

**FALLING WEIGHT DEFLECTOMETER FOR ESTIMATING SUBGRADE
RESILIENT MODULI**

FINAL REPORT

by

K.P. George

Conducted by the

DEPARTMENT OF CIVIL ENGINEERING
UNIVERSITY OF MISSISSIPPI

In cooperation with

THE MISSISSIPPI DEPARTMENT OF TRANSPORTATION

And

U.S. DEPARTMENT OF TRANSPORTATION
FEDERAL HIGHWAY ADMINISTRATION

The University of Mississippi
University, Mississippi
October 2003

1. Report No. FHWA/MS-DOT-RD-03-153		2. Government Accession No.		3. Recipient's Catalog No.	
4. Title and Subtitle Falling Weight Deflectometer for Estimating Subgrade Moduli				5. Report Date December 2003	
				6. Performing Organization Code	
7. Author(s) K.P. George				8. Performing Organization Report No. MS-DOT-RD-03-153	
9. Performing Organization Name and Address University of Mississippi Department of Civil Engineering University, MS 38677				10. Work Unit No. (TRAIS)	
				11. Contract or Grant No. State Study 153	
12. Sponsoring Agency Name and Address Mississippi Department of Transportation Research Division P.O. Box 1850 Jackson, MS 39215-1850				13. Type Report and Period Covered January 2002 – December 31, 2003 Final Report	
				14. Sponsoring Agency Code	
15. Supplementary Notes					
16. Abstract <p>Subgrade soil characterization expressed in terms of resilient modulus, M_R, has become crucial for pavement design. For new pavement design, M_R values are generally obtained by conducting repeated load triaxial tests on reconstituted/undisturbed cylindrical specimens, employing TP46 protocol. Because of the complexities encountered with the test, in situ tests would be desirable if reliable correlation can be established. In evaluating existing pavements for rehabilitation selection, subgrade characterization is even more complex. The focus of this study is to investigate the viability of Falling Weight Deflectometer (FWD) for direct testing of subgrade with the object of deriving resilient modulus, via a correlation between FWD modulus and M_R. In support of this research, side-by-side Automated Dynamic Cone Penetrometer (ADCP) tests were also conducted.</p> <p>Ten as-built subgrade sections reflecting typical subgrade soil materials of Mississippi were selected and tested with FWD. Both fine- and coarse-grain soils were included in the program. Undisturbed samples were extracted using a Shelby tube and tested in a repeated load triaxial machine for M_R, employing TP46 protocol. Other routine laboratory tests are conducted to determine physical properties, and, in turn, classify the soil being tested.</p> <p>Employing seven FWD sensor deflections, elastic moduli, E_1 to E_7, are calculated employing forward equations (assuming static half-space). E_1 and E_{3-5} (average of E_3, E_4, and E_5) are regressed against M_R, advancing two models for M_R prediction. Employing E_1 and E_{3-5}, two distinct resilient moduli are derived, with the lesser of the two serving as the design resilient modulus. A feature of the model is that both center sensor modulus and offset sensor moduli enter in the process, yielding a representative, but conservative, resilient modulus for design. Having been derived from multiple sensor moduli, this procedure promises to be a viable method for subgrade characterization, considering significant nonhomogeneity expected of built-up subgrades. Also suggested is a short-cut procedure for predicting resilient modulus which employs an E_{3-5} section average for a low moduli range, that is, $E_1 < 9000$ psi (62 MPa), and lesser of E_1 and E_{3-5} for $E_1 > 9000$ psi (62 MPa).</p> <p>An exclusive program, FWDSUBGRADE, is developed to analyze FWD deflection data from subgrade tests, extracting first sensor modulus E_1, and average of three offset sensor moduli, E_{3-5}, from which only design resilient modulus is derived. The program, in addition to calculating station-by-station resilient modulus, relying on what is known as "cumulative difference" technique, delineates homogenous units of the subgrade, outputting mean and standard deviation of the resilient modulus for each homogenous section. A graphical plot of resilient modulus of each station is another output of the program.</p>					
17. Key Words Subgrade, Resilient Modulus, Falling Weight Deflectometer, Elastic Modulus, Correlation Analysis			18. Distribution Statement Unclassified		
19. Security Classif. (of this report) Unclassified		20. Security Classif. (of this page) Unclassified		21. No. of Pages	
				22. Price	

Form DOT F 1700.7 (8-72)

Reproduction of completed page authorized

ACKNOWLEDGMENT

This report includes the results of a study titled “Falling Weight Deflectometer for Estimating Subgrade Moduli”, conducted by the Department of Civil Engineering, The University of Mississippi, in cooperation with the Mississippi Department of Transportation (MDOT), and the U.S. Department of Transportation, Federal Highway Administration (FHWA). Funding of this project by MDOT and FHWA is gratefully acknowledged.

The author wishes to thank Bill Barstis with MDOT’s Research Division for his efforts in coordinating the overall work plan of the project. Johnny Hart of MDOT coordinated the fieldwork, including FWD tests; Alan Hatch of MDOT conducted ADCP tests. Richard Stubstad’s (ERES/ARA) assistance in the data analysis phase of this project is acknowledged.

Manil Bajracharya and Madan Gaddam were the key personnel from the University conducting laboratory work and providing support in the field. The service of Sherra Jones in preparing this report is gratefully acknowledged.

ABSTRACT

Subgrade soil characterization expressed in terms of resilient modulus, M_R , has become crucial for pavement design. For new pavement design, M_R values are generally obtained by conducting repeated load triaxial tests on reconstituted/undisturbed cylindrical specimens, employing TP46 protocol. Because of the complexities encountered with the test, in situ tests would be desirable if reliable correlation can be established. In evaluating existing pavements for rehabilitation selection, subgrade characterization is even more complex. The focus of this study is to investigate the viability of Falling Weight Deflectometer (FWD) for direct testing of subgrade with the object of deriving resilient modulus, via a correlation between FWD modulus and M_R . In support of this research, side-by-side Automated Dynamic Cone Penetrometer (ADCP) tests were also conducted.

Ten as-built subgrade sections reflecting typical subgrade soil materials of Mississippi were selected and tested with FWD. Both fine- and coarse-grain soils were included in the program. Undisturbed samples were extracted using a Shelby tube and tested in a repeated load triaxial machine for M_R , employing TP46 protocol. Other routine laboratory tests are conducted to determine physical properties, and, in turn, classify the soil being tested.

Employing seven FWD sensor deflections, elastic moduli, E_1 to E_7 , are calculated employing forward equations (assuming static half-space). E_1 and E_{3-5} (average of E_3 , E_4 , and E_5) are regressed against M_R , advancing two models for M_R prediction. Employing E_1 and E_{3-5} , two distinct resilient moduli are derived, with the lesser of the two serving as the design resilient modulus. A feature of the model is that both center sensor modulus and offset sensor moduli enter in the process, yielding a representative, but conservative, resilient modulus for design. Having been derived from multiple sensor moduli, this procedure promises to be a viable method

for subgrade characterization, considering significant nonhomogeneity expected of built-up subgrades. Also suggested is a short-cut procedure for predicting resilient modulus which employs an E_{3-5} section average for a low moduli range, that is, $E_1 < 9000$ psi (62 MPa), and lesser of E_1 and E_{3-5} for $E_1 > 9000$ psi (62 MPa).

An exclusive program, FWDSUBGRADE, is developed to analyze FWD deflection data from subgrade tests, extracting first sensor modulus E_1 , and average of three offset sensor moduli, E_{3-5} , from which only design resilient modulus is derived. The program, in addition to calculating station-by-station resilient modulus, relying on what is known as “cumulative difference” technique, delineates homogenous units of the subgrade, outputting mean and standard deviation of the resilient modulus for each homogenous section. A graphical plot of resilient modulus of each station is another output of the program.

TABLE OF CONTENTS

1.	INTRODUCTION	1
1.1	How to Characterize Subgrade.....	1
1.2	Critique of Resilient Modulus Test (TP46).....	3
1.3	Objective.....	4
1.4	Scope.....	5
2.	REVIEW OF LITERATURE	7
2.1	Introduction.....	7
2.2	Deflection Tests for Material Characterization.....	7
2.2.1	Deflection Analysis Methods.....	8
2.3	Nonlinear Characterization of Subgrade (Unbound Material).....	12
2.4	Relation Between Resilient Modulus, M_R , and FWD Modulus, E_{back} or E	15
2.4.1	Small-Scale Devices for Measuring Elastic Stiffness and Its Relation to FWD Modulus.....	17
2.5	Relation Between M_R and E : A Critique.....	17
2.6	Conclusion.....	19
3.	EXPERIMENTAL WORK AND DATA COLLECTED	21
3.1	Introduction.....	21
3.2	Field Tests.....	21
3.2.1	FWD Test On Prepared Subgrade and Modulus Calculation.....	21
3.2.2	Automated Dynamic Cone Penetrometer (ADCP) Test.....	41
3.2.3	Geogauge Modulus.....	42
3.2.4	In-Place Density and Moisture.....	45
3.2.5	Soil Sampling and Tests.....	47
3.3	Summary.....	51
4.	ANALYSIS AND DISCUSSION OF RESULTS	54
4.1	Introduction.....	54
4.2	How Layering Affects Elastic Modulus.....	54
4.3	FWD Elastic Modulus Compared to Geogauge Modulus.....	57
4.4	Are the Resilient Moduli of Shelby Tube Samples Overestimated?.....	58
4.5	Selecting Appropriate Resilient Modulus from TP46 Results.....	63
4.6	FWD Plate Dimension and Sensor Tip Size for Subgrade Test.....	68
4.6.1	General.....	68
4.6.2	Comparison of Moduli from 18-in. (450-mm) and 12-in. (300-mm) Plates.....	68
4.6.3	Comparison of Moduli Employing 10 mm and 16 mm Tips.....	71
4.7	Selecting Appropriate FWD Test Results.....	73
4.7.1	FWD Test Results, Outliers Deleted.....	73
4.7.2	Selecting FWD Elastic Modulus.....	73
4.7.3	Elastic Modulus and Resilient Modulus Variabilities Compared.....	77

4.8	Prediction of Design Resilient Modulus Employing FWD Modulus E ₁ and/or E ₃₋₅	79
4.8.1	General.....	79
4.8.2	Linear Relation Between E ₁ and M _R	80
4.8.3	Linear Relation Between E ₃₋₅ and M _R	83
4.8.4	One-to-One Relation Between E ₁ and M _R	83
4.8.5	Resilient Modulus Prediction Using Both E ₁ and E ₃₋₅	86
4.9	Three Resilient Modulus Prediction Methods Critiqued.....	91
4.10	Data Analysis Software.....	93
4.11	Summary.....	94
5.	PLANNING FWD TEST AND CALCULATION OF DESIGN RESILIENT MODULUS.....	95
5.1	Overview.....	95
5.2	Planning FWD Test in the Field.....	95
5.2.1	Equipment Selection.....	96
5.2.2	When and Where To Test?.....	97
5.3	Selection of Design Unit.....	97
5.4	Computer Program, FWDSUBGRADE, to Calculation Design Modulus.....	99
5.5	Summary.....	100
6.	SUMMARY AND CONCLUSIONS.....	103
6.1	Summary.....	103
6.2	Conclusions.....	104
6.3	Recommendations for Further Research.....	105
6.4	Implementation.....	106
6.5	Benefits.....	106
	REFERENCES.....	108
	APPENDIX A (FWD Deflection Basins, Typical Station From Each Section).....	113
	APPENDIX B (Automated Dynamic Cone Penetrometer Test Data).....	119
	APPENDIX C (Resilient Modulus of Sample 1 (0-12 in. Depth) As Function of Stress State.....	125
	APPENDIX D (Detailed Flow Chart of Software Program FWDSUBGRADE).....	148

LIST OF TABLES

2.1	Summary of the Median and Mean Values for Each Coefficient of Constitutive Equation 2.6 for Subgrade Soils, $k_6 = 0$ (37).....	14
2.2	AASHTO Modulus Correction Values From Long-term Pavement Performance Sections (43). (Backcalculated values shall be multiplied by a correction factor to get resilient modulus).....	16
3.1	Summary Section Locations and Tests Performed.....	22
3.2	Summary of FWD Tests Using Two Plate Sizes and Two Sensor Tip Sizes.....	23
3.3	Backcalculated Moduli Based on FWD Deflection Basin, Section # 1.....	25
3.4	Comparison of Modulus (Expressed As A Ratio) Calculated for Offset Sensors Employing Equation 3.1, and Exact Equation with Distributed Loads.....	27
3.5	Elastic Moduli For All Four Load Drops For Nine Stations of Section # 4.....	28
3.6	Summary of Elastic Modulus Calculated from FWD Sensor Deflections Using 18-in. (450-mm) Plate, Montgomery County, Section # 1.....	29
3.7	Summary of Elastic Modulus Calculated from FWD Sensor Deflections Using 18-in. (450-mm) Plate, Coahoma County, Section # 2.....	29
3.8	Summary of Elastic Modulus Calculated from FWD Sensor Deflections Using 18-in. (450-mm) Plate, Coahoma County, Section # 3.....	30
3.9	Summary of Elastic Modulus Calculated from FWD Sensor Deflections Using 18-in. (450-mm) Plate, Montgomery County, Section # 4.....	30
3.10	Summary of Elastic Modulus Calculated from FWD Sensor Deflections Using 18-in. (450-mm) Plate, Montgomery County, Section # 5.....	31
3.11	Summary of Elastic Modulus Calculated from FWD Sensor Deflections Using 18-in. (450-mm) Plate, Hinds County, Section # 6.....	31
3.12	Summary of Elastic Modulus Calculated from FWD Sensor Deflections Using 18-in. (450-mm) Plate, Wayne County, Section # 7.....	32
3.13	Summary of Elastic Modulus Calculated from FWD Sensor Deflections Using 18-in. (450-mm) Plate, Wayne County, Section # 8.....	32
3.14	Summary of Elastic Modulus Calculated from FWD Sensor Deflections Using 18-in. (450-mm) Plate, Wayne County, Section # 9.....	33

3.15	Summary of Elastic Modulus Calculated from FWD Sensor Deflections Using 18-in. (450-mm) Plate, Madison County, Section #10.....	33
3.16	Summary of Elastic Modulus Calculated from FWD Sensor Deflections Using 12-in. (300-mm) Plate, Coahoma County, Section #2.....	34
3.17	Summary of Elastic Modulus Calculated from FWD Sensor Deflections Using 12-in. (300-mm) Plate, Coahoma County, Section #3.....	34
3.18	Summary of Elastic Modulus Calculated from FWD Sensor Deflections Using 12-in. (300-mm) Plate, Montgomery County, Section #4.....	35
3.19	Summary of Elastic Modulus Calculated from FWD Sensor Deflections Using 12-in. (300-mm) Plate, Montgomery County, Section #5.....	35
3.20	Summary of Elastic Modulus Calculated from FWD Sensor Deflections Using 12-in. (300-mm) Plate, Hinds County, Section #6.....	36
3.21	Summary of Elastic Modulus Calculated from FWD Sensor Deflections Using 12-in. (300-mm) Plate, Wayne County, Section #7.....	36
3.22	Summary of Elastic Modulus Calculated from FWD Sensor Deflections Using 12-in. (300-mm) Plate, Wayne County, Section #8.....	37
3.23	Summary of Elastic Modulus Calculated from FWD Sensor Deflections Using 12-in. (300-mm) Plate, Wayne County, Section #9.....	37
3.24	Summary of Elastic Modulus Calculated from FWD Sensor Deflections Using 12-in. (300-mm) Plate, Madison County, Section #10.....	38
3.25	Summary of Dynamic Cone Penetration Index (DCPI) Results of Ten Test Sections.....	43
3.26	Geogauge Modulus Compared With FWD First Sensor Modulus, E_1 , and Offset Modulus, E_{3-5} (18-in. Load Plate).....	44
3.27	Density and Moisture Determined (i) by Nuclear Device (ii) from Shelby Tube Samples, and (iii) Optimum Moisture and Density.....	46
3.28	Physical Properties and AASHTO Classification of (Grouped) Shelby Tube, and Bag Samples.....	49
3.29	Resilient Modulus of Reconstituted Samples Compared With Modulus of Shelby Tube Samples.....	52
4.1	TP46 Resilient Modulus Compared to That Predicted by Equation 4.2.....	62

4.2	Typical Regression Constants (k – values) of Constitutive Equation 2.8, Sample 1.....	64
4.3	Calculated Stress States in Subgrade Under Different Loads Including Overburden.....	65
4.4	Resilient Modulus Calculated Employing Two Stress States at Depths 6 in. Below and 18 in. Below Surface, Respectively. Load 2500 lb on 18-in. Plate.....	66
4.5	Comparison of Average Density and Moisture of Sample 1 (0 - 12 in. depth) and sample 2 (12 - 24 in. depth) Shelby Tube Samples.....	67
4.6	Comparison of Coefficient of Variation of Sample 1 (0 - 12 in. depth) and Sample 2 (12 - 24 in. depth) Resilient Modulus.....	68
4.7	Summary of Statistical Test Results Comparing 18-in. (450-mm) Plate Modulus to 12-in. (300-mm) Plate Modulus.....	70
4.8	Comparison of Coefficient of Variation of 12-in. and 18-in. Plate Moduli.....	70
4.9	Average Section Elastic Moduli at Each Sensor, Load Plate = 12 in., Sensor Tip 10 mm/18 mm, Sections 7 – 9.....	72
4.10	How Sensor Tips, 10 mm and 16 mm, Affect Elastic Moduli (E_1 and E_{3-5}), 12-in. Plate.....	72
4.11	Predicted Resilient Modulus Compared with Experimental Value.....	91

LIST OF FIGURES

2.1	Typical FWD Load Impulse and Geophone Response With Time.....	11
2.2	Frequency Response Function.....	12
3.1.a	Elastic Moduli at Each Sensor Location. Nine Stations of Section #4, 1 psi = 6.89 kPa, 1 in. = 25.4 mm.....	38
3.1.b	Elastic Moduli at Each Sensor Location. Nine Stations of Section #7, 1 psi = 6.89 kPa, 1 in. = 25.4 mm.....	39
3.2.a	Deflection Ratios of 12-in. and 18-in. Plates at Station 907+50 of Section #4, 1 in. = 25.4 mm.....	40
3.2.b	Deflection Ratios of 12-in. and 18-in. Plates at Station 7+382.5 of Section #9, 1 in. = 25.4 mm.....	40
4.1	Geogauge Modulus Compared with FWD Modulus, $E_{1(av)}$, Section Averages, FWD with 18-in. (450-mm) Plate, 1 psi = 6.89 kPa.....	58
4.2	Comparison of Normalized Deflections of 12-in. (300-mm) and 18-in.(450-mm) Plates. Section #8, 1 in. = 25.4mm, 1 lb. = 4.448N.....	71
4.3	Comparison of Normalized Deflections of 10 mm and 16 mm tip, Section # 8, 12-in. Plate, 1 in. = 25.4 mm.....	74
4.4	Photograph of Imprint Showing Loose Coarse Particles Congregating Around the First Sensor Tip.....	76
4.5	Coefficient of Variation of E_{3-5} Plotted Against Coefficient of Variation of M_R of Nine Sections, 18-in. (450-mm) Plate.....	78
4.6	Scatter Plot of Station-by-Station Values of E_1 and M_R , Nine Sections, 18-in. (450-mm) Plate, 1 psi = 6.89 kPa.....	81
4.7	Scatter Plot of Station-by-Station Values of E_1 and M_R , Eight Sections, (Section 1 Not Included), 12-in. (300-mm) Plate, 1 psi = 6.89 kPa.....	81
4.8	Scatter Plot of Section Average E_1 vs. Section Average M_R , Nine Sections, 18-in. (450-mm) Plate, 1 psi = 6.89 kPa.....	82
4.9	Scatter Plot of Section Average E_{3-5} vs. Section Average M_R , Nine Sections, 18-in. (450-mm) Plate, 1 psi = 6.89 kPa.....	84
4.10	Scatter Plot of Section Average E_1 vs. Section Average M_R , Nine Sections, 18-in.	

	(450-mm) Plate, Intercept Zero, 1 psi = 6.89 kPa.....	84
4.11	Scatter Plot of Section Average E_{3-5} vs. Section Average M_R , Nine Sections, 18-in. (450-mm) Plate, Intercept Zero, 1 psi = 6.89 kPa.....	85
4.12	E_1 and E_{3-5} Each Plotted Against Resilient Modulus M_R , (Station-by-Station Values), Nine Sections, 18-in. (450-mm) Plate, 1 psi = 6.89 kPa.....	87
4.13	Scatter Plot of Station-by-Station Values of E_1 and M_R , 18-in. (450-mm) Plate, 1 psi = 6.89 kPa.....	88
4.14	Scatter Plot of Average Modulus of Sensors 3-5 vs. Resilient Modulus, 18-in. (450-mm) Plate, 1 psi = 6.89 kPa.....	88
4.15	Section Averages E_1 and E_{3-5} , Each Plotted Against Average Resilient Modulus M_R , Eight Sections, 18-in. (450-mm) Plate, Section 1 Deleted in E_1 vs. M_R Plot & Section 5 Deleted in E_{3-5} vs. M_R Plot, 1 psi = 6.89 kPa.....	89
5.1	FN(40) Results versus Distance Along Project (Adapted From Reference 2).....	98
5.2	Delineating Analysis Units by Cumulative Difference Approach (Adapted From Reference 2).....	100
5.3	Flow Chart of Program FWDSUBGRADE.....	102

APPENDIX A

	FWD DEFLECTION BASINS, TYPICAL STATION FROM EACH SECTION.....	113
Figure A1	Deflection Basins for Four Loads, Section #1, Station #854+25, US 82W, Montgomery County, 18-in. (450-mm) Plate.....	114
Figure A2	Deflection Basins for Four Loads, Section #2, Station #56+00, US 61N, Coahoma County, 18-in. (450-mm) Plate.....	114
Figure A3	Deflection Basins for Four Loads, Section #3, Station #152+50, US 61N, Coahoma County, 18-in. (450-mm) Plate.....	115
Figure A4	Deflection Basins for Four Loads, Section #4, Station #907+50, US 82W, Montgomery County, 18-in. (450-mm) Plate.....	115
Figure A5	Deflection Basins for Four Loads, Section #5, Station #833+20, US 82W, Montgomery County, 18-in. (450-mm) Plate.....	116
Figure A6	Deflection Basins for Four Loads, Section #6, Station #26+50, Norell W, Hinds County, 18-in. (450-mm) Plate.....	116

Figure A7	Deflection Basins for Four Loads, Section #7, Station #6+530, US 45N, Wayne County, 18-in. (450-mm) Plate.....	117
Figure A8	Deflection Basins for Four Loads, Section #8, Station #7+405, US 45N, Wayne County, 18-in. (450-mm) Plate.....	117
Figure A9	Deflection Basins for Four Loads, Section #9, Station #7+435, US 45N, Wayne County, 18-in. (450-mm) Plate.....	118
Figure A10	Deflection Basins for Four Loads, Section #10, Station #48+50, Nissan W. Parkway, Madison County, 18-in. (450-mm) Plate.....	118

APPENDIX B

AUTOMATED DYNAMIC CONE PENETROMETER TEST DATA.....119

Figure B1	ADCP Test Results in Section #1, US 82W, Montgomery County.....	120
Figure B2	ADCP Test Results in Section #2, US 61N, Coahoma County.....	120
Figure B3	ADCP Test Results in Section #3, US 61N, Coahoma County.....	121
Figure B4	ADCP Test Results in Section #4, US 82W, Montgomery County.....	121
Figure B5	ADCP Test Results in Section #5, US 82W, Montgomery County.....	122
Figure B6	ADCP Test Results in Section #6, Norrell W, Hinds County.....	122
Figure B7	ADCP Test Results in Section #7, US 45N, Wayne County.....	123
Figure B8	ADCP Test Results in Section #8, US 45N, Wayne County.....	123
Figure B9	ADCP Test Results in Section #9, US 45N, Wayne County.....	124
Figure B10	ADCP Test Results in Section #10, Nissan W. Parkway, Madison County.....	124

APPENDIX C

RESILIENT MODULUS OF SAMPLE # 1 (0 – 12 in. DEPTH) AS FUNCTION OF STRESS STATE.....125

Figure C1	Resilient Modulus Test Results, Station 852+50, Section 1, Sample #1, 1 MPa = 145 psi.....	126
Figure C2	Resilient Modulus Test Results, Station 853+50, Section 1, Sample #1, 1 MPa = 145 psi.....	126
Figure C3	Resilient Modulus Test Results, Station 853+75, Section 1, Sample #1, 1 MPa = 145 psi.....	127

Figure C4	Resilient Modulus Test Results, Station 854+00, Section 1, Sample #1, 1 MPa = 145 psi.....	127
Figure C5	Resilient Modulus Test Results, Station 55+00, Section 2, Sample #1, 1 MPa = 145 psi.....	128
Figure C6	Resilient Modulus Test Results, Station 56+00, Section 2, Sample #1, 1 MPa = 145 psi.....	128
Figure C7	Resilient Modulus Test Results, Station 57+50, Section 2, Sample #1, 1 MPa = 145 psi.....	129
Figure C8	Resilient Modulus Test Results, Station 58+50, Section 2, Sample #1, 1 MPa = 145 psi.....	129
Figure C9	Resilient Modulus Test Results, Station 152+00, Section 3, Sample #1, 1 MPa = 145 psi.....	130
Figure C10	Resilient Modulus Test Results, Station 152+50, Section 3, Sample #1, 1 MPa = 145 psi.....	130
Figure C11	Resilient Modulus Test Results, Station 153+00, Section 3, Sample #1, 1 MPa = 145 psi.....	131
Figure C12	Resilient Modulus Test Results, Station 153+50, Section 3, Sample #1, 1 MPa = 145 psi.....	131
Figure C13	Resilient Modulus Test Results, Station 153+90, Section 3, Sample #1, 1 MPa = 145 psi.....	132
Figure C14	Resilient Modulus Test Results, Station 905+50, Section 4, Sample #1, 1 MPa = 145 psi.....	132
Figure C15	Resilient Modulus Test Results, Station 906+00, Section 4, Sample #1, 1 MPa = 145 psi.....	133
Figure C16	Resilient Modulus Test Results, Station 906+50, Section 4, Sample #1, 1 MPa = 145 psi.....	133
Figure C17	Resilient Modulus Test Results, Station 907+00, Section 4, Sample #1, 1 MPa = 145 psi.....	134
Figure C18	Resilient Modulus Test Results, Station 907+50, Section 4, Sample #1, 1 MPa = 145 psi.....	134

Figure C19	Resilient Modulus Test Results, Station 833+20, Section 5, Sample #1, 1 MPa = 145 psi.....	135
Figure C20	Resilient Modulus Test Results, Station 834+00, Section 5, Sample #1, 1 MPa = 145 psi.....	135
Figure C21	Resilient Modulus Test Results, Station 834+40, Section 5, Sample #1, 1 MPa = 145 psi.....	136
Figure C22	Resilient Modulus Test Results, Station 25+00, Section 6, Sample #1, 1 MPa = 145 psi.....	136
Figure C23	Resilient Modulus Test Results, Station 25+50, Section 6, Sample #1, 1 MPa = 145 psi.....	137
Figure C24	Resilient Modulus Test Results, Station 26+00, Section 6, Sample #1, 1 MPa = 145 psi.....	137
Figure C25	Resilient Modulus Test Results, Station 26+50, Section 6, Sample #1, 1 MPa = 145 psi.....	138
Figure C26	Resilient Modulus Test Results, Station 27+00, Section 6, Sample #1, 1 MPa = 145 psi.....	138
Figure C27	Resilient Modulus Test Results, Station 6+500, Section 7, Sample #1, 1 MPa = 145 psi.....	139
Figure C28	Resilient Modulus Test Results, Station 6+515, Section 7, Sample #1, 1 MPa = 145 psi.....	139
Figure C29	Resilient Modulus Test Results, Station 6+530, Section 7, Sample #1, 1 MPa = 145 psi.....	140
Figure C30	Resilient Modulus Test Results, Station 6+545, Section 7, Sample #1, 1 MPa = 145 psi.....	140
Figure C31	Resilient Modulus Test Results, Station 6+560, Section 7, Sample #1, 1 MPa = 145 psi.....	141
Figure C32	Resilient Modulus Test Results, Station 7+375, Section 8, Sample #1, 1 MPa = 145 psi.....	141
Figure C33	Resilient Modulus Test Results, Station 7+390, Section 8, Sample #1, 1 MPa = 145 psi.....	142

Figure C34	Resilient Modulus Test Results, Station 7+405, Section 8, Sample #1, 1 MPa = 145 psi.....	142
Figure C35	Resilient Modulus Test Results, Station 7+420, Section 8, Sample #1, 1 MPa = 145 psi.....	143
Figure C36	Resilient Modulus Test Results, Station 7+375, Section 9, Sample #1, 1 MPa = 145 psi.....	143
Figure C37	Resilient Modulus Test Results, Station 7+390, Section 9, Sample #1, 1 MPa = 145 psi.....	144
Figure C38	Resilient Modulus Test Results, Station 7+420, Section 9, Sample #1, 1 MPa = 145 psi.....	144
Figure C39	Resilient Modulus Test Results, Station 7+435, Section 9, Sample #1, 1 MPa = 145 psi.....	145
Figure C40	Resilient Modulus Test Results, Station 47+00, Section 10, Sample #1, 1 MPa = 145 psi.....	145
Figure C41	Resilient Modulus Test Results, Station 47+50, Section 10, Sample #1, 1 MPa = 145 psi.....	146
Figure C42	Resilient Modulus Test Results, Station 48+00, Section 10, Sample #1, 1 MPa = 145 psi.....	146
Figure C43	Resilient Modulus Test Results, Station 48+50, Section 10, Sample #1, 1 MPa = 145 psi.....	147
Figure C44	Resilient Modulus Test Results, Station 49+00, Section 10, Sample #1, 1 MPa = 145 psi.....	147

APPENDIX D

DETAILED FLOWCHARTS OF SOFTWARE PROGRAM FWDSUBGRADE.....148

Figure D1	Flow Chart of First Phase of Program calculating Resilient Modulus from Elastic Modulus.....	149
Figure D2	Flow Chart of Second Phase of Program Delineating Homogeneous Section...	150

CHAPTER 1

INTRODUCTION

1.1 HOW TO CHARACTERIZE SUBGRADE?

Subgrade soil stiffness is an important parameter in pavement design. In recent years, mechanistic-empirical design procedures have attracted the attention of both pavement engineers and researchers. These design procedures require knowledge of the mechanical properties of the materials that make up the pavement structure. The resilient modulus (M_R) has become a well-known parameter to characterize unbound pavement materials because a large amount of evidence has shown that the elastic (resilient) pavement deflection possesses a better correlation to field performance than the total pavement deflection (1). Resilient modulus is defined as the ratio of deviator stress, σ_d , to the recoverable strain, ϵ_r ,

$$M_R = \sigma_d / \epsilon_r \quad (1.1)$$

The 1993 AASHTO Pavement Design Guide recommends using M_R as an input parameter to evaluate subgrade support (2). To meet this recommendation, AASHTO tests (laboratory) T-274-87 and TP292-92 were proposed, the latest being the provisional standard TP46-94. Meanwhile, the complexity of the laboratory test procedures has prompted highway agencies to explore other test methods, especially in-situ field tests. Deflection measurements with the Falling Weight Deflectometer (FWD) and, in turn, modulus calculation through backcalculation have been routinely employed in evaluating pavement layers, and the underlying subgrade. The modulus of a multilayer system, calculated from surface deflections employing a backcalculation routine, is referred to as “backcalculated modulus,” E_{back} , in contrast to “resilient modulus,” M_R , which results from a laboratory test, for example, TP46 protocol. When using

forward calculation, employing surface deflection(s) and Boussinesq equations, the modulus resulting is designated “elastic modulus,” E .

Highway agencies have also attempted to correlate resilient modulus with other test parameters. The California Bearing Ratio (CBR)-resilient modulus correlation has been studied extensively (3). The Dynamic Cone Penetrometer (DCP), a penetration device, introduced in the 1960s for pavement evaluation, is another device that has been employed for characterization for subgrade soils (4, 5, 6, 7).

The AASHTO Guide allows the use of both laboratory and in situ backcalculated moduli, but recognizes that the moduli determined by both procedures are not equal. The guide, therefore, suggests that the subgrade modulus determined from deflection measurements on the pavement surface, E_{back} , be adjusted by a factor of 0.33. However, other ratios have been documented. Ali and Khosla (8) compared the subgrade soil resilient modulus determined in the laboratory and backcalculated values from three pavement sections in North Carolina. The ratio of laboratory- measured modulus values to the corresponding backcalculated values varied from 0.18 to 2.44. Newcomb (9) reported the results of similar tests in Washington State, suggesting a ratio in the range of 0.8 to 1.3. Von Quintus et al. (10) reported ratios in the range of 0.1 to 3.5 in a study based on data obtained from the Long Term Pavement Performance (LTPP) database. In the same reference, different average ratios were reported based on the type of layers atop the subgrade layer. Laboratory values were consistently higher (nearly double) than the backcalculated values, according to Chen et al. (11). Note that the previous studies relied on backcalculated moduli from deflection measurements on the top of the pavement structure. Many factors may have contributed to the disagreement between the laboratory measured and backcalculated moduli. One reason is the difficulty of obtaining representative samples from the

field because of the inherent variability of the subgrade layer itself. A detailed discussion of the differences between laboratory measured $M_R(\text{lab})$ and backcalculated moduli can be found elsewhere (12).

While numerous studies have attempted FWD measurements on the pavement surface, only a few have targeted FWD tests conducted directly on the subgrade surfaces. In their study of the Minnesota Research Road Project (Mn/ROAD), Van Deusen et al. (13) reported difficulties analyzing FWD measurements performed directly on subgrade surfaces. Their results showed a weak correlation between laboratory and backcalculated moduli. Chai (6) employed the FWD during subgrade construction, backcalculated modulus and comparing these values to the field modulus calculated from the Dynamic Cone Penetration Index (DCPI). Resilient modulus vs. elastic modulus, E , relation was explored in a recent study titled “The Virginia Smart Road Project” (14). The relationship, however, was less than satisfactory. A recent investigation, conducted by the author’s group, showed that the backcalculated moduli (E_{back}) obtained from testing directly on the subgrade are in satisfactory agreement with the laboratory values with certain restrictions (15).

1.2 CRITIQUE OF RESILIENT MODULUS TEST (TP46)

Since AASHTO recommends using a laboratory resilient modulus test in a relatively small soil sample – one that is undisturbed or reconstituted – it is worthwhile to examine how realistic this test is. Despite several improvements made over the years, researchers have cited several uncertainties as well as limitations associated with this laboratory test procedure, a list of which follows (16):

1. The laboratory resilient modulus sample is not completely representative of in situ conditions because of sample disturbance and differences in aggregate orientation,

moisture content, in-situ soil suction and level of compaction (or recompaction).

2. Inherent equipment flaws make it difficult to simulate the state of stress of the material in situ.
3. Inherent instrumentation flaws create uncertainty in the measurement of sample displacements.
4. Lack of uniform equipment calibration and verification procedures lead to differences not only between labs but also within a given lab.
5. Laboratory specimens represent the properties of a small quantity of material, and not necessarily the average of the mass of material that responds to a typical truck axle.
6. The time, expense and potential impact associated with a statistically adequate sampling plan as well as testing add up to large expenditure.

Overall, these issues have kept the resilient modulus test from achieving general acceptance by the pavement and materials testing community, whereas a nondestructive test such as the FWD deflection test is credited with providing in situ modulus, and is also capable of identifying inherent spatial variation. This research explores the viability of FWD in estimating subgrade material modulus, a surrogate for resilient modulus for pavement design.

1.3 OBJECTIVE

This project addresses the issue of employing FWD deflection test data for subgrade characterization. Recognizing the need for the resilient modulus of subgrade soil in AASHTO design methodology, this research seeks a relationship between deflection-based elastic modulus, E , and laboratory determined resilient modulus, M_R . Once a statistically significant relationship is established, the FWD could become a viable device for direct in-situ testing of subgrades and for estimating the subgrade resilient modulus (via a derived relationship), the standard input into

the AASHTO 1993 Design Guide, as well as in the 2002 Mechanistic Design Guide.

1.4 SCOPE

Ten as-built subgrades, representing a wide range of soil types, were tested with Mississippi Department of Transportation (MDOT) FWD employing the low-load package and two load plates (12-in. (300-mm) and 18-in. (450-mm)). Shelby tube samples (three depths from each station) were retrieved from the same locations and tested for resilient modulus, M_R . For direct verification of the stiffness of the subgrade, Geogauge modulus was determined at each location. Side-by-side (automated) dynamic cone penetrometer tests were also performed, to a depth of 3 ft. 3 in. (1000 mm), identifying layering of subgrade, which became useful in interpreting deflection-based elastic modulus. Because of their importance on soil properties, density and moisture were determined using nuclear gauge, again at the same test locations. Bag samples collected from each section enabled us to identify and classify the soil in each test section, further substantiating the classification test results of Shelby tube samples.

This report comprises six chapters and three appendices. Chapter 2 presents a literature review of the use of deflection testing devices for material characterization with special reference to FWD deflections for subgrade modulus calculation, and its relation to resilient modulus. Field data collected from ten test sections, five stations from each test section, are presented in Chapter 3. A comprehensive data analysis, culminating in a relation between elastic modulus, E , and resilient modulus, M_R , comprises Chapter 4. A methodology for FWD tests is described in the first part of chapter 5. Presented in the latter part is an outline of a computer program designated “FWDSUBGRADE,” for analyzing FWD data, arriving at a design resilient modulus – mean and standard deviation of so-called “uniform section.” A summary and observations regarding the findings of the study constitute Chapter 6. Typical deflection basins are presented in *Appendix*

A. *Appendix B* includes the entire DCP data of ten test sections. Resilient modulus test results comprise *Appendix C*. Detailed flow charts of the program, FWDSUBGRADE, are included in *Appendix D*.

CHAPTER 2

REVIEW OF LITERATURE

2.1 INTRODUCTION

The 1986 AASHTO Guide has stipulated and the 2002 Guide reaffirmed that resilient modulus should be the parameter for characterizing subgrade. Consequently, AASHTO Tests (laboratory) T274-87 and TP292-91 were proposed, the latest being the provisional standard TP46-94 and the “harmonized” M_R test protocol developed in the NCHRP 1-28A study. The complexity of the laboratory test procedures has prompted highway agencies to explore other test methods, primarily nondestructive deflection tests, and subsequent backcalculation of moduli (17). Some of the impulse devices currently in use are Falling Weight Deflectometer, Loadman, and TRL Foundation Tester (TFT). Correlation of laboratory moduli with other test methods has been attempted. The California Bearing Ratio–resilient modulus correlation has been studied extensively in the past. The Dynamic Cone Penetrometer (DCP), a penetration device, introduced in the 1960s for pavement evaluation, is another device that has been employed for characterization of subgrade soils, again via a correlation between laboratory M_R and DCP index (4, 7).

2.2 DEFLECTION TESTS FOR MATERIAL CHARACTERIZATION

Nondestructive testing (NDT) of pavements, especially deflection testing, has been a vital part evaluating the structural capacity of pavement. The following discusses different deflection measuring methods and analysis techniques to derive material property of the layered system. A detailed discussion of these topics can be seen in reference (18).

The NDT equipment used in making the measurements includes a variety of modes for applying loads to a pavement and a number of sensors for measuring the pavement response.

The loading methods include: (a) static or slowly moving loads, (b) vibration, (c) “near field” impulse methods, and (d) wave propagation methods. Output responses are measured on the surface or with depth below the surface. Surface measurements are made with the following: (a) geophones that sense the velocity of motion, (b) accelerometers, and (c) linear voltage differential transformers (LVDT) that measure displacement. Measurements below the surface are made with all of the same sensors, but the loading methods may include moving traffic.

The Benkelman Beam, the LaCroix Deflectograph, and the Curviameter apply static or slow moving loads. Vibratory loads are applied by the Dynaflect, the Road Rater, the Corps of Engineers 71-kN (16-kip) Vibrator, and the Federal Highway Administration’s Cox Van. “Near field” impulse loads, a term which will be explained subsequently, are applied by the Dynatest, KUAB, and Phoenix falling weight deflectometers. Small-scale impulse test devices include Loadman (19), German Dynamic Plate Bearing Test (GBP) (20), and TRL Foundation Tester (TFT) (21). “Far field” impulse loads are applied by the impact devices used in Spectral Analysis of surface wave technique. Wave propagation is used by the Shell Vibrator, which loads the pavement harmonically and sets up standing surface waves, the peaks and nodes of which are found by using moveable sensors.

2.2.1 Deflection Analysis Methods

The analytical methods covered in this review are categorized as follows: (a) closed-form multilayered solution, (b) backcalculation of moduli, and (c) impulse methods for near-field measurements.

2.2.1.1 Closed-Form Multilayered Solution

The first closed-form, multilayer solution for the backcalculation of layer moduli was developed by Hou (22). The central feature of this method was the least squares method

(Newton method) used for searching for the set of moduli that will reduce the sum of the squared differences between the calculated and measured deflections to a minimum. An algorithm based on the modified Newton method was employed by Harichandran et al. (23) to obtain the least squares solution of an over-determined set of equations. The algorithm was implemented in a new backcalculation program named MICHBACK.

Another closed-form solution makes use of Odemark's assumption (24), which was developed for the purpose of estimating surface deflections of multilayered pavements. According to Odemark, the deflection of a multilayered pavement with moduli, E_i and layer thickness, h_i , may be represented by a single layer thickness, H , and a single modulus, E_0 , if the thickness is chosen to be:

$$H = \sum_{i=1}^m C * h_i * \left(\frac{E_i}{E_0} \right)^{1/3} \quad (2.1)$$

where, C = a constant, approximately 0.8 to 0.9

This useful assumption makes it possible to use the Boussinesq theory for a one-layer to estimate stresses, strains, and displacements in the half-space, which are assumed to occur in the real multilayered pavement at the same radius and at the depth corresponding to the transformed depth where they were calculated.

An equivalent layer method of special mention here is the one developed by Ullidtz (25), which permits the use of a stress-softening nonlinear stress-strain relation in the subgrade. Calculations of rutting and fatigue life of test pavements, using strains and deflections computed using this method, have proven to be realistic. Backcalculation of layer moduli also appears to give reasonable results for pavements in which the layer decreases in stiffness with depth.

2.2.1.2 Backcalculation of Moduli

Backcalculation procedure is widely employed for analyzing deflection data from FWD. There are three general techniques into which these methods may be grouped.

1. There is a traditional backcalculation technique that matches measured deflections against those calculated from theory. Some of the programs that make use of this technique include EVERCALC (26), MODCOMP (27), and WESDEF (28).
2. A pattern search technique is employed in MODULUS (29) to obtain a match between measured and calculated deflections.
3. BOUSDEF (30) and ELMOD (31) are examples of a technique based on an equivalent layer method.

The traditional backcalculation technique uses deflection test conditions (i.e., load, plate geometry, layer thicknesses) and estimated layer moduli to generate a theoretical deflection basin. The theoretical deflections are compared with the measured deflections, and the error is computed. If the error is not within a specified tolerance, the process is repeated with revised layer modulus values until the two deflection basins are considered to be sufficiently close or until the modulus for any given layer reaches a given limit.

2.2.1.3 Impulse and Response Analysis Methods in the Near Field

When the falling weight drops to a pavement surface, an impulse generates body waves and surface waves. The geophone sensors pick up the vertical velocity of the pavement surface, and a single analog integration of the signal produces the deflection versus time trace. *Figure 2.1* shows a typical set of force versus time impulses and deflection versus time responses. Usually these signals are used to extract the maximum force and the maximum deflection from each geophone and to print them out for analysis by elastic methods. But, there is much more useful

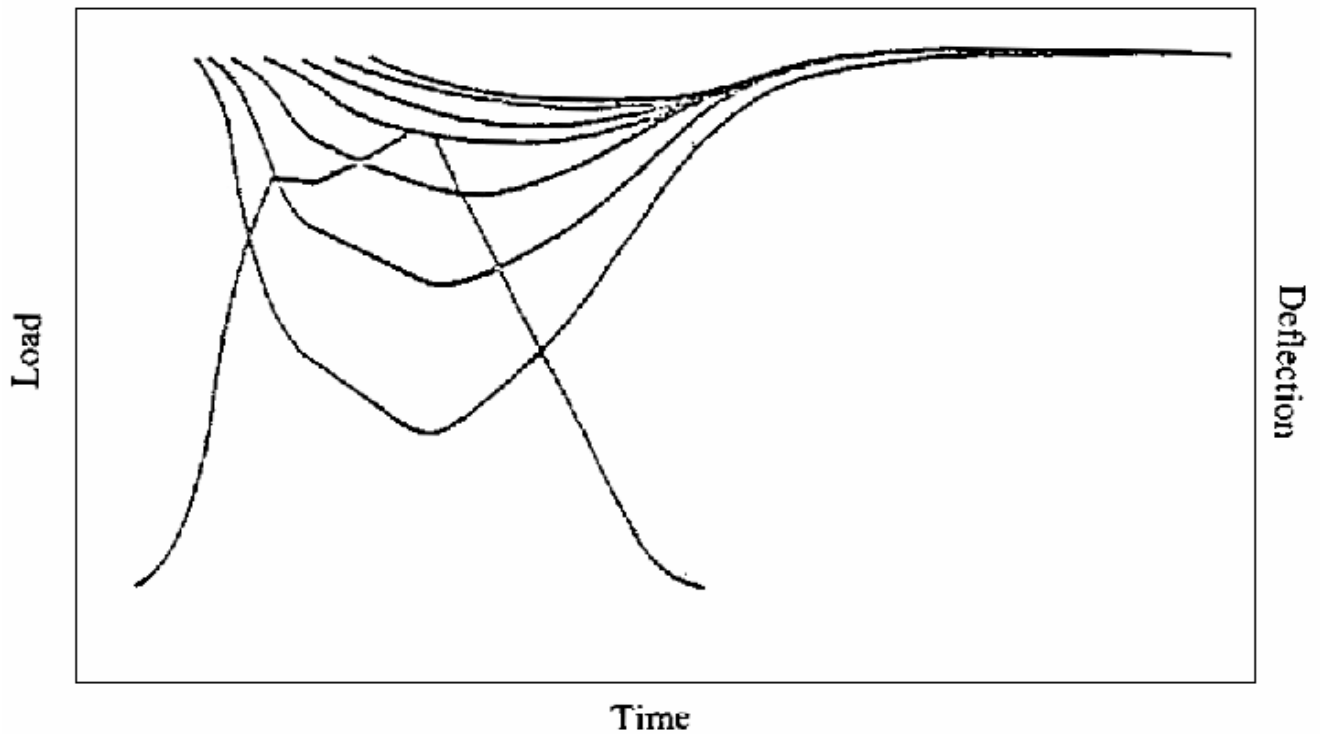


Figure 2.1 Typical FWD Load Impulse and Geophone Response With Time

information in these signals than simply their maxima.

One method of tapping this additional information is to perform a Fast Fourier Transform on the force-time impulse and on each deflection-time response. The transform breaks up a signal into its component frequencies and produces a complex number for each frequency, $a(f) + ib(f)$. The magnitude of this complex number is $(a^2 + b^2)^{1/2}$, and the phase angle, Φ , ($\text{arc tan } (b/a)$). If the transform of the deflection signal is divided, frequency-by-frequency, by the transform of the load impulse, the result is a transfer function, which is also a complex number and a function of frequency. A graph of the magnitude for typical transfer functions is shown in *Figure 2.2* for the geophones placed 1, 3, and 5 ft (0.3, 0.9, and 1.5m) from the center of the loaded area. In *Figure 2.2*, the magnitude is the deflection per unit of force at each frequency.

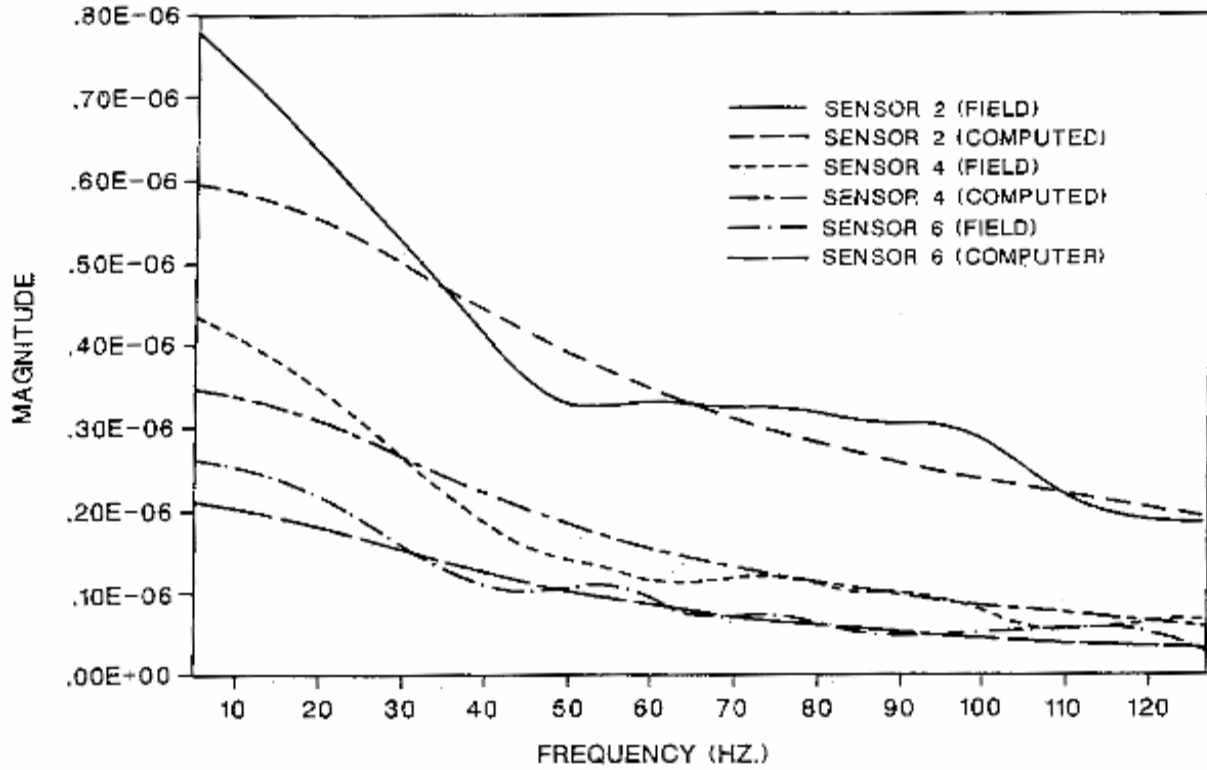


Figure 2.2 Frequency Response Function

2.3 NONLINEAR CHARACTERIZATION OF SUBGRADE (UNBOUND MATERIAL)

Ever since resilient modulus officially replaced earlier design parameters such as soil support value, its nonlinear behavior has been recognized. Ullditz (25) asserted that the difference between field modulus and laboratory modulus can be overcome by treating the subgrade as a nonlinear material. Over the years, numerous models have been proposed, a brief review of which follows:

$$M_R = k_1 \left(\frac{\sigma_d}{p_a} \right)^{k_2} \quad (\text{Moossadeh and Witczak (32)}) \quad (2.2)$$

$$M_R = k_1 \left(\frac{\sigma_3}{p_a} \right)^{k_2} \quad (\text{Dunlap, (33)}) \quad (2.3)$$

$$M_R = k_1 \left(\frac{\theta}{p_a} \right)^{k_2} \quad (\text{Seed et al. (34)}) \quad (2.4)$$

where σ_d = deviator stress;

σ_3 = confining pressure;

θ = bulk stress;

p_a = atmospheric pressure; and

k_1, k_2 = regression constants.

May and Witzak (35) and Uzan (36) proposed another model

$$M_R = k_1 \left(\frac{\theta}{p_a} \right)^{k_2} \left(\frac{\sigma_d}{p_a} \right)^{k_3} \quad (2.5)$$

An expanded version of *Equation 2.5*, that has been used is,

$$M_R = k_1 p_a \left[\frac{\theta - 3k_6}{p_a} \right]^{k_2} \left[\frac{\tau_{oct}}{p_a} + 1 \right]^{k_3} \quad (2.6)$$

where τ_{oct} = octahedral shear stress = $\frac{1}{3} [(\sigma_1 - \sigma_2)^2 + (\sigma_2 - \sigma_3)^2 + (\sigma_3 - \sigma_1)^2]^{1/2}$

Coefficient k_1 is proportional to Young's modulus. Thus, the values for k_1 should be positive since M_R can never be negative. Increasing the volumetric stress (θ) should produce a stiffening or hardening of the material, which results in a higher M_R . Therefore, the exponent k_2 of the bulk stress term for the above constitutive equation should also be positive. Coefficient k_6 is intended to account for pore water pressure or cohesion and is a measure of the material's ability to resist tension. The values for k_6 are expected to be negative or, when positive, less than or equal to a third of the bulk stress. Coefficient k_3 is the exponent of the octahedral shear stress term, and

its value should be negative since increasing the shear stress will produce a softening of the material, i.e., a lower M_R . Having found k_6 to be zero (37), it is deleted from Equation 2.6, and the resulting equation is recommended in the 2002 AASHTO Guide. Table 2.1 presents a summary statistic of k_1 , k_2 and k_3 compiled from the LTPP materials test program. Note $k_6 = 0$. Table 2.1 shows that the median value for coefficient k_2 increases as the amount of fines in the material/soil decreases (fine grain soils to unbound aggregate base material). Similarly, the median value for k_3 becomes more negative as the material/soil becomes more fine-grained. Von Quintus et al. (37) reported that in some unbound base materials and coarse grain soils, k_3 tends to become zero. It is interesting to note that the regressed k -coefficients from the LTPP- M_R test results are consistent with previous experiments.

Table 2.1 Summary of the Median and Mean Values for Each Coefficient of Constitutive Equation 2.6 for Subgrade Soils, $k_6 = 0$ (37).

Coefficient		Material/Soil Group	
		Coarse-Grained Soils	Fine-Grained Soils
k_1	Median	0.764	0.804
	Mean	0.802	0.896
	Standard Deviation	0.266	0.313
k_2	Median	0.446	0.243
	Mean	0.452	0.282
	Standard Deviation	0.193	0.155
k_3	Median	-1.052	-1.399
	Mean	-1.140	-1.576
	Standard Deviation	0.736	1.101
Number of Tests		257	105

Yet another model, proposed by Ni et al. (38), takes the following form:

$$M_R = k_1 \left(\frac{\sigma_3}{p_a} + 1 \right)^{k_2} \left(\frac{\sigma_d}{p_a} + 1 \right)^{k_3} \quad (2.7)$$

A recent LTPP study (39) included an additional power term to the universal model of Uzan,

$$\log \left(\frac{M_R}{p_a} \right) = k_1 + k_2 \log \left(\frac{\theta}{p_a} \right) + k_3 \log \left(\frac{\tau_{oct}}{p_a} \right) + k_4 \left(\log \left(\frac{\tau_{oct}}{p_a} \right) \right)^2 \quad (2.8)$$

According to the authors, there is a reasonably strong trend for the TP46 results to be somewhat nonlinear for the log octahedral shear stress term. Nonlinear behavior of log bulk stress, however, is not as common, but does exist in some cases.

2.4 RELATION BETWEEN RESILIENT MODULI, M_R , AND FWD MODULUS, E_{back} OR E

The results of comparison overwhelmingly suggest that the laboratory resilient modulus is less than that determined from backcalculation, E_{back} . The AASHTO Guide (2) asserted that laboratory modulus is only a third of that determined from in situ deflection of pavements. Other researchers, for example, Daleiden (40), Akram (41) and Nazarian (42) could not identify a unique relationship between moduli from laboratory and field tests. Having failed to establish a meaningful relationship between laboratory and backcalculated moduli, Von Quintus and Killingsworth (43) recommended correction factors (see *Table 2.2*) to be used with the AASHTO Design Guide. Based on the comparison study performed in regard to the WESTRACK road test, Seed et al. (16) asserted that their findings were enough to support the consensus that laboratory and NDT-based backcalculated moduli do not agree.

Whereas all of the above investigations relied on FWD measurements on pavement surface, only a few investigations had conducted the FWD test directly on the subgrade surface. In their study of the Minnesota Research Road Project (Mn/ROAD), difficulties were

encountered in analyzing FWD measurements performed directly on a subgrade surface (17). Their results showed weak correlation between laboratory and backcalculated moduli. Yet another attempt to estimate resilient modulus via subgrade deflection testing and Boussinesq

Table 2.2 AASHTO Modulus Correction Values From Long-term Pavement Performance Sections (43). (Backcalculated value shall be multiplied by correction factor to get resilient modulus)

Layer Type and Location	C-Value, Correction Factor
Granular base/subbase under PCC	1.32
Granular base/subbase under AC	0.62
Granular base/subbase between stabilized layer and AC	1.43
Subgrade soils under stabilized subgrade	1.32
Subgrade under full-depth AC or PCC	0.52
Subgrade under granular base/subbase	0.35

Note: PCC, Portland cement concrete; AC, asphalt concrete

equation was made in the Virginia test road (14). Elastic modulus was calculated employing Equation 2.9.

$$E_0 = \frac{2(1-\nu^2)\sigma_0 a}{d_1} \quad (2.9)$$

where E_0 = subgrade resilient modulus;

σ_0 = (peak) pressure of FWD impact load under loading plate;

a = radius of FWD loading plate

d_1 = (peak) center FWD deflection; and

ν = Poisson's ratio

The one-to-one relation between elastic modulus and resilient modulus, turned out to be weak.

In a recent study completed for MDOT, twelve finished subgrades were tested for deflection employing FWD. As the subgrade exhibited three layers, indicated by the Dynamic Cone Penetrometer (DCP), modulus of those layers were backcalculated using MODULUS 5.0.

Shelby tube samples from the twelve sections were tested in accordance with TP-46, and the resulting M_R showed satisfactory agreement with the backcalculated value E_{back} (7, 15). However, E_{back} of the same sections increased, 40 and 100 percent for fine- and coarse-grain soil, respectively, upon completion of pavement construction and deflection measurements conducted on top of the pavement.

2.4.1 Small-Scale Devices for Measuring Elastic Stiffness and Its Relation to FWD

Modulus

There are an increasing number of small-scale dynamic plate test devices available, which reportedly measure elastic stiffness modulus of foundation material: Loadman (19), German Dynamic Plate Bearing Test (GDP) (20), and TRL Foundation Tester (TFT) (21). Shahid (44) compared results from field tests to suggest the following stiffness relationship, $TFT = 0.9 FWD$ and $GDP = 0.6 FWD$, and with very significant scatter. To account for large variability, it would appear prudent to carry out many tests and apply some form of statistical analysis to come up with a representative value. As discussed earlier, the Dynamic Cone Penetrometer, a penetration device introduced in the 1960s for pavement evaluation, is another device that has been employed for characterization of subgrade soils, again via a correlation between laboratory M_R and DCP index (4, 7, 15).

2.5 RELATION BETWEEN M_R AND E: A CRITIQUE

In comparing laboratory M_R and in situ modulus, for example, back-figured from deflection studies, it is important to recognize spatial variability as well as variability in the vertical direction. No doubt, spatial variability would have strong influence on in situ modulus, as the test encompasses a large volume of material, and, therefore, a large variation. What follows is a discussion of important factors that could result in the two moduli – laboratory M_R

and in situ modulus – being different, nonetheless, portraying the basic stiffness characteristics of the material being tested.

Besides variability in the prepared subgrade, there are fundamental differences in the procedural aspects of the two test methods, yielding different moduli at a given location. Possible causes of difference in the moduli are briefly explained herein. First, different volumes of material are tested in the laboratory and in the field. Accordingly, the size effect phenomenon should result in the laboratory modulus being larger than the field modulus, provided the material tested is “homogeneous.” Second, the confinement in TP46 protocol is generated by compressed air, whereas in the field it is due to self-induced passive earth pressure. Air medium is compressible and, therefore, the laboratory sample is vulnerable to relatively large lateral and, in turn, increased axial deformation with the laboratory test resulting in smaller resilient modulus as compared to backcalculated field values. While these two factors are recognized as influencing the resilient moduli, their quantification is somewhat obscure at this time. It could be that the effects of those factors offset each other while averaging the results for some length of a subgrade.

While testing material compacted in the field (employing either static or vibratory rollers), residual stress becomes an issue. It has been documented that vertical compaction – especially under a roller compactor – causes lateral stress to increase with only partial recovery when the roller “walks out.” The stress remaining, otherwise known as residual stress, has a profound effect on the deflection tests in situ, whereas it has minimal effect on Shelby tube samples. Residual stresses are partially removed when the sample is being extruded from the thin wall tube, an explanation for residual stress being not significant in TP46 samples. That the residual stress, fully operational in material in situ, could cause the resulting modulus to be larger

than that obtained from tube sample in which residual stress is practically nonexistent.

The stress-dependent nonlinearity of subgrade soil is yet another factor that influences a realistic comparison of the two sets of values. The laboratory sample being of finite size, the stress state is practically uniform for induced triaxial stress state. Besides, in the laboratory test only resilient deformation is measured and used in resilient modulus calculation. Whereas in FWD test the stress distribution is uniform neither in the vertical nor in the horizontal directions. More important, total deflections are monitored in contrast to the resilient deformation in the FWD test. The effect of nonlinearity alone, therefore, could likely bring about a decrease in FWD modulus, in relation to TP46 resilient modulus.

Another important factor is the dynamic effect of FWD loading. For example, the deflection of the bearing plate is out of phase (in time) with the maximum applied contact stress, and this phase difference becomes exaggerated for the largest bearing plate inertia and stiffest damper. Also, with the dynamic test (for example, FWD), stress in the material under testing extends to proportionally a larger depth, i.e. produces a more elongated pressure bulb. What it amounts to is that utilizing conventional static load theory for interpretation of dynamic deflection is inconsistent and will tend to underestimate the actual stiffness modulus (45).

With several factors influencing laboratory and in situ moduli in a rather complicated manner, it is unlikely that they exhibit a one-to-one relation. More on this will be presented in Chapter 4, while discussing the test results.

2.6 CONCLUSION

The AASHTO Pavement Design Guide as well as the 2002 Mechanistic Pavement Design Guide require that resilient modulus of subgrade be the parameter for characterizing subgrade. The complexity of the laboratory resilient modulus test has prompted highway

engineers to explore nondestructive test methods, especially the deflection test by FWD. The literature includes numerous studies evaluating FWD-based backcalculated modulus of in-service pavements and relating it to resilient modulus. In regard to characterizing a subgrade with FWD deflection test for new pavement design, again, in situ modulus must be correlated to laboratory resilient modulus. Studies of this type are few, however.

There seems to be hardly any consensus as to the relation between FWD-based modulus and laboratory resilient modulus. Besides presenting a comprehensive review of studies related to this topic, this chapter critiques why elastic modulus not necessarily showing a one-to-one relation with laboratory resilient modulus.

CHAPTER 3

EXPERIMENTAL WORK AND DATA COLLECTED

3.1 INTRODUCTION

With the primary objective of deriving a relationship between FWD-based modulus and resilient modulus determined from TP46, field tests were programmed in several finished subgrades – ten test sections mostly 200 ft. (61 m) long – whose soil properties reflect typical soils of Mississippi. *Table 3.1* presents a summary of various tests, including the location and test dates. Automatic Dynamic Cone Penetrometer (ADCP) tests were performed, determining homogeneity of subgrade, especially the top 3 ft. (910 mm) or so, because deflection analysis needs to be tailored accordingly. Field density and moisture were determined to assess the degree of compaction, which may affect in situ modulus. With provision to directly measure modulus, Geogauge served as an alternate to determine in situ modulus. Shelby tube samples retrieved during field tests were transported to the MDOT laboratory in Jackson, MS, to be tested for resilient modulus in accordance with TP46 protocol. What follows is a description of each field test, the data collected, and preliminary analysis corroborating the field data.

3.2 FIELD TESTS

3.2.1 FWD Test On Prepared Subgrade and Modulus Calculation

Ten as-built test sections reflecting typical soils throughout the State of Mississippi were selected and tested (see *Table 3.1*). The Mississippi Department of Transportation (MDOT) FWD was used for the deflection testing discussed in this study. The testing pattern for each section was designed for a series of nine test stations located longitudinally at 25 ft. (8m) intervals with a few exceptions. Typical deflection basins of one station of each test section can be seen in *Appendix A*.

Table 3.1 Summary Section Locations and Tests Performed

Section #	County/Road	Date Tested	Section Length, (ft)	Tests Performed
1	Montgomery/ US 82W	04/17/02	200	FWD ^a , ADCP ^b , Geogauge Nuclear Moisture & Density
2	Coahoma/ US 61N	04/18/02	500	FWD, ADCP, Geogauge Nuclear Moisture & Density
3	Coahoma/ US 61N	04/18/02	200	FWD, ADCP, Geogauge Nuclear Moisture & Density
4	Montgomery/ US 82W	05/21/02	200	FWD, ADCP, Geogauge Nuclear Moisture & Density
5	Montgomery/ US 82W	05/21/02	200	FWD, ADCP, Geogauge Nuclear Moisture & Density
6	Hinds/ Norrell W	05/22/02	200	FWD, ADCP, Geogauge Nuclear Moisture & Density
7	Wayne/ US 45N	06/12/02	200	FWD, ADCP, Geogauge Nuclear Moisture & Density
8	Wayne/ US 45N	06/12/02	200	FWD, ADCP, Geogauge Nuclear Moisture & Density
9	Wayne/ US 45N	06/12/02	200	FWD, ADCP, Geogauge Nuclear Moisture & Density
10	Madison/ Nissan W. Parkway	08/26/02	200	FWD, ADCP, Geogauge Nuclear Moisture & Density

^aFWD – Falling Weight Deflectometer

^bADCP – Automated Dynamic Cone Penetrometer

1 ft = 0.3048 m

For all of the tests, the nominal 18-in. (450-mm) and 12-in. (300-mm) diameter plates were used; except, in section #1 where only the 18-in. (450-mm) plate was employed (see *Table 3.2*). For measuring surface deflection, velocity transducers were located at the center of the plate and at offset distances of 8 in. (200 mm), 12 in. (305 mm) 18 in. (457 mm), 24 in. (610 mm), 36 in. (914 mm), 48 in. (1214 mm) and 60 in. (1524 mm) from the center. Other

Table 3.2 Summary of FWD Tests Using Two Plate Sizes and Two Sensor Tips

Section #	FWD tests	
	12-in. load plate	18-in. load plate
1	-	X ^a
2	X ^a	X ^a
3	X ^a	X ^a
4	X ^b	X ^b
5	X ^b	X ^b
6	X ^b	X ^b
7	X ^{ab}	X ^b
8	X ^{ab}	X ^b
9	X ^{ab}	X ^b
10	X ^b	X ^b

^a 10mm sensor tip

^b 16mm sensor tip

1 in. = 25.4 mm

modifications in the test equipment included replacing the 0.4 in. (10 mm) transducer tips with large 0.6 in. (16 mm) tips to investigate the effect of tip size on deflection. Large tips were employed in sections 4 through 9. In sections 7, 8, and 9, employing the 12-in. (300-mm) plate, two series of tests were performed, one with a 0.4 in. (10 mm) tip followed by a 0.6 in. (16 mm) tip. Section 10, set aside for model verification, was tested with both plates, each time installing the large tip. Various combinations of plate sizes and tips can be seen in Table 3.2.

All of the tests were conducted with the light load package of the FWD. Two seating loads, approximately 1700 lbs. (7.6 kN) each, followed by two load drops at four different drop heights, generated four different loads, ±1700 lbs (7.6 kN), ±2,500 lbs (11.2 kN), ±3,200 lbs (14.3 kN) and ±4,300 lbs (19.3 kN). The repeat readings of loads and deflections were averaged before calculating modulus.

In cases where the station was unsuitable for testing due to loose surface material, wheel ruts, or other reasons, the surface was leveled to eliminate as far as possible erratic sensor deflections. Some sections were bladed and re-compacted before FWD testing to ensure surface smoothness. Nonetheless, debris and improper sensor seating resulted in a few sporadic deflection basins.

By necessity, sensor deflections with negative slope were excluded from the analysis. These erroneous deflections might be due to unevenness of the soil surface attributable to either a soft layer or debris at the surface. It could also be due in part to spatial variation resulting in soft pockets along the road leading to punching of the sensor tip. Abnormal deflections due in part to plate vibration and/or soft surface layers, were critically reviewed prior to data analysis.

3.2.1.1 Modulus from FWD Deflection Data

Researchers in previous studies employed a backcalculation routine for deriving subgrade modulus from deflection data ([15](#), [17](#)). The Minnesota Test Road Program adopted EVERCALC, and Mississippi researchers used MODULUS 5.1. One reason for resorting to backcalculation in the Mississippi study stems from the fact that subgrades exhibited layering, as determined by Dynamic Cone Penetrometer tests. The layering observed was more due to moisture fluctuations and lack of confinement at the surface than due to material variation. Invariably, the top 6 to 12 in. (152 to 305 mm) of the material remained at a lower moisture content than the underlying material. In this study, side-by-side Automated DCP (ADCP) tests had detected a desiccated layer at the top, on average 12 in. (305 mm) deep.

A few deflection basins were analyzed and modulus backcalculated employing MODULUS 5.1. Two- and three-layer analyses were attempted; however, three-layer analysis is discouraged because second-layer modulus is always much smaller and third-layer modulus is

Table 3.3 Backcalculated Moduli Based on FWD Deflection Basin, Section # 1

Station	Backcalculated Moduli, psi	
	Layer 1	Layer 2 (Semi-infinite)
852+50	10000	15500
853+00	10000	15000
853+50	8000	15700
853+75	7000	18000
854+00	5000	14900
854+25	6000	14200
854+50	5000	18300

1 psi = 6.89 kPa

relatively larger (15). The results presented in *Table 3.3*, compared with the DCP Index (DCPI) of corresponding layers, show good correspondence between the backcalculated modulus and DCPI. The backcalculation methodology often posed problems of non-uniqueness, demanding several trial-and-error calculations, which become time consuming. Also, a question arises as to selecting a design modulus from the two values with a two-layer assumption. The idea of selecting the most conservative value for design was rejected for the reason that this approach often leads to conservative design driving up the cost. The average of the two values does not seem appropriate either.

To reiterate, a representative/unique modulus value characterizing the entire subgrade is required for pavement design. Such a modulus can alternately be estimated from the load and deflection data using the Boussinesq solution for a uniformly distributed load on the surface of an isotropic, elastic half-space. Equations with distributed load and concentrated load will be employed. Two equations adopted for calculating elastic modulus, E , from sensor deflections

are: one using the first sensor (peak) deflection and the other utilizing any other offset sensor deflection. Respectively, they are:

$$E_1 = \frac{2(1-\nu^2)\sigma_0 a}{d_1} \quad (2.9)$$

$$E_r = \frac{(1-\nu^2)\sigma_0 a^2}{rd_r} \quad (3.1)$$

where E_1 = “surface” or composite modulus of the subgrade beneath the load plate;

E_r = “surface” or composite modulus of the subgrade beneath offset sensor;

ν = Poisson’s ratio, suggested value 0.4 to 0.45;

σ_0 = (peak) pressure of FWD impact load under loading plate;

a = radius of FWD loading plate;

d_1 = (peak) center FWD deflection;

d_r = (peak) FWD deflection at offset distance r ; and

r = distance of sensor where d_r is registered.

Note that *Equation 3.1* is derived for a concentrated load. If d_r is a reasonably large distance from the edge of the plate, however, the point load equation (that is, *Equation 3.1*) can be justified for the FWD test where the load is, in fact, distributed uniformly over the plate. The modulus calculated employing exact equation for each offset deflection is now compared with that employing *Equation 3.1* (see *Table 3.4*), to note that both equations result in practically the same moduli, except that from the second sensor deflection. Therefore, *Equation 3.1* will be used in place of the exact equation, which can be seen in Harr (47).

Now the research has two options: multilayered backcalculation approach or direct forward calculation. A Minnesota study concluded that the multilayered backcalculation

Table 3.4 Comparison of Modulus (Expressed As A Ratio) Calculated for Offset Sensors Employing Equation 3.1, and Exact Equation with Distributed Loads

Modulus Calculation	Sensor Distance, in.					
	12	18	24	36	48	60
$E \times d_r / \sigma_o \times a$ <u>Concentrated load equation</u>	5.4	3.37	2.53	1.68	1.26	1.01
$E \times d_r / \sigma_o \times a$ <u>Distributed load equation</u>	4.86	3.49	2.58	1.69	1.27	0.99

σ_o – distributed load

d_r – sensor deflection at radial distance r

a – radius of the loaded area

E – modulus of homogeneous layer

1 in. = 25.4 mm

approach does not provide any advantage in interpreting FWD deflection from subgrade testing relative to the homogeneous approach (17). Concurring with this premise, *Equations 2.9 and 3.1* were employed for calculating elastic modulus corresponding to each sensor location. These values have been subjected to checks for outliers. For detecting spurious readings plot of moduli vs. sensor distance is prepared and moduli values “way” off the general pattern are deleted. A typical section data of elastic moduli of all nine stations, with four load drops in each station, is shown in *Table 3.5* with the outliers, if any, identified. The remaining moduli (maximum of four) for each sensor are averaged for the 18-in. plate (450-mm) and reported in *Tables 3.6 to 3.15*. A similar tabulation of test results with the 12-in. (300-mm) plate is presented in *Tables 3.16 to 3.24*. Outliers amongst the station averages for each section are now identified by *Cheavnaut’s Criterion (46)*, and the section average of each sensor is now listed in the last row in each table. Graphical representation of elastic moduli, calculated from seven sensor deflections and averaged over four loads, for two typical test stations, can be seen in *Figures 3.1.a and 3.1.b*. *Figure 3.1.a* depicts moduli variation for a soft-over-stiff profile where we note

Table 3.5 Elastic Moduli For All Four Load Drops For Nine Stations of Section # 4

Station	Load, lbs	Elastic Moduli, psi						
		E ₁	E ₂	E ₃	E ₄	E ₅	E ₆	E ₇
905+50	1741	13703	12870	21237	23264	24100	23338	24379
	2473	13673	11905	20603	22579	24768	22776	23543
	3273	13881	11613	20139	22510	24849	22657	23304
	4355	13984	11319	20098	22391	24405	22610	23354
905+75	1618	11498	19610	26034	27089	26877	27414	26360
	2362	10872	18634	25174	26333	28030	27491	27415
	3113	10719	17843	24693	26267	30105	26163	26372
	4233	10682	17358	24852	26604	30340	27334	26964
906+00	1753	16728	21341	26265	28346	28292	27104	28564
	2535	16150	20413	26030	28406	30332	27115	27889
	3223	15578	19313	25077	27752	28806	26878	27866
	4306	15274	18983	25496	28152	29518	27640	27851
906+25	1760	35371	23853	30394	31992	23330	27205	35496
	2535	33393	25087	32686	32937	27962	31956	31123
	3359	32677	25321	31623	32195	33641	31764	29647
	4528	31736	26901	32537	32182	33127	31341	30206
906+50	1704	8986	28477	32851	32084	37020	31942	26492
	2510	8737	27471	33751	32813	35087	32022	27614
	3248	8567	26823	33726	32453	31852	32150	27248
	4441	8577	26954	34938	33717	33717	32216	29397
906+75	1772	16391	17179	24961	28116	30893	30516	28064
	2571	13525	16305	24285	27786	32130	30256	26246
	3310	12163	15754	23967	27930	33623	29455	26963
	4491	11291	15658	24674	28737	32189	30293	27571
907+00	1722	24028	21241	25805	27848	29842	26246	26293
	2498	19193	19594	23911	26584	29148	24954	24896
	3298	17794	19137	23758	26660	29472	26259	26609
	4368	16181	18265	23407	26738	29370	26894	26433
907+25	1771	14361	20447	24827	28000	30319	30754	29427
	2547	12673	18604	23280	26842	27456	24978	27317
	3334	12501	18178	23482	26550	27859	26751	27162
	4466	12138	17567	22975	26205	26952	25707	26278
907+50	1845	15756	14463	20763	23060	25673	25056	22177
	2621	13848	13706	19789	22293	24346	24561	23129
	3334	12675	13176	19296	22349	23899	24021	23346
	4478	11898	12958	19398	22967	24416	24574	23714

1 psi = 6.89 kPa

1 lb = 4.448 N

Table 3.6 Summary of Elastic Modulus Calculated from FWD Sensor Deflections Using 18-in. (450-mm) Plate, Montgomery County, Section # 1

Station	Modulus, psi							
	E ₁	E ₂	E ₃	E ₄	E ₅	E ₆	E ₇	Ave. E ₃₋₅
852+50	2837	3882	9464	13685	17694	16909	17096	13614
853+00	4099	4084	7883	11662	16364	15361	17183	11970
853+50	3376	4479	8853	15102	18890	17002	15467	14282
853+75	3090	5722	13282	22393	20483	18776	18851	18719
854+00	2717	3199	11912	18793	17737	15672	15045	16147
854+25	5938 ^a	6268 ^a	12119	16463	16473	16286	13678	15018
854+50	3336	NA	NA	NA	22736	18307	18039	22736 ^a
Average	3240	3560	10590	14010	18630	16900	16480	14410

^a Outlier according to Chauvenet's criterion

NA - Data not available

1 psi = 6.89 kPa

Table 3.7 Summary of Elastic Modulus Calculated from FWD Sensor Deflections Using 18-in. (450-mm) Plate, Coahoma County, Section # 2

Station	Modulus, psi							
	E ₁	E ₂	E ₃	E ₄	E ₅	E ₆	E ₇	Ave. E ₃₋₅
54+00	19870	14757	13201	13249	14782	14057	13825	13744
54+50	6661	23346 ^a	18043	16409	17638	16794	16122	17363
55+00	5608	15020	16771	15417	15396	14544	13778	15861
55+50	15733	14019	15465	15295	15660	14924	14681	15473
56+00	10227	7717	9240	9399	10461	10786 ^a	11589 ^a	9700
57+25	12606	11803	12012	12650	12485	12722	13286	12382
57+50	11531	13747	14576	14749	15466	15149	14843	14930
58+00	5004	7860	9061	9904	12306	14852	14892	10423
58+50	7843	11012	12631	12741	13756	13096	13720	13043
Average	10570	11990	13440	13310	14220	14520	14390	13660

^a Outlier according to Chauvenet's criterion

1 psi = 6.89 kPa

Table 3.8 Summary of Elastic Modulus Calculated from FWD Sensor Deflections Using 18-in. (450-mm) Plate, Coahoma County, Section # 3

Station	Modulus, psi							
	E ₁	E ₂	E ₃	E ₄	E ₅	E ₆	E ₇	Ave. E ₃₋₅
152+00	7079	10298	17702	16900	20325	19963	17688	18309
152+25	10733	12073	22007	22066	20244	17719	18965	21439
152+50	9027	10461	17963	17810	20104	19463	16281	18626
152+75	7037	11317	17672	19277	19192	18443	18176	18713
153+00	8391	10712	15730	14474	17562	13945	15394	15922
153+25	8089	11426	16347	18037	16059	16026	15387	16814
153+50	6999	13667	20776	16840	18664	17275	14794	18760
153+75	7127	19830 ^a	17045	16204	15456	13870	13178	16235
153+90	3805 ^a	4922 ^a	6599 ^a	8204 ^a	7937 ^a	8150 ^a	7252 ^a	7580 ^a
Average	8060	11420	18160	17700	18450	17090	16230	18100

^a Outlier according to Chauvenet's criterion

1 psi = 6.89 kPa

Table 3.9 Summary of Elastic Modulus Calculated from FWD Sensor Deflections Using 18-in. (450-mm) Plate, Montgomery County, Section # 4

Station	Modulus, psi							
	E ₁	E ₂	E ₃	E ₄	E ₅	E ₆	E ₇	Ave. E ₃₋₅
905+50	13810	11927	20520	22686	24531	22845	23645	22084
905+75	10942	17601	24773	26435	30223	26748	26668	25670
906+00	15932	20012	25717	28164	29237	27184	28042	26879
906+25	32206 ^a	26111	32080	32189	33384	31553	29926	28197
906+50	8572	26889	34332	33085	32785	32183	28322	33401
906+75	13736	16381	24640	28213	31737	30355	27293	32551
907+00	19299	19559	24220	26958	29458	26088	26058	27706
907+25	12320	17873	23229	26377	27405	26229	26720	27144
907+50	12807	13280	19494	22536	24220	24385	23396	22579
Average	13400	18850	25450	27410	29220	27510	26680	27360

^a Outlier according to Chauvenet's criterion

1 psi = 6.89 kPa

Table 3.10 Summary of Elastic Modulus Calculated from FWD Sensor Deflections Using 18-in. (450-mm) Plate, Montgomery County, Section # 5

Station	Modulus, psi							
	E ₁	E ₂	E ₃	E ₄	E ₅	E ₆	E ₇	Ave.E ₃₋₅
833+20	18439	28708	34459	36412	39496	39977	36445	36789
833+40	37643 ^a	29826	31156	32519	38273	38810	36196	33982
833+60	14822	20577	29307	34940	39836	38994	37702	34694
833+80	25028	23776	30193	33664	39952	41332	41754	34603
834+00	23231	18720	32326	35708	40583	44451	45887	36206
834+20	19915	29941	39362	48286	52387	51827	55853	46679
834+40	11031	12874	17907	24056	28596	28245	28857	23520
834+60	10756	17895	19452	19583	21395	20942	21233	20143
834+80	12129	11190	10241	10792	16158	16337	17513	12397
Average	16920	21500	27160	30660	35190	35660	35720	31000

^a Outlier according to Chauvenet's criterion

1 psi = 6.89 kPa

Table 3.11 Summary of Elastic Modulus Calculated from FWD Sensor Deflections Using 18-in. (450-mm) Plate, Hinds County, Section # 6

Station	Modulus, psi							
	E ₁	E ₂	E ₃	E ₄	E ₅	E ₆	E ₇	Ave.E ₃₋₅
25+00	12735	12788	14456	19749	21300	19945	19912	18501
25+25	16213	15308	15693	22583	21372	21547	19930	19883
25+50	12944	16079	15565	21397	21180	20282	18981	19381
25+75	11830	21176	17540	22424	24163	19446	18256	21376
26+00	12455	23505	17506	24431	23856	21408	20219	21931
26+25	14336	14481	14615	21809	21881	21622	20773	19435
26+50	11484	19233	15273	19098	19222	20349	19060	17864
26+75	9528	17075	13873	18148	19982	14533	17540	17334
27+00	NA	13480	10172 ^a	12185 ^a	11946 ^a	12070 ^a	14321 ^a	11434 ^a
Average	12690	17010	15570	21210	21620	19890	19330	19460

^a Outlier according to Chauvenet's criterion

1 psi = 6.89 kPa

Table 3.12 Summary of Elastic Modulus Calculated from FWD Sensor Deflections Using 18-in. (450-mm) Plate, Wayne County, Section # 7

Station ^a	Modulus, psi							
	E ₁	E ₂	E ₃	E ₄	E ₅	E ₆	E ₇	Ave.E ₃₋₅
6+500	22336	19071	20586	24106	27522	23971	26941	24071
6+507.5	21113	22156	25009	27039	28465	28259	30263	26838
6+515	27820	25423	26850	27699	29462	27872	30206	28004
6+522.5	25366	29899 ^b	30386 ^b	31808 ^b	33718	31859	34810	31971 ^b
6+530	20318	23116	24828	26547	28944	29624	30329	26773
6+537.5	20071	22406	23642	26453	32647	35604	35044	27581
6+545	20164	18079	21226	23976	29789	31641	30268	24997
6+552.5	33462	20600	24006	24864	28056	30211	31191	25642
6+560	32306	23697	22994	24055	26630	27488	27598	24560
Average	24770	21820	23640	25590	29470	29610	30740	26240

^a Stations in meters

^b Outlier according to Chauvenet's criterion

1 psi = 6.89 kPa

Table 3.13 Summary of Elastic Modulus Calculated from FWD Sensor Deflections Using 18-in. (450-mm) Plate, Wayne County, Section # 8

Station ^a	Modulus, psi							
	E ₁	E ₂	E ₃	E ₄	E ₅	E ₆	E ₇	Ave.E ₃₋₅
7+375	15605	23901	23274	24763	27381	23935	20123	25140
7+382.5	38756	31238	26577	28744	30311	26838	28015	28544
7+390	31966	22265	23064	24078	35238	28828	23568	27460
7+397.5	21672	13570 ^b	13994 ^b	24902	21764	19456	18785	20220 ^b
7+405	37187	23265	28232	29928	32349	32576	33830	30170
7+412.5	66572 ^b	33652	28867	27437	34454	33292	27742	30253
7+420	19971	21983	23507	29077	36428	36656	25764	29671
7+427.5	18752	25859	27048	27307	34085	32356	29253	29480
7+435	19162	27587	23586	27824	24028	28682	25603	25146
Average	25380	26220	25520	27120	30670	29180	25850	27770

^a Stations in meters

^b Outlier according to Chauvenet's criterion

1 psi = 6.89 kPa

Table 3.14 Summary of Elastic Modulus Calculated from FWD Sensor Deflections Using 18-in. (450-mm) Plate, Wayne County, Section # 9

Station ^a	Modulus, psi							
	E ₁	E ₂	E ₃	E ₄	E ₅	E ₆	E ₇	Ave.E ₃₋₅
7+375	20049	24150	40826	34919	32178	28178	28001	35975
7+382.5	36385	23641	21206	21145	30505	27326	25905	24285
7+390	58566 ^b	35235	31184	31130	32011	35188	34519	31442
7+397.5	43672 ^b	44734 ^b	38074	36346	37174	35959	36040	37198
7+405	27092	23208	23181	35239	32223	33198	29039	30214
7+412.5	53416 ^a	36647	32574	33411	34640	42536 ^a	31032	33542
7+420	31237	30004	26420	23968	31106	27004	27519	27164
7+427.5	26761	25411	21384	21570	26700	28483	25435	23218
7+435	42773 ^b	25702	23282	25386	26716	26972	25318	25128
Average	28310	28000	28680	29240	31470	30290	29200	29800

^a Stations in meters

^b Outlier according to Chauvenet's criterion

1 psi = 6.89 kPa

Table 3.15 Summary of Elastic Modulus Calculated from FWD Sensor Deflections Using 18-in. (450-mm) Plate, Madison County, Section # 10

Station	Modulus, psi							
	E ₁	E ₂	E ₃	E ₄	E ₅	E ₆	E ₇	Ave.E ₃₋₅
47+00	6999	8435	10647	11497	13466	12718	12394	11870
47+25	10513	6955	9348	10949	11283	11709	11146	10527
47+50	7931	6720	7360	7358	7646	6792	6945	7455
47+75	5812	5007	5244	4887	5529	5355	5502	5220
48+00	17994 ^a	10999 ^a	10695	9865	9136	9014	8256	9899
48+25	7918	7188	7969	7632	7646	6802	6282	7749
48+50	8337	5753	5268	5105	5272	5613	5336	5215
48+75	7350	4165	4009	4024	4903	5518	5284	4312
49+00	6066	4473	4704	4950	6348	6849	5837	5334
Average	7620	6090	7250	7360	7910	7820	7440	7510

^a Outlier according to Chauvenet's criterion

1 psi = 6.89 kPa

Table 3.16 Summary of Elastic Modulus Calculated from FWD Sensor Deflections Using 12-in. (300-mm) Plate, Coahoma County, Section # 2

Station	Modulus, psi							
	E ₁	E ₂	E ₃	E ₄	E ₅	E ₆	E ₇	Ave. E ₃₋₅
54+00	11712	14660	13203	13532	13895	14004	13847	13543
54+50	13152	22978	17182	15502	16131	15559	15290	16272
55+00	10691	19757	15451	14907	15837	15296	14722	15398
56+00	9710	9164	9100	9334	10196	10623 ^a	10760 ^a	9543
57+25	17567	15370	13442	13330	13183	13801	13652	13318
57+50	12656	14764	12664	12524	13072	13240	13044	12753
58+00	4157	7974	8988	10094	12440	14028	14502	10508
58+50	5400	15468	14073	12417	14660	13859	13594	13717
Average	10630	15020	13010	12710	13680	14260	14090	13130

^a Outlier according to Chauvenet's criterion

1 psi = 6.89 kPa

Table 3.17 Summary of Elastic Modulus Calculated from FWD Sensor Deflections Using 12-in. (300-mm) Plate, Coahoma County, Section # 3

Station	Modulus, psi							
	E ₁	E ₂	E ₃	E ₄	E ₅	E ₆	E ₇	Ave. E ₃₋₅
152+00	8823	20731	29281	26400	20618	19775	18417	25433
152+25	7594	26627	25089	24143	21845	17939	19034	23692
152+50	8788	22348	22357	21694	21477	20753	19564	21842
152+75	7440	24002	25517	24315	20965	19286	18860	23599
153+00	8685	11556	15432	17973	18656	16563	16060	17353
153+25	5934	36115	38164	30633	19021	15010	14217	29273
153+50	7581	23263	24514	23185	18503	16082	16226	22067
153+75	8110	19823	24216	23107	18892	16839	16572	22072
153+90	3540 ^a	5095 ^a	8591 ^a	11421 ^a	11267 ^a	10508 ^a	10444 ^a	10426
Average	7870	23060	25560	23930	20000	17780	17370	23170

^a Outlier according to Chauvenet's criterion

1 psi = 6.89 kPa

Table 3.18 Summary of Elastic Modulus Calculated from FWD Sensor Deflections Using 12-in. (300-mm) Plate, Montgomery County, Section # 4

Station	Modulus, psi							
	E ₁	E ₂	E ₃	E ₄	E ₅	E ₆	E ₇	Ave. E ₃₋₅
905+50	17548	19514	21832	23671	25840	23832	23516	23781
905+75	15569	23272	24821	24871	27579	27332	25183	25757
906+00	18125	24684	26617	27784	28888	28428	26668	27763
906+25	19332	21835	28971	27819	33766	27720	27704	30185
906+50	14827	32047	36459 ^a	36872 ^a	34725	33324	31750	36019 ^a
906+75	13032	20900	31552	31505	29816	29230	31231	30958
907+00	11734	18492	23971	23989	26687	26036	27289	24882
907+25	17754	18598	22950	23197	23860	21107	26832	23336
907+50	14014	18236	21361	22630	25762	26240	25394	23251
Average	15770	21950	25260	25680	28550	27030	27290	26500

^a Outlier according to Chauvenet's criterion

1 psi = 6.89 kPa

Table 3.19 Summary of Elastic Modulus Calculated from FWD Sensor Deflections Using 12-in. (300-mm) Plate, Montgomery County, Section # 5

Station	Modulus, psi							
	E ₁	E ₂	E ₃	E ₄	E ₅	E ₆	E ₇	Ave. E ₃₋₅
833+20	18787	30198	34536	35517	36343	37808	36770	35465
833+40	19376	25715	36710	35205	34754	30139	34012	35556
833+60	29413	22299	30209	31255	36176	35388	39322	32547
833+80	18856	23437	30263	33872	40964	41535	41345	35033
834+00	19839	24091	31678	33638	38259	40326	40838	34525
834+20	11180	22325	28427	33420	34746	36891	39850	32198
834+40	11218	16803	20822	22564	25827	21565	36196	23071
834+60	7426	15720	18999	18803	20368	19251	19097	19390
834+80	23266	8298 ^a	8657 ^a	11058 ^a	16026	17964	18694	11914 ^a
Average	17710	22570	28960	30530	31500	31210	34010	30330

^a Outlier according to Chauvenet's criterion

1 psi = 6.89 kPa

Table 3.20 Summary of Elastic Modulus Calculated from FWD Sensor Deflections Using 12-in. (300-mm) Plate, Hinds County, Section # 6

Station	Modulus, psi							
	E ₁	E ₂	E ₃	E ₄	E ₅	E ₆	E ₇	Ave.E ₃₋₅
25+00	8114 ^a	18446	19682	20924	20867	20672	19906	20491
25+25	16607	17068	20921	21762	21098	18757	19522	21261
25+50	15443	18214	19276	21363	17909	19140	17031	19516
25+75	17263	22129	24284	23591	22960	19389	18703	23612
26+00	14865	23080	23922	22770	23602	20330	20100	23432
26+25	14320	21701	20533	21480	20933	20223	18946	20982
26+50	15764	18575	20088	17851	20566	19198	18665	19502
26+75	13350	18111	18341	17617	19025	17550	16979	18328
27+00	13430	18661	16038	15235	13480 ^a	10026 ^a	13807 ^a	14918
Average	15130	19550	20340	20290	20870	19410	18730	20500

^a Outlier according to Chauvenet's criterion

1 psi = 6.89 kPa

Table 3.21 Summary of Elastic Modulus Calculated from FWD Sensor Deflections Using 12-in. (300-mm) Plate, Wayne County, Section # 7

Station ^a	Modulus, psi							
	E ₁	E ₂	E ₃	E ₄	E ₅	E ₆	E ₇	Ave.E ₃₋₅
6+500	29157	20933	24391	25974	27898	27330	28306	26088
6+507.5	27509	24587	26271	27550	30635	30453	31424	28152
6+515	38688	26522	25827	27626	30499	30749	31703	27984
6+522.5	46126 ^b	29858	30352 ^b	30913	32002	33338	34465	31089
6+530	28444	20999	24724	27524	29732	31238	31675	27327
6+537.5	32869	21226	23077	25854	30071	30798	33019	26334
6+545	30256	24042	25609	26937	30772	32148	31185	27773
6+552.5	39952	25887	25987	27027	31209	29394	32891	28074
6+560	34823	21020	21589	22838 ^b	27540	26898	27165	23989
Average	32710	23900	24680	27430	30040	30260	31320	27380

^a Stations in meters

^b Outlier according to Chauvenet's criterion

1 psi = 6.89 kPa

Table 3.22 Summary of Elastic Modulus Calculated from FWD Sensor Deflections Using 12-in. (300-mm) Plate, Wayne County, Section # 8

Station ^a	Modulus, psi							
	E ₁	E ₂	E ₃	E ₄	E ₅	E ₆	E ₇	Ave.E ₃₋₅
7+375	30307	19228	23184	25069	27596	25209	26826	25283
7+382.5	34012	25871	25255	26237	30782	27940	27597	27424
7+390	25304	20034	20875	24454	30494	25814	24391	25274
7+397.5	29352	38311 ^b	31338	30629	29666	29029	26354	30544
7+405	43117 ^b	28405	30899	30460	38194 ^b	32183	28689	33184
7+412.5	34471	32078	27755	28104	35431	31217	30181	30430
7+420	28665	22014	25696	40915 ^b	29283	26468	28416	31965
7+427.5	42921 ^b	28784	30508	29687	33122	30188	29648	31106
7+435	36906	23644	30756	27409	30638	31131	29966	29601
Average	31290	25010	27360	27760	30880	28800	28010	28670

^a Stations in meters

^b Outlier according to Chauvenet's criterion

1 psi = 6.89 kPa

Table 3.23 Summary of Elastic Modulus Calculated from FWD Sensor Deflections Using 12-in. (300-mm) Plate, Wayne County, Section # 9

Station ^a	Modulus, psi							
	E ₁	E ₂	E ₃	E ₄	E ₅	E ₆	E ₇	Ave.E ₃₋₅
7+375	24509	21721	20552	24994	25556	27478	26927	23700
7+382.5	32239	22622	22467	22091	30964	27786	27195	25174
7+390	33126	32557	29656	27440	37020	31925	27868	31372
7+397.5	37214	34416	34684	36283	34594	36376	37712 ^b	35187
7+405	33942	36772	35291	37817	32751	37076	29093	35286
7+412.5	47659 ^b	36288	29859	29286	36504	34287	33421	31883
7+420	39993	37231	31404	36029	36988	32395	31182	34807
7+427.5	28734	24842	23450	23603	29109	27779	28473	25387
7+435	38079	21462	20409	21735	25962	26371	27534	22702
Average	33480	29770	27530	28810	32160	31280	28960	29500

^a Stations in meters

^b Outlier according to Chauvenet's criterion

1 psi = 6.89 kPa

Table 3.24 Summary of Elastic Modulus Calculated from FWD Sensor Deflections Using 12-in. (300-mm) Plate, Madison County, Section # 10

Station	Modulus, psi							
	E ₁	E ₂	E ₃	E ₄	E ₅	E ₆	E ₇	Ave.E ₃₋₅
47+00	8061	7410	9542	8487	10008	NA	10296	9346
47+25	13991	11294 ^a	11055	10854	11367	10974 ^a	11918	11092
47+50	10206	6455	6057	5773	5450	5916	6028	5760
47+75	6505	5074	5210	5163	5285	5132	5365	5219
48+00	13532	8529	9838	9165	8530	8284	8248	9178
48+25	10272	5801	6635	6877	6985	7573	NA	6832
48+50	6914	4539	4679	4593	5014	5352	5345	4762
48+75	5169	2948	3047	3002	3649	4648	4489	3233
49+00	6718	3766	3876	4134	5274	6133	5389	4428
Average	9040	5570	6660	6450	6840	6150	7140	6650

^a Outlier according to Chauvenet's criterion

NA - Data not available

1 psi = 6.89 kPa

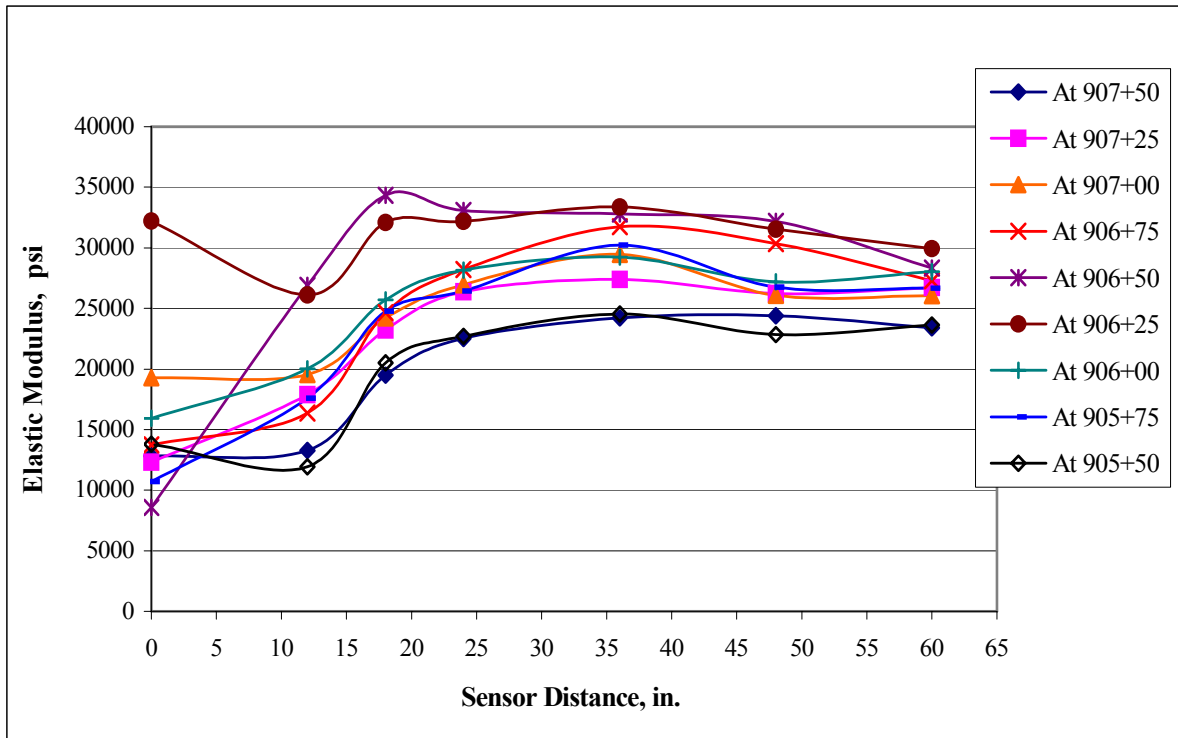


Figure 3.1.a Elastic Moduli at Each Sensor Location. Nine Stations of Section # 4, 1 psi = 6.89 kPa, 1 in. = 25.4 mm

that the first sensor modulus is smaller than that from offset sensors. On the other hand, in a relatively stiff subgrade, section #7 (see *Figure 3.1.b*), the difference between the first sensor- and offset sensor-modulus is statistically insignificant.

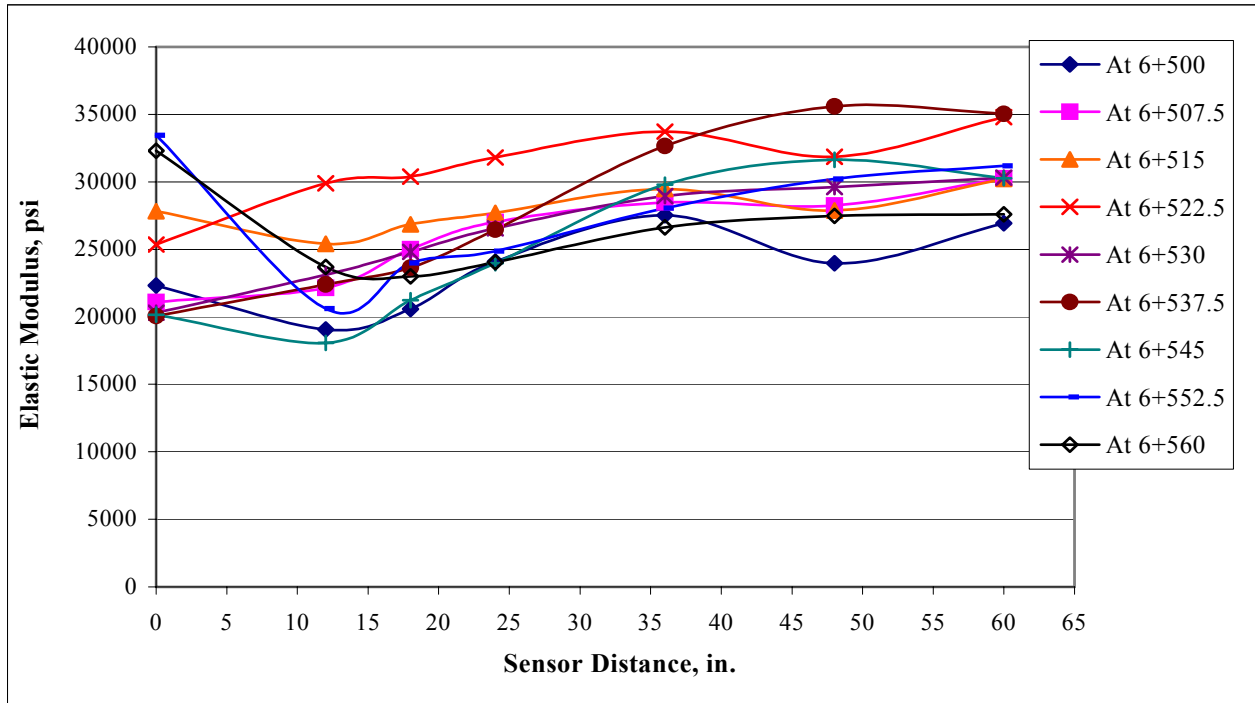


Figure 3.1.b Elastic Moduli at Each Sensor Location. Nine Stations of Section # 7, 1 psi = 6.89 kPa, 1 in. = 25.4 mm

3.2.1.2 Verification of Linear Elastic Behavior of Soils

Justification for homogeneous material assumption with elastic equations for modulus determination is presented in this section. Three different procedures are described to suggest that, for loads corresponding to the light load package, the soil behavior is close to elastic.

- (i) If the test material is linear elastic, the ratio of deflections of the 12-in. (300-mm) plate to the 18-in. (450-mm) plate are fixed numbers, namely, the first sensor deflection ratio = 1.5 and offset deflection ratios (for sensors two through seven) = 1.0. Two plots of those ratios, graphed in *Figure 3.2.a and 3.2.b*, suggest that with

the exception of the second sensor, deflection ratios of offset sensors correspond to the theoretical number

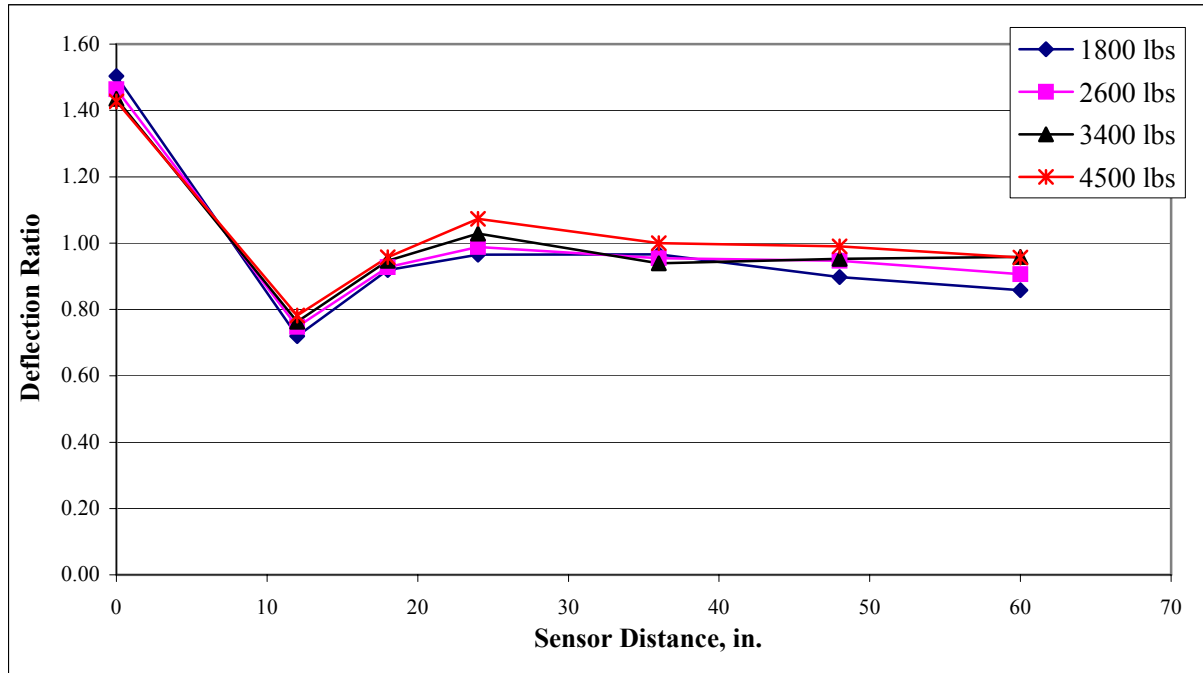


Figure 3.2.a Deflection Ratios of 12-in. and 18-in. Plates at Station 907+50 of Section # 4, 1 in. = 25.4 mm

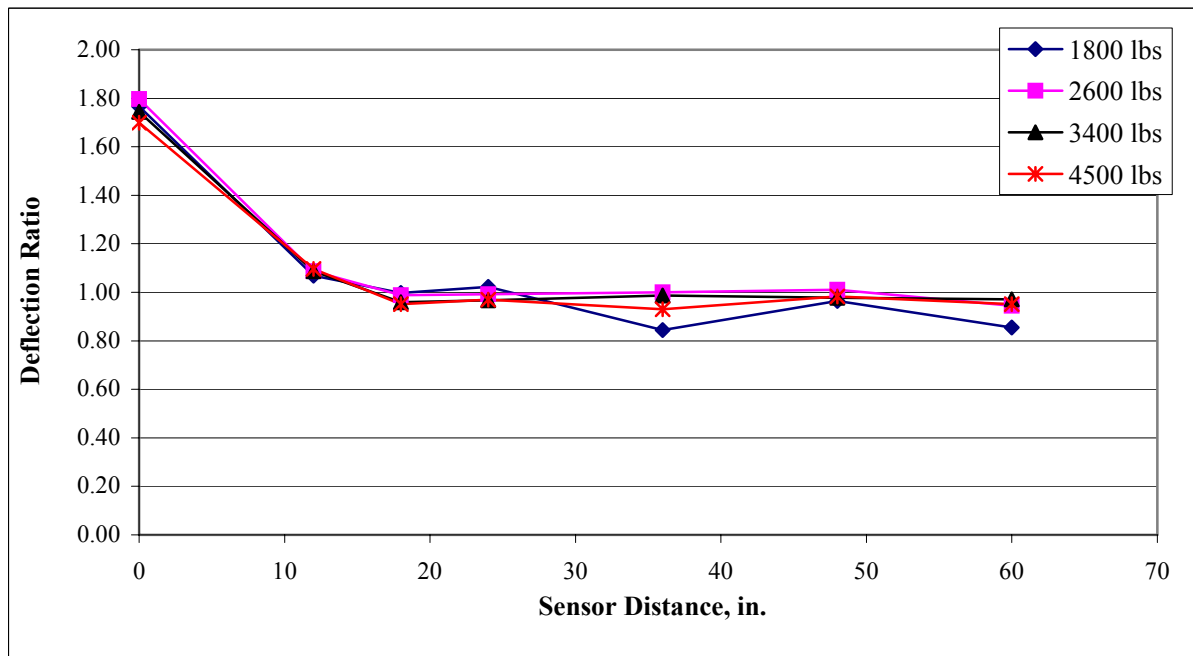


Figure 3.2.b Deflection Ratios of 12-in. and 18-in. Plates at Station 7+382.5 of Section # 9, 1 in. = 25.4 mm

- ($d_{r12}/d_{r18} = 1.0$). While the first sensor ratio of section #4 is nearly 1.5 as expected, the ratio of section #9 exceeds 1.5. Overall, the results support the premise that the load package, indeed, resulted in stresses and strains in the linear elastic range.
- (ii) If the material is linear elastic and/or stress independent, the modulus calculated from each of the seven sensors will be the same. What the test results show are that vibrations of the circular loading plate, because of the second sensor's proximity to the plate, adversely affect this sensor. The first sensor deflection is influenced by layering, along with other test uncertainties. Apart from these two exceptions, the moduli calculated from sensors three to seven are nearly constant for all of the ten sections (see *Tables 3.6 to 3.24*).
 - (iii) If the material is linear elastic, the moduli calculated from deflections generated by increasing loads should be nearly identical. A cursory examination of the data in *Table 3.5* confirms that the moduli determined at different load levels (1700 lbs (7.6 kN) to 4300 lbs (19.3 kN)) are nearly identical, discounting for inherent variation expected in the field test results.

3.2.2 Automated Dynamic Cone Penetrometer (ADCP) Test

The MDOT ADCP device was used in conducting penetration tests on prepared subgrade. The scheme of ADCP investigation consisted of penetration tests at 50 ft. (15 m) intervals adjacent to FWD plate imprint. ADCP tests in a given section were performed following FWD test to a depth in excess of 3 ft. (915 mm) in the subgrade. The ADCP is fully automated, with the penetration data collected by a laptop computer, the latter controlling the ADCP operation. The objective of ADCP test at each station was to detect layering, if any, in the top 3 ft. (915 mm) of the subgrade, which could influence FWD deflection, and, in turn the

calculated elastic modulus.

Plotting cumulative penetration data against number of blows (see *Figures B1 to B10, Appendix B*), it was possible to identify layering at each station, as indicated by the change in the slope. The slope change was visually identified and the results tabulated in *Table 3.25*. Note that DCPI of each layer and the corresponding layer thickness, from top to bottom, are tabulated for each station. How layering affects sensor deflection, and, in turn, computed moduli is discussed in section 4.2.

3.2.3 Geogauge Modulus

In addition to FWD, Geogauge is employed to determine in situ modulus of subgrade, conducting the test adjacent to the FWD foot imprint. Geogauge is a device that induces vibration on the surface and picks up resulting force and deformation to calculate stiffness, and, in turn elastic modulus employing an empirical correlation between stiffness and modulus. A complete description of the Geogauge can be seen in *reference (48)*. Geogauge moduli were determined at five sample locations for each section; those values are tabulated in column 3 of *Table 3.26*.

The purpose of testing with Geogauge was to authenticate the use of the device for quick estimation of stiffness, and, in turn, the modulus. A secondary objective was to have a check on the consistency of FWD-based modulus determination. Though a previous comparison study failed to confirm a one-to-one relation between the moduli determined by the two devices (*49*), this is another effort to explore the same issue. In a recent Federal Highway Administration (FHWA) sponsored pooled study, Geogauge has been investigated for QC/QA, by monitoring field density and correlating to stiffness.

Table 3.25 Summary of Dynamic Cone Penetration Index (DCPI) Results of Ten Test Sections

Section #	DCPI (mm/blow) / LAYER THICKNESS (mm)				
1	852+50	853+00	853+50	853+75	854+00
	50.0/300	NA	38.6/425	44.4/400	36.6/440
	20.9/960		11.4/775	12.3/800	10.0/540
2	54+00	55+00	56+00	57+50	58+50
	50.0/100	20.8/125	25.0/100	30.0/120	50.0/100
	6.3/700	6.1/800	8.6/525	6.2/655	7.3/750
3	152+00	152+50	153+00	153+50	153+90
	12.5/300	18.1/200	22.2/200	19.6/1275	22.7/500
	26.3/975	5.8/275	16.8/925		44.4/800
4	905+50	906+00	906+50	907+00	907+50
	16.7/1125	18.3/625	23.4/375	21.1/400	16.1/1112
		11.9/500	12.2/737	12.3/712	
5	833+20	833+60	834+00	834+40	834+80
	12.0/312	9.1/1125	8.6/1125	10.0/1112	3.3/175
	8.1/838				12.8/437
6	25+00	25+50	26+00	26+50	27+00
	10.8/1137	9.0/325	7.0/225	8.9/537	9.3/575
		13.9/825	10.3/350	15.4/600	25.5/562
7	6+500	6+515	6+530	6+545	6+560
	8.3/320	10.0/280	10/350	10.7/375	9.4/375
	3.63/425		5.0/625	5.5/660	5.6/350
8	7+375	7+390	7+405	7+420	7+435
	5.0/350	6.0/450	4.1/475	5.2/700	2.2/525
	14.4/1100	8.5/700	14/700	12.1/425	11.4/625
9	7+375	7+390	7+405	7+420	7+435
	4.4/350	5.0/450	4.8/442	4.6/475	5.0/275
	10.1/625	8.4/675	10.8/683	8.9/662	9.1/345
10	47+00	47+50	48+00	48+50	49+00
	8.67/260	12/960	7.41/200	9.52/200	11.38/410
	15/690		14.42/750	18.26/420	
				71/710	

NA - Data not available

1mm = 0.039 in.

Table 3.26 Geogauge Modulus Compared With FWD First Sensor Modulus, E₁, and Offset Modulus, E₃₋₅ (18-in. Load Plate)

Section #	Station	Modulus, psi		
		Geogauge	FWD E ₁	FWD E ₃₋₅
1	852+50	7560	2837	13614
	853+00	9720	4099	11970
	853+50	8620	3376	14282
	853+75	10470	3090	18719
	854+00	4680	2717	16147
2	54+00	10500	19870	13744
	55+00	9240	5608	15861
	56+00	7720	10227	9700
	57+50	13920	11531	14930
	58+50	8240	7843	13043
3	152+00	5990	7079	18309
	152+50	6430	9027	18626
	153+00	5710	8391	15922
	153+50	6640	6999	18760
	153+90	4890	3805 ^a	7580 ^a
4	905+50	12690	12807	22579
	906+00	11960	19299	27706
	906+50	13320	8572	33401
	907+00	12480	15932	26879
	907+50	12520	13810	22084
5	833+20	14170	18439	36789
	833+60	10750	14822	34694
	834+00	10600	23231	36206
	834+40	10970	11031	23520
	834+80	19030	12129	12390
6	25+00	20880	12735	18501
	25+50	20300	12944	19381
	26+00	19720	12455	21931
	26+50	19140	11484	17864
	27+00	18560	NA	11434 ^a
7	6+500	18890	22336	24071
	6+515	16500	27820	28004
	6+530	11980	20318	26773
	6+545	15770	20164	24997
	6+560	17070	32306	24560

^a Outlier according to Chauvenet's criterion

NA - Data not available

1psi = 6.89 kPa

Table 3.26 (Ctd) Geogauge Modulus Compared With FWD First Sensor Modulus, E₁, and Offset Modulus, E₃₋₅ (18-in. Load Plate)

Section #	Station	Modulus, psi		
		Geogauge	FWD E ₁	FWD E ₃₋₅
8	7+375	12050	15605	25140
	7+390	11840	31966	27460
	7+405	10410	37187	30170
	7+420	12570	19971	29671
	7+435	13600	19162	25146
9	7+375	14730	20049	35975
	7+390	10970	58566 ^a	31442
	7+405	11380	27092	30214
	7+420	12110	31237	27164
	7+435	12270	42773 ^a	25128
10	47+00	3790 ^a	6999	11870
	47+50	10240	7931	7455
	48+00	10780	17994 ^a	9899
	48+50	8240	8337	5215
	49+00	9760	6066	5334

^a Outlier according to Chauvenet's criterion

1 psi = 6.89 kPa

3.2.4 In-Place Density and Moisture

As the resilient modulus, or any strength parameter for that matter, is dependent on density and moisture of the material in place, and recognizing those attributes generally exhibit significant spatial variation, they were determined in place. At each station, where the FWD test was performed, density (moist density, and in turn, dry density) and moisture content were determined by nuclear device. Both 6-in. (15-mm) and 12-in. (30mm) probes were successively used, estimating density and moisture at two depths. The average of the two values is tabulated in *Table 3.27*, comparing them with those determined from Shelby tube samples, and also with the optimum density and corresponding moisture content of bag samples.

The Shelby tube sample densities are generally larger than field density as well as the maximum optimum density, especially in samples taken from places where moisture was below

Table 3.27 Density and Moisture Determined (i) by Nuclear Device (ii) from Shelby Tube Samples, and (iii) Optimum Moisture and Density

Section #	Station	Nuclear Device		Shelby Tube, First Sample		Bag Sample, Optimum	
		Density, lbs/ft ³	Moisture, %	Density, lbs/ft ³	Moisture, %	Density, lbs/ft ³	Moisture, %
1	852+50	109.2	15.8	111.3	14.3	115.2	13.8
	853+00	NA	NA	NA	NA		
	853+50	110.2	13.4	116.5	11.7		
	853+75	116.8	11.9	118.7	12		
	854+00	111.6	17.7	109	17.7		
2	54+00	114	14.4	NA	NA	113.7	14.1
	55+00	112	16.3	114.1	10.8		
	56+00	109.8	16.3	106.8	16.3		
	57+50	113	15.8	113	13.8		
	58+50	111	14.9	114.3	11.9		
3	152+00	115.3	13.2	112.7	13.2	116.2	12.9
	152+50	116.8	11.4	111.1	12.4		
	153+00	114.1	11.3	116.5	10.4		
	153+50	117.1	11.4	116.2	9.9		
	153+90	112.4	14.1	111.8	12.4		
4	905+50	116.8	11.3	121.6	11.7	115.5	13.8
	906+00	115.4	11.8	120	12.6		
	906+50	119.9	12.2	119.1	13.4		
	907+00	117.8	11.5	119	12.4		
	907+50	117.4	10.6	119.3	12.1		
5	833+20	113.2	10.7	113.6	15.4	108.2	17.8
	833+60	106.7	14.7	NA	NA		
	834+00	112.3	12.6	109.6	16.8		
	834+40	114.6	11.5	120.5	10.9		
	834+80	123.1	7.1	NA	NA		
6	25+00	111.3	12.3	110.4	15	105.6	17.8
	25+50	115.2	11.2	115	13.4		
	26+00	115.6	13.4	115.8	15		
	26+50	111	13.1	113.4	14.6		
	27+00	111.8	14	113.1	13.9		
7	6+500	116.5	8.5	121.1	8.5	118	11
	6+515	120.1	10	120.7	10		
	6+530	115.3	7.9	120.8	7.9		
	6+545	116.2	6	119.8	6		
	6+560	116.3	6	118.2	6		
8	7+375	125.7	6.8	130.4	6.3	118.9	12
	7+390	124.1	5.8	129.3	5.8		
	7+405	123.5	8.9	127.3	8.9		
	7+420	124.3	6.6	129.9	5.8		
	7+435	126.5	6.1	NA	NA		
9	7+375	124.3	6.4	128.9	5.9	118.9	12
	7+390	124.2	6.2	128.2	5.9		
	7+405	126.3	6.4	NA	NA		
	7+420	127.5	6.1	128.3	6.1		
	7+435	122.9	8.1	126.7	8.1		
10	47+00	107.7	8.2	110.2	14.1	106.1	18.6
	47+50	108.7	10.3	112	10.3		
	48+00	106.4	9.8	110	9.8		
	48+50	107.8	9.8	110.3	9.8		
	49+00	115.4	10.5	114.5	10.5		

NA - Data not available

1 lb/ft³ = 0.157 kN/m³

the optimum. This could be attributed to disturbance/densification resulting from pushing Shelby tube for sample extraction. Since M_R is significantly affected by sample density, modulus values could be higher for those samples. A correction to account for this re-compaction effect was attempted, a description of which will be presented in a later section.

3.2.5 Soil Sampling and Tests

Two independent sampling procedures were performed: Shelby tube samples from every station where FWD test was performed, and a bag sample representative of each test section. Three Shelby tube samples were retrieved from each station, at 1 ft. (304 mm) intervals reaching a depth in excess of 3 ft. (912 mm). These core samples were sealed in wax paper and shipped to the laboratory for resilient modulus testing in accordance with TP 46 protocol. The coring not only corroborated the layering, if any, identified by ADCP, but also helped to explore the presence of possible water table/rigid bottom. In order for the bag sample to be representative of the section, it was collected from three sampling locations digging to a depth of 16 in. (406 mm) minimum. This composite sample was shipped to the laboratory for further tests.

3.2.5.1 Laboratory Tests on Shelby Tube Samples

Trimmed from Shelby tube samples, three 2.8 in. (71 mm) diameter by 5.6 in. (142 mm) tall specimens were tested for resilient modulus, in accordance with AASHTO TP 46 protocol. All M_R tests were carried out in the MDOT Soils Laboratory. The deformation in the samples was recorded using two Linear Variable Differential Transducers (LVDTs) mounted outside of the testing chamber. Deformation and applied load readings were digitally recorded, from which the deviator stresses and resilient strains were calculated. The average M_R values for the last five loading cycles of a 100-cycle sequence yielded the resilient modulus. Typical laboratory M_R test results for the first samples (0–12-in, 0–305-mm) are presented in *Appendix C*. In all of the soils,

laboratory M_R decreases with decrease in confining stress. The effect of deviator stress on M_R appears mixed, though in a majority of soils M_R decreases with increase in deviator stress. Upon completion of M_R test, its density and moisture content were determined as well.

The Shelby tube samples tested for resilient modulus were preserved for further laboratory tests. Based on visual appearance, dry density values, and resilient modulus for every sample, they were grouped, reducing the number of samples for classification. Nonetheless, 89 classification tests were required from an original pool of 148 samples. These tests included particle size analysis in accordance with AASHTO T88-90, Liquid Limit in accordance with AASHTO T-89-90, and Plastic Limit AASHTO T-90-87. This information was employed to classify the subgrade soil of Shelby tube samples in accordance with the AASHTO procedure. *Table 3.28* lists the results of the aforementioned tests for all of the samples from the ten sections included in the study.

3.2.5.2 Routine Laboratory Tests on Bag Samples

In order to double-check the soil classification based on Shelby tube samples, a bag sample from each section was subjected to particle size analysis (AASHTO T88-90), Atterberg limits (AASHTO T89-90 and T90-87), and Standard Proctor test (AASHTO T99-90). *Table 3.28* lists the results of those tests for all of the ten sections. These tests were intended to establish benchmark properties of the soils being studied. As reported, each Shelby tube sample, after being tested for resilient modulus, was subjected to classification tests. Comparison of those results with the bag sample properties enabled us to assess the (natural) spatial variability in each section.

Besides classification tests, 2.8 in. by 5.6 in. (71 mm by 142 mm) samples (three for each section) were reconstituted at the respective optimum moisture and maximum density and tested

Table 3.28 Physical Properties and AASHTO Classification of (Grouped) Shelby Tube, and Bag Samples

Section #	Station/Sample	Shelby Tube Samples				Bag Sample			
		Material passing # 200, %	LL, %	PI, %	AASHTO Classification	Material passing # 200, %	LL, %	PI, %	AASHTO Classification
1	852+50/1	47	29	11	A6	55	22	6	A-4
	852+50/2	NA	NA	NA	NA				
	853+00/1	NA	NA	NA	NA				
	853+00/2	NA	NA	NA	NA				
	853+50/1	47	29	11	A6				
	853+50/2	NA	NA	NA	NA				
	853+75/1	47	29	11	A6				
	853+75/2	NA	NA	NA	NA				
	854+00/1	56	25	15	A6				
854+00/2	NA	NA	NA	NA					
2	54+00/1	NA	NA	NA	NA	56	27	8	A-4
	54+00/2	NA	NA	NA	NA				
	55+00/1	31	20	NP	A-2-4				
	55+00/2	NA	NA	NA	NA				
	56+00/1	31	20	NP	A-2-4				
	56+00/2	NA	NA	NA	NA				
	57+50/1	31	20	NP	A-2-4				
	57+50/2	91	54	23	A-7-6				
	58+50/1	48	27	8	A-2-4				
58+50/2	NA	NA	NA	NA					
3	152+00/1	39	20	1	A-4	40	25	7	A-4
	152+00/2	87	47	24	A-7-5				
	152+50/1	39	20	1	A-4				
	152+50/2	NA	NA	NA	NA				
	153+00/1	39	20	5	A-4				
	153+00/2	87	47	24	A-7-5				
	153+50/1	39	20	5	A-4				
	153+50/2	39	20	5	A-4				
	153+90/1	39	20	5	A-4				
153+90/2	NA	NA	NA	NA					
4	905+50/1	63	32	10	A-4	60	28	12	A-6
	905+50/2	68	29	11	A-6				
	906+00/1	63	32	10	A-4				
	906+00/2	68	29	11	A-6				
	906+50/1	63	32	10	A-4				
	906+50/2	68	29	11	A-6				
	907+00/1	63	32	10	A-4				
	907+00/2	68	29	11	A-6				
	907+50/1	63	32	10	A-4				
907+50/2	68	29	11	A-6					

NA - Data not available

NP - Non Plastic

Table 3.28 (Ctd) Physical Properties and AASHTO Classification of (Grouped) Shelby Tube, and Bag Samples

Section #	Station/Sample	Shelby Tube Samples				Bag Sample			
		Material passing # 200, %	LL, %	PI, %	AASHTO Classification	Material passing # 200, %	LL, %	PI, %	AASHTO Classification
5	833+20/1	83	32	11	A-6	NA	NA	NA	NA
	833+20/2	83	32	11	A-6				
	833+60/1	NA	NA	NA	NA				
	834+60/2	87	40	19	A-6				
	834+00/1	83	32	11	A-6				
	834+00/2	87	40	19	A-6				
	834+40/1	83	32	11	A-6				
	834+40/2	83	32	11	A-6				
	834+80/1	87	40	19	A-6				
834+80/2	83	32	11	A-6					
6	25+00/1	96	40	17	A-6	98	37	13	A-6
	25+00/2	98	40	12	A-6				
	25+50/1	96	40	17	A-6				
	25+50/2	98	40	12	A-6				
	26+00/1	96	40	17	A-6				
	26+00/2	98	40	12	A-6				
	26+50/1	96	40	17	A-6				
	26+50/2	98	40	12	A-6				
	27+00/1	96	40	17	A-6				
27+00/2	98	40	12	A-6					
7	6+500/1	29	23	NP	A-2-4	29	21	NP	A-2-4
	6+500/2	33	18	NP	A-2-4				
	6+515/1	29	23	NP	A-2-4				
	6+515/2	33	18	NP	A-2-4				
	6+530/1	29	23	NP	A-2-4				
	6+530/2	33	18	NP	A-2-4				
	6+545/1	29	23	NP	A-2-4				
	6+545/2	33	18	NP	A-2-4				
	6+560/1	29	23	NP	A-2-4				
6+560/2	33	18	NP	A-2-4					
8	7+375/1	52	22	5	A-4	42	24	5	A-4
	7+375/2	55	22	6	A-4				
	7+390/1	52	22	5	A-4				
	7+390/2	39	20	NP	A-4				
	7+405/1	52	22	5	A-4				
	7+405/2	53	23	4	A-4				
	7+420/1	52	22	5	A-4				
	7+420/2	53	23	4	A-4				
	7+435/1	NA	NA	NA	NA				
7+435/2	53	22	6	A-4					

NA - Data not available

NP - Non Plastic

Table 3.28 (Ctd) Physical Properties and AASHTO Classification of (Grouped) Shelby Tube, and Bag Samples

Section #	Station/Sample	Shelby Tube Samples				Bag Sample			
		Material passing # 200, %	LL, %	PI, %	AASHTO Classification	Material passing # 200, %	LL, %	PI, %	AASHTO Classification
9	7+375/1	69	22	4	A-4	42	24	5	A-4
	7+375/2	49	20	3	A-4				
	7+390/1	69	22	4	A-4				
	7+390/2	NA	NA	NA	NA				
	7+405/1	NA	NA	NA	NA				
	7+405/2	70	23	5	A-4				
	7+420/1	69	22	4	A-4				
	7+420/2	70	23	5	A-4				
	7+435/1	69	22	4	A-4				
7+435/2	49	20	3	A-4					
10	47+00/1	98	36	13	A6	98	36	13	A-6
	47+00/2	98	37	12	A6				
	47+50/1	98	36	13	A6				
	47+50/2	98	37	12	A6				
	48+00/1	98	36	13	A6				
	48+00/2	98	37	12	A6				
	48+50/1	98	36	13	A6				
	48+50/2	98	37	12	A6				
	49+00/1	98	36	13	A6				
49+00/2	98	37	12	A6					

NA - Data not available

for resilient modulus. A seven-day waiting period from molding to testing was allowed. The resilient modulus values, along with the respective moisture and density, are reported in *Table 3.29*.

3.3 SUMMARY

For relating FWD-backcalculated elastic modulus to resilient modulus of subgrade soils, a battery of field tests were conducted in ten finished subgrades. The field tests included:

- (i) FWD tests employing two different size plates, 12-in. and 18-in. (300-mm and 450-mm), and low load package
- (ii) Automatic Dynamic Cone Penetrometer tests

Table 3.29 Resilient Modulus of Reconstituted Samples Compared With Modulus of Shelby Tube Samples

Section #	Sample	Reconstituted Samples			Station	Shelby Tube Samples		
		Resilient Modulus, psi	Density, lbs/ft ³	Moisture, %		Resilient Modulus, psi	Density, lbs/ft ³	Moisture, %
1	1	9761	114.9	13.6	852+50	9866	111.3	14.3
	2	10241	115.1	13.4	853+00	NA	NA	NA
	3	9977	115	13.5	853+50	12528	116.5	11.7
					853+75	11687	118.7	12
					854+00	7711	111.6	17.7
	Average	9990			Average	10450		
2	1	12160	113.6	13.6	54+00	NA	NA	NA
	2	12930	113.7	13.7	55+00	15880	114.1	10.8
	3	12667	113.6	13.8	56+00	7998		
					57+50	15407	113	13.8
					58+50	14312	114.3	11.9
	Average	12590			Average	13400		
3	1	7549	116.2	12.6	152+00	11176	112.7	13.2
	2	7587	116.1	12.7	152+50	11198	111.1	12.4
	3	7510	116.3	12.5	153+00	10641	116.5	10.4
					153+50	8936	116.2	9.9
					153+90	11217	111.8	12.4
	Average	7550			Average	10630		
4	1	13611	115.6	13.9	905+50	21337	121.6	11.7
	2	15577	115.8	13.8	906+00	17880	120	12.6
	3	14402	116	13.6	906+50	21235	119.1	13.4
					907+00	19471	119	12.4
					907+50	20264	119.3	12.1
	Average	14530			Average	20040		
5	1	Data not available			833+20	15752	113.6	15.4
	2				833+60	NA	NA	NA
	3				834+00	9723	109.6	16.8
					834+40	20951	120.5	10.9
					834+80	NA	NA	NA
	Average							Average
6	1	12235	105.3	17.9	25+00	11193	110.4	15
	2	13043	105.8	17.5	25+50	15236	115	13.4
	3	13856	105.8	17.5	26+00	16395	115.8	15
					26+50	12221	113.4	14.6
					27+00	12306	113.1	13.9
	Average	13050			Average	13470		

NA - Data not available

1 psi = 6.89 kPa

1 lb/ft³ = 0.157 kN/m³

Table 3.29 (Ctd), Resilient Modulus of Reconstituted Samples Compared With Modulus of Shelby Tube Samples

Section #	Sample	Reconstituted Samples			Station	Shelby Tube Samples		
		Resilient Modulus, psi	Density, lbs/ft ³	Moisture, %		Resilient Modulus, psi	Density, lbs/ft ³	Moisture, %
7	1	12162	118.1	10.9	6+500	18449	121.1	8.5
	2	12463	118.2	10.8	6+515	24365	120.7	10
	3	12666	118.4	10.7	6+530	26885	120.8	7.9
					6+545	23977	119.8	6
					6+560	23031	118.2	6
	Average	12430			Average	23340		
8	1	14421	118.9	10.9	7+375	20815	130.4	6.3
	2	15450	119.1	10.7	7+390	23928	129.3	5.8
	3	16598	119.1	10.8	7+405	22554	127.3	8.9
					7+420	24765	129.9	5.8
					7+435	NA	NA	
	Average	15490			Average	23020		
9	1	14421	118.9	10.9	7+375	22787	128.9	5.9
	2	15450	119.1	10.7	7+390	22904	128.2	5.9
	3	16598	119.1	10.8	7+405	NA	NA	
					7+420	23000	128.3	6.1
					7+435	18229	126.7	8.1
	Average	15490			Average	21730		
10	1	10864	105	19.4	47+00	16902	110.2	14.1
	2	11539	105	19.1	47+50	20979	114	10.3
	3	11752	105.2	19.2	48+00	18268	110	9.8
					48+50	18214	110.3	9.8
					49+00	24394	114.5	10.5
	Average	11390			Average	19750		

NA - Data not available

1 psi = 6.89 kPa

1 lb/ft³ = 0.157 kN/m³

(iii) Direct estimation of modulus employing Geogauge, and

(iv) In-place density and moisture content by a nuclear device

Undisturbed samples were obtained by Shelby tubes and subsequently tested for resilient modulus employing TP-46 protocol. For identification of soil in each section, a bag sample was collected and tested in the laboratory. This chapter presents a detailed report of test results and some preliminary analyses indicating how best the data fit in the overall scheme of this research study. A detailed discussion of the results and correlation analysis will be the topic of the next chapter.

CHAPTER 4

ANALYSIS AND DISCUSSION OF RESULTS

4.1 INTRODUCTION

With in situ elastic modulus from FWD deflection, and resilient modulus from TP46 tests, a relation will be sought between the two. Prior to attempting a regression analysis, the calculated elastic moduli (*Equations 2.9 and 3.1*) will be qualitatively justified in light of the DCP index of each test station. TP46 resilient modulus values needed to be critically reviewed as well, the purpose of which is to assess whether the sample recompaction (brought about by Shelby tube sampling technique) affected the resilient modulus values. Whether Geogauge modulus agrees with the elastic modulus and/or resilient modulus is also explored.

4.2 HOW LAYERING AFFECTS ELASTIC MODULUS

The ADCP plots (*Figures B1 to B10*) were visually analyzed identifying any layering as indicated by change in slope of graph relating penetration and number of blows. Note penetration (expressed in mm per blow) is designated as DCP index. With a few exceptions, the top layer, 12 in. to 18 in. (305 mm to 457 mm) of section #1 appeared softer than the bottom layer, as can be verified in *Table 3.25*. The top material is classified as A-6, whereas the bottom turned out to be A-2-4. The elastic moduli calculated from sensors 1, 2, and 3 are significantly lower than those from sensors 4 through 7.

In section 2, except for a thin layer (approximately 4 in. (100 mm) thick) the top 27 in. to 32 in. (686 mm to 813 mm) appeared very stiff with DCPI of the order of 6 to 9 mm/blow. Underlying this stiff layer, classified as A-2-4, is a relatively loose layer with DCPI 25 to 43 mm/blow. Deflection-based moduli are reasonably uniform from sensor 2 to 7 at all nine

stations, though the first sensor modulus tends to be smaller than those from offset sensors (see *Table 3.7*).

Revealed from the study of borehole material in section #3, two layers were identified: a top layer of dense sand and a bottom layer of stiff gray clay. The ADCP data, however, failed to show this layering. It may be that the material is so interspersed that at 153 + 50 it appeared uniform to a depth of 1275 mm. A partial explanation for the increased DCPI with depth, especially at 152 + 00 and 153 + 90, could be the stiff clay being wet. In general, the section profile here is mixed or stiff over soft material; nonetheless, the first sensor modulus tends to be smaller than those of the offset moduli.

The first indication of uniformity of material in section #4 was obtained from the study of borehole material. Up to approximately 500 mm in depth, the material is described as “hard tan light gray sandy clay.” Judging from the DCPI values of the profile, especially at stations 906 + 00, 906 + 50, and 907 + 00, soft material overlies a stiff material, though the end stations are pretty much uniform. On average, the first sensor modulus is smaller than the offset sensor moduli characteristic of soft over stiff profile.

Judging from ADCP results, section #5 appears to be uniform to a depth of 1100 mm. Station 834 + 80 may be an exception in that stiffness tends to decrease with depth. Contrary to expectations, the first sensor modulus is lower than that of the other offset sensors, a finding uncharacteristic of uniform soil profile. The soil is classified as A-6.

Section 6 may be categorized as having a uniform profile or some non-uniformity with a moderately stiff top layer. Though the material is classified as A-6, its fine content is larger than that in section #5 (96 percent vs. 86 percent), accordingly the average elastic modulus is low as well. Again, the first sensor modulus is slightly lower than that of the offset sensors.

Though a relatively soft layer was identified on the surface in section #7, the thick layer underneath appeared very stiff with DCPI, approximately 5mm/blow. The dominance of stiff layer is clear, in that the elastic moduli calculated are extremely high, with the first sensor deflection resulting in a modulus compared to those from the offset sensors. This high moduli may be attributed not only to relative compaction of this section, but also, to the desiccated state of material. The material is indeed superior, with A-2-4 classification.

Based on ADCP results, section #8 appears as stiff as section #7; however, the upper surface layer is stiffer than the material immediately below. Regardless, the elastic moduli are as large as those for section #7, with the first sensor moduli almost equal to the offset sensor moduli. The material being A-4, it received good compaction and had undergone desiccation prior to being tested.

Section 9 is adjacent to section 8 and, therefore, the same layering is observed in this section as well. Again, the first sensor modulus is close to those obtained from offset sensors. The soil is again classified as A-4.

The latter half of section #10 showed some layering with stiff soil at the top with soft at the bottom. As per the design drawing of MDOT, the top stiff layer resulted from compacting borrow soil, whereas the bottom soft layer comprises nothing but the virgin soil. In general, in-situ tests revealed relatively low elastic modulus, with the first sensor showing mixed comparison with offset sensor moduli. The presence of shallow uncompacted virgin ground could have contributed to larger FWD deflection and, in turn, lower moduli.

The foregoing discussion led to the following observations:

- (i) Unless the material is completely homogeneous and isotropic, moduli based on center and offset sensor deflections can hardly be identical. Those two requirements are

hardly satisfied in case of a compacted subgrade. For a prepared subgrade, the soil for each compacted layer (approximately 8 in. (203 mm) thick) could be of different properties, violating the homogeneity requirement. And, for having compacted unidirectionally, the isotropy property is violated as well.

- (ii) Should there be a soft layer overlying a stiff layer, the first sensor modulus would be smaller than those from offset sensors.
- (iii) Another scenario of a stiff layer underlain by a less stiff layer or two or more stiff layers of nearly uniform properties, the first sensor modulus may equal those from the offset sensor moduli.

An overall conclusion is that elastic modulus from a single sensor, for example, the first sensor modulus alone, would not be adequate to characterize the subgrade. A host of factors, for example, material homogeneity, state factors and load factors, to mention a few, affect the elastic modulus as derived from FWD deflections. How to select a modulus, from an array of seven moduli values from each deflection bowl, will be again discussed in a later section.

4.3 FWD ELASTIC MODULUS COMPARED TO GEOGAUGE MODULUS

As was indicated, Geogauge measures the soil stiffness and from which modulus is calculated via an equation (48). Comparing the Geogauge modulus with FWD elastic modulus (see *Figure 4.1*), it is noted that, barring two outliers, namely section 1 and section 6, the Geogauge modulus is smaller than, or somewhat equal to the FWD elastic modulus. In sections 7, 8, and 9, they are totally different in that FWD modulus is on average 80 percent larger than the Geogauge modulus.

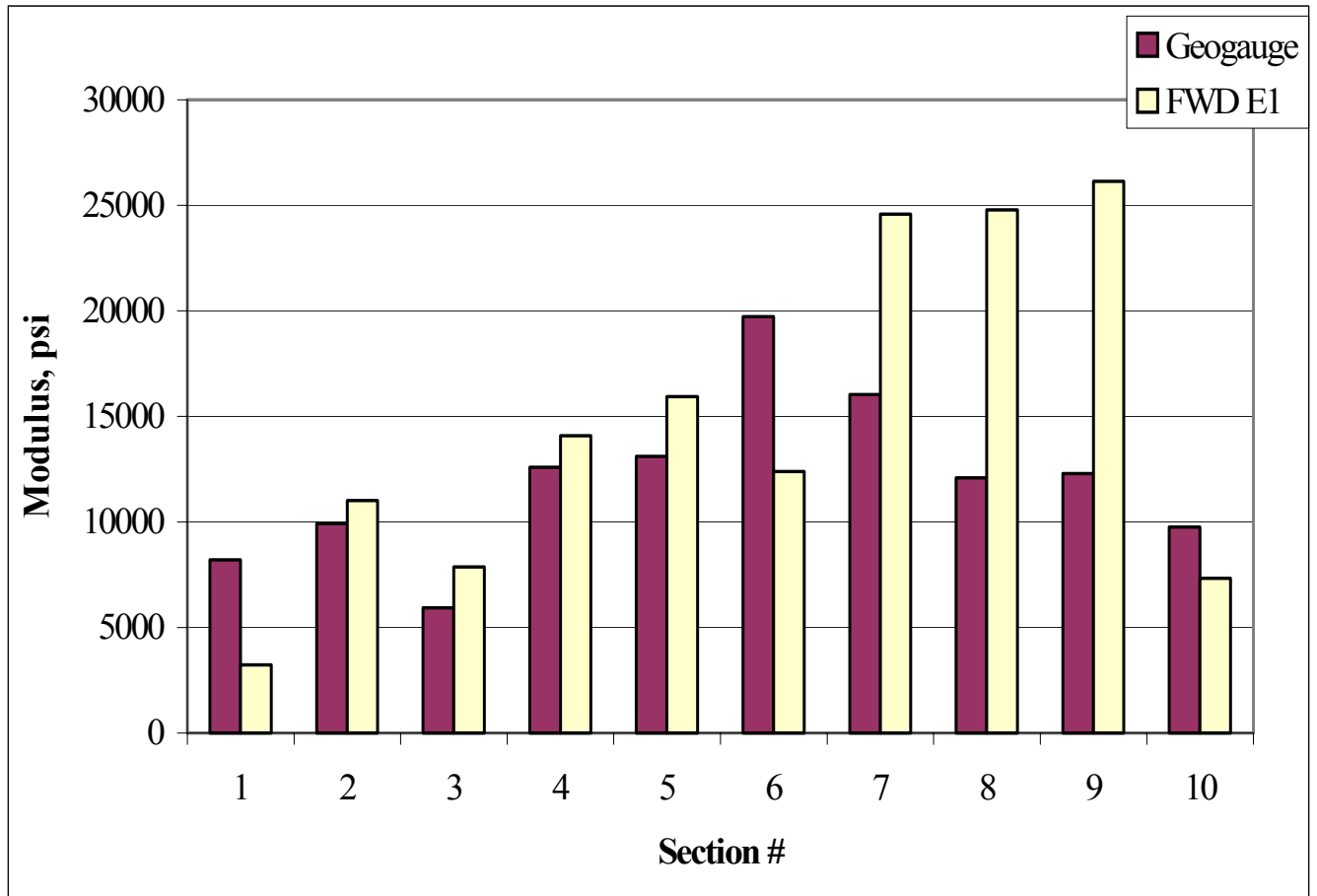


Figure 4.1 Geogauge Modulus Compared with FWD Modulus, $E_{1(av)}$, Section Averages, FWD with 18-in. (450-mm) Plate, 1 psi = 6.89 kPa

4.4 ARE THE RESILIENT MODULI OF SHELBY TUBE SAMPLES OVERESTIMATED?

As reported in a previous section, excessive force was required to extract samples using Shelby tube, especially when top layer had undergone desiccation. Also, sections 6, 7, 8, 9, and 10 had their in-place moisture relatively low compared to their respective optimums. A question now arises whether Shelby tube resilient modulus had been overestimated for apparent recompaction during sample retrieval. Comparing Shelby tube densities with the field densities – obtained by a nuclear device – it becomes clear that the Shelby tube samples had indeed been

recompacted by 2 to 3 percent, on average (see *Table 3.27*). The moisture change – loss of moisture during sampling and storage – had been minor, as can be verified by comparing the nuclear moisture with Shelby tube sample moisture. Whether TP46 modulus warrants adjustment to account for sampling/storage is addressed in the following section.

The following data is compiled from *Table 3.27* seeking a correction equation.

- (i) Field (nuclear device) density and moisture at five locations in each section
- (ii) Laboratory density and moisture content of each Shelby tube sample 1, retrieved from five locations in each test section
- (iii) Optimum moisture and maximum density of bag sample collected from each test section. Also available on bag sample are physical properties, for example, Atterberg limits and material passing #200 sieve (see *Table 3.28*)

The procedure proposed here entails developing a regression equation relating TP46 resilient modulus as a function of density and moisture. First, we use Shelby tube sample resilient modulus, and corresponding density and moisture for developing the model. Had this modeling been successful, each Shelby tube sample resilient modulus will be corrected to correspond to the field density and moisture measured by nuclear device. In developing the model, resilient modulus ratio (Shelby tube sample M_R/M_R of reconstituted sample at optimum density, as listed in *Table 3.29*) will be regressed against the density ratio (Shelby tube sample density/Optimum density) and moisture ratio (Shelby tube sample moisture/optimum moisture). Two options are available for this purpose: First, one equation for each section, which would be the most desirable. For want of adequate data, however, section-wise model could not be attempted. Second, an overall model covering all ten sections was considered. This approach necessitated inclusion of some soil property as an independent variable. Following several preliminary trials

with several combinations of soil properties, a transformed independent variable was chosen – a ratio of plasticity index and fines passing #200. The regression model, therefore, takes the following form:

$$M_{R(s/0)} = K_1 + K_2 D_{(s/0)} + K_3 M_{(s/0)} + K_4 PI/P_{200} + \varepsilon$$

where, $M_{R(s/0)}$ = resilient modulus ratio of Shelby tube sample and reconstituted sample (optimum density and optimum moisture sample);

$D_{(s/0)}$ = density ratio of Shelby tube density to optimum density;

$M_{(s/0)}$ = moisture ratio of Shelby tube moisture to optimum moisture;

PI/P_{200} = plasticity index (percent) divided by material passing #200 sieve as a ratio;

K_1, K_2, K_3, K_4 = regression constants; and

ε = error term

Section #5 data was incomplete and, therefore, not included in the model building.

Statistical Package for the Social Science (SPSS) program, with nonlinear analysis capabilities, was employed in developing the model. Several trials were attempted with power functions of the independent variables. The best model (one with the highest R^2 and least standard error) turned out to be a linear model, as listed below:

$$M_{R(s/0)} = 1.384 + 0.600 D_{(s/0)} - 0.167 M_{(s/0)} - 0.0286 PI/P_{200} \quad (4.1)$$

$$R^2 = 0.71$$

A sensitivity study of the model indicates that the predictions are more influenced by the PI/P_{200} ratio than the density ratio. What seems to be happening is that the PI/P_{200} ratio varies over one order of magnitude, whereas the density and moisture ratios vary by a small magnitude, as each individual density/moisture was divided by the corresponding optimum density/moisture.

Another option was to designate absolute values of density and moisture as independent variables. After preliminary investigations with one-on-one plots with Shelby tube modulus (M_{RS}) with each independent variable, density and PI/P_{200} were transformed to $density/62.4$ (designated specific density, SD) and $\log PI/P_{200}$. Again, employing SPSS, the following regression equation is derived:

$$M_{RS} = 15.3828 + 8.0263 SD - 0.542M - 6.0809 \log PI/P_{200} \quad (4.2)$$

$$R^2 = 0.65$$

where, M_{RS} = Resilient modulus of Shelby tube samples, ksi;

SD = Specific density; and

M = Moisture content, percent

The probable field resilient modulus, predicted by inputting (in *Equation 4.2*) density and moisture content in the field (determined by nuclear device), are tabulated in *Table 4.1*. A sensitivity study shows that a 10% change in each of the independent variables, density, moisture and PI/P_{200} , (keeping the other variable constant) would bring about a change in modulus of 5%, 0.35% and 1.5%, respectively. With a ten-fold variation in PI/P_{200} for the nine soils tested, it seems to overshadow the effects of density and moisture variation. That the predicted moduli hardly influenced by Shelby tube density or moisture attests to this premise. As can be seen in *Table 4.1*, out of the ten test sections, one-half of the predicted moduli are lower than the corresponding Shelby tube values, whereas the trend of the other half is exactly opposite, despite the fact that the Shelby tube samples were, in general, recompacted during sample retrieval. A decision has, therefore, been made to employ Shelby tube sample resilient modulus without correcting for the recompaction effect.

Table 4.1 TP46 Resilient Modulus Compared to That Predicted by Equation 4.2

Section #	Station	Sample 1 Shelby Tube Resilient Modulus, psi	Nuclear Device (Field)		Predicted M _R (for field density and moisture), psi
			Density, lbs/ft ³	Moisture, %	
1	852+50	9866	109.2	15.8	12528
	853+00	NA	NA	NA	NA
	853+50	12528	110.2	13.4	13957
	853+75	11687	116.8	11.9	15619
	854+00	7711	111.6	17.7	11521
2	54+00	NA	114	14.4	NA
	55+00	15880	112	16.3	17857
	56+00	7998	109.8	16.3	17574
	57+50	15407	113	15.8	18257
	58+50	14312	111	14.9	14079
3	152+00	11176	115.3	13.2	19679
	152+50	11198	116.8	11.4	20848
	153+00	10641	114.1	11.3	17188
	153+50	8936	117.1	11.4	17520
	153+90	11217	112.4	14.1	15452
4	905+50	21337	116.8	11.3	17107
	906+00	17880	115.4	11.8	16656
	906+50	21235	119.9	12.2	17018
	907+00	19471	116.8	11.5	16998
	907+50	20264	117.4	10.6	17563
5	833+20	15752	113.2	10.7	17263
	833+60	NA	106.7	14.7	NA
	834+00	9723	112.3	12.6	16117
	834+40	20951	114.6	11.5	17009
	834+80	NA	123.1	7.1	NA
6	25+00	11193	110	15	13865
	25+50	15236	115.2	13.4	15401
	26+00	16395	113.6	15	14328
	26+50	12221	111	14.6	14210
	27+00	12306	110.6	14	14484
7	6+500	18449	116.5	8.5	22487
	6+515	24365	120.1	10	22137
	6+530	26885	115.3	7.9	22658
	6+545	23977	116.2	6	23804
	6+560	23031	116.3	6	23817
8	7+375	20815	125.7	6.8	21828
	7+390	23928	124.1	5.8	22164
	7+405	22554	123.5	8.9	20407
	7+420	24765	124.3	6.6	21756
	7+435	NA	126.5	6.1	NA

NA - Data not available

1 psi = 6.89 kPa

1 lb/ft³ = 0.157 kN/m³

Table 4.1 (Ctd) TP46 Resilient Modulus Compared to That Predicted by Equation 4.2

Section #	Station	Sample 1 Shelby Tube Resilient Modulus, psi	Nuclear Device (Field)		Predicted M_R (for field density and moisture) psi
			Density, lbs/ft ³	Moisture, %	
9	7+375	22787	124.3	6.4	23418
	7+390	22904	124.2	6.2	23622
	7+405	NA	126.3	6.4	NA
	7+420	23000	127.5	6.1	24046
	7+435	18229	122.9	8.1	23671
10	47+00	16902	110.2	14.1	15079
	47+50	20979	108.7	10.3	17488
	48+00	18268	106.4	9.8	17246
	48+50	18214	107.8	9.8	17751
	49+00	24394	115.4	10.5	18078

NA - Data not available

1 psi = 6.89 kPa

1 lb/ft³ = 0.157 kN/m³

4.5 SELECTING THE APPROPRIATE RESILIENT MODULUS FROM TP46

RESULTS

The TP46 test is performed over a range of axial stresses and confining pressures (five and three, respectively) to measure the nonlinear (stress-sensitive) elastic behavior of soils. Numerous relationships have been employed for describing nonlinear behavior of subgrade soil; a summary of those models is presented in Chapter 2 (section 2.3). As recommended in the recent LTPP Study, Stubstad et al. (39), (Equation 2.8) is adopted in this study.

$$\log\left(\frac{M_R}{P_a}\right) = k_1 + k_2 \log\left(\frac{\Theta}{P_a}\right) + k_3 \log\left(\frac{\tau_{oct}}{P_a}\right) + k_4 \left(\log\left(\frac{\tau_{oct}}{P_a}\right)\right)^2 \quad (2.8)$$

Equation 2.8 serves to model stress dependency of resilient modulus. The k_1 to k_4 coefficients are determined from the 15 stress states employed in the TP46 test. Multiple regression analysis of 15 sets of M_R and corresponding stress states for each sample resulted in k_1 to k_4 . As expected, k_1 is positive. Constant k_2 also turns out to be positive, signifying stress hardening

with increasing bulk stress. Stress softening is equally dominant, as indicated by a negative k_3 exponent. For all practical purposes, k_3 is negative as well. Typical k -values of each section can be seen in *Table 4.2*.

Table 4.2 Typical Regression Constants (k – values) of Constitutive Equation 2.8, Sample 1

Section #	Station	Sample Location (Depth), in.	k_1	k_2	k_3	k_4
1	854+00	6	2.2729	0.4227	-0.7029	-0.0358
		18	NA	NA	NA	NA
2	57+50	6	2.8577	0.3744	-0.3269	-0.0825
		18	2.2818	0.3377	-1.0385	-0.3814
3	153+50	6	2.5196	0.3306	-0.4015	0.0174
		18	2.5547	0.4623	-0.8068	-0.3651
4	906+00	6	3.0071	0.2892	-0.2212	-0.1085
		18	3.0990	0.3006	-0.0496	0.0828
5	833+20	6	2.9056	0.2524	-0.3191	-0.1548
		18	2.5172	0.5805	-0.4633	-0.0836
6	27+00	6	2.8888	0.2039	-0.1257	-0.0652
		18	2.9756	0.1641	-0.3825	-0.2490
7	6+545	6	3.1331	0.3171	-0.1513	-0.0043
		18	2.8126	0.5808	-0.3356	-0.0709
8	7+405	6	3.0861	0.4978	-0.3172	-0.1931
		18	3.1264	0.5033	0.0471	0.0810
9	7+375	6	3.0283	0.3941	-0.4339	-0.2365
		18	2.7833	0.5459	-0.7865	-0.3385
10	48+50	6	2.9829	0.3309	-0.2926	-0.1430
		18	2.8610	0.3368	-0.2947	-0.0782

1 in. = 25.4 mm

NA – Data not available

The question now arises as to what stress state should be used to calculate the representative resilient moduli for correlation to field-test elastic moduli. Two load scenarios were considered: first, a stress state resulting from a typical 18-in. pavement overlying subgrade, in conjunction with a 9000-lb. (9-kN) wheel load at 100 psi (690 kPa) tire pressure. Second, a 2500-lb. (11-kN) load on a FWD plate (either 12-in. or 18-in. as the case may be) on top of

Table 4.3 Calculated Stress State in Subgrade Under Different Loads Including Overburden

Load Description	Stress		
	Location	σ_1 , psi	$\sigma_2 = \sigma_3$, psi
9000 lb wheel load over 18 in. pavement	6 in. below subgrade surface	4.3	1
	18 in. below subgrade surface	4	1.3
2500 lb load on 12 in. FWD plate	6 in. below subgrade surface	14.6	2.6
	18 in. below subgrade surface	4.4	0.6
2500 lb load on 18 in. FWD plate	6 in. below subgrade surface	8.5	2.5
	18 in. below subgrade surface	4	0.7

1 psi = 6.89 kPa
1 in. = 25.4 mm

the subgrade. The stress states calculated at various depths, employing KENLAYER, are tabulated in *Table 4.3*. Stress states at 6 in. and 18 in. depths, including overburden, were subsequently employed in resilient moduli computation of Shelby tube samples retrieved from corresponding depths. The results in entirety are not presented in the report for brevity; however, the resilient moduli of first sample (0 to 12 in.) and second sample (12 to 24 in.) employing, respectively, the two stress scenarios (stresses $\sigma_1 = 8.5$ psi, $\sigma_3 = 2.5$ psi and $\sigma_1 = 4.0$ psi, $\sigma_3 = 0.7$ psi) are presented in *Table 4.4*.

Comparing the two sets, it is noted that the second sample (under the corresponding load stresses, column 4) appears significantly softer than the first sample, as evidenced by its lower modulus. The percentage reduction varies from 14% in section #3 to 50% in section 7. Some of this decrease in M_R could be attributed to the lower bulk stress and/or confining stress employed in calculating the second sample moduli. Also, the moisture content of the second sample is invariably

Table 4.4 Resilient Modulus Calculated Employing Two Stress States at Depths 6 in. Below and 18 in. Below Surface, Respectively. Load 2500 lb on 18-in. Plate

Section #	Station	Resilient Modulus, psi	
		Stress State $\sigma_1 = 8.5, \sigma_2 = \sigma_3 = 2.5$ First sample	Stress State $\sigma_1 = 4, \sigma_2 = \sigma_3 = 0.7$ Second sample
1	854 + 00	7711	NA ^a
	853 + 75	11687	NA
	853 + 50	12528	NA
	852 + 50	9866	NA
2	54 + 00	NA	NA
	55 + 00	15880	NA
	56 + 00	7998	NA
	57 + 50	15407	8608
	58 + 50	14312	NA
3	152 + 00	11176	11733
	152 + 50	11198	NA
	153 + 00	10641	7602
	153 + 50	8936	8892
	153 + 90	11217	NA
4	905 + 50	21337	10361
	906 + 00	17880	15630
	906 + 50	21235	15088
	907 + 00	19471	15025
	907 + 50	20264	15309
5	833 + 20	15752	6185
	833 + 60	NA	7220
	834 + 00	9723	8775
	834 + 40	20951	7147
	834 + 80	NA	NA
6	25 + 00	11193	8279
	25 + 50	15236	15024
	26 + 00	16395	17535
	26 + 50	12221	12420
	27 + 00	12306	15646
7	6 + 500	18449	12760
	6 + 515	24365	7789
	6 + 530	26885	19161
	6 + 545	23977	9463
	6 + 560	23031	8193
8	7 + 375	20815	18335
	7 + 390	23928	17371
	7 + 405	22554	12444
	7 + 420	24765	10314
	7 + 435	NA ^a	16179

NA - Data not available

1 psi = 6.89 kPa

Table 4.4 (Ctd) Resilient Modulus Calculated Employing Two Stress States at Depths 6 in. Below and 18 in. Below Surface, Respectively. Load 2500 lb on 18-in. Plate

Section #	Station	Resilient Modulus, psi	
		Stress State $\sigma_1 = 8.5, \sigma_2 = \sigma_3 = 2.5$ First sample	Stress State $\sigma_1 = 4, \sigma_2 = \sigma_3 = 0.7$ Second sample
9	7 + 375	22787	14050
	7 + 390	22904	NA
	7 + 405	NA	11018
	7 + 420	23000	17302
10	47+00	16902	15262
	47+50	20979	11877
	48+00	18268	12346
	48+50	18214	12031
	49+00	24394	14619

NA - Data not available

1 psi = 6.89 kPa

Table 4.5 Comparison of Average Density and Moisture of First Sample (0 - 12 in. depth) and Second Sample (12 - 24 in. depth) Shelby Tube

Section #	Density, lbs/ft ³		Moisture, %	
	Sample # 1	Sample # 2	Sample # 1	Sample # 2
1	113.8	NA	13.9	NA
2	112	102.1	13.2	21.3
3	113.6	106.2	11.3	17.6
4	118.6	118.3	12.6	13.1
5	120	110.5	14.4	17.2
6	113.5	113.2	14.4	15.1
7	120.1	118.7	7.7	9.2
8	129.2	126.5	6.7	7.4
9	128	125.4	6.5	8.9
10	111.4	109.1	10.9	13.8

NA - Data not available

1 lb/ft³ = 0.157 kN/m³

higher than that of the first sample (see *Table 4.5*). The fact that the density of the first sample is high contributed significantly to the disparity between the moduli values: Namely, the second sample showed consistently lower modulus for all of the sections. Not only is the modulus of the second sample (column 4, *Table 4.4*) smaller, but also its variation within a section is

Table 4.6 Comparison of Coefficient of Variation of First Sample (0 - 12 in. depth) and Second Sample (12 - 24 in. depth) Resilient Modulus

Section #	Coefficient of Variation, percent	
	First Sample	First Sample
1	17.7	NA
2	23.6	NA
3	8.2	18.3
4	6.4	13.8
5	29.6	12.6
6	14.7	23.2
7	11.8	36.8
8	6.5	20.4
9	9.3	15.6
10	13.5	10.7

NA – Data not available

significantly larger, as can be seen in *Table 4.6*.

Explanation of the selection of stress state for M_R calculation follows: First, the 2500-lb load, is appropriate because the four FWD load levels employed in the test program bracket the 2500-lb load. Second, it is gratifying to note that this load results in stresses, typically sustained by subgrades (namely, $\sigma_1 = 8.5$ psi and $\sigma_3 = 2.5$ psi). Accordingly, modulus values from column 3 of *Table 4.4* are chosen to relate to FWD-modulus from *Tables 3.6 to 3.15*.

4.6 FWD PLATE DIMENSION AND SENSOR TIP SIZE FOR SUBGRADE TEST

4.6.1 General

FWD deflection tests were conducted on ten test sections with two variations from the normal set up, namely, an 18-in. (450-mm) plate and a modified 16-mm sensor tip (see *Table 3.2*). The purpose of this investigation was to investigate whether the 18-in. plate (300-mm) would have advantage over the 12-in. (450-mm) plate and also whether large sensor tips (16 mm) would work better than the standard 10-mm tips.

4.6.2 Comparison of Moduli from 18-in. (450-mm) and 12-in. (300-mm) Plates

Average moduli of nine test stations in each section, for each sensor, are presented in the last row of *Tables 3.6 to 3.15 and 3.16 to 3.24*, respectively, for the large and small plates. The first question is: Are they statistically equal? A Mann-Whitney-Wilcoxon test for comparison of two independent variables (50) was performed to test the difference between the first sensor modulus (E_1) obtained from the large and the small plates. The same comparison test was performed on the offset sensor E_{3-5} (average of third, fourth and fifth sensors) and both of the results are tabulated in *Table 4.7*. Evidence is lacking to suggest that plate size has any effect on E_1 and E_{3-5} .

Coefficient of Variation (COV) of E_1 of both plates is listed in columns 2 and 3 while COV of E_{3-5} in columns 4 and 5 of *Table 4.8*. It is noted that E_1 values from the large plate show large variations within a section, as signified by larger COV values. It could be that uneven seating of large plate adversely affects E_1 . Unpredictable plate vibration could be another reason. The COV of the offset sensors (E_{3-5}) with large plate, however, is improved compared to that for the small plate results.

The side-by-side tests with two plates revealed another compelling result that the first sensor moduli indeed shows a large variation regardless of the size of the plate, as can be seen in *Figure 4.2*, for a typical section (#8). Normalized deflections (deflection per unit load) of sensor 1 shows significant variation compared to those of sensor 4. Some 36 sensor 4 data points bunch together right on the equality line, whereas the, corresponding points for the first sensor deflections, hardly show any trend. Also, the theoretical result that first sensor deflections of 12-in. and 18-in. plates conform to a ratio of 1:5 is not satisfied. More than plate size, sensor position affects the precision of deflection results.

Table 4.7 Summary of Statistical Test Results Comparing 18-in. (450-mm) Plate Modulus to 12-in. (300-mm) Plate Modulus

Section #	Average E_1 , psi		Mann-Whitney-Wilcoxon Test Comparing 12- and 18-in. Plate Moduli, E_1	Average E_{3-5} , psi		Mann-Whitney-Wilcoxon Test Comparing 12- and 18-in. plate Moduli, E_{3-5}
	18-in. Plate	12-in. Plate		18-in. Plate	12-in. Plate	
1	3240	NA	NA	14410	NA	NA
2	10570	10630	No difference	13660	13130	No difference
3	8060	7870	No difference	18100	23170	Different
4	13400	15770	No difference	27360	26500	No difference
5	16920	17710	No difference	31000	30330	No difference
6	12690	15130	No difference	19460	20500	No difference
7	24770	32710	Different	26240	27380	No difference
8	25380	31290	No difference	25850	28670	No difference
9	28310	33480	No difference	29800	29500	No difference
10	7620	9040	No difference	7510	6650	No difference

NA - Data not available

1 psi = 6.89 kPa

Table 4.8 Comparison of Coefficient of Variation of 12-in. and 18-in. Plate Moduli

Section #	Coefficient of Variation, percent			
	E_1		E_{3-5}	
	12-in. plate	18-in. plate	12-in. plate	18-in. plate
1	NA	13.9	NA	20.8
2	37.9	44.2	16	17.5
3	11.5	15.3	13.7	9.1
4	15.4	22.6	10.9	13.2
5	36.1	30.7	28.1	31.5
6	8.7	14.5	12.3	7.6
7	17.3	20.1	6.6	5.2
8	11.8	33.6	9	7
9	14.2	19	16.7	16.2
10	32.9	18.1	37.6	34.2

NA - Data not available

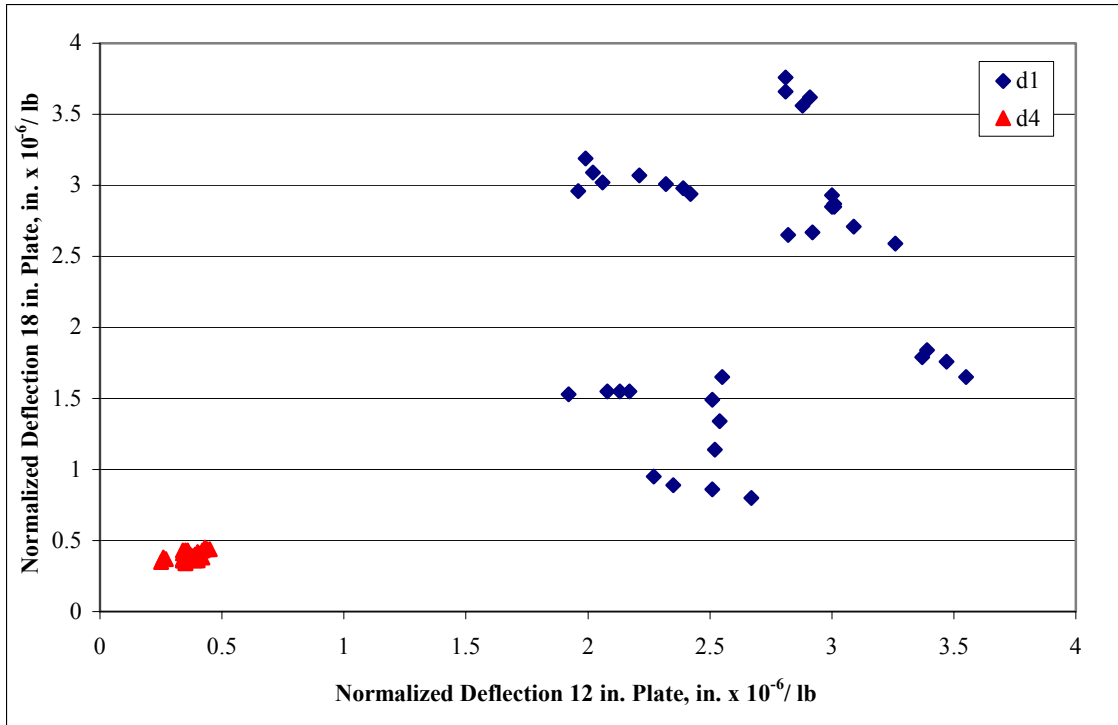


Figure 4.2 Comparison of Normalized Deflections of 12-in. (300-mm) and 18-in. (450-mm) Plates. Section # 8, 1 in. = 25.4mm, 1 lb. = 4.448 N

A point of significance in this comparison is the stress level under both plates. The stresses under the 2500-lb. load with a large plate seems very much reasonable: compare large plate stresses $\sigma_1 = 8.5$ psi, and $\sigma_3 = 2.5$ psi, small plate stresses $\sigma_1 = 14.6$ psi, and $\sigma_3 = 2.6$ psi. For the purpose of mitigating nonlinear effects only, lower stresses are preferred in FWD testing of subgrade soils. Based on stress criteria, therefore, the large plate would be desirable for subgrade testing.

Accordingly, 18-in plate moduli are utilized in regression modeling. In a later section (section 4.8.5), it will be shown that the 18-in. (450-mm) plate moduli show better correlation than that resulted from the smaller 12-in. (300-mm) plate, yet another reason for our preference for the 18-in. (450-mm) plate results (*Tables 3.6 to 3.15*).

**Table 4.9 Average Section Elastic Moduli at Each Sensor, Load Plate = 12 in.,
Sensor Tip 10mm/18mm, Sections 7 - 9**

Section #	Average Elastic Modulus, psi, (10mm tip/16mm tip)						
	Sensor 1	Sensor 2	Sensor 3	Sensor 4	Sensor 5	Sensor 6	Sensor 7
7	32340/ 32710	23340/ 23900	24380/ 24680	26870/ 27430	29900/ 30040	29730/ 30260	31070/ 31320
8	31440/ 31290	26960/ 25010	27160/ 27360	27990/ 27760	30980/ 30880	28410/ 28800	26470/ 28010
9	34650/ 33480	28810/ 29770	29970/ 27530	31250/ 28810	33000/ 32160	30900/ 31280	29610/ 28960

1 psi = 6.89 kPa

**Table 4.10 How Sensor Tips, 10mm and 16mm, Affect Elastic Moduli (E_1 and E_{3-5}),
12-in. Plate**

Section #	E_1 , psi		Mann-Whitney-Wilcoxon Test Results	E_{3-5} , psi		Mann-Whitney-Wilcoxon Test Results
	Mean value 10mm tip	Mean value 16mm tip		Mean value 10mm tip	Mean value 16mm tip	
7	32340	32710	No difference	27050	27380	No difference
8	31440	31290	No difference	28710	28670	No difference
9	34650	33480	No difference	31400	29500	Different

1 psi = 6.89 kPa

4.6.3 Comparison of Moduli Employing 10mm and 16mm Tips

Side-by-side FWD tests with 12-in. (300-mm) plate and, respectively, 10 mm and 16 mm tips, were conducted in three sections, sections #7, #8 and #9. Results from two sensor tips are compared in *Table 4.9*. Again, the Mann-Whitney-Wilcoxon test for comparison of means are conducted, with the results listed in columns 4 and 7 of *Table 4.10*. The results are encouraging in that both tips result in statistically similar moduli, in five out of six cases.

Yet another test performed compares normalized deflections registered by the two tips with the 12-in. (300-mm) plate. The plot in *Figure 4.3* for section #8 signifies that fourth sensor deflections are indeed identical, whereas first sensor deflections not only vary over a moderate range but some plotted points deviate from the line of equality, especially at large deflections. Again, the sensor position matters more than the sensor tip size. For all practical purposes, therefore, the smaller tip, standard on many FWD machines, is appropriate for subgrade tests.

4.7 SELECTING APPROPRIATE FWD RESULTS

4.7.1 FWD Test Results, Outliers Deleted

The field test program comprised of ten test sections. As alluded to in a previous section, test section #10 was meant to substantiate the regression model (FWD-modulus vs. resilient modulus), the focus of this study. Not only had section #10's response failed to fit the overall trend of the other nine sections, it was brought to our attention that two deflection sensors had malfunctioned during the field tests. Accordingly, a decision was made to exclude moduli data of section #10 from regression modeling, and/or from utilizing it for substantiating the model.

4.7.2 Selecting FWD Elastic Modulus

In section 4.5, it was argued that one single value of resilient modulus (TP46 modulus applicable to 0-12 in. (0-30 mm) sample depth) would be correlated with elastic modulus.

Elastic modulus, seven values calculated from seven sensors, (see *Tables 3.6 to 3.14*), are now available for comparing with a single resilient modulus. Had the soils tested been perfectly elastic, homogeneous and isotropic (discounting for FWD testing errors), all seven values should have been identical. Unfortunately, none of those criteria are satisfied; therefore, deflection-

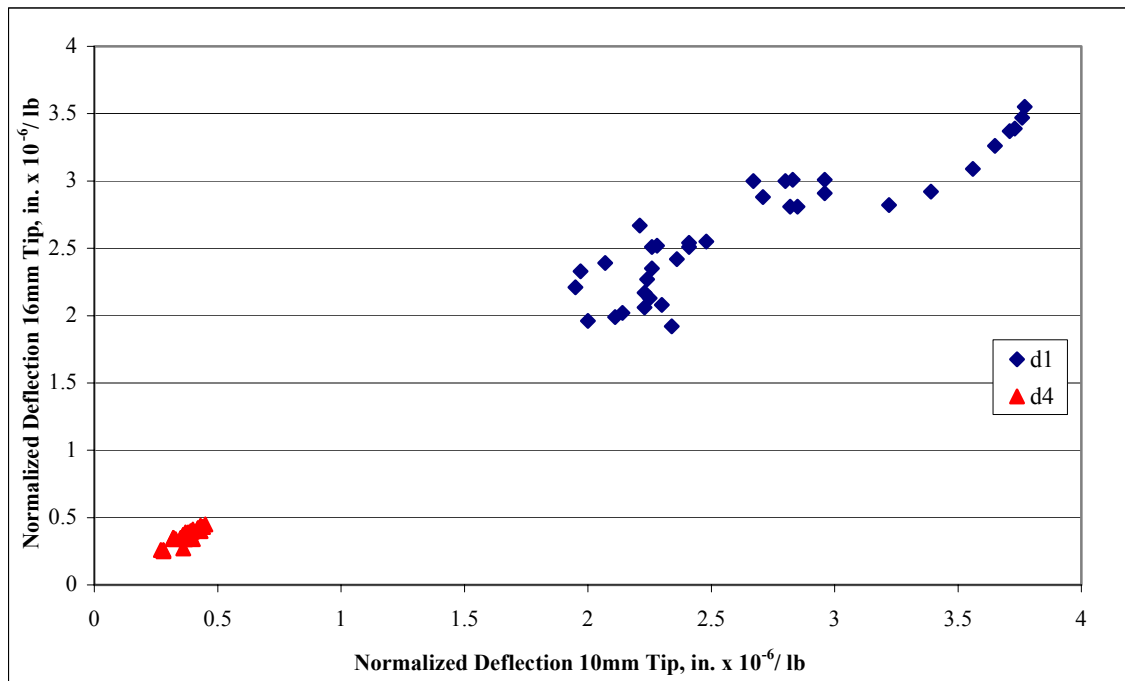


Figure 4.3 Comparison of Normalized Deflections of 10mm and 16 mm tip, Section # 8, 12-in. Plate, 1 in. = 25.4 mm

based modulus may not necessarily be uniform. As discussed in a previous section (4.2), the first sensor modulus is smaller than the offset sensors, should a soft finite layer overlay a stiff layer. If the material tested is uniform (satisfying homogeneity criterion), or relatively stiff to a reasonable depth, the first sensor modulus may equal the collective average of the offset sensor moduli, excluding sensor 2 modulus.

Since subgrade is constructed in layers (approximately 8 in.) employing a roller or vibratory compactor, residual horizontal stresses remain in the soil after the roller has “walked out.” This so-called “passive condition” could promote better energy dispersion, and, in turn,

lower stress/deflection under the FWD plate. That is, subgrade anisotropy could impede surface deflection; in all likelihood, not a set percentage at each sensor location, however.

Another factor that affects FWD deflections pertains to the reality that soil is composed of discrete aggregate particles that are connected by cementing agents or interlocking forces that present states far from homogeneity and isotropy. The particulate nature of soil defies classical continuity. Unlike in a continuous medium, when external loads are applied, particle arrangements are altered and deformation occurs. When particulate nature of soil is considered, load spreading under FWD load would be significantly altered in relation to assuming classical continuity. For example, fine (clay) soils show improved ability to distribute stresses, as do well-packed soils. What this amounts to is that in loose coarse soil deposits, the first sensor deflection could be accentuated, resulting in lower elastic modulus.

Without a question, there could be inherent spatial variation of material property, from the first to the seventh sensor location, which in all likelihood would be random. Nonetheless, random variation of material is a minor issue, as the measurements are confined to a short length of 5 ft. (1.8 m).

In addition, it has been observed that vibration caused by the falling weight tends to alter first sensor deflection and the second sensor deflection as well. In fine-grain soils, the sensor tip might pierce through, enhancing the deflection registered by the sensor. In coarse-grain soils, where the surface is sprinkled with loose particles, we noted particles congregating around the sensor tip. Note in *Figure 4.4*, the 1 in.-diameter depression in the soil (section #7) corresponds to the hole in the plate with loose particles forming a mound around the sensor tip. This shifting of particles in granular soils seems to have minor effect on first sensor deflection, and in turn, the corresponding modulus.

Observations confirm that the plate vibrations also affect the second sensor deflection, as it is only 3-in. (76-mm) from the edge of an 18-in. (300-mm) plate. That the modulus calculation is based on an equation (*Equation 3.1*), which relies on the simplifying assumption of concentrated load, is another reason for placing less reliance on the second sensor modulus. The second sensor modulus, therefore, will not be considered for further analysis.



Figure 4.4 Photograph of Imprint Showing Loose Coarse Particles Congregating Around the First Sensor Tip

The foregoing suggests that one can expect the first sensor modulus to be smaller than or equal to any one of the five (second sensor modulus excluded) offset sensors. Nonetheless, the

modulus from the first sensor needs to be reckoned with in arriving at a “design resilient modulus.” Why first sensor modulus? Because the first sensor deflection typifies the entire subgrade as opposed to the offset sensors, each of which characterizes only a fractional depth of subgrade; the farther the sensor, the deeper layers influencing its deflection. Accordingly, a decision has been made to treat the first sensor modulus separately from the five offset sensor moduli. Out of those five offset sensor moduli, E_6 and E_7 are considered less reliable for having been calculated from sixth and seventh sensor deflections that are extremely small, less than a mil in some cases. Also, those sensors do not capture the response of the top approximately 40 in. (1 m) of the subgrade. Therefore, E_6 and E_7 are deleted from the data set and the remaining three sensor moduli (E_3 , E_4 and E_5) are averaged and tabulated in column 9 of *Tables 3.6 to 3.14*. E_1 -values are listed in column 2 of *Tables 3.6 to 3.14*. For now, with two elastic moduli representative of the soil deposit being tested by FWD and one resilient modulus characterizing the subgrade, two relations would be attempted: first, E_1 vs. the resilient modulus, and second average of E_3 through E_5 vs. the resilient modulus.

4.7.3 Elastic Modulus and Resilient Modulus Variabilities Compared

The variability of subgrade resilient modulus has been emphasized in the 2002 AASHTO Guide, which mandates both mean value and standard deviation of subgrade resilient modulus for pavement design. As can be verified in *Tables 3.6 to 3.14*, the first sensor modulus, E_1 , exhibited a high degree of variability whereas E_{3-5} scatter was relatively small. Postulating that spatial variability and test errors contribute to the total variability, we assert that test errors dominate the first sensor modulus more than E_{3-5} . Now, resilient modulus determined in the laboratory also experienced some variability (see *Table 3.29*), perhaps due to the same two causal factors – material variability and test errors.

With variabilities of both elastic moduli (E_1 and E_{3-5}) and resilient modulus expressed by coefficient of variation, COV, two plots are prepared: first, COVs of E_1 vs. M_R , and second, COVs of E_{3-5} vs M_R . The first plot exhibited no clear indication of being equal. On the contrary, COV of E_1 was significantly larger than that of M_R , with hardly any trend whatsoever.

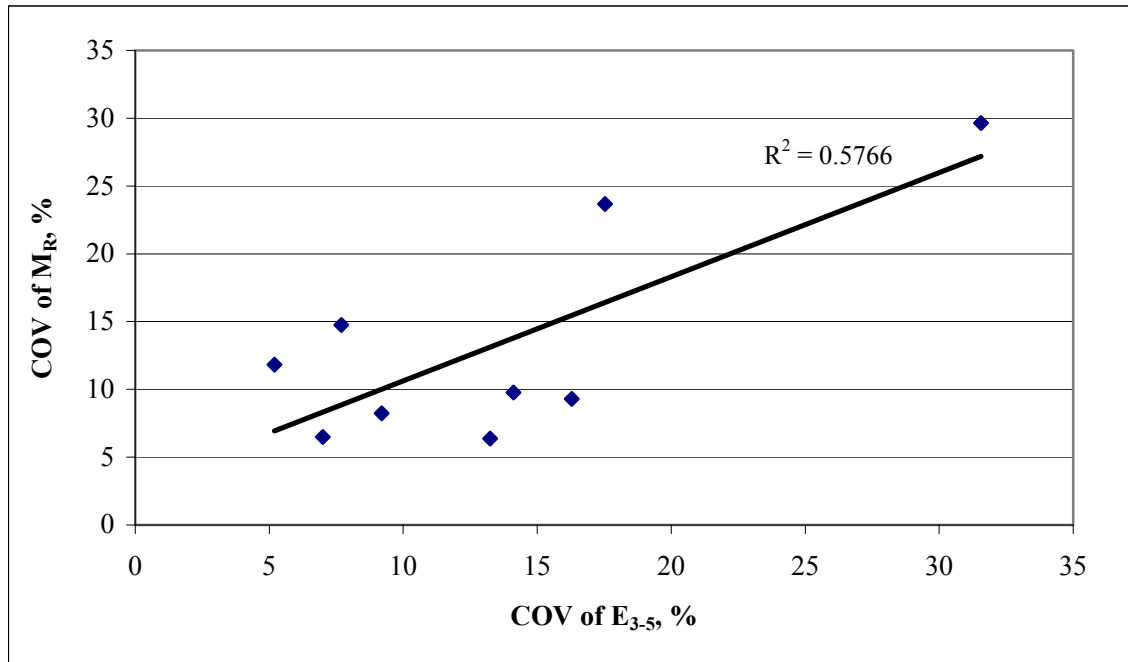


Figure 4.5 Coefficient of Variation of E_{3-5} Plotted Against Coefficient of Variation of M_R of Nine Sections, 18-in. (450-mm) Plate

For the sake of brevity, this plot is not presented here. As can be verified in *Figure 4.5*, the COVs of E_{3-5} and M_R , utilizing all nine stations, is close to one-to-one, with a satisfactory R-square value of 0.58. That the COVs of both moduli are nearly identical attests to the fact that the variation resulted more from spatial variation than from test errors.

Another point is in regards to the COVs of either the FWD or TP46 Test methods: Generally speaking, as succeeding layers are constructed above the subgrade, the COV of the subgrade (derived from FWD tests) becomes less and less. On the other hand, what starts out as a relatively large COV ends up with a relatively large COV as well (though not as large as each

succeeding layer is placed). In other words, the COVs “track” one another, from one layer to the next, but as expected, the relation is not one-to-one. This is probably due to a variety of reasons, including but not limited to greater confining pressures, lower deviator stresses, decrease in moisture content, and post-consolidation. With PCC pavements, the “evening out” of the subgrade modulus is especially pronounced. The end result of all this is an even more conservative pavement design, whether one uses the FWD or TP46 test method for subgrade characterization.

4.8 PREDICTION OF DESIGN RESILIENT MODULUS EMPLOYING FWD-MODULUS E_1 AND/OR E_{3-5}

4.8.1 General

As discussed in a previous section, only resilient modulus of the first sample, extracted from a depth of 0-12 in. (0-30 mm), will be employed for correlation with elastic modulus. Again, justification for simultaneously using the first sensor modulus, E_1 , and the average of third to fifth sensor modulus, E_{3-5} , are presented in section 4.7.2. First, station-by-station resilient modulus is correlated to corresponding elastic modulus, E_1 or E_{3-5} . Second, section average M_R is correlated to section average E_1 or E_{3-5} .

In order to arrive at a representative design resilient modulus from FWD elastic modulus, three different methods are proposed and critiqued. First, a linear relation is touted between elastic modulus E_1 and resilient modulus M_R of the first sample. Second, a one-to-one relationship between the aforementioned two moduli are postulated with E_{3-5} complimenting the selection procedure. Third, two power equations are proposed: (i) relating M_R and E_1 , and (ii) relating M_R and E_{3-5} , both concurrently deciding design resilient modulus.

4.8.2 Linear Relation between E_1 and M_R

Now, we have seven elastic moduli corresponding to each sensor deflection of a FWD test. Encouraged by the recent work of LTPP (39), it was decided to correlate E_1 with M_R directly. In all of the ensuing analysis, M_R values of first sample, tabulated in column 3 of *Table 4.4* will be used. Another issue is why first sensor modulus? Because the first sensor deflection reflects the entire subgrade as opposed to the offset sensors, each of which characterizes only a partial depth of the subgrade. In other words, the offset sensors capture only a part of the subgrade material, in contrast to the first sensor, which captures the entire subgrade.

A simple linear relationship is sought with all of the data pairs (34 in total using 18-in. (450-mm) load plate) from nine test sections. The scatter plot shown in *Figure 4.6* has a satisfactory coefficient of determination ($R^2 = 0.56$); however, the best-fit line does not pass through the origin, a necessary physical condition that elastic modulus and resilient modulus each be zero at the limit. Instead, the best-fit line results in an intercept, signifying that when elastic modulus is zero, resilient modulus could have a value of $\approx 10,000$ psi (70 MPa). A recent LTPP study (39) reported a similar intercept in their correlation analysis. Another plot with the same resilient modulus and elastic modulus resulting from the 12-in. (300-mm) plate is now prepared (see *Figure 4.7*), to note that the best-fit line again does not go through the origin. Interestingly, identical intercepts have been observed with each load plate results, so also indistinguishable confidence intervals.

Another plot is prepared where section average E_1 (average of nine stations) is related to section average M_R (see *Figure 4.8*). The R-squared value is improved (increased from 0.56 to 0.82) and the best-fit line slightly closer to the origin, nonetheless, with an intercept of $\approx 8,000$

psi

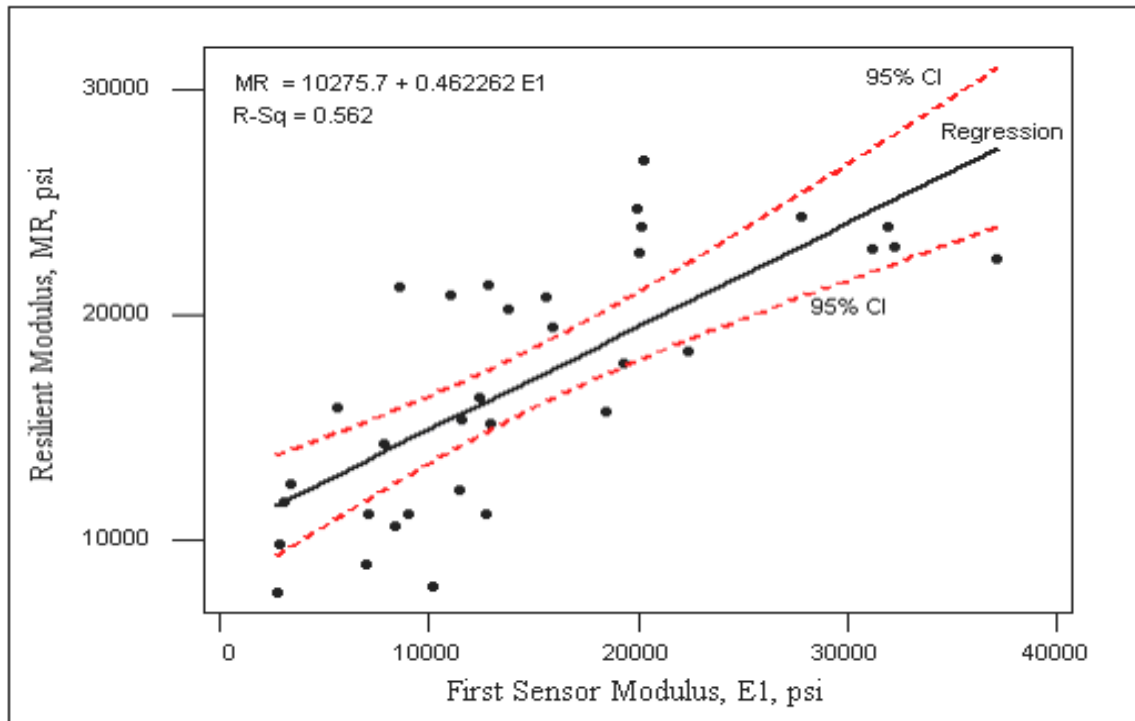


Figure 4.6 Scatter Plot of Station-by-Station Values of E_1 and M_R , Nine Sections, 18-in. (450-mm) Plate, 1 psi = 6.89 kPa

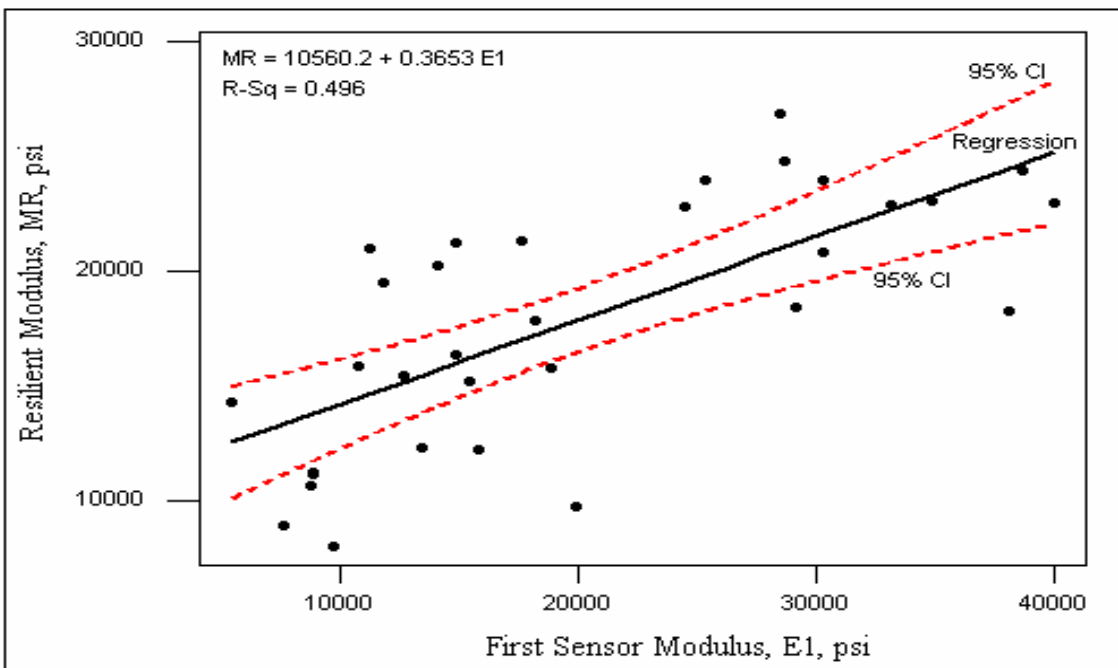


Figure 4.7 Scatter Plot of Station-by-Station Values of E_1 and M_R , Eight Sections,

(Section 1 Not Included), 12-in. (300-mm) Plate, 1 psi = 6.89 kPa

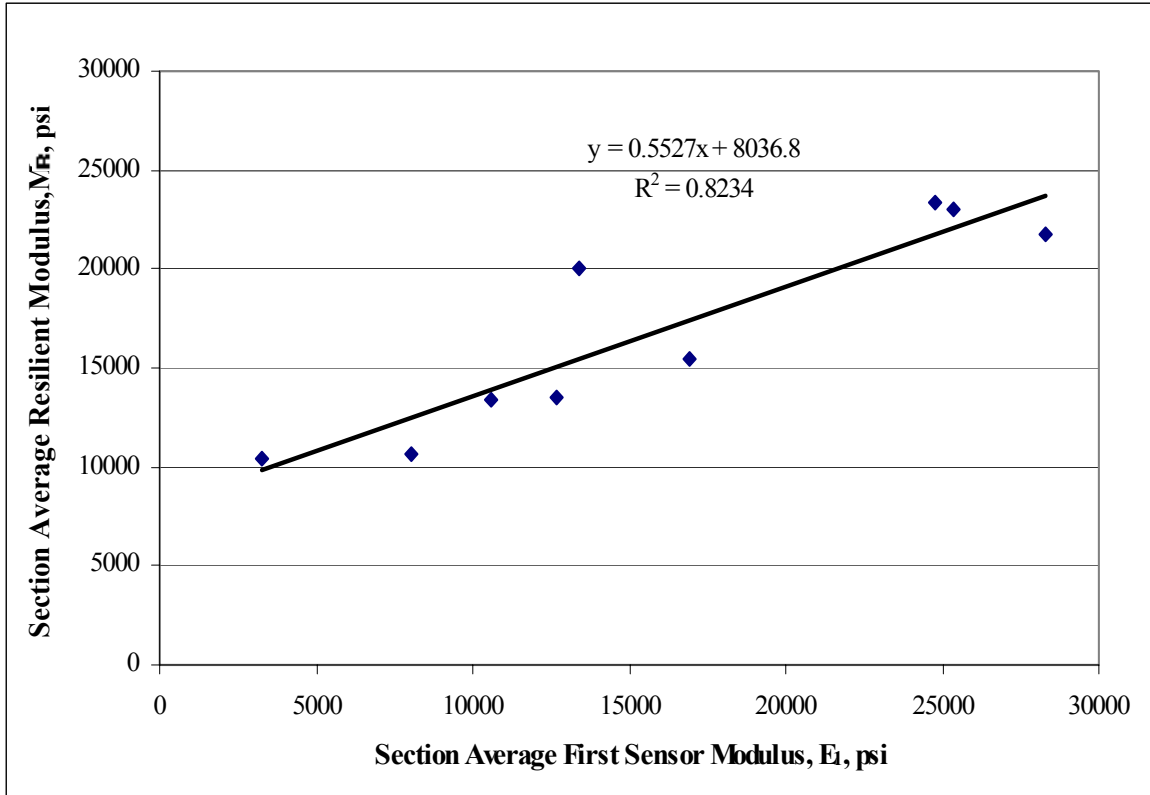


Figure 4.8 Scatter Plot of Section Average E_1 vs. Section Average M_R , Nine Sections, 18-in. (450-mm) Plate, 1 psi = 6.89 kPa

(55 MPa). The reason for this anomaly could be that the TP46 test procedure causes the material under test to be better confined than what the material would experience when the FWD load is dropped. For very weak soils, this may pose a limitation in using the FWD test method, especially using the center deflection. Because the offset sensor deflections are hardly influenced by the top layer of subgrade, which in all probability is poorly confined, the modulus calculated from those sensors should be more stable. In other words, for reasonably stiff soils first sensor modulus may be appropriate; however, for soft soils, one or an average of some of the offset sensors would be the right choice.

A close scrutiny of the data suggests that it was the low-stiffness sections, especially #1 and #3 (respectively, with E_1 values 3240 psi and 8060 psi (22 MPa and 56 MPa) that

precipitated the large intercept on the resilient modulus ordinate. Note that the ADCP tests suggest that those two sections have a soft layer underlain by a stiff layer, allegedly the reason for relatively low elastic modulus. Asserting that the first sensor moduli of sections #1 and #3 are less reliable than the rest, another scatter plot, along with a best-fit-line, is prepared (using only data of 7 sections), only to note that the intercept still persists, though smaller than 8000 psi (55 MPa). For brevity, that plot is not presented in this report.

Of the three alternate relations discussed herein, the section average plot in *Figure 4.8* may be promoted in view of its large R^2 value. With the first sensor modulus calculated from the FWD test results, a corresponding resilient modulus may be estimated from *Figure 4.8*.

4.8.3 Linear Relation between E_{3-5} and M_R

With a dubious relation between E_1 and M_R , for the reason that the best-fit-line is unable to pass through the origin, another relation is sought for, between E_{3-5} and M_R , using only section averages. The best-fit-line for this plot also fails to pass through the origin, but the resulting intercept is relatively small (see *Figure 4.9*). That the R^2 value decreased from that of the $E_1 - M_R$ plot in *Figure 4.8*, plus the fact that the best-fit-line does not pass through the origin, diminishes the usefulness of this relation. Also, for the reason that offset moduli cannot capture the top layers of the subgrade, its viability as a stand-alone parameter is suspect. Therefore, an E_{3-5} vs. M_R linear relation cannot be promoted. By necessity, therefore, the physical condition, that the best-fit-line results in zero intercept, is introduced in the data analysis, the results of which constitutes the next section.

4.8.4 One-to-One Relation between E_1 and M_R

The same E_1 data in *Figure 4.8* is replotted in *Figure 4.10*, seeking a best-fit-line with zero intercept. Note the best-fit-regression line is, for all practical purposes, a virtual 45° line,

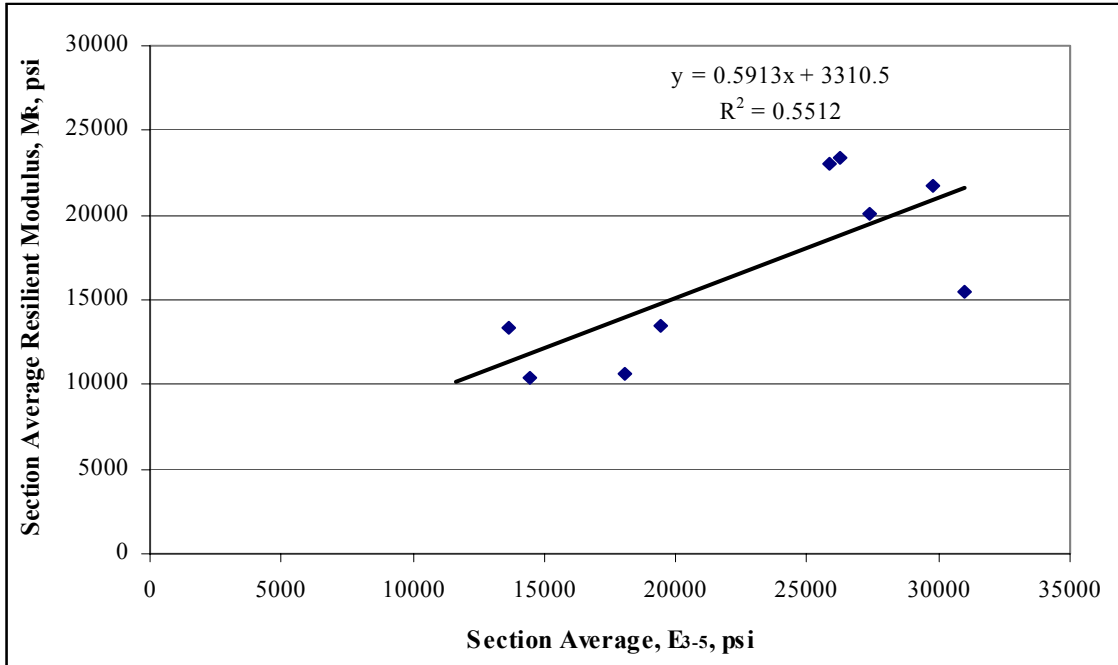


Figure 4.9 Scatter Plot of Section Average E_{3-5} vs. Section Average M_R , Nine Sections, 18-in. (450-mm) Plate, 1 psi = 6.89 kPa

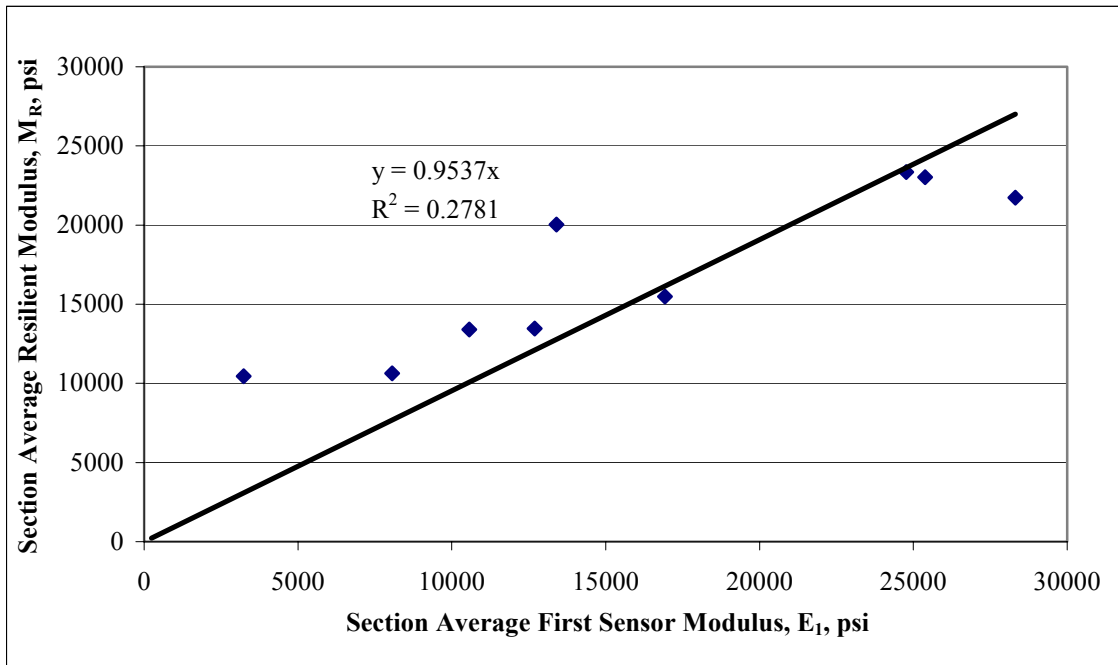


Figure 4.10 Scatter Plot of Section Average E_1 vs. Section Average M_R , Nine Sections, 18-in. (450-mm) Plate, Intercept Zero, 1 psi = 6.89 kPa

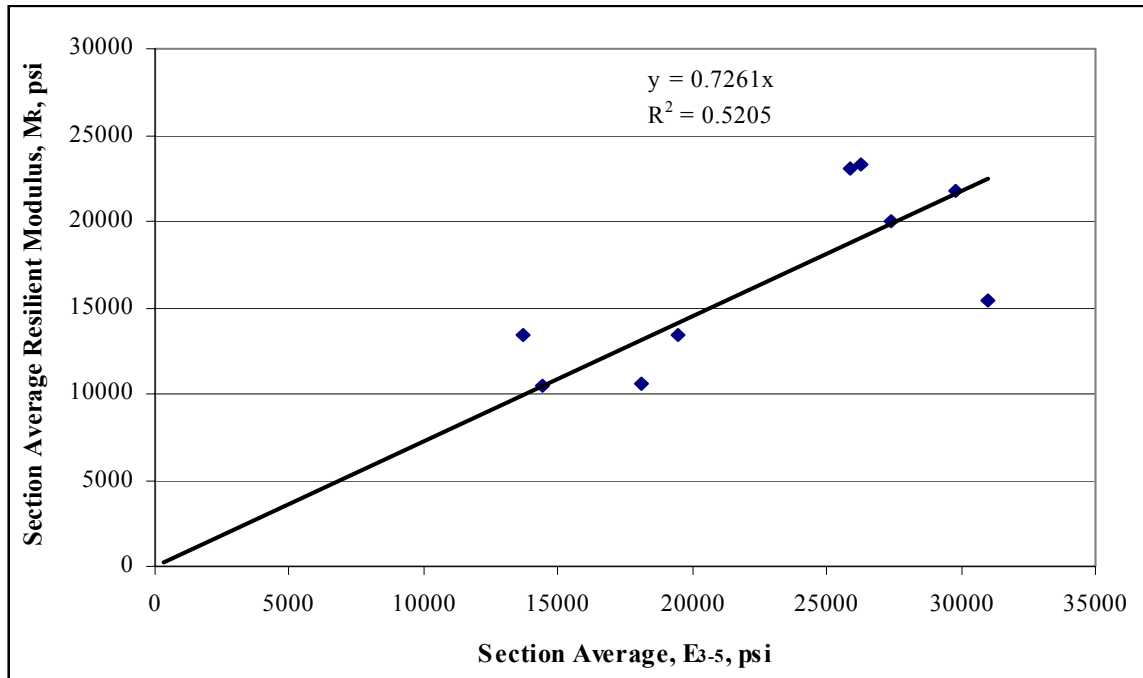


Figure 4.11 Scatter Plot of Section Average E_{3-5} vs. Section Average M_R , Nine Sections, 18-in. (450-mm) Plate, Intercept Zero, 1 psi = 6.89 kPa

though with marginal R-square. A close scrutiny of the data points suggests a reasonable one-to-one relation between E_1 and M_R , especially in the middle range, namely between 9,000 psi (62 MPa) and 25,000 psi (172 MPa). A similar plot of E_{3-5} vs. M_R , presented in *Figure 4.11*, deviates further from a one-to-one relation in comparison to that in *Figure 4.10*, however, with an improved R^2 value (0.28 vs. 0.52). Encouraged by the LTPP study (39), relating E_1 and M_R , a one-to-one relation between those two variables is pursued herein. In promoting the relation for data plotted in *Figure 4.10*, it is tantamount that both low and high ends of the relation be adequately represented. For moderately soft soils, FWD first sensor modulus tends to become small and generally with high variability, primarily due to test errors. Therefore, it is proposed that E_1 be substituted by E_{3-5} , signifying $E_{3-5} = M_R$, extending the one-to-one relation below 9,000 psi (62 MPa). E_{3-5} is believed to infer a test result under more confined conditions, and, therefore, preferred in soft subgrade. At the upper reach, namely when E_1 exceeds 25,000 psi

(172 MPa), especially in stiff soils, M_R becomes asymptotic, showing fair agreement with the lesser of E_1 and E_{3-5} . In summary, some evidence promotes a one-to-one relation between E_1 and M_R , where for the two extreme reaches (lower and upper), E_1 is replaced by E_{3-5} when $E_1 < 9,000$ psi, and the lesser of E_1 and E_{3-5} when $E_1 > 25,000$ psi. With a substantial range of data satisfying a 1:1 relation, this method is promoted for “quick” and “dirty” calculation of “design resilient modulus. A five-step procedure is listed here for general use:

1. Calculate station- E_1 and $-E_{3-5}$ or averages if replicate tests are performed. Respectively, *Equations 2.9 and 3.1* will be used in conjunction with FWD sensor deflection data and (suggested) Poisson’s ratio range of 0.4 to 0.45.
2. If station (average) E_1 is less than 9,000 psi, utilize station (average) E_{3-5} as design resilient modulus.
3. If E_1 is equal or larger than 9,000 psi and less than 25,000 psi, choose E_1 as design resilient modulus.
4. If station (average) E_1 is equal or larger than 25,000 psi, choose the lesser of averages E_1 and E_{3-5} as the design resilient modulus, limiting resilient modulus for design to 35,000 psi (240 MPa).
5. The section average resilient modulus calculated from station values, selected from step 2, 3, or 4 shall be reported along with the section standard deviation.

4.8.5 Resilient Modulus Prediction Using Both E_1 and E_{3-5}

Though there seems to be a piecewise one-to-one relation between E_1 or E_{3-5} and M_R , it lacks generality for having to include ad hoc assumptions in both soft soils and very stiff soils. Realizing that the best-fit-line, for any viable relation should pass through the origin and also satisfy asymptotic trend at higher end of the trend line, other model forms were tried, for

example, a power equation. The scatter plots in *Figure 4.12* include two sets of data points from all nine sections, with the best-fit power curves depicting the two relations. The R^2 value is only minimally improved from a linear relation, for example, 0.56 to 0.58 for E_1 vs. M_R . However, the physically intuitive condition is satisfied, namely, both E_1 or E_{3-5} and M_R identically approach zero.

It may be of interest to the reader to assess the robustness of the two plots in *Figure 4.12*.

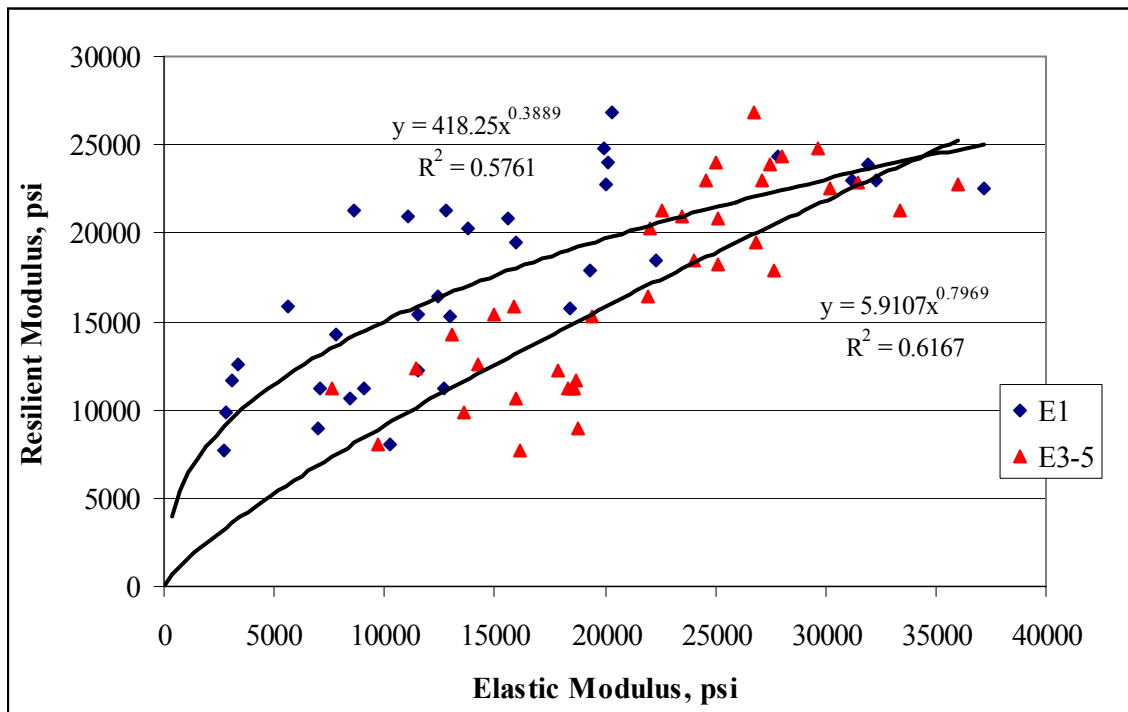


Figure 4.12 E_1 and E_{3-5} Each Plotted Against Resilient Modulus M_R , (Station-by-Station Values), Nine Sections, 18-in. (450-mm) Plate, 1 psi = 6.89 kPa

With this in mind, 95 percent confidence intervals are determined for the two best-fit-curves. For each relation, confidence levels are plotted in separate figures (see *Figures 4.13 and 4.14*) to avoid crowding.

Instead of relating station-by-station data, section averages are graphed, and the resulting scatter plots and best-fit-lines are presented in *Figure 4.15*. The R^2 -value of both plots are

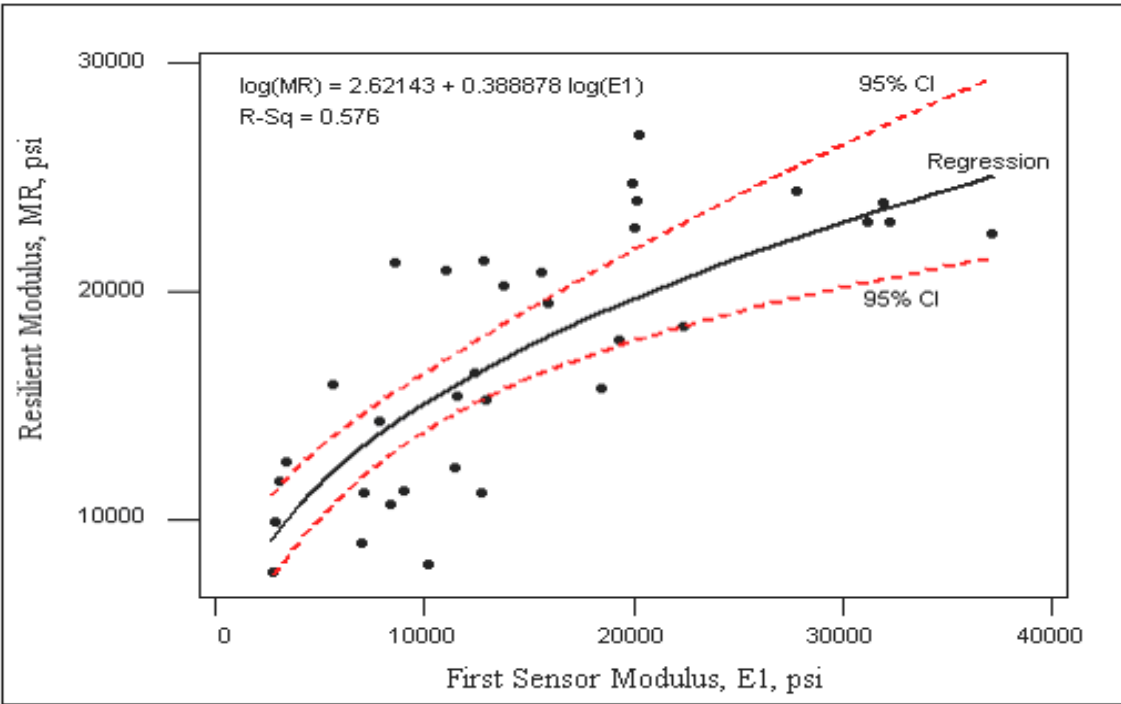


Figure 4.13 Scatter Plot of Station-by-Station Values of E_1 and M_R , 18-in. (450-mm) Plate, 1 psi = 6.89 kPa

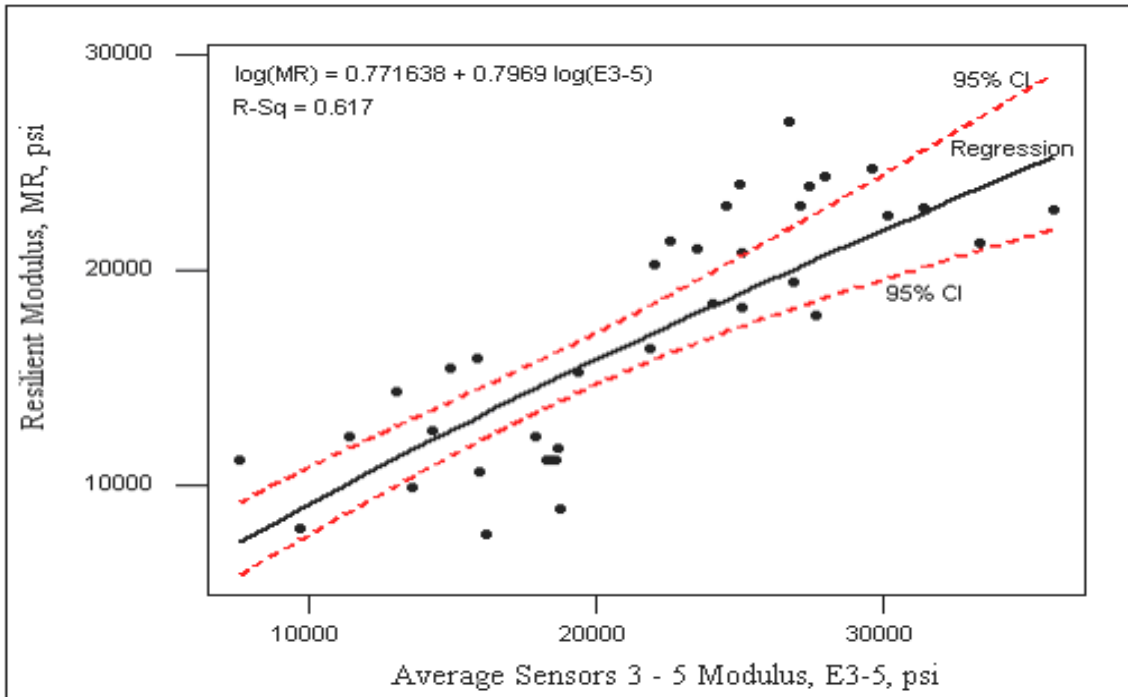


Figure 4.14 Scatter Plot of Average Modulus of Sensors 3-5 vs. Resilient Modulus, 18-in. (450-mm) Plate, 1 psi = 6.89 kPa

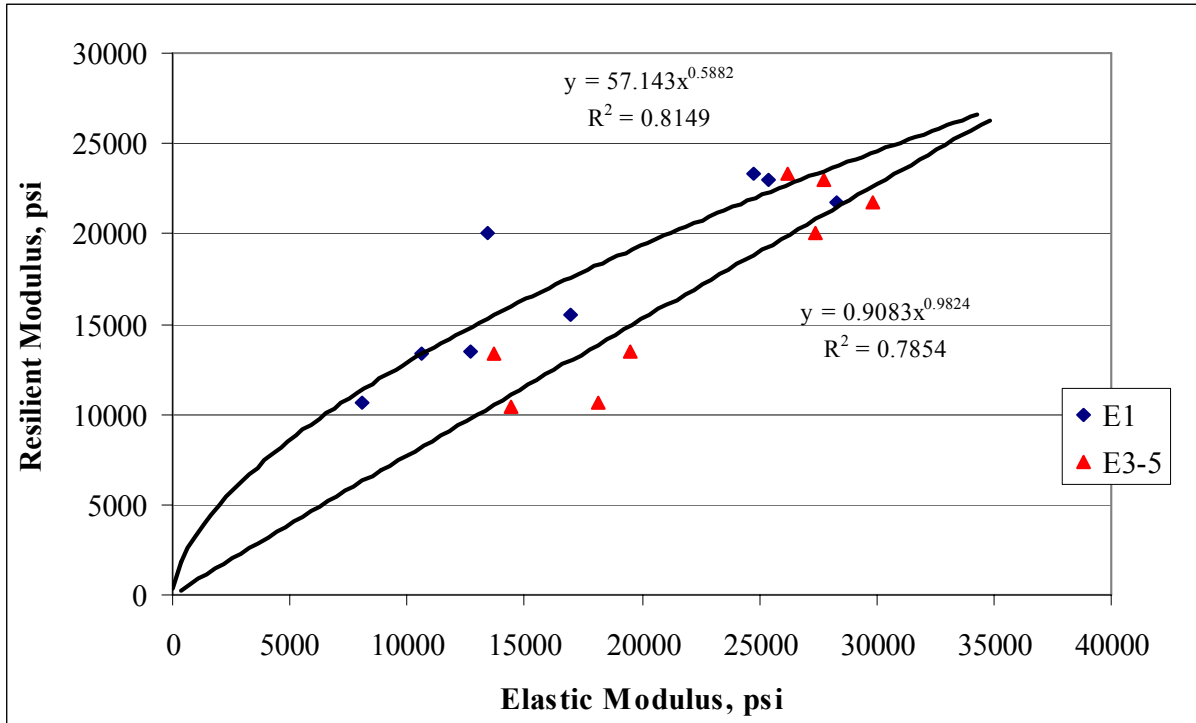


Figure 4.15 Section Averages E_1 and E_{3-5} , Each Plotted Against Average Resilient Modulus M_R , Eight Sections, 18-in. (450-mm) Plate, Section 1 Deleted in E_1 vs. M_R Plot & Section 5 Deleted in E_{3-5} vs. M_R Plot, 1 psi = 6.89 kPa

significantly improved with section averages. It is also interesting to note that E_{3-5} vs. M_R obeys a straight-line relationship, as judged from the power of the equation being close to unity. Yet another point of interest is that linear and power relations suggest M_R to be a constant ratio of E_{3-5} , respectively, 73 and slightly lower than 91 percent (see *Figures 4.11 and 4.15*).

A question now arises as to whether one of the relationships (either E_1 vs. M_R or E_{3-5} vs. M_R) would suffice to derive a design resilient modulus or if both should enter in the decision process. As was discussed in connection with the ADCP results, subgrade soils can be homogeneous and isotropic, or completely heterogeneous, or anything in between. Convincing results are presented to postulate that when a soft layer overlies a relatively stiff layer, E_1 is smaller than E_{3-5} . Lack of confinement of loose surface material in case of soft deposits could be a reason for E_1 being smaller than E_{3-5} , though this situation would improve with the

pavement overburden. It would, therefore, appear that E_1 for soft-over-stiff system or a completely soft system can be unreliable, while, as the test data suggests, E_3 , E_4 and E_5 are reasonably uniform, and show minor variation with different load levels. For homogeneous subgrades, with practically no layering, E_1 is close to E_{3-5} and shows negligible variation with load levels as well. Another scenario that may be of interest would be to present itself with a stiff layer atop a soft layer, in which case E_1 could be equal or slightly larger than those resulting from the offset sensors, E_{3-5} . Simply put, E_1 could be different from E_{3-5} depending on the homogeneity of the deposit and also the vertical profile, for example, soft-over-stiff or stiff-over-soft configuration.

Why the layer configuration affects E_1 and E_{3-5} differently warrants some discussion. Based on the load dispersion concept, it is clear that each sensor response is affected by material at different depths. Put it differently, the depth of layers sampled by each sensor is different depending on its distance from the load (FWD plate). Sensor 1 captures the properties of the entire subgrade (to a depth of say 3 to 4 ft.), as contrasted by offset sensors E_3 , E_4 , and E_5 , which characterize only lower reaches with no contribution from surface material. Recognizing that $E_1 < E_{3-5}$ or $E_1 \geq E_{3-5}$, a logical approach would be to employ both E_1 and E_{3-5} in the decision process, that is, make use of both E_1 vs. M_R and E_{3-5} vs. M_R relationships. With this premise only, *Figures 4.12 and 4.15* are prepared each with two relationships, where E_1 is graphed against M_R and a second plot where E_{3-5} is plotted against the same M_R .

How does one select a design resilient modulus from the two equations (or graphical plots) in *Figure 4.15*? The two representative elastic moduli, E_1 and E_{3-5} , in *Figure 4.15* capture subgrade properties at different depths; nonetheless, they are related. In fact, they must be equal under ideal conditions. A conservative approach, therefore, would be to calculate two M_R -

values, one employing E_1 and another employing E_{3-5} , and subsequently choose the lower of the two M_R values as the design resilient modulus. Accordingly, a step-by-step procedure is presented as follows:

- (i) Based on the FWD deflection tests, calculate for each station E_1 and E_{3-5} .
- (ii) With E_1 and E_{3-5} , employing the respective equations in *Figure 4.15*, calculate two M_R values (for each station).
- (iii) Choose the lower of the two M_R -values as the design resilient modulus for each station.
- (iv) With the design resilient modulus of each station computed, the mean and standard deviation of each section (or subsections or homogeneous units as the case may be) are calculated, employing them for design. (Software to subdivide the section into homogeneous units will be described in a later section).

4.9 THREE RESILIENT MODULUS PREDICTION METHODS CRITIQUED

Relying on the three regression relations, *Figures 4.8, 4.10 and 4.15*, and employing elastic modulus E_1 and E_{3-5} from FWD tests, the design resilient modulus for the nine sections are predicted and listed in *Table 4.11* along with the first-foot Shelby tube M_R values.

Table 4.11 Predicted Resilient Modulus Compared with Experimental Value

Section #	Average TP46-MR, First Sample, psi	Predicted Resilient Modulus, psi		
		Linear Relation, Figure 4.8	1:1 Relation, Section 4.8.4	Power Relation, Figure 4.15
1	10450	9830	14410	6640
2	13400	13880	10570	10220
3	10630	12490	18100	11340
4	20040	15440	13400	15290
5	15480	17390	16920	17540
6	12360	15050	12690	14810
7	23340	21730	24770	19930
8	23020	22060	25380	21070
9	21730	23680	28310	22580

1psi = 6.89 kPa

The resilient modulus predicted by linear relation is in good agreement with the laboratory M_R . Despite good predictions, the relation violates a necessary physical boundary condition that both moduli should approach zero identically. Instead, with the first sensor elastic modulus zero, a resilient modulus in excess of 10,000 psi (70 MPa) is predicted. In soft soils, therefore, this resilient modulus prediction is suspect. The viability of linear model is questionable, because of its inability to make reasonable M_R predictions for a range of soils.

As indicated at the outset, the one-to-one relation predicts reasonable design resilient modulus, should the subgrade tested be homogeneous and moderately stiff. Due in part to the top stiff surface layer perhaps, the resilient moduli of sections #3, and #9 are overpredicted. While testing a subgrade with a soft layer overlying a stiff layer, as in section #4, the resilient modulus is underpredicted, however, (20,040 psi (138 MPa) vs. 12,780 psi (88 MPa)). With a soft top layer why section #1 departed from under-prediction is still not clear. These differences in resilient moduli arise from the fact that the overall response under the FWD test and the TP46 test happen to be different, attributable to the non-homogeneity of the subgrade and nonlinearity of soil. To summarize, though a one-to-one relation is preferred for its simplicity, when implementing that relationship in low stiffness soils, the resilient modulus prediction becomes ad hoc for the reason that E_1 needs to be replaced by E_{3-5} . Replacing E_1 by E_{3-5} can give rise to overprediction of resilient moduli, as we note in sections #1 and #3. One also has to contend with the likelihood of overprediction of resilient modulus in stiff soils.

Compared to linear and one-to-one relations, the power relation makes fewer assumptions in predicting design resilient modulus from FWD elastic modulus, E_1 and E_{3-5} . Employing E_1 and E_{3-5} , resilient modulus values are computed and the lesser of the two is selected as the design value. Relying on both E_1 and E_{3-5} in predicting a representative resilient modulus is desirable

for the following reasons: First, the subgrade can seldom be homogeneous. In soft soils or soft soil atop a stiff soil, E_1 is generally smaller than E_{3-5} . However, if the soil deposit is stiff, despite possible layering (that is, slight variations in stiffness with depth), E_1 tends to be comparable to E_{3-5} . Realizing that E_1 and E_{3-5} are affected by layering, which seldom is known during FWD test, an argument may be made in employing both E_1 and E_{3-5} . Should the two M_R values be different, the lesser of the two is selected, resulting in a conservative design. Note, no ad hoc assumptions are introduced in selecting a probable resilient modulus for the subgrade, and finally the design modulus. Second, in high stiffness soils, the resilient modulus is not over predicted. The leveling off of the E_1 vs. M_R curve ensures that high FWD elastic moduli do not result in large predicted M_R values. The fact that the two curves cross over at approximately 35,000 psi (241 MPa) beyond which E_1 surpassing E_{3-5} agrees with our field results. A stiff or stiff atop a soft soil resulting in E_1 equal to or larger than E_{3-5} is a relevant finding in this regard. Typical examples being sections #7, #8 and #9, where E_1 is close to E_{3-5} , though not slightly larger. Third, this method gives better correlation than that of one-to-one relation and as good a correlation as linear method as indicated by the R-squared values (*Figures 4.8, 4.10 and 4.15*). In addition, it satisfies the intuitive physical condition as well. This method where E_1 and E_{3-5} are both contributing to the selection of design resilient modulus is by far our recommendation.

4.10 DATA ANALYSIS SOFTWARE

The task at hand in determining a design resilient modulus for new pavement design starts with FWD tests followed by an analysis of deflection data. Each subgrade section tested may show substantial spatial variation in response (deflection) and, in turn, modulus, so that the section in question may, in effect, comprise one or more uniform sections or homogeneous units. A software program to perform these two tasks--namely, data reduction and subsectioning, if

warranted--is developed as a part of this study, the details of which can be seen in Chapter 5. This program, following the calculation of elastic modulus from FWD deflection data, estimates station-by-station resilient modulus utilizing elastic modulus. With the resilient modulus, we employ cumulative difference approach technique (2) for testing and delineating homogeneous units for the subgrade in question. By way of output, the program prints out the length of each uniform section, the mean and standard deviation of design resilient modulus for each uniform section, and a resilient modulus of each station plotted with distance along the road.

4.11 SUMMARY

With the objective of correlating FWD-based elastic modulus with resilient modulus from TP46 results, the two sets of data obtained from nine test sections are scrutinized ensuring that the data is reasonable in view of the unique nature of (for example, layering) each subgrade section. Whether the sampling (by Shelby tube) has any effect on resilient modulus test results is discussed. A side-by-side test with two plate sizes and two sensor tip sizes led us to select an 18-in. plate and standard 10 mm tip for subgrade investigation. In selecting the appropriate resilient modulus value, the stress dependency of modulus is taken into account. After a discussion of elastic modulus computed from seven deflection sensors, a decision has been made to use both E_1 (first sensor modulus) and the offset sensor modulus E_{3-5} (average of third, fourth, and fifth sensor modulus), seeking independent correlations with M_R .

Of the three procedures described to estimate probable resilient modulus for a test station, the recommended procedure employs both E_1 and E_{3-5} sequentially, choosing the lesser resilient modulus for design purpose. A software program titled FWDSUBGRADE, developed as a part of this study, performs all of the calculations, and identifies subsections, if any, in the section in question. A detailed discussion of this program will be presented in Chapter 5.

CHAPTER 5

PLANNING FWD TEST AND CALCULATION OF DESIGN RESILIENT MODULUS

5.1 OVERVIEW

A methodology for choosing a design resilient modulus, relying on FWD test deflections and corresponding elastic modulus, has been the topic of Chapter 4. Planning FWD test and collecting field data is an important component that supports this methodology. A brief description of FWD test configuration and advance field preparation will be covered in the first part of the chapter. Each subgrade project under consideration may be a fraction of a mile or a few miles in length. Inherent spatial variation along the road shall be recognized. And, if the variation of modulus is statistically significant, the project should be divided into subsections or homogeneous units, as described in the second part of this chapter. Included in the third part of this chapter is a brief description of the exclusive computer program, FWDSUBGRADE, for arriving at homogeneous unit(s), if warranted.

5.2 PLANNING FWD TEST IN THE FIELD

The field test shall be planned with extreme care ensuring that data collected from FWD tests be minimally affected by spatial variations in the field. The planning of the field test includes the following:

1. Equipment selection
2. When and where to test?
3. Validation of deflection data

Data collected during the FWD test include the load applied and the resulting peak sensor deflections. A validation procedure of deflection data is included in section 3.2.1 and is

implemented in the computer program described in the latter part of this chapter. It entails checking each deflection basin for negative slopes. That is, the sensor deflection shall not increase as the sensor distance from the load center increases.

5.2.1 Equipment Selection

A FWD with a seven-sensor configuration shall be used for the field deflection study. A load package inducing a load of $2,500 \pm 100$ pounds is recommended. An 18-in. (450-mm) load plate is preferred for subgrade testing. The velocity sensor spacing shall be adjusted such that they are positioned with one at the center of the load plate and the remaining six sensors at 12 in. (305 mm), 18 in. (457 mm), 24 in. (610 mm), 36 in. (914 mm), 48 in. (1219 mm), and 60 in. (1524 mm), respectively, from the center of the plate.

5.2.1.1 Test Procedure

At each station two seating loads followed by three or more load drops of $2,500 \pm$ pounds shall be applied. The peak load and peak deflection of each sensor (total of seven sensors) shall be monitored and recorded, with the data collection repeated for all of the load repetitions (except for the two seating loads). Tests shall be repeated at constant intervals (or uniform spacing) along the road till the end of the proposed subgrade. Because FWDSUBGRADE software does not use the beginning station modulus, it shall not be tested; however, the last station (or the project end) must be tested, regardless if the last section is equal to or smaller than the predetermined interval. Though the test interval (spacing) is left to the discretion of the project engineer, based on the precision required and practicality, a test interval of 50 ft. (15 m) is recommended.

5.2.2 When and Where to Test?

Subgrade soil, though compacted to specified density and moisture, could become soft should it absorb excessive moisture resulting from precipitation for an extended period of time. Likewise, it could become hard if the soil becomes dry, as can be expected during a long drought. Additionally, some coarse-grain soils could lose strength when subject to extreme drought. For these reasons, it is important to schedule FWD testing when the moisture of the subgrade is close to optimum moisture. Approximately, the moisture during tests shall be within the upper limit of optimum moisture +2 percent, and the lower limit of 75 percent of optimum.

Test locations along the road shall be so chosen as to avoid loose surface material and wheel ruts due to construction traffic. Uneven subgrade surface could result in load plate not being seated properly giving rise to asymmetrical stress distribution affecting sensor deflections. Loose surface material also affects the sensor deflections. Experience suggests that loose particulate material shifts while the load is being dropped. *Figure 4.4* is an illustration of a sensor imprint where coarse loose particles congregate around the sensor tip, caused primarily by vibration due to impacting load. If subgrade to be tested is uneven and/or rutted, it shall be bladed and lightly recompact before FWD testing to ensure a reasonably smooth surface for proper seating of the plate, and the sensors, as well. Finally, test locations shall be aligned such that they are within 10 ft. of the centerline of the paved surface for 14 ft. wide lanes or 8 ft. for 12 ft. wide lanes.

5.3 SELECTION OF DESIGN UNIT

When considering a reasonably large pavement project, deflections along the prepared subgrade and, in turn, the moduli could experience changes of large magnitude signaling statistically different units within a given project. Frequently, the engineer must rely on the

analysis of a measured pavement response variable (e.g., modulus) for unit delineation. The designer could develop a plot of the measured response variable as a function of the distance along the project. This can be done manually or through computerized data analysis-graphic systems. To illustrate the approach, the problem of sectioning a highway based on friction

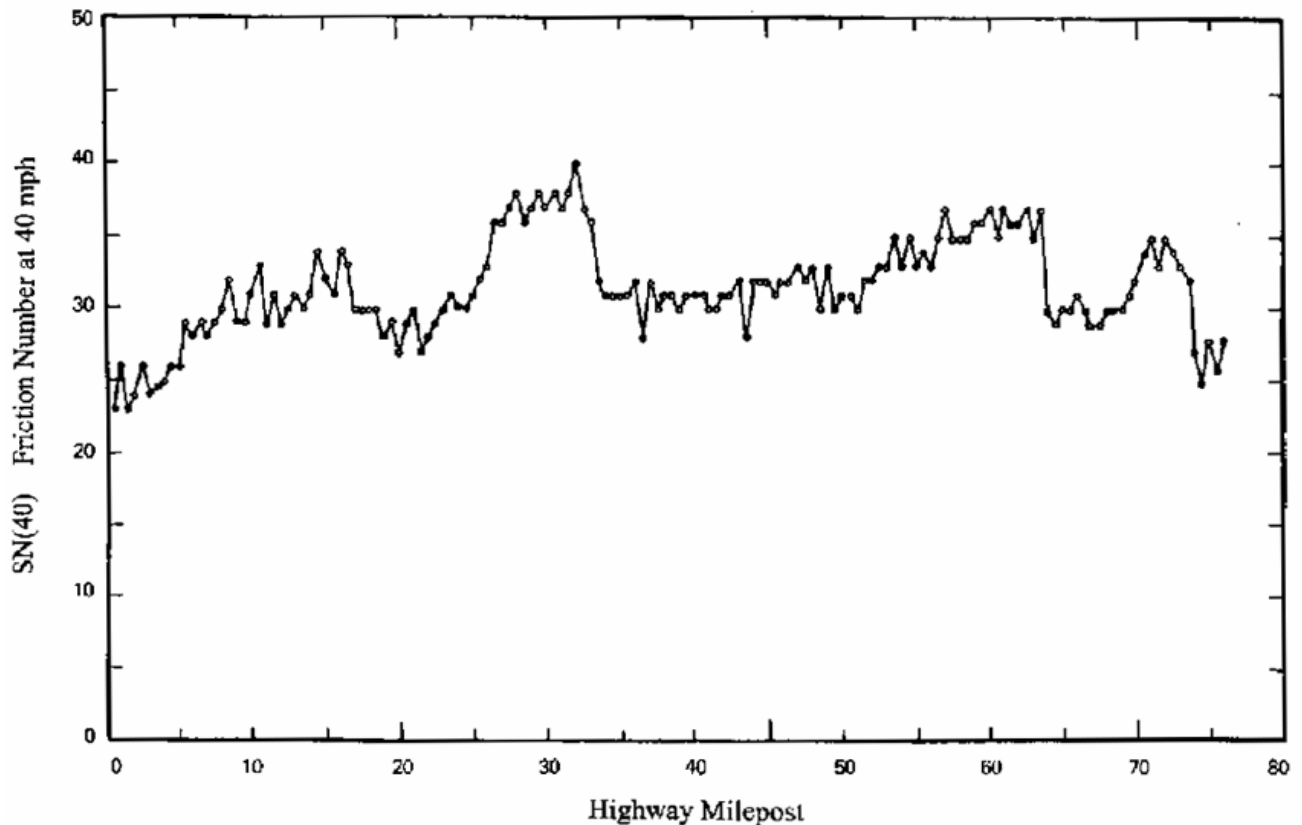


Figure 5.1 FN(40) Results versus Distance Along Project (Adapted From Reference 2)

number (FN (40)) is included herein. *Figure 5.1* is a plot of friction number results, FN (40), versus station number along an actual highway system. The proposed methodology is adopted from reference 2.

Once the plot of a pavement response variable has been generated, it may be used to delineate units through several methods. The simplest of these is visual examination to subjectively determine where relatively unique units occur. In addition, several analytical

methods are available to help delineate units, with the recommended procedure being the “cumulative difference.” This analytical procedure, readily adaptable to computerized evaluation, relies on the simple mathematical fact that when the variable Z_c (defined as the difference between the area under the response curve at any distance and the total area developed from the overall project average response at the same distance) is plotted as a function of distance along the project, unit boundaries occur at the location where the slopes (Z_c vs distance) change sign. *Figure 5.2* is a plot of the cumulative difference variable (Z_c) for the data shown in *Figure 5.1*. For this example, 11 preliminary analysis units are defined. The engineer must then evaluate the resulting length of each unit to determine whether two or more units should be combined for practical construction considerations and economic reasons. The combination of units should be done relative to the sensitivity of the mean response values for each unit upon performance of future designs.

5.4 COMPUTER PROGRAM, FWDSUBGRADE, TO CALCULATE DESIGN MODULUS

As alluded to before, the program, FWDSUBGRADE, performs two major tasks in arriving at a design modulus. First, accepting deflection data, it calculates elastic modulus and, in turn, derives resilient modulus of soil at each station. Employing these station-by-station moduli in an analytical procedure known as cumulative difference, the program delineates homogeneous units, outputting the length of each unit (in the event of identifying multiple units) and the corresponding resilient moduli – both mean and standard deviation – which shall form the design resilient moduli. The logic of these operations is presented in the flow chart in *Figure 5.3*. Detailed operations of the program can be seen in *Appendix D*.

Note the output of the program includes a plot of the resilient modulus at each station as a function of distance along the project. This plot should serve as a guide in combining adjacent units to form “design units.” Practical construction considerations and economic reasons likely

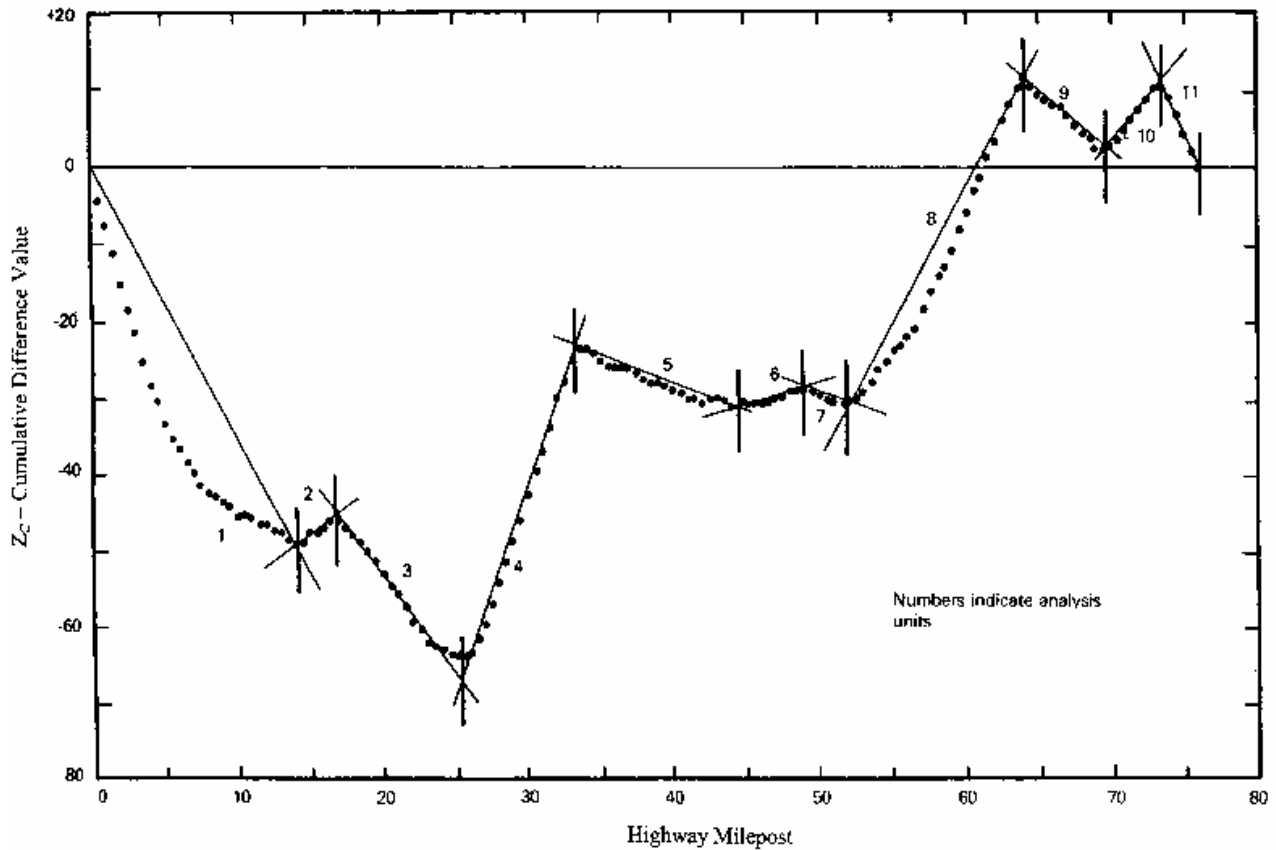


**Figure 5.2 Delineating Analysis Units by Cumulative Difference Approach
(Adapted From Reference 2)**

govern these decisions. For example, should there be short sections of relatively soft material, they shall be upgraded with additives (cement, lime, lime-fly ash, etc.) to facilitate merger with contiguous homogeneous units.

5.5 SUMMARY

Planning the FWD test in the field, including equipment selection and site preparation for subgrade deflection measurements, is described. Test specifics, for example, seating load and

repetitions required, are also a part of this discussion. With the calculated modulus response in each project, a methodology for unit delineation is presented. Finally, a flow chart outlining the operations necessary to accept FWD deflection data and to output homogeneous units (with boundaries identified) and corresponding design modulus constitute the last section of this chapter.

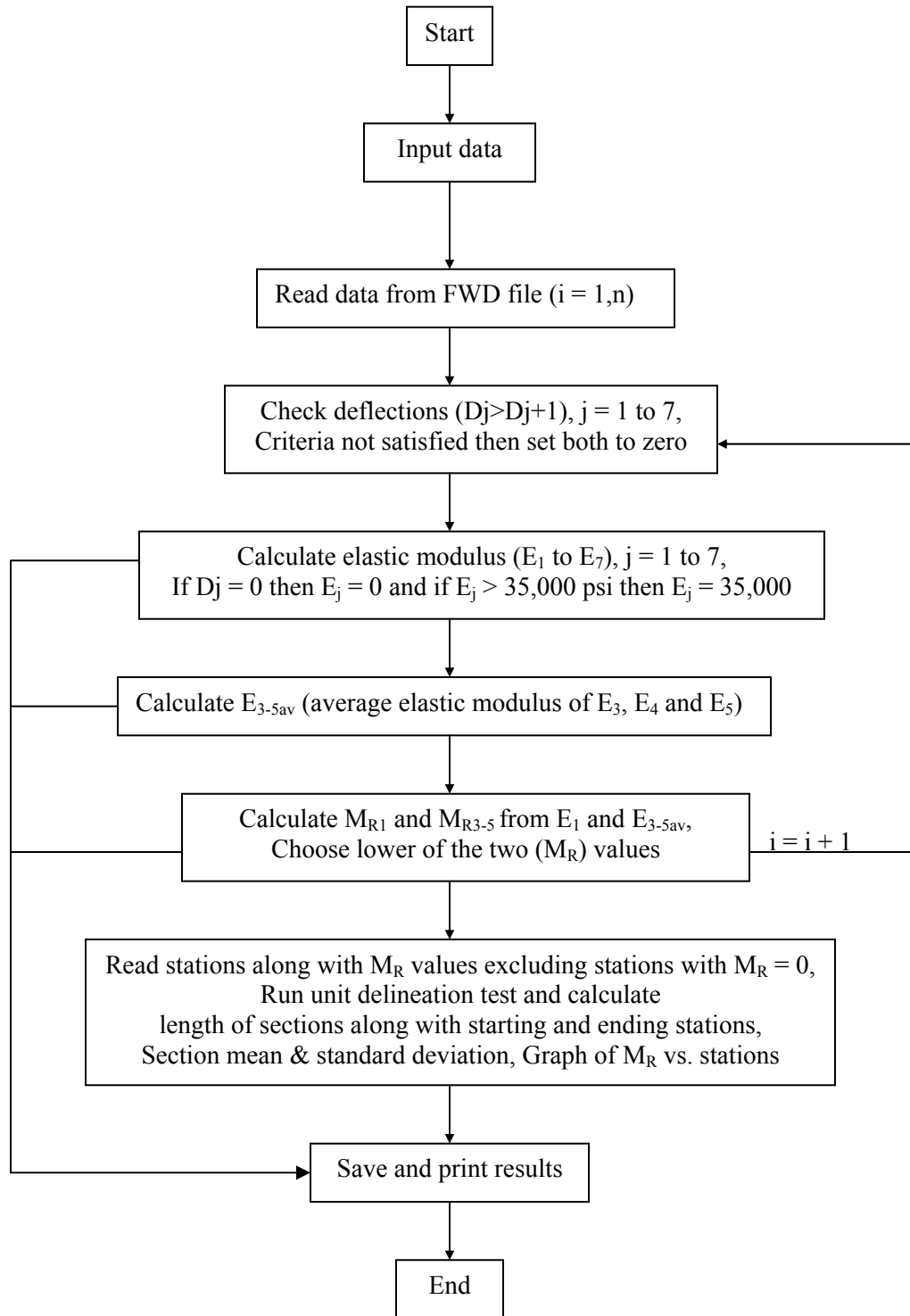


Figure 5.3 Flow Chart of Program FWDSUBGRADE

CHAPTER 6

SUMMARY AND CONCLUSIONS

6.1 SUMMARY

This project addresses the issue of employing a FWD test for subgrade characterization. A research program, including field and laboratory tests, is initiated seeking a relation between deflection-based elastic modulus, E , and laboratory resilient modulus, M_R . Ten as-built subgrade sections were tested using the FWD followed by the Dynamic Cone Penetrometer to detect soil layering, if any. Undisturbed soil samples were retrieved utilizing a thin wall Shelby tube and tested in the laboratory employing TP46 protocol. Elastic modulus calculations employing forward calculation equations (assuming an elastic half-space) was regressed against laboratory resilient modulus, advancing various approaches (models) for M_R prediction. A feature of the chosen approach is that both center sensor modulus and offset sensor moduli enter in the process independently resulting in two equations. With two equations, two resilient moduli can be derived, and the lesser of the two yield a conservative value for design. Having been derived with multiple sensor moduli, it promises to be a viable method for subgrade characterization, especially when sizeable nonhomogeneity is expected in built-up subgrades. A short-cut procedure suggesting a one-to-one relation between E_1 and M_R is also presented, where, for the two extreme reaches (lower and upper), E_1 is replaced by E_{3-5} when $E_1 < 9000$ psi, and lesser of E_1 and E_{3-5} when $E_1 > 25,000$ psi.

An exclusive program, FWDSUBGRADE, was developed to analyze FWD deflection data obtained from subgrade tests, extracting the first sensor modulus E_1 , and average of three offset sensors, E_{3-5} . Employing E_1 and E_{3-5} , two distinct resilient moduli are derived with the

lesser of the two serving as the design resilient modulus. The program, in addition to calculating station-by-station resilient modulus, relying on what is known as cumulative difference technique, delineates homogeneous units of the subgrade, outputting mean and standard deviation of resilient modulus for each homogenous section. A graphical plot of resilient modulus at each station along the project is another output of the program.

6.2 CONCLUSIONS

The analysis of test results focused on relating FWD elastic modulus to resilient modulus of undisturbed Shelby tube samples and recommending this model for estimating a design resilient modulus. Summarized herein are the major conclusions/observations, related to test set-up, modulus results and data analysis:

1. FWD is a viable test device for testing subgrade soil provided the stress in the subgrade can be kept low, ensuring elastic behavior (a $2,500 \pm$ lb load on an 18-in. plate meets the stress criteria).
2. The first sensor deflection exhibits large variability compared to those of the offset sensors, except the second sensor deflection that also shows large fluctuation especially with an 18-in. plate.
3. The standard 10 mm sensor tip performed as satisfactorily as the larger tip, 16 mm size.
4. Forward calculation employing elastic equations is found to result in consistent elastic moduli values from all of the offset sensor deflections except sensor 2.
5. The first sensor modulus tends to be lower than each of the offset sensor modulus when the surface material is softer than the underlying soil, while the first sensor modulus is either equal to or slightly larger than the offset sensor modulus when the subgrade is uniformly stiff or a stiff material overlies a softer material.

6. Disturbance caused by pushing the Shelby tube sampler into a desiccated top layer resulted in re-compaction of samples, and, in turn, increased resilient modulus values. Moisture also influenced the resilient modulus results.
7. Though tested at appointed stresses, resilient modulus based on TP46 protocol exhibits stress dependency, warranting the use of universal model to adjust the resilient modulus values with respect to stress state.
8. Field, as well as laboratory test results, show that subgrade in all of the test sections is non-uniform, with more variation spatially than in the vertical direction.
9. Though the data revealed a one-to-one relationship between E_1 and M_R for a limited range of moduli values, the relation is not robust enough nor could be justified on a theoretical basis.
10. Neither first sensor modulus nor offset sensor moduli (E_{3-5} : average of third, fourth and fifth sensor moduli) could independently capture subgrade response characteristic, therefore, employing E_1 and E_{3-5} concurrently, two resilient modulus values are chosen. Lesser of the two values constitutes the design resilient modulus.

6.3 RECOMMENDATIONS FOR FURTHER RESEARCH

This research has charted a viable procedure for characterizing subgrade employing FWD, a device that has been used for some time for pavement evaluation including the in-place subgrade. In the overall pavement evaluation scheme, the nonhomogeneity of subgrade plays a minor role as compared to when a subgrade is being tested directly on the surface. In order to account for the nonhomogeneity only, both center sensor and offset sensor moduli have been brought into prominence in choosing the appropriate design resilient modulus. Now the two relationships/equations derived in this research needs to be continually refined as more field test

data becomes available. More test data on relatively soft soils, whose modulus falls below 10,000 psi (70 MPa), would indeed improve the robustness of the two relations, that form the backbone of the correlation methodology.

Also studies are encouraged to map out the change in subgrade moduli, as other layers, for example, subbase/base and surface, are emplaced over the subgrade. This would help to substantiate the 0.33 factor for translating subgrade FWD modulus (backcalculated), to resilient modulus in the context of pavement evaluation.

6.4 IMPLEMENTATION

The subgrade soils selected for this study covered a wide variety of Mississippi soil types, plasticity indices, and gradations. Accordingly, the procedures described for determining design M_R -values using the FWD shall be widely applicable, at least for unbound, fine-grain subgrade soils. Design resilient modulus may be calculated employing equations in Figure 4.15 followed by a plot similar to that in Figure 5.1, in choosing homogeneous sections. Alternately, the computer program FWDSUBGRADE performs all of the above steps.

The entire procedure of reading the FWD data in real time and making calculations, outputting homogeneous units with mean and standard deviation of resilient modulus, is programmed and furnished for ready-use by MDOT. The ability to perform real time data analysis in the field enables the engineer to verify the accuracy of sub-sectioning and to some extent validate the resilient modulus values predicted by the analysis procedure.

6.5 BENEFITS

The principle benefit of the correlations developed in this research resides in being able to use FWD for subgrade characterization. Subgrade resilient modulus for pavement design (in accordance with AASHTO Guide and the 2002 Guide) can now be determined employing

relationships developed in this study. FWD deflection-based characterization is preferred primarily for two reasons: (i) in-situ tests circumvent disturbance (recompaction/decompaction) affecting the test outcome, and (ii) in-situ tests simulate the stress state in the material better than that can be attained in TP46 test, for example. With the results accomplished in this research incorporated in a user-friendly program, feasibility of the FWD test directly on subgrade is indeed enhanced.

Recognition of spatial variability of soil compaction uncovered in this study could lead to better construction control specifications, in terms of employing statistical quality control. As FWD is extensively used in pavement evaluation, receiving widespread recognition, its use in subgrade evaluation is a logical choice and is likely to be embraced by pavement engineers.

REFERENCES

1. Witczak, M., Qi, X. and Mirza, M.W., "Use of Nonlinear Subgrade Modulus in AASHTO Design Procedure", *ASCE Journal of Transportation Engineering*, Vol. 121, No. 3, 1995, pp. 273-282.
2. *AASHTO Guide for Design of Pavement Structures 1993*. AASHTO, Washington, DC, 1993.
3. Heukelom, W., and Klomp, A.J.G., "Dynamic Testing as a Means of Controlling Pavements During and After Construction", *Proceedings of the First International Conference on Structural Design of Asphalt Pavements*, University of Michigan, 1962.
4. Hassan, A., "The Effect of Material Parameters on Dynamic Cone Penetrometer Results For Fine-grained Soils and Granular Materials", *Ph.D. Dissertation*, Oklahoma State University, Stillwater, Oklahoma, 1996.
5. Burnham, T., and Johnson, D., "In-Situ Characterization Using the Dynamic Cone Penetrometer", *Report MN-93/05*, Minnesota Department of Transportation, Maplewood, Minnesota, 1993.
6. Chai, G., and Roslie, N., "The Structural Response and Behavior Prediction of Subgrade Soils Using Falling Weight Deflectometer in Pavement Construction", *Proceedings, Third International Conference on Road & Airfield Pavement Technology*, Beijing, China, April 1998.
7. George, K.P. and Uddin, W., "Subgrade Characterization for Highway Pavement Design", *Final Report*, Submitted to Mississippi Department of Transportation, The University of Mississippi, December 2000.
8. Ali, N.A., and Khosla, N.P., "Determination of Layer Moduli Using a Falling Weight Deflectometer", *Transportation Research Record 1117*, TRB, National Research Council, Washington, D.C., 1987, pp. 1-10.
9. Newcomb, D.E., "Comparison of Field and Laboratory Estimated Resilient Moduli of Pavement Materials", *Asphalt Paving Technology, Association of Asphalt Paving Technologists*, Vol. 56, February 1987, pp. 91-106.
10. Von Quintus, H.L., and Killingsworth, B.M., "Comparison of Laboratory and In-Situ Determined Elastic Moduli", A paper presented at the 76th Annual Meeting of the *Transportation Research Board*, Washington, D.C., January 1998.
11. Chen, Bilyeu, and He, "Comparison of Resilient Moduli Between Field and Laboratory Testing: A Case Study", A Paper Presented at the 76th Annual Meeting of the *Transportation Research Board*, Washington, D.C., January 1998.

12. Houston, W.N., Mamlouk, M.S., and Perera, R.W.S., "Laboratory versus Nondestructive Testing for Pavement Design", *ASCE Journal of Transportation Engineering*, Vol. 118, No. 2, 1992, pp. 207-222.
13. Van Deusan, D.A., Lenngren, C.A., and Newcomb, D.E., "A Comparison of Laboratory and Field Subgrade Moduli at the Minnesota Road Research Project", *Nondestructive Testing of Pavements and Backcalculation of Moduli*, ASTM STP 1198, H.L. Von Quintus et al., eds., ASTM, 1994.
14. Nassar, W., Al-Qadi, I., Flinlsch, G.W., and Appea, A., "Evaluation of Pavement Layer Response at the Virginia Smart Road", Virginia Polytechnic Institute, Blacksburg, VA, 1990.
15. Rahim, A., and George, K.P. "Falling Weight Deflectometer for Estimating Subgrade Elastic Modulus", *ASCE Journal Transportation Engineering*, Vol. 129, No. 1, 2003, pp. 100-107.
16. Seeds, S.B., Ott, W.C., Milchail, M., and Mactutis, J.A. "Evaluation of Laboratory Determined and Nondestructive Test Based Resilient Modulus Values From WesTrack Experiment", *Nondestructive Testing of Pavements and Backcalculation of Moduli* ASTM STP 1375, S. Tayabji and O. Lukanen eds., ASTM, 2000.
17. Newcomb, D.E., Chabourn, B.A., Van-Deusen, D.A., and Burnham, T.R., "Initial Characterization of Subgrade Soils and Granular Base Materials at the Minnesota Road Research Project", *Report No. MN/RC-96/19*, Minnesota Department of Transportatino, St. Paul, Minnesota, December 1995.
18. Newcomb, D.E. and Birgisson, B., "Measuring In-Situ Mechanical Properties of Pavement Subgrade Soils", *NCHRP Synthesis 278*, Transportation Research Board, Washington, D.C., 1999.
19. Gros, C., "Use of a Portable Falling Weight Deflectometer: Loadman", University of Oulu, Publications of Road and Transportation Laboratory, No. 20, 1993.
20. Kudla, W., Floss, R., and Trautmann, C., "Dynamic Plate Compression Test - Rapid Testing Method for Quality Assurance of Unbound Course", *Autobahn 42*, No. 2. (Published in German), 1991.
21. Rogers, C.D.F., Brown, A.J. and Fleming, P.R., "Elastic Stiffness Measurement of Pavement Foundation Layers", *Unbound Aggregates in Roads 4*, Edited by Dawson A. and Jones R.H., Nottingham University, 1995.
22. Hou, T.Y., "Evaluation of Layered Material Properties from Measured Surface Deflections", *Ph.D. Thesis*, University of Utah, Salt Lake City, Utah, 1977.

23. Harichandran, R.S., Mahmood, T., Raab, A.R., and Baladi, G.Y., "Modified Newton Algorithm for Backcalculation of Pavement Layer Properties", *Transportation Research Record 1384*, TRB, National Research Council, Washington, D.C., 1993, pp. 15-22.
24. Odemark, N., "Undersokning av elasticitetegenskaperna hos olika jordarter samt teori for berakning av belagningar enligt elasticitesteorin", Statens Vaginstitute, meddelande 77, 1949.
25. Ullidtz, Per, "Will Nonlinear Backcalculation Help?" *Nondestructive Testing of Pavements and Backcalculation of Moduli*, Volume 3, ASTM STP 1375, S. Tayabj and E.D. Lukanen, eds., ASTM, 2000.
26. Lee, S.W., Backcalculation of Pavement Moduli by Use of Pavement Surface Deflections, Ph.D. dissertation, University of Washington, Seattle, Washington, 1988.
27. Irwin, L.H., *User's Guide to MODCOMP 2, Version 2.4, Report No. 83-8*, Cornell Local Roads Program, Cornell University, Ithaca, N.Y., November 1983.
28. Van Cauwelaert, F.J., Alexander, D.R., White, T.D. and Barker, W.R. "Multilayer Elastic Program for Backcalculating Layer Moduli in Pavement Evaluation", *Nondestructive Testing of Pavements and Backcalculation of Moduli*, ASTM STP 1026, A.J. Bush III and Gilbert Baladi, eds., American Society for Testing and Materials, Philadelphia, PA, 1989.
29. Uzan, J., et al., A Microcomputer Based Procedure for Backcalculating Layer Moduli from FWD Data, *Research Report No. 1123-1*, Texas Transportation Institute, College Station, TX, September 1988.
30. Haiping, Z., Hicks, R.G. and Bell, C.A. "BOUSDEF: A Backcalculation Program for Determining Moduli of a Pavement Structure", *Transportation Research Record 1260*, TRB, National Research Council, Washington, D.C., 1990.
31. Ullidtz, P. and Stubstad, R.N. "Analytical-Empirical Pavement Evaluation Using the Falling Weight Deflectometer", *Transportation Research Record 1022*, TRB, National Research Council, Washington, D.C., 1985.
32. Moossazadeh, J.M. and Witczak, W. "Prediction of Subgrade Moduli for Soil That Exhibits Nonlinear Behavior", *Transportation Research Record 810*, TRB, National Research Council, Washington, D.C., 1981.
33. Dunlap, W.S. "A Report On A Mathematical Model Describing the Deformation Characteristics of Granular Materials", *Technical Report 1, Project 2-8-62-27*, TTI, Texas A & M University, 1963.

34. Seed, H.B., Mitry, F.G., Monosmith, C.L., and Chan, C.K. "Prediction of Pavement Deflection From Laboratory Repeated Load Tests", *NCHRP Report 35*, Transportation Research Board, Washington, D.C., 1967.
35. May, R.W. and Witczak, M.W. "Effective Granular Modulus to Model Pavement Response", *Transportation Research Record 810*, TRB, National Research Council, Washington, D.C., 1981.
36. Uzan, J., "Characterization of Granular Materials", *Transportation Research Record 1022*, TRB, National Research Council, Washington, D.C., 1985.
37. Yau, A. and Von Quintus, H.L., "Study of LTPP Laboratory Resilient Modulus Test Data and Response Characteristics", *Report No. FHWA-RD-01*, FHWA, USDOT, Washington, D.C., 2001.
38. Ni, B., Hopkins, T.C., Sun, L., and Beckham, T.L., "Modeling the Resilient Modulus of Soils", *Proceedings, Sixth International Conference Bearing Capacity of Roads, Railways and Airfields*, Lisbon, Portugal, 2002.
39. Stubstad, R.N., et al., "LTPP Data Analysis: Feasibility of Using FWD Deflection Data to Characterize Pavement Construction Quality" NCHRP Web Document #52: Project 20-59 (9), Washington, D.C., 2002.
40. Daleiden, J.F., Killingsworth, B.M., Simpson, A.L., and Zamora, R.A., "Analysis of Procedures for Establishing In Situ Subgrade Moduli", *Transportation Research Record 1462*, TRB, National Research Council, Washington, D.C., 1994.
41. Akram, T., Scullion, T., and Smith, R.E., "Comparing Laboratory and Backcalculated Layer Moduli on Instrumented Pavement Sections", Special Technical Publication (STP) 1198, ASTM, Philadelphia, PA, 1994.
42. Nazarian, S., Yuan, D., and Baker, M.R. "Rapid Determination of Pavement Moduli With Spectral-Analysis-of-Surface-Waves Method", *Research Record 1243-1F*, Center for Geotechnical and Highway Materials Research, University of Texas at El Paso, 1995.
43. Von Quintus, H. and Killingsworth, B., "Design Pamphlet for the Backcalculation of Pavement Layer Moduli in Support of the 1993 AASHTO Guide for the Design of Pavement Structures", *Report No. FHWA-RD-97-076*, FHWA, USDOT, Washington, D.C., 1997.
44. Shahid, M.A., Thom, N.H., and Fleming, P.R. "In Situ Assessment of Road Foundations", *Journal of the Institute of Highways and Transportation and IHIE, Vol. 44, No. 11*, 1997.

45. Fleming, P.R., "Small-scale Dynamic Devices for the Measurement of Elastic Stiffness Modulus on Pavement Foundations", *Nondestructive Testing of Pavements and Backcalculation of Moduli: ASTM STP 1375*, S. Tayabji and O. Lukanen, eds., ASTM, 2000.
46. Cooleman, H.W. and Steele, W.G. "*Experimentation and Uncertainty Analysis for Engineers*", John Wiley & Sons, Inc., New York, N.Y., 1989.
47. Harr, M.E., "*Mechanics of Particulate Media*", McGraw-Hill, New York, N.Y., 1977.
48. "Humboldt Stiffness Gauge, A Field Instrument for Measuring Lift Stiffness and Soil Modulus" Humboldt Manufacturing Co., Norridge, IL.
49. George, K.P., "Soil-Cement Field Trial" *Interim Report* to Mississippi Department of Transportation, University of Mississippi, University, M.S., 2001.
50. Netter, J., Wasserman, W., and Whitmore, G.A. *Applied Statistics*, Allyn and Bacon, Inc., 1988.

APPENDIX A

FWD DEFLECTION BASINS, TYPICAL STATION FROM EACH

SECTION

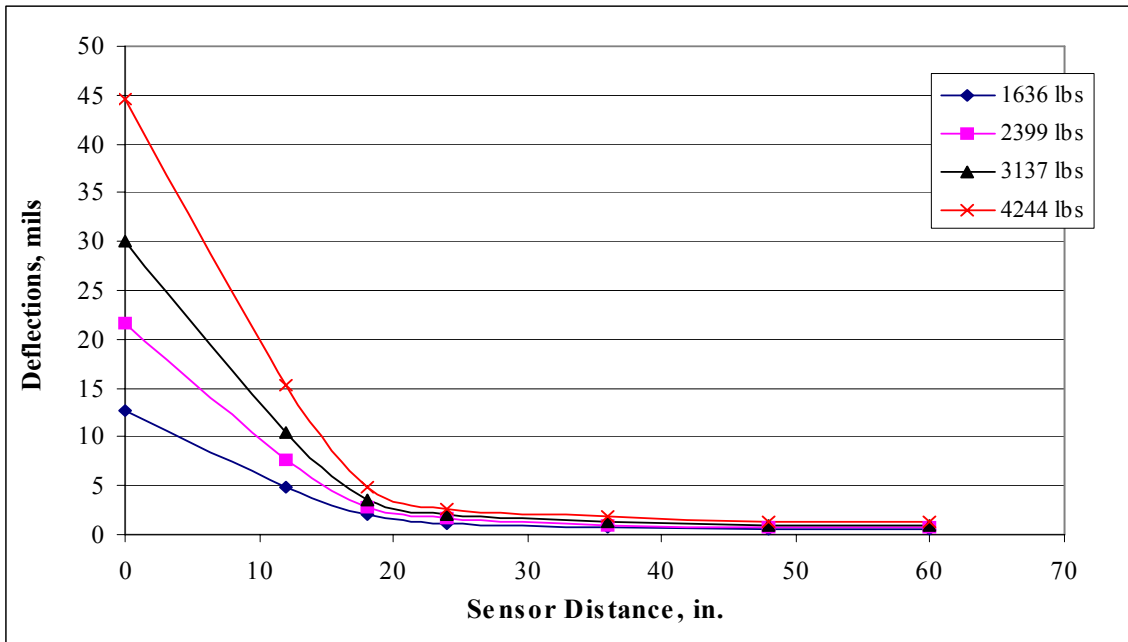


Figure A1 Deflection Basins for Four Loads, Section # 1, Station # 854+25, US 82W, Montgomery County, 18-in. (450-mm) Plate

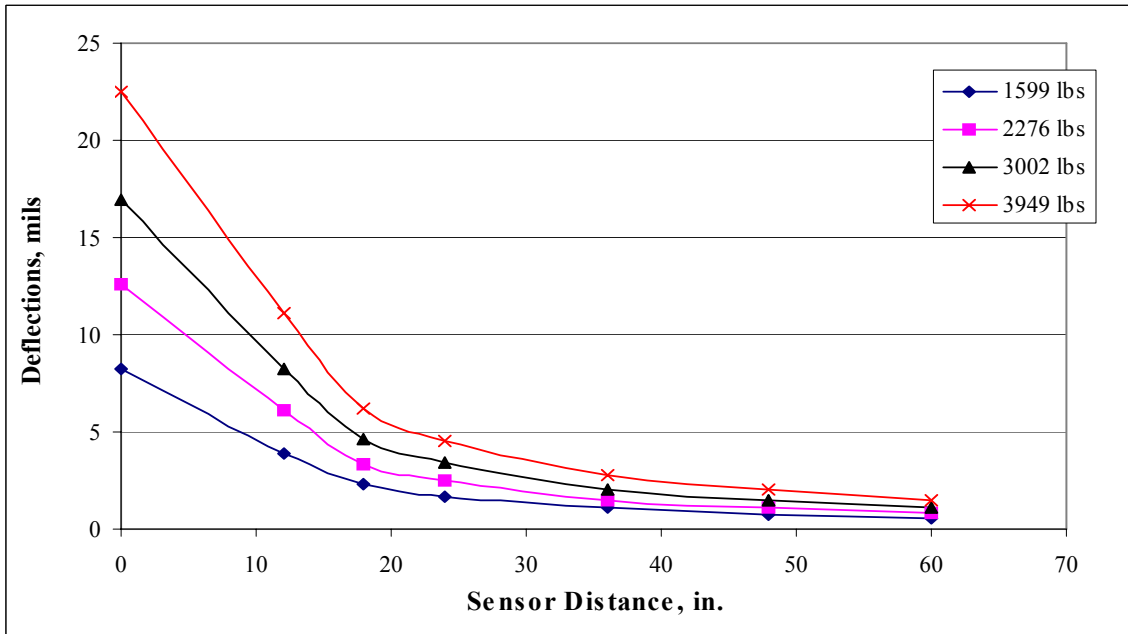


Figure A2 Deflection Basins for Four Loads, Section # 2, Station # 56+00, US 61N, Coahoma County, 18-in. (450-mm) Plate

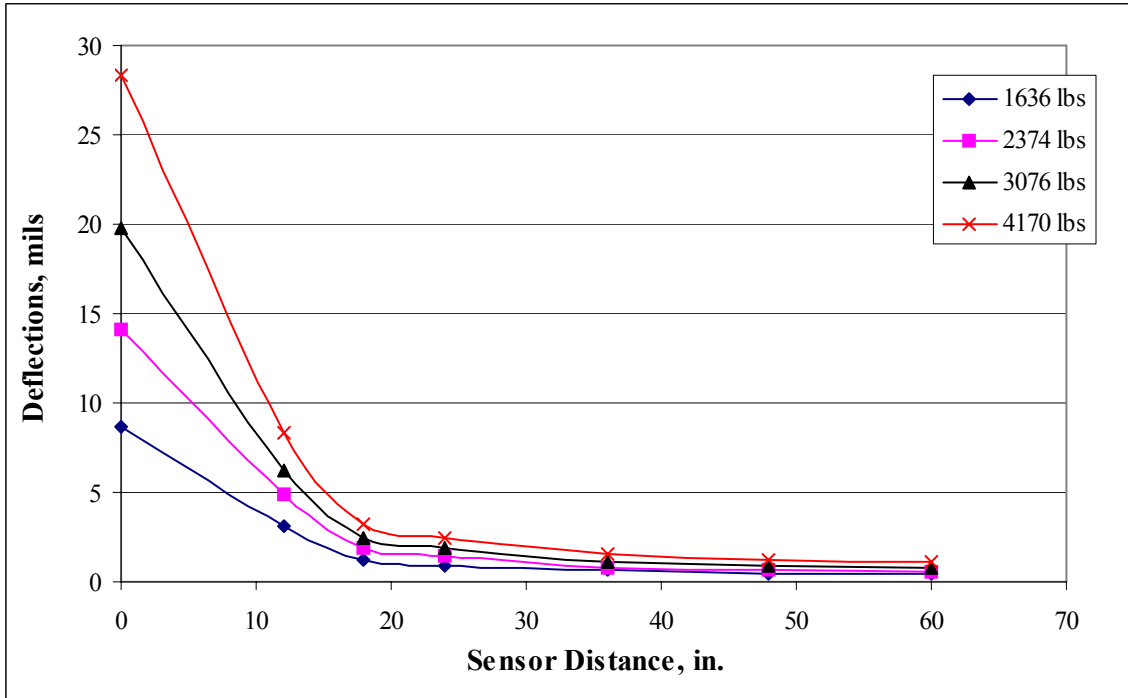


Figure A3 Deflection Basins for Four Loads, Section # 3, Station # 152+50, US 61N, Coahoma County, 18-in. (450-mm) Plate

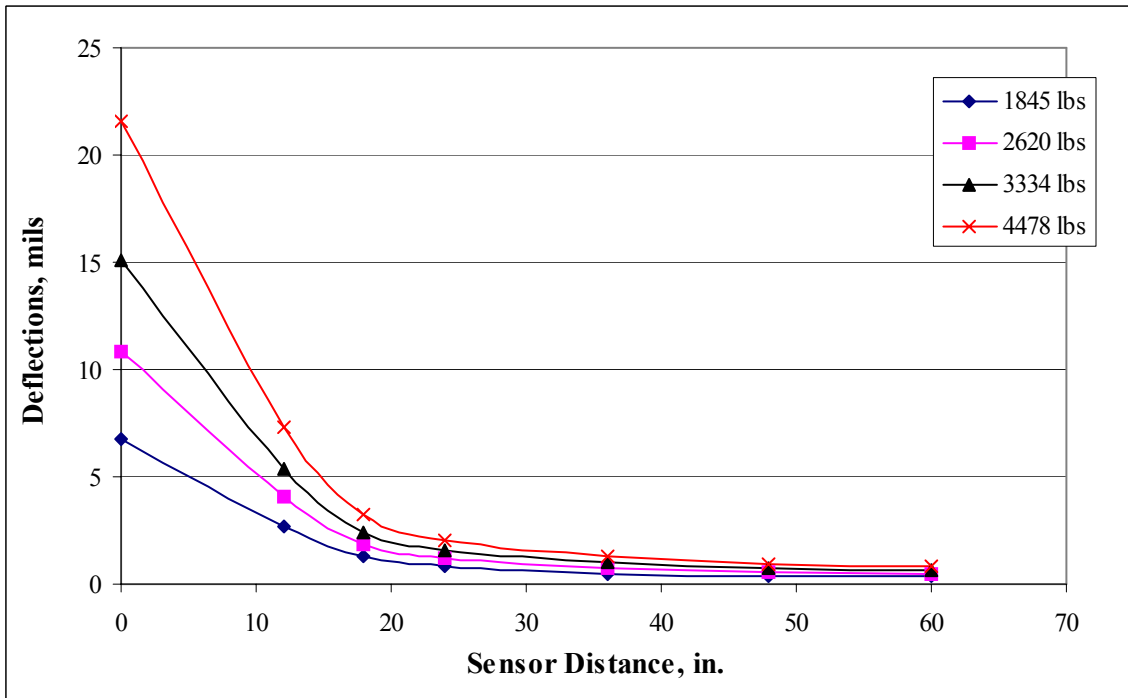


Figure A4 Deflection Basins for Four Loads, Section # 4, Station # 907+50, US 82W, Montgomery County, 18-in. (450-mm) Plate

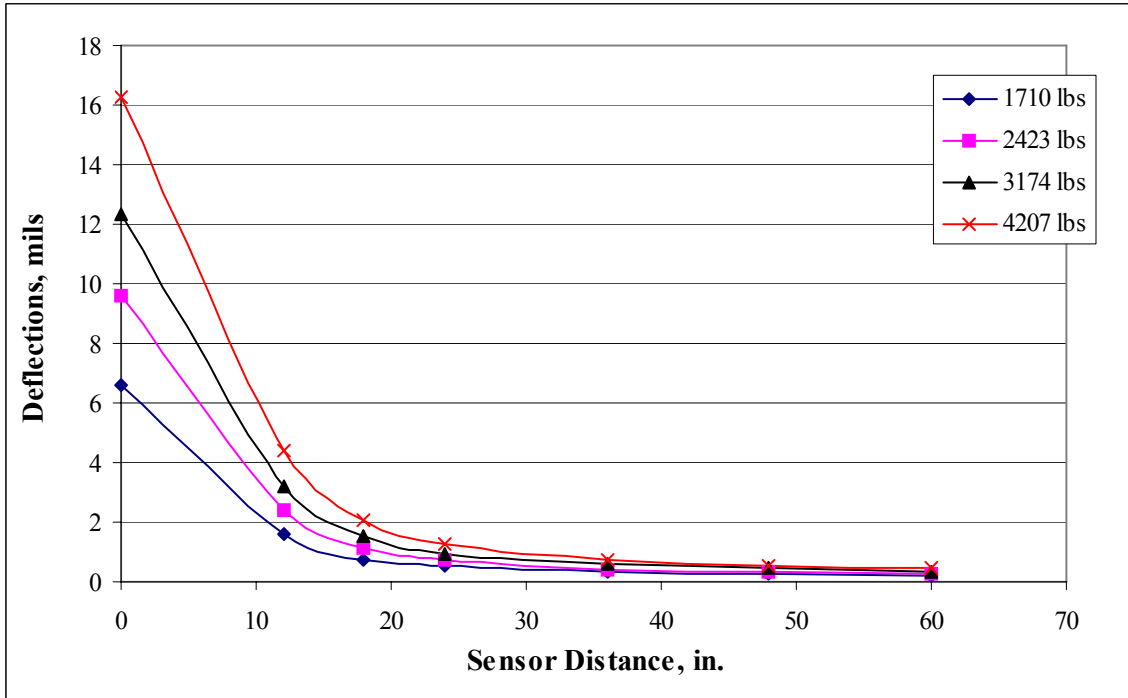


Figure A5 Deflection Basins for Four Loads, Section # 5, Station # 833+20, US 82W, Montgomery County, 18-in. (450-mm) Plate

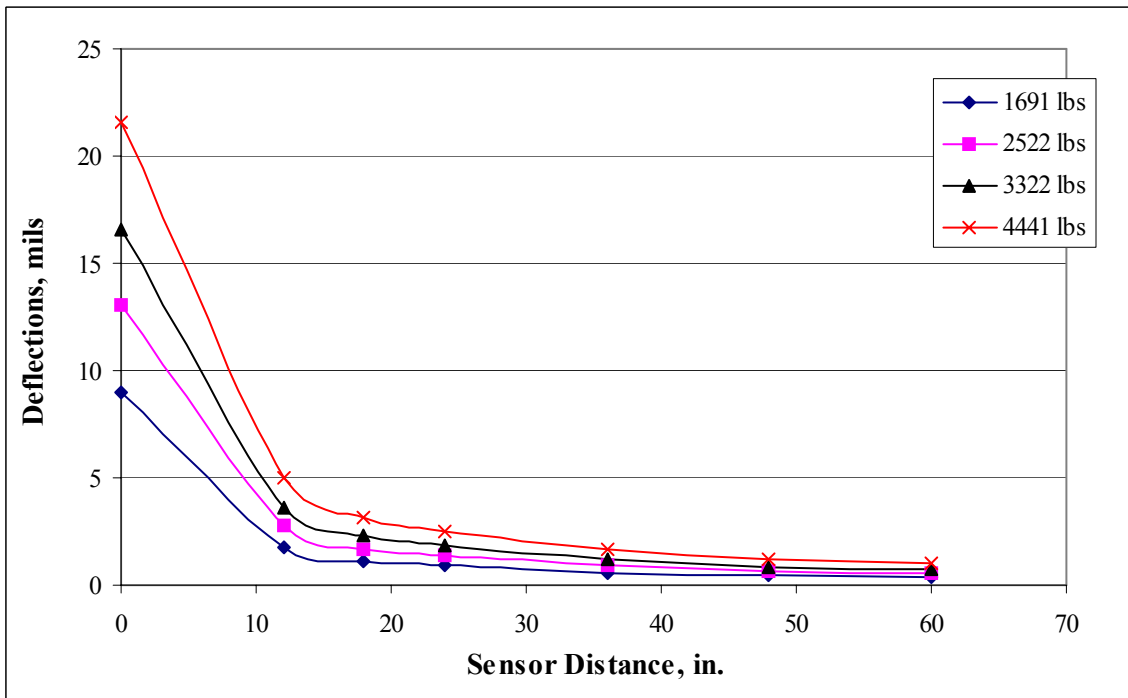


Figure A6 Deflection Basins for Four Loads, Section # 6, Station # 26+50, Norell W, Hinds County, 18-in. (450-mm) Plate

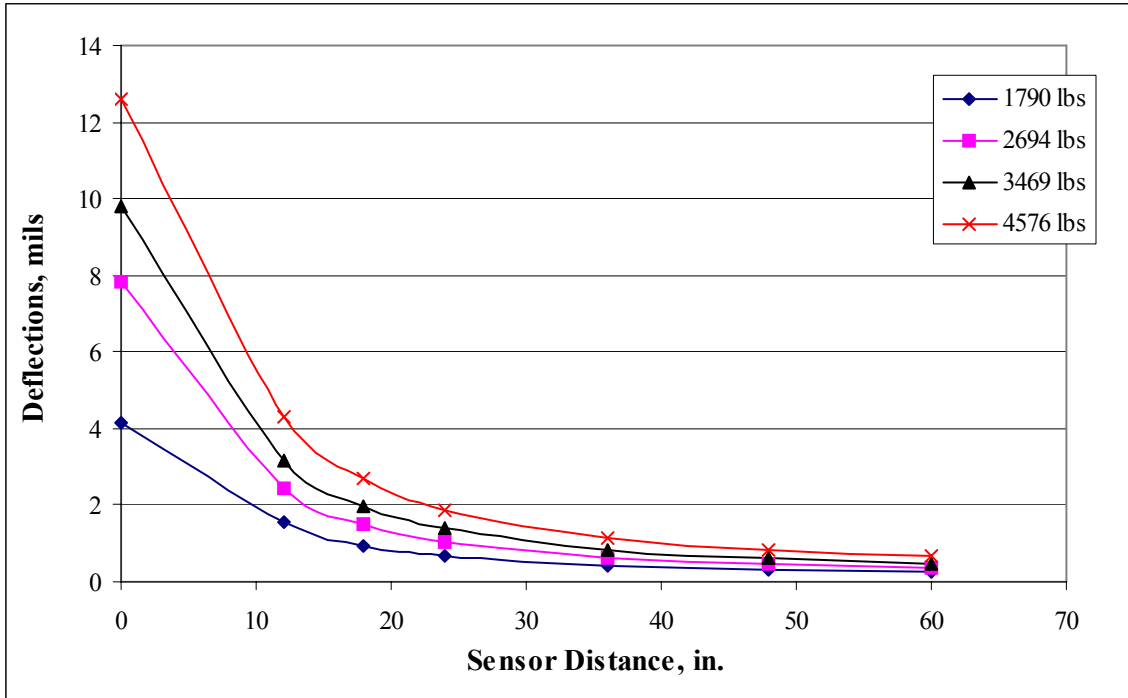


Figure A7 Deflection Basins for Four Loads, Section # 7, Station # 6+530, US 45N, Wayne County, 18-in. (450-mm) Plate

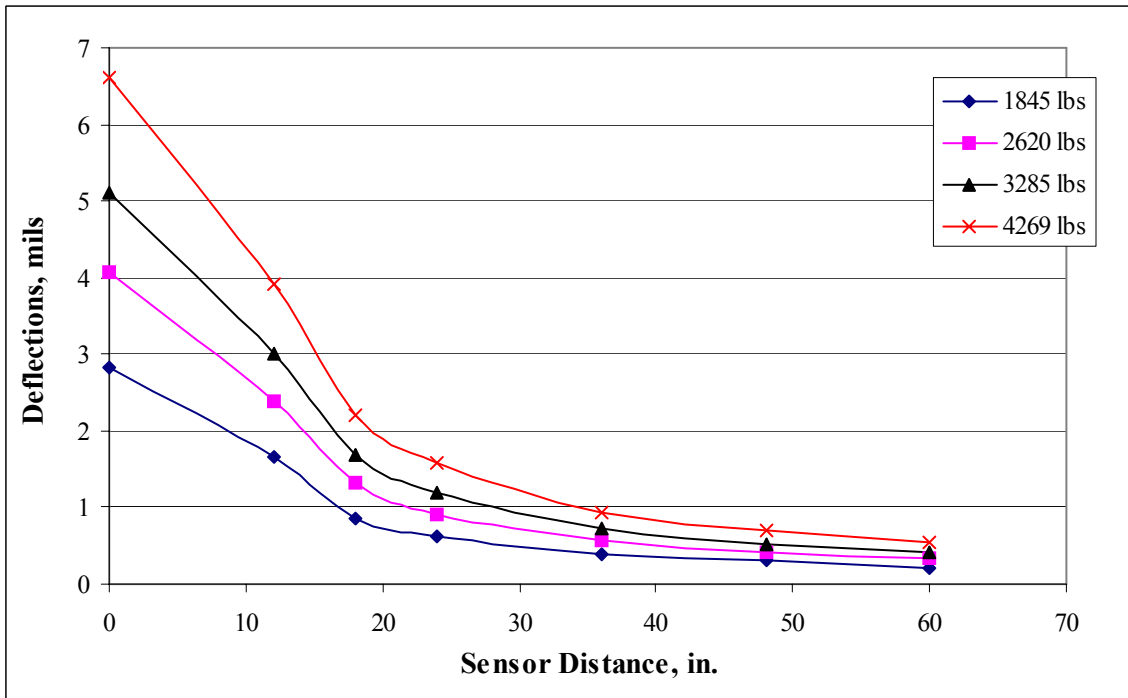


Figure A8 Deflection Basins for Four Loads, Section # 8, Station # 7+405, US 45N, Wayne County, 18-in. (450-mm) Plate

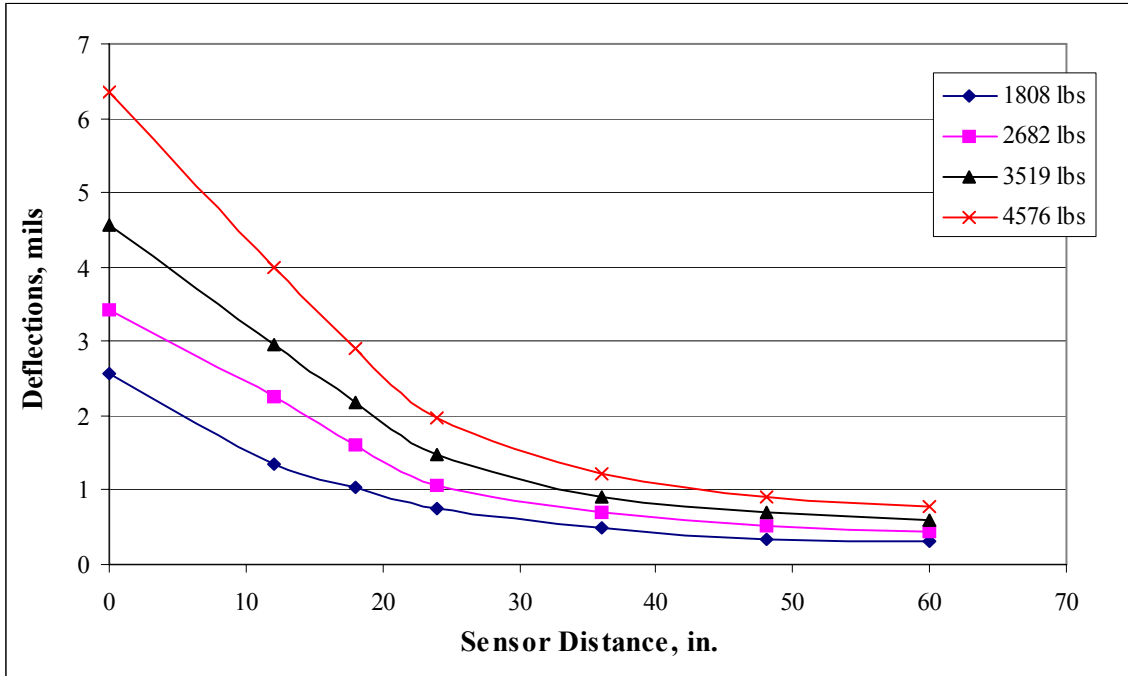


Figure A9 Deflection Basins for Four Loads, Section # 9, Station # 7+435, US 45N, Wayne County, 18-in. (450-mm) Plate

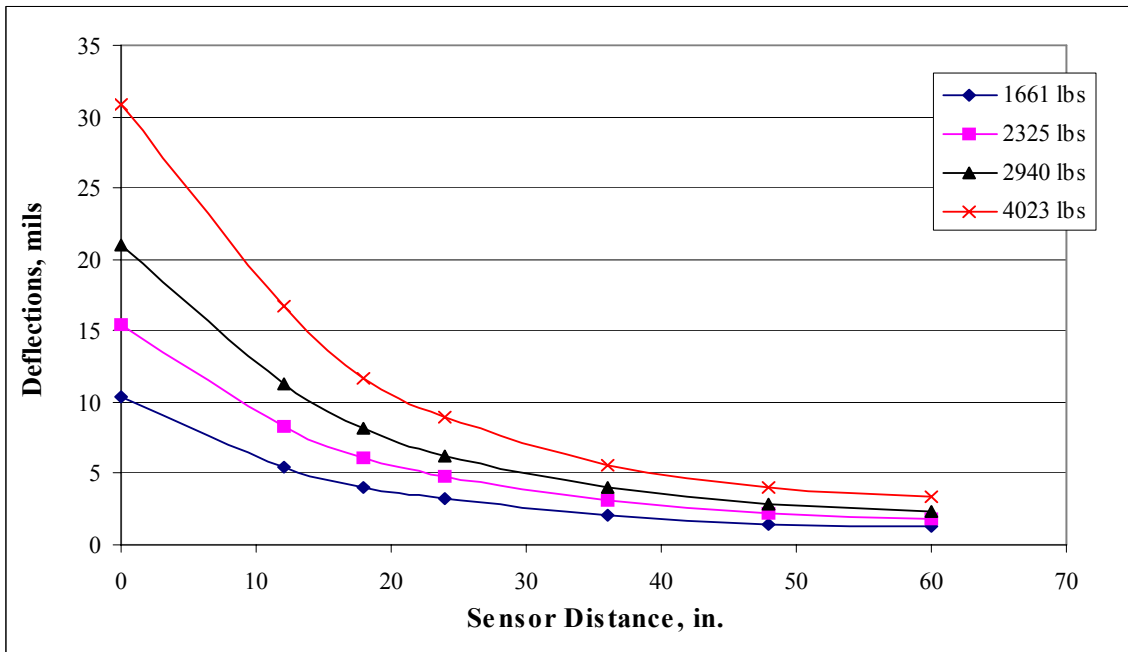


Figure A10 Deflection Basins for Four Loads, Section # 10, Station # 48+50, Nissan W. Parkway, Madison County, 18-in. (450-mm) Plate

APPENDIX B
AUTOMATED DYNAMIC CONE PENETROMETER TEST DATA

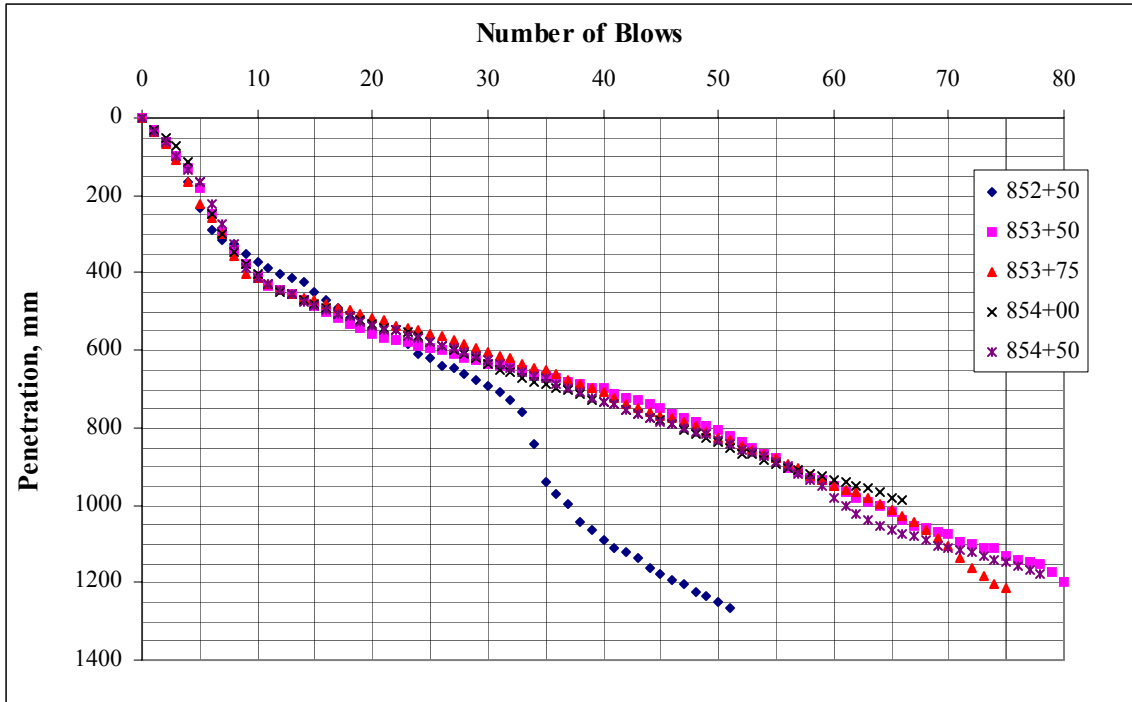


Figure B1 ADCP Test Results in Section # 1, US 82W, Montgomery County

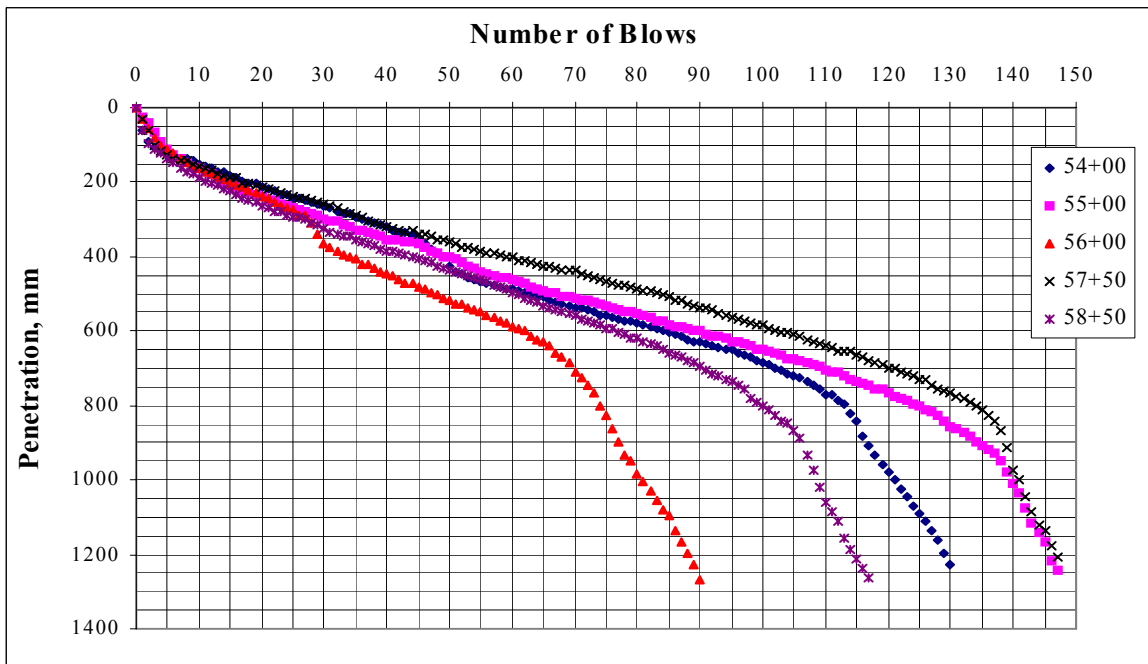


Figure B2 ADCP Test Results in Section # 2, US 61N, Coahoma County

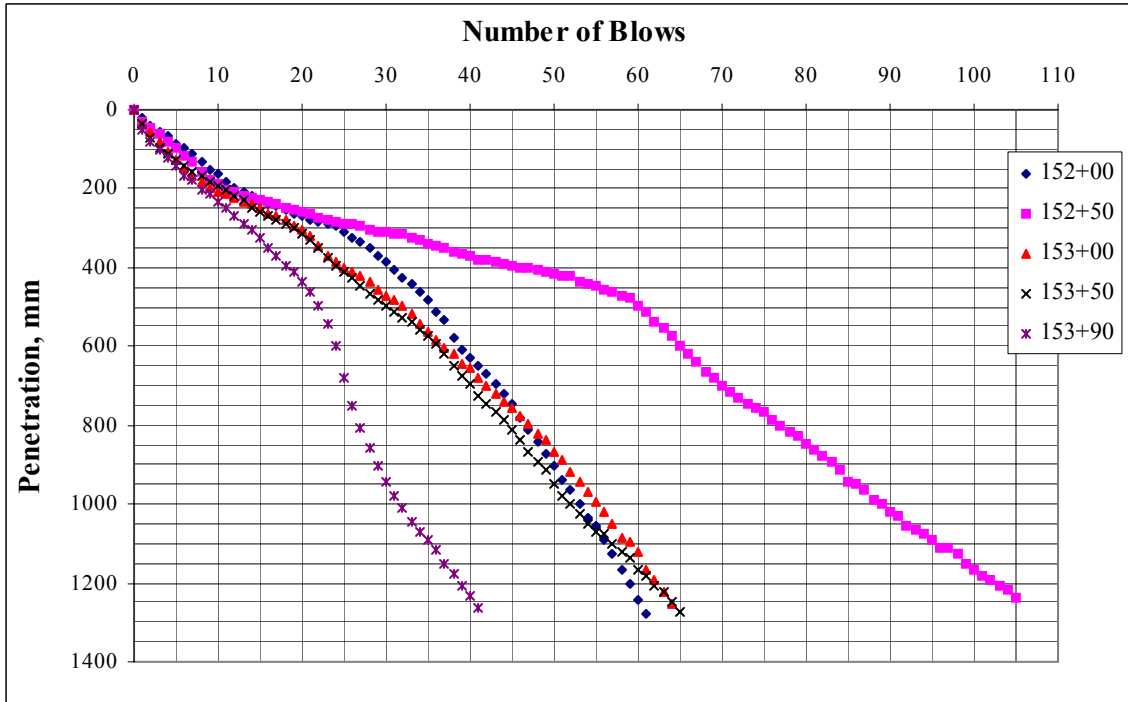


Figure B3 ADCP Test Results in Section # 3, US 61N, Coahoma County

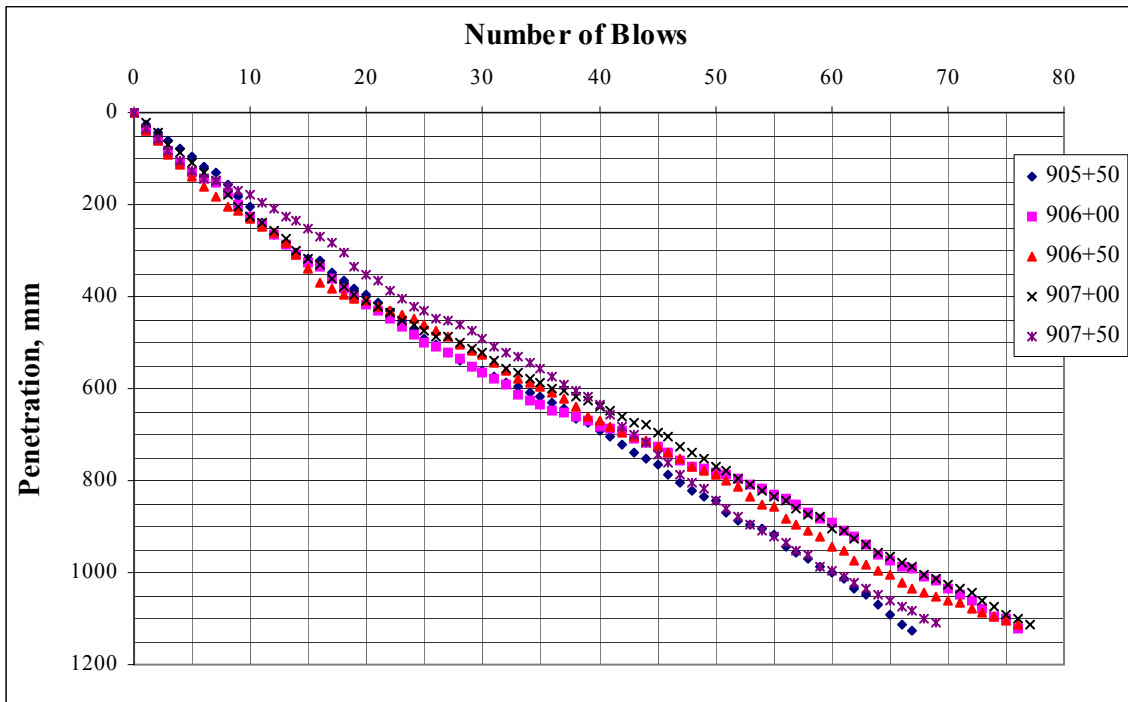


Figure B4 ADCP Test Results in Section # 4, US 82W, Montgomery County

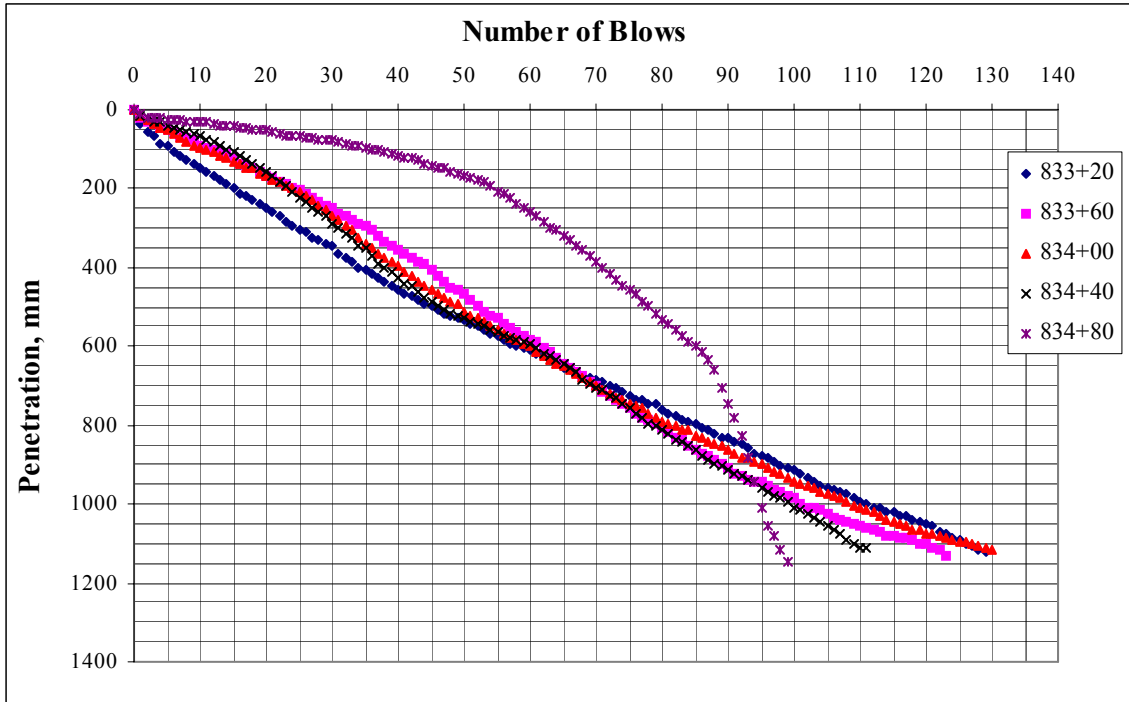


Figure B5 ADCP Test Results in Section # 5, US 82W, Montgomery County

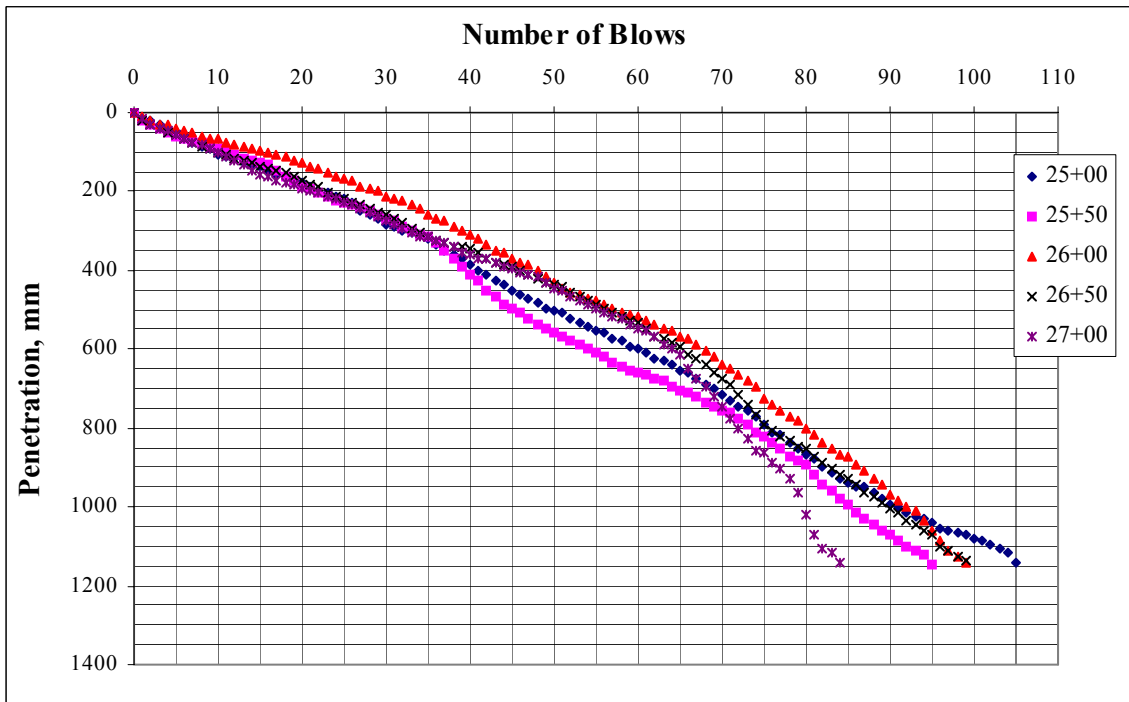


Figure B6 ADCP Test Results in Section # 6, Norrell W., Hinds County

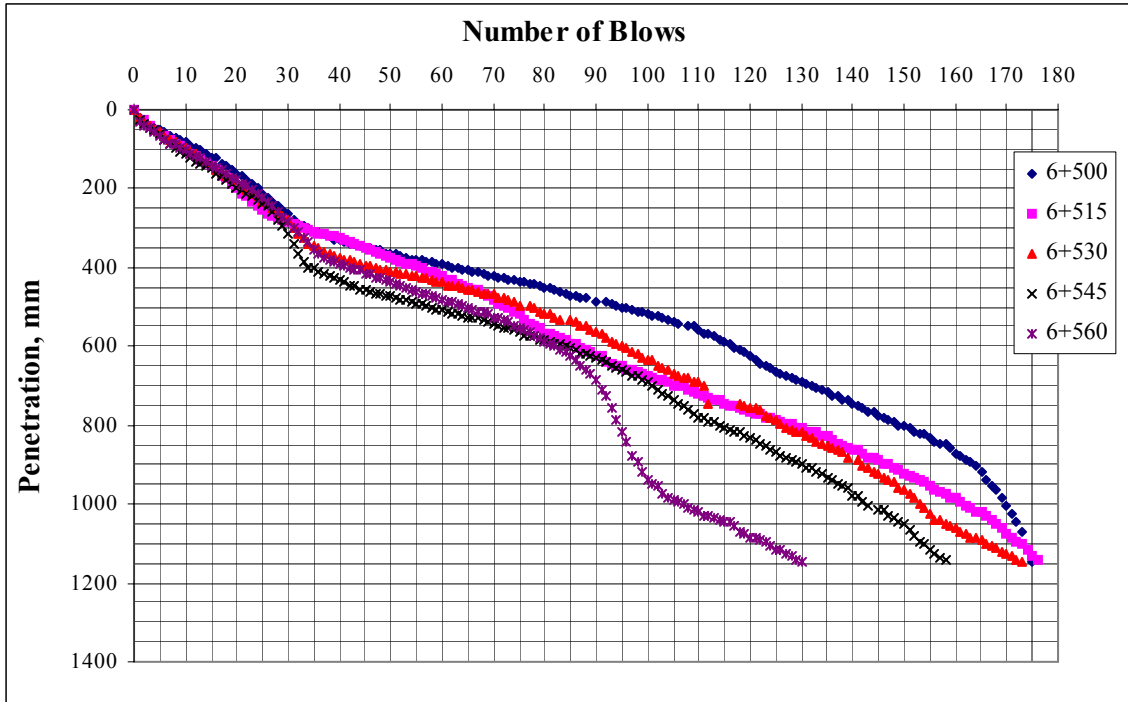


Figure B7 ADCP Test Results in Section # 7, US 45N, Wayne County

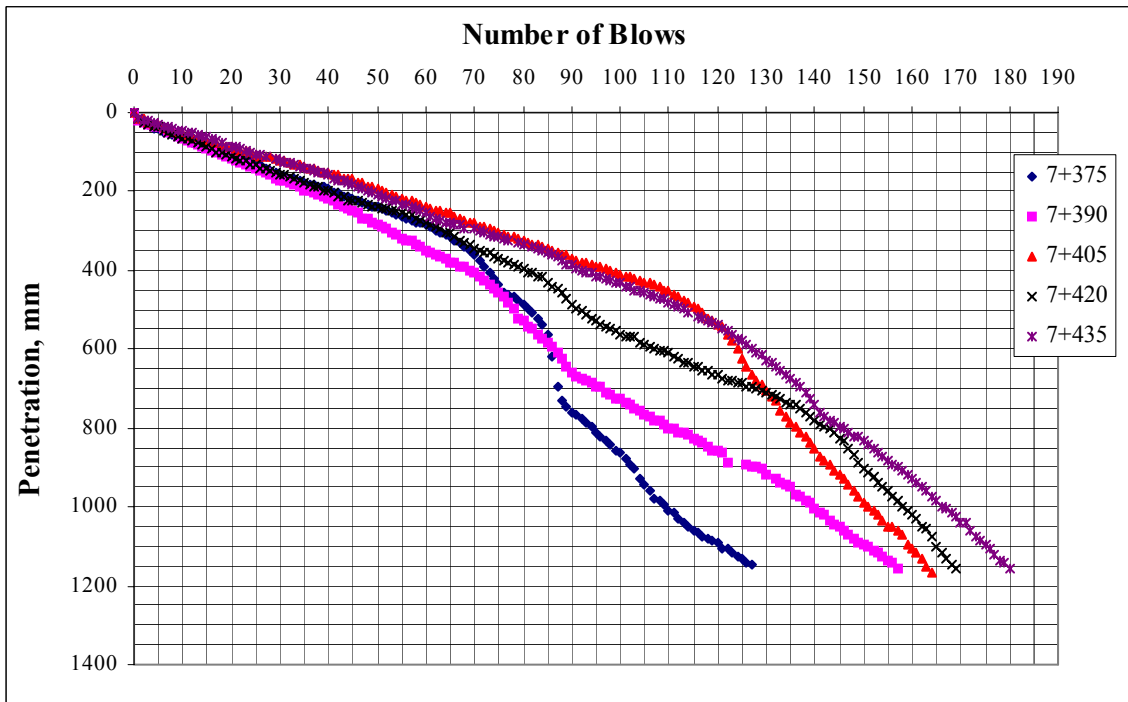


Figure B8 ADCP Test Results in Section # 8, US 45N, Wayne County

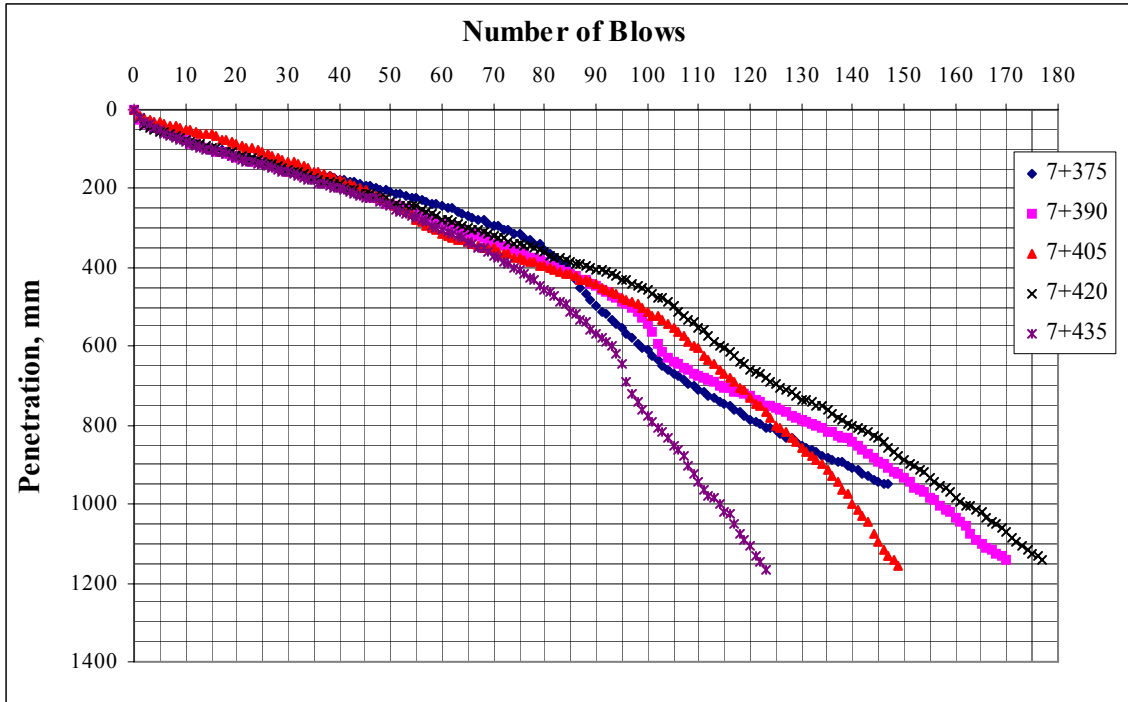


Figure B9 ADCP Test Results in Section # 9, US 45N, Wayne County

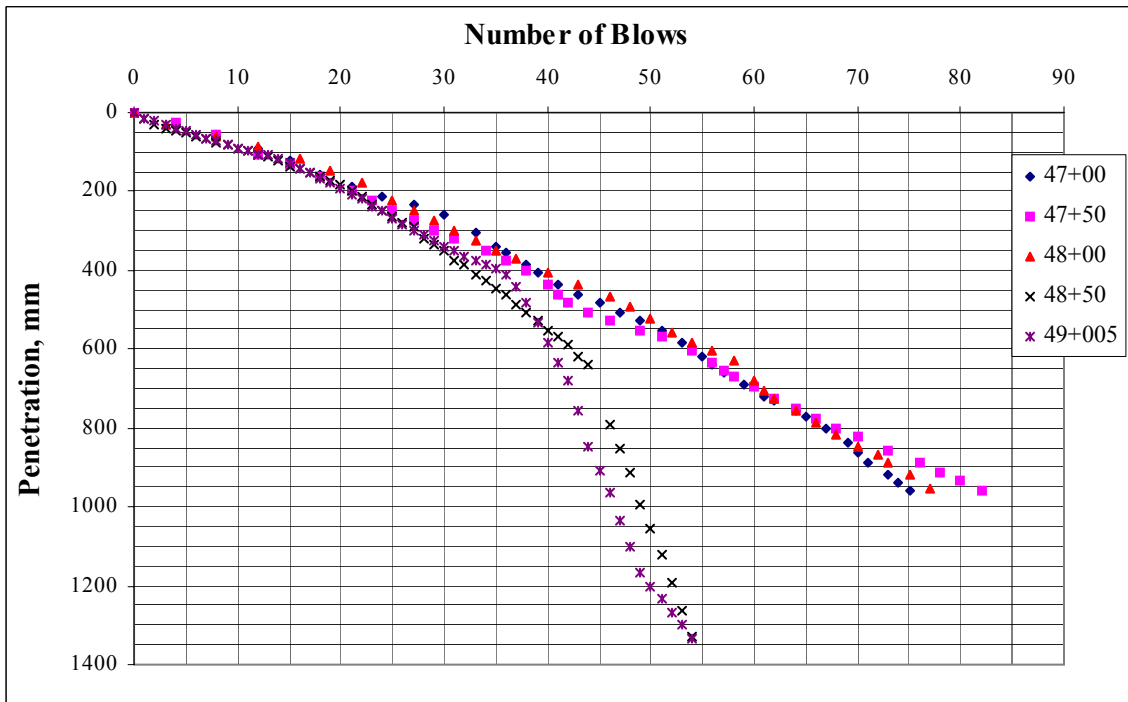


Figure B10 ADCP Test Results in Section # 10, Nissan W. Parkway, Madison County

APPENDIX C
RESILIENT MODULUS OF SAMPLE 1 (0-12 IN. DEPTH) AS FUNCTION
OF STRESS STATE

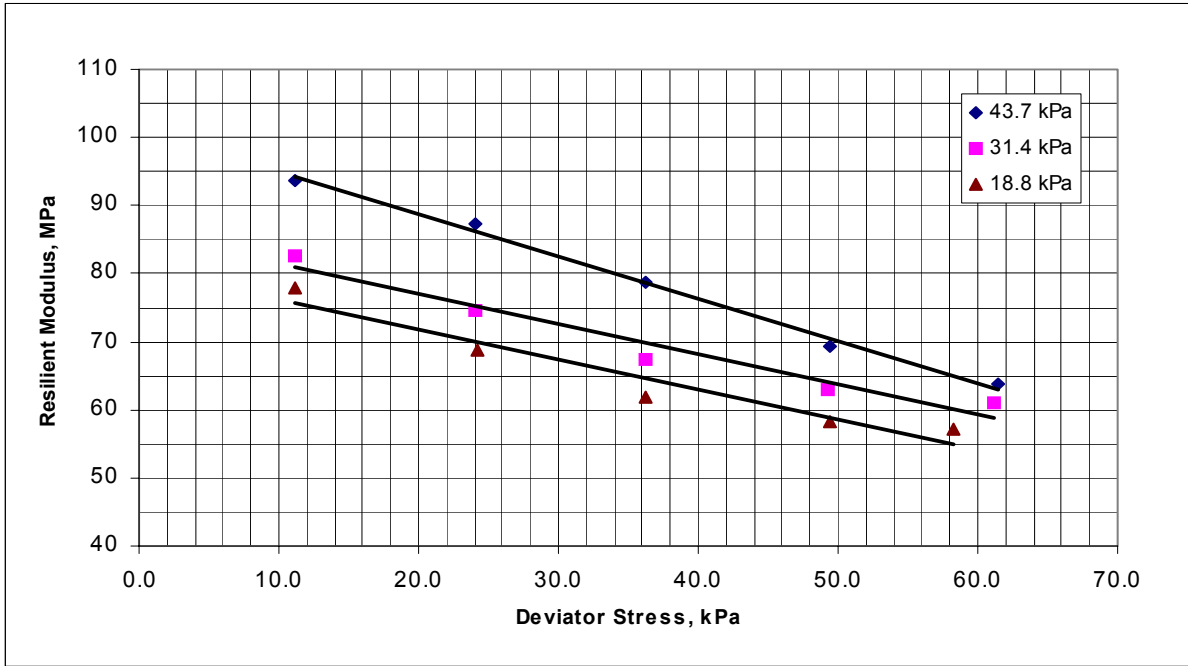


Figure C1 Resilient Modulus Test Results, Station 852+50, Section 1, Sample # 1, 1 MPa = 145 psi

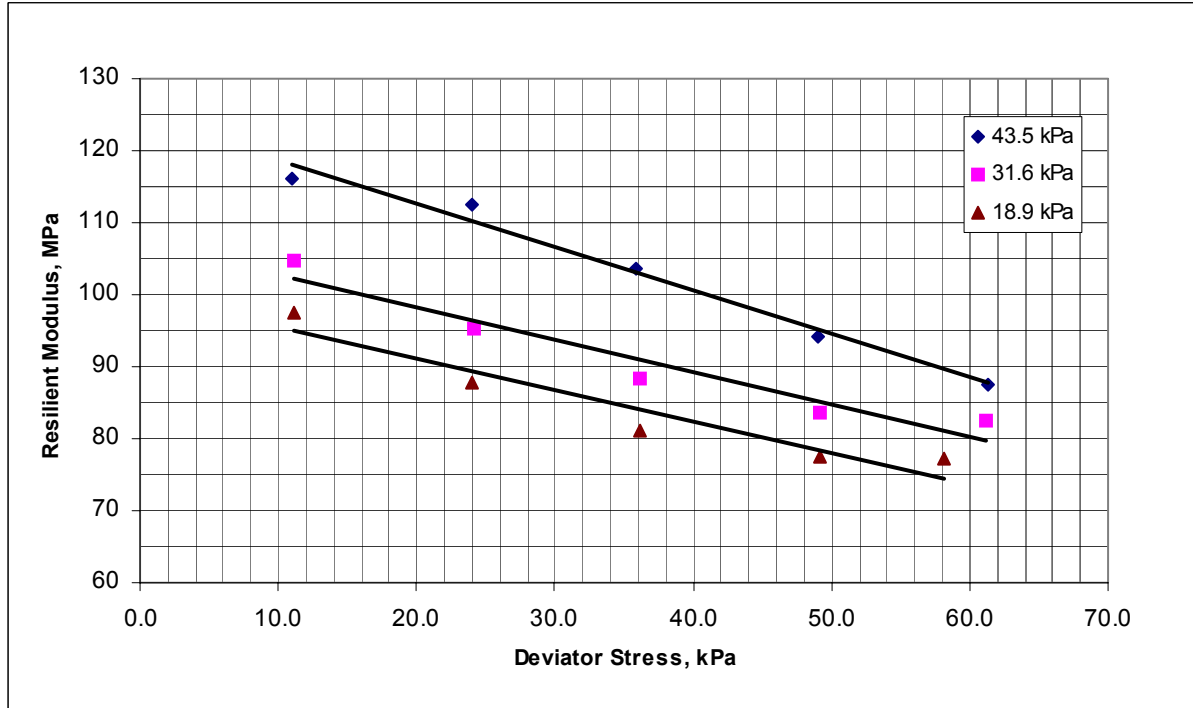


Figure C2 Resilient Modulus Test Results, Station 853+50, Section 1, Sample # 1, 1 MPa = 145 psi

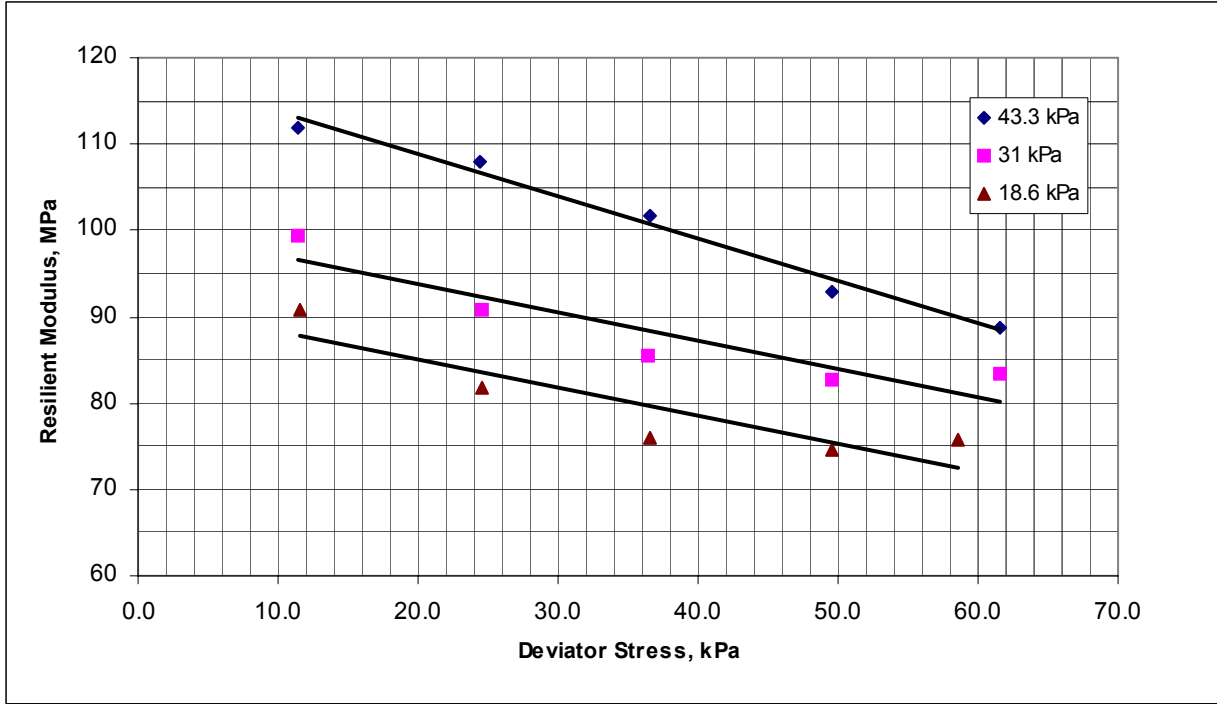


Figure C3 Resilient Modulus Test Results, Station 853+75, Section 1, Sample # 1, 1 MPa = 145 psi

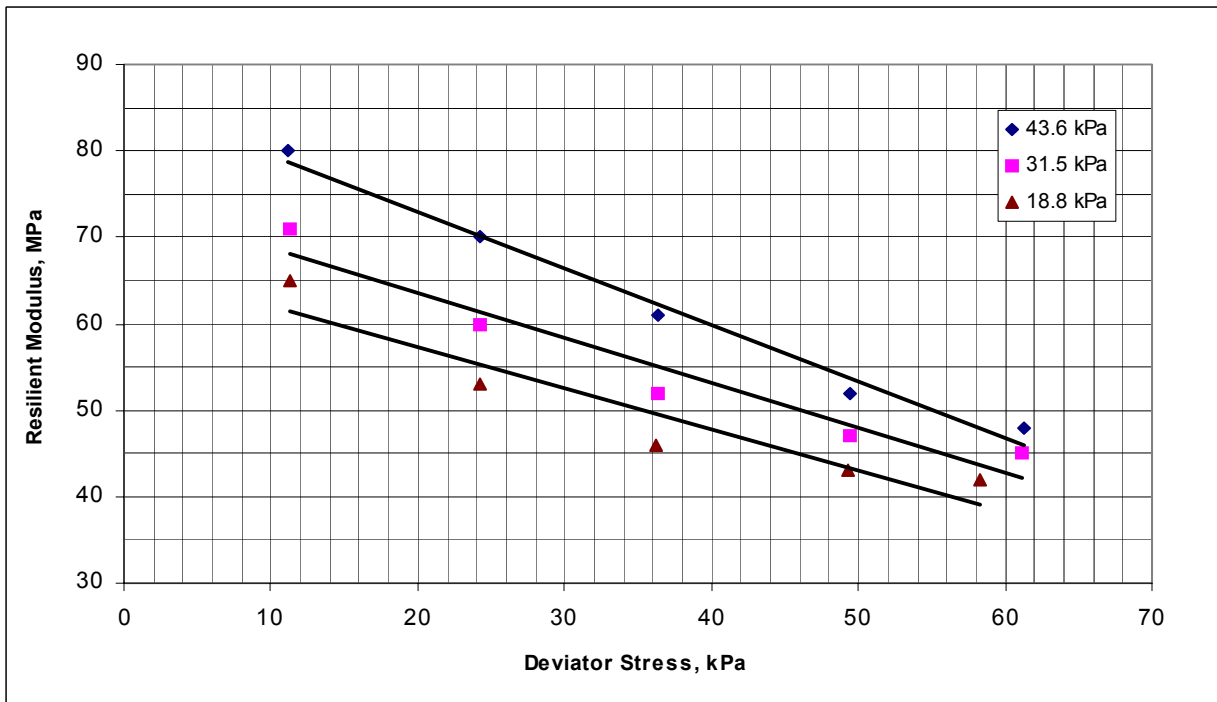


Figure C4 Resilient Modulus Test Results, Station 854+00, Section 1, Sample # 1, 1 MPa = 145 psi

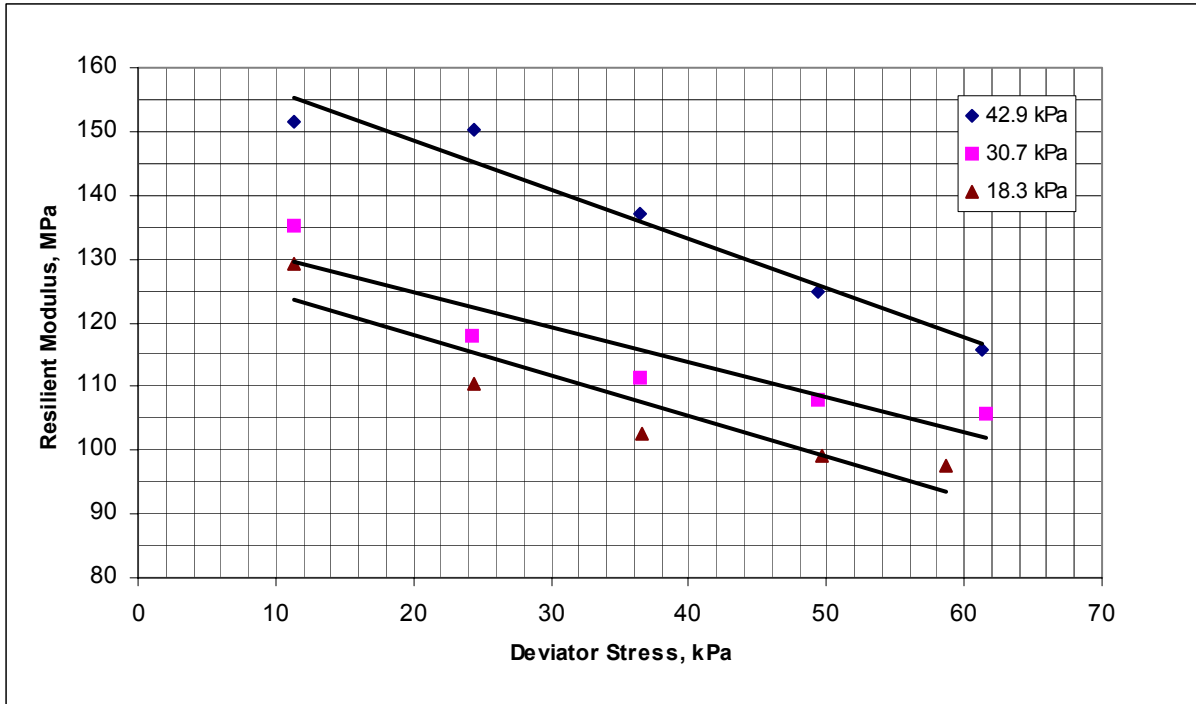


Figure C5 Resilient Modulus Test Results, Station 55+00, Section 2, Sample # 1, 1 MPa = 145 psi

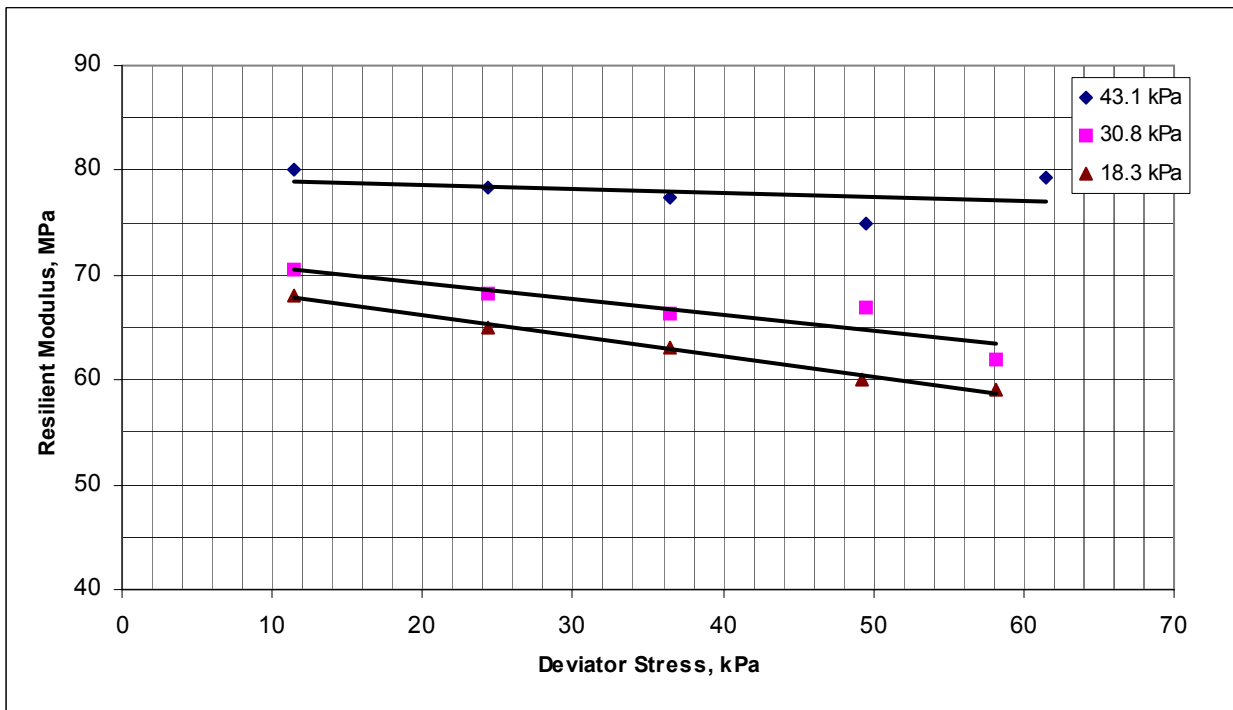


Figure C6 Resilient Modulus Test Results, Station 56+00, Section 2, Sample # 1, 1 MPa = 145 psi

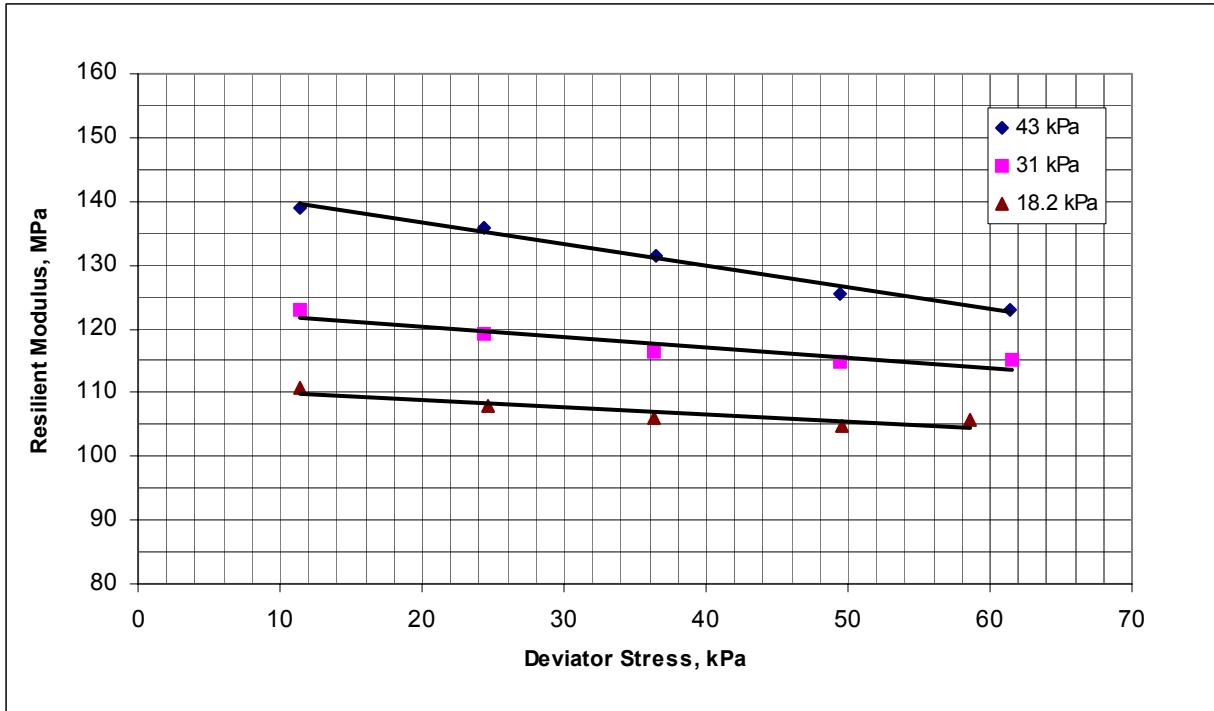


Figure C7 Resilient Modulus Test Results, Station 57+50, Section 2, Sample # 1, 1 MPa = 145 psi

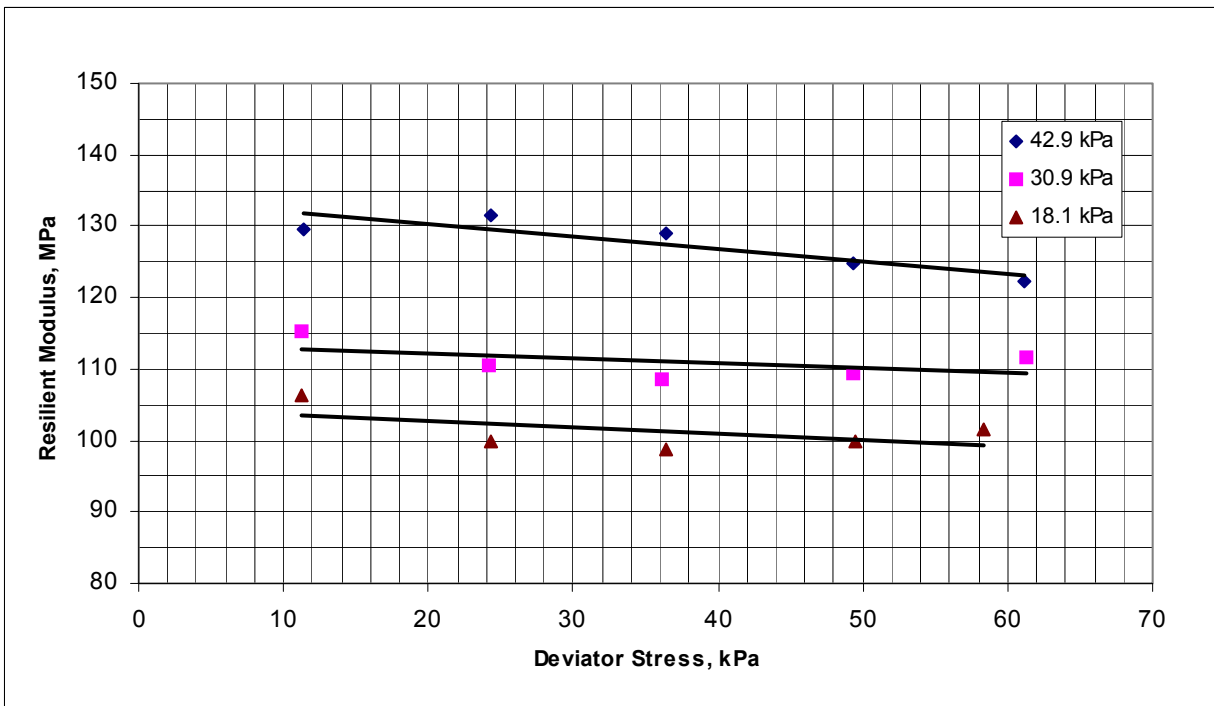


Figure C8 Resilient Modulus Test Results, Station 58+50, Section 2, Sample # 1, 1 MPa = 145 psi

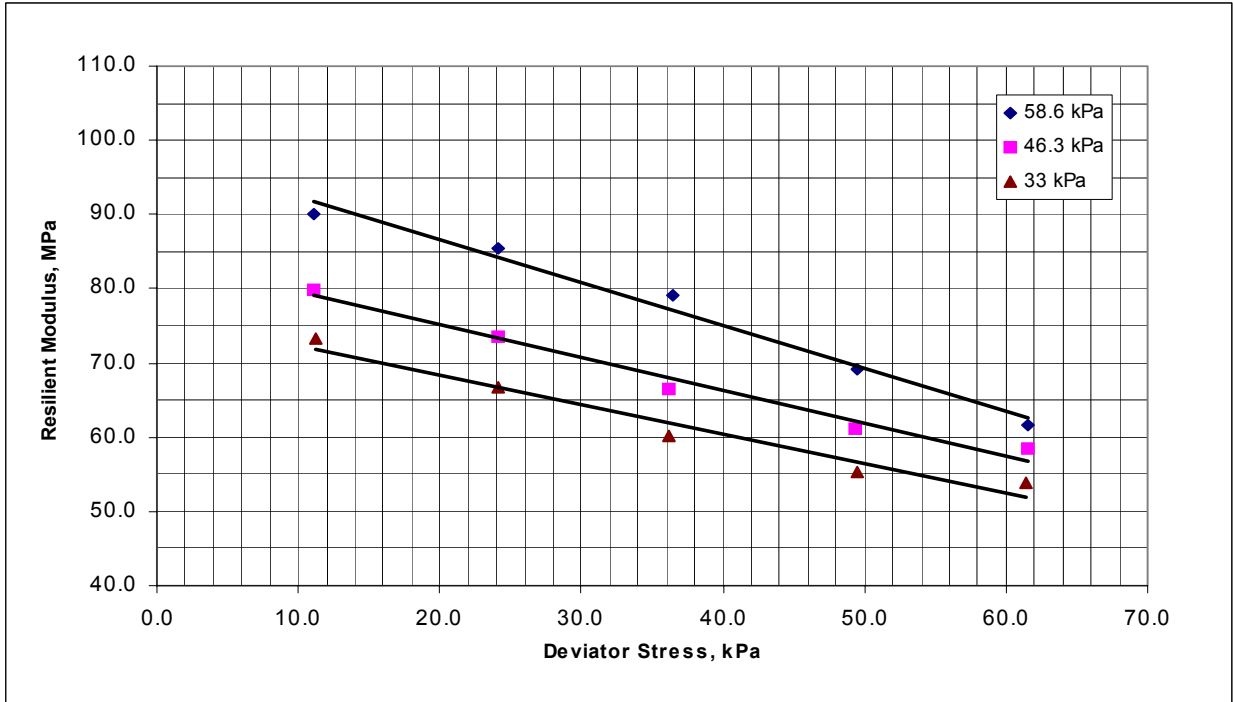


Figure C9 Resilient Modulus Test Results, Station 152+00, Section 3, Sample # 1, 1 MPa = 145 psi

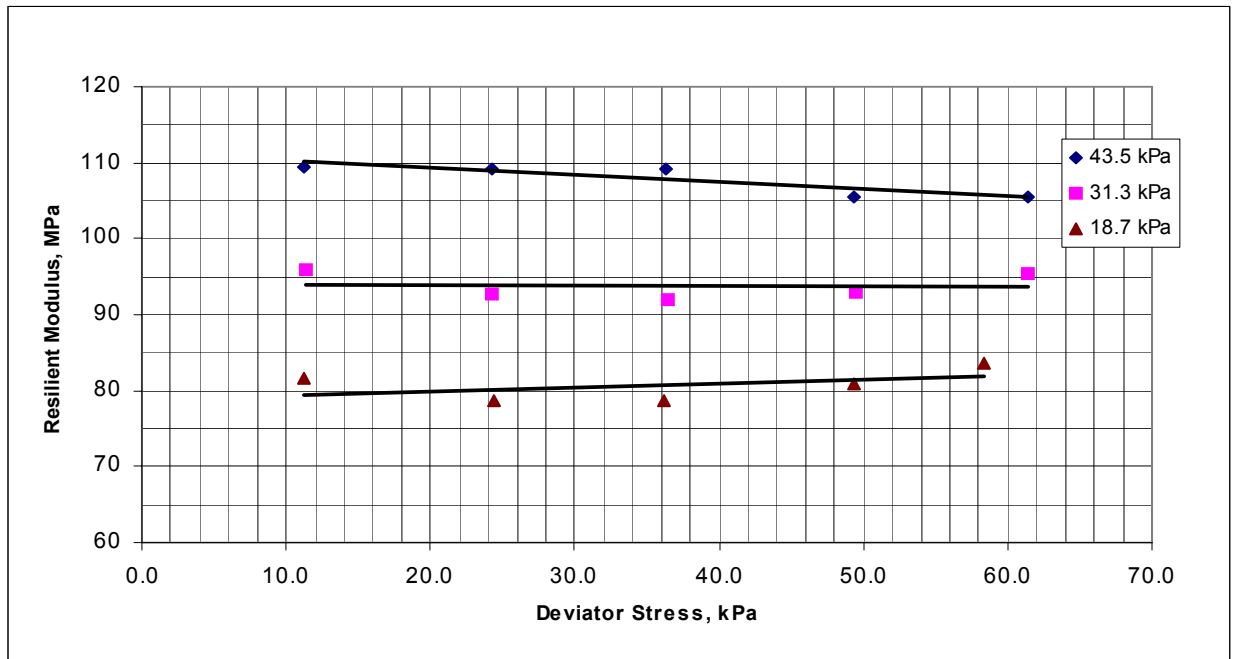


Figure C10 Resilient Modulus Test Results, Station 152+50, Section 3, Sample # 1, 1 MPa = 145 psi

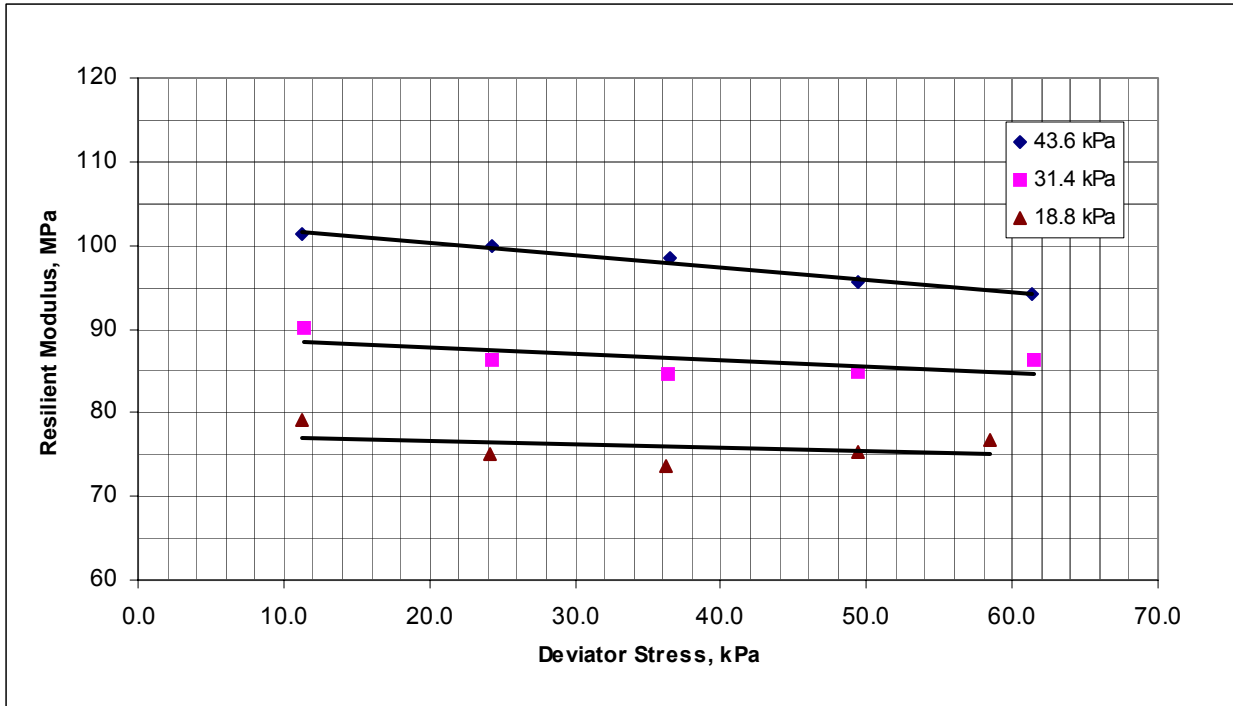


Figure C11 Resilient Modulus Test Results, Station 153+00, Section 3, Sample # 1, 1 MPa = 145 psi

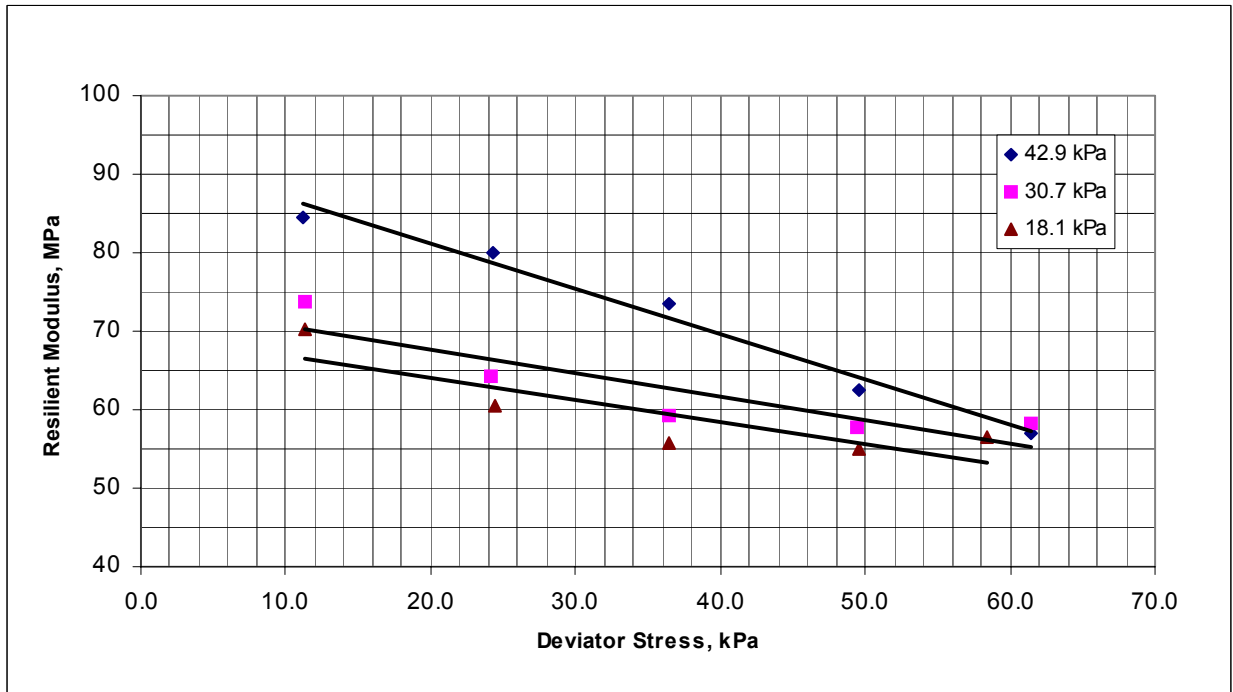


Figure C12 Resilient Modulus Test Results, Station 153+50, Section 3, Sample # 1, 1 MPa = 145 psi

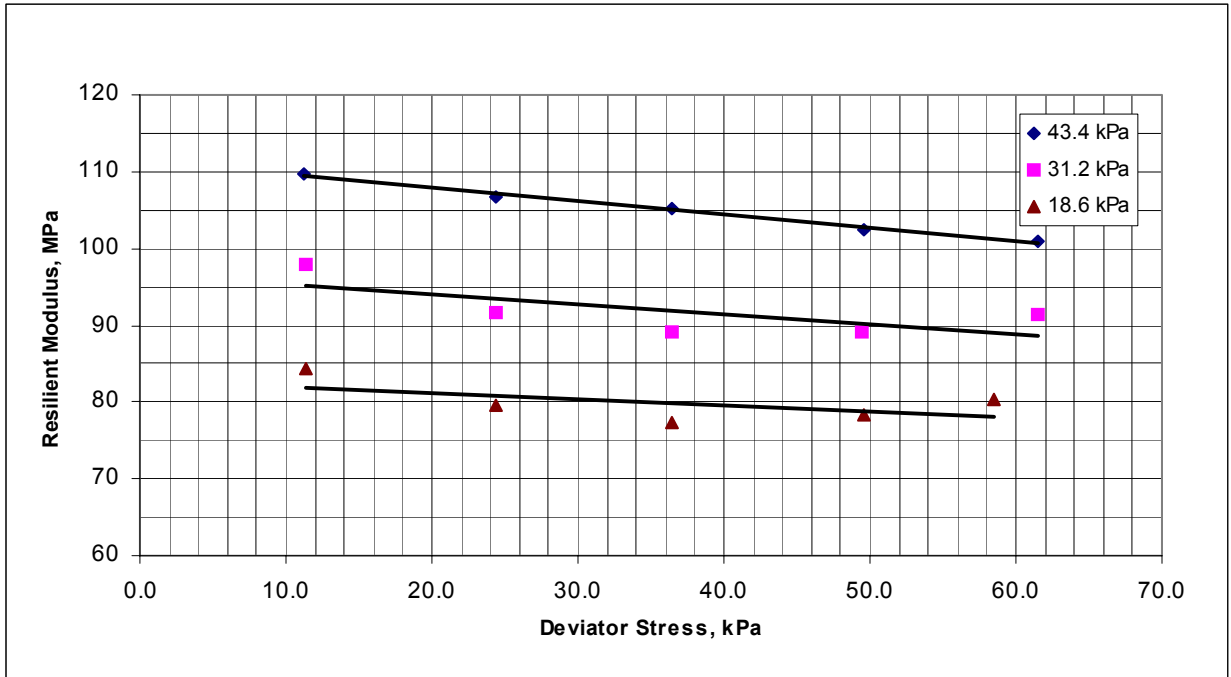


Figure C13 Resilient Modulus Test Results, Station 153+90, Section 3, Sample # 1, 1 MPa = 145 psi

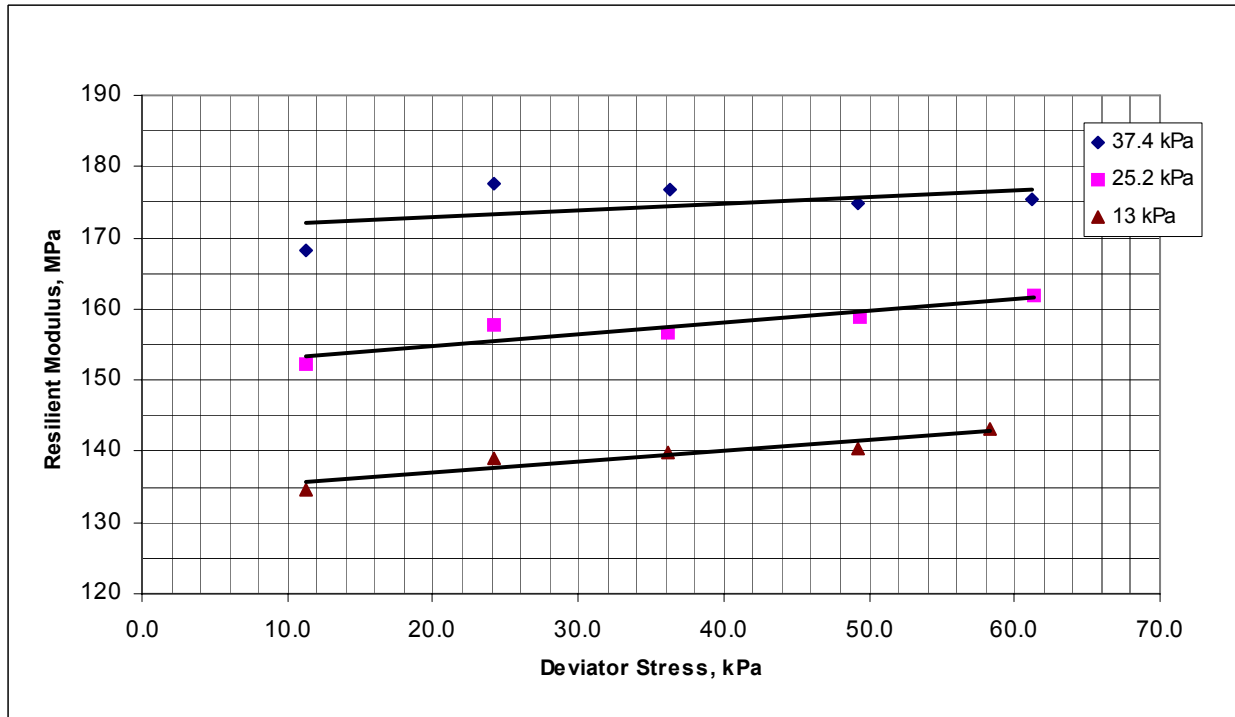


Figure C14 Resilient Modulus Test Results, Station 905+50, Section 4, Sample # 1, 1 MPa = 145 psi

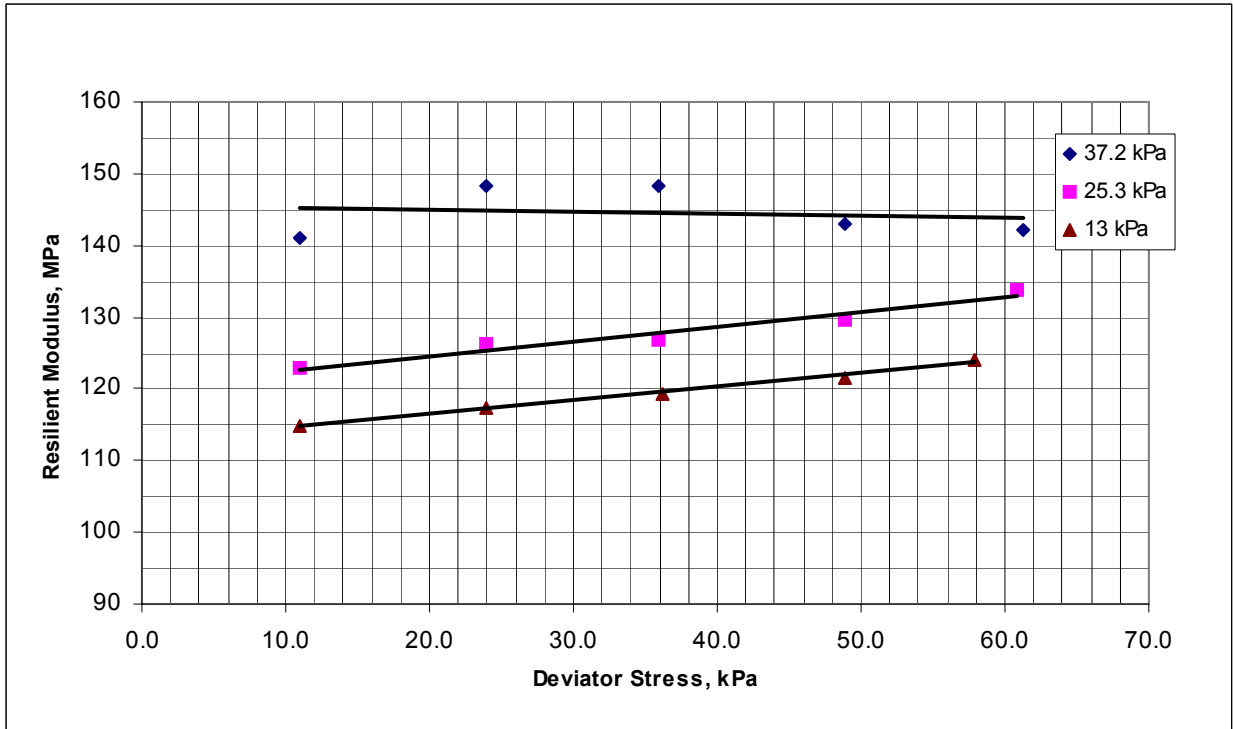


Figure C15 Resilient Modulus Test Results, Station 906+00, Section 4, Sample # 1, 1 MPa = 145 psi

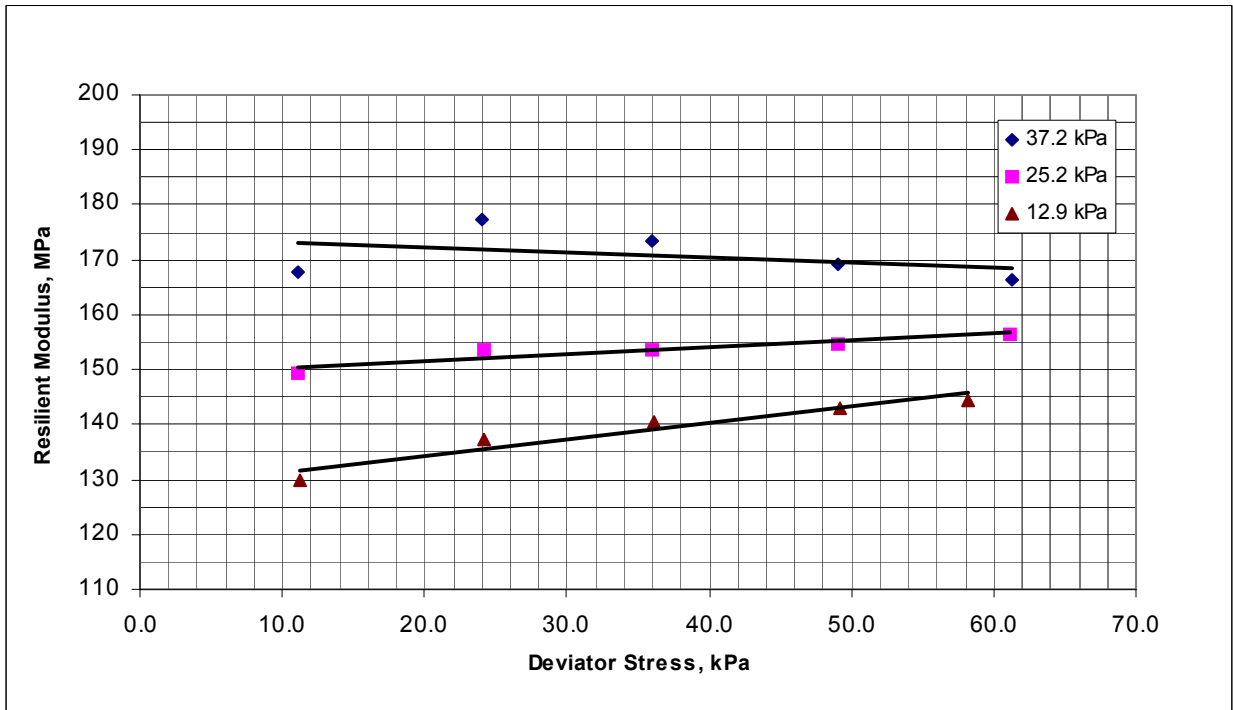


Figure C16 Resilient Modulus Test Results, Station 906+50, Section 4, Sample # 1, 1 MPa = 145 psi

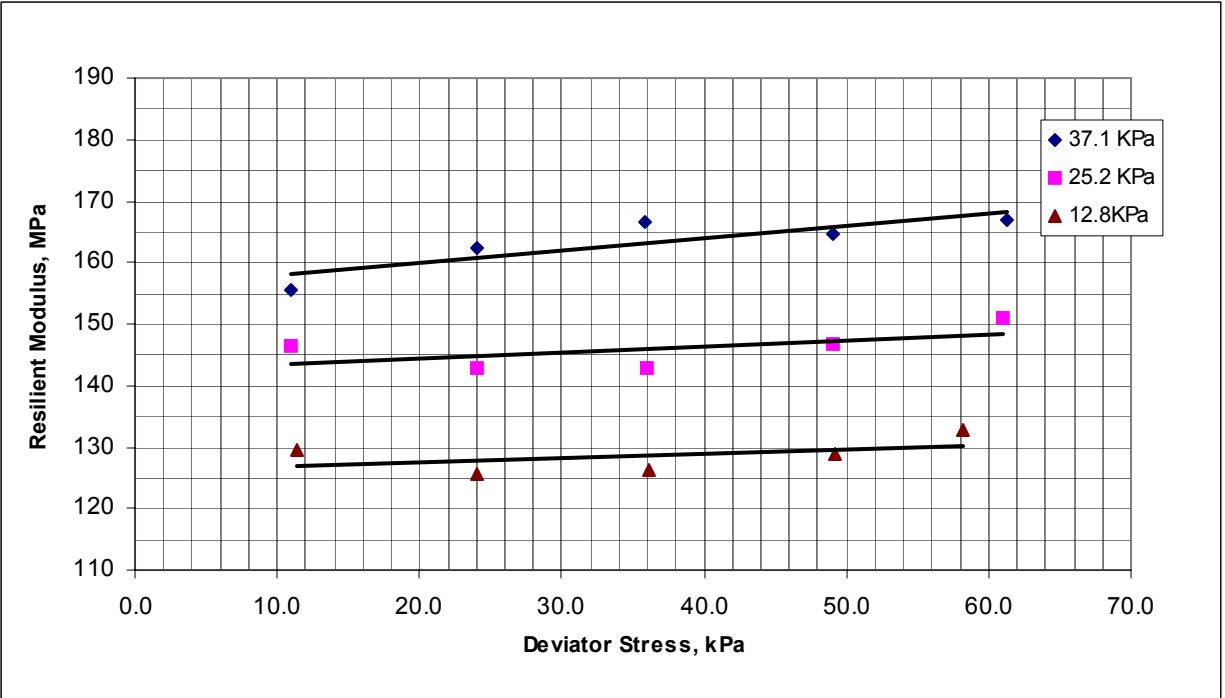


Figure C17 Resilient Modulus Test Results, Station 907+00, Section 4, Sample # 1, 1 MPa = 145 psi

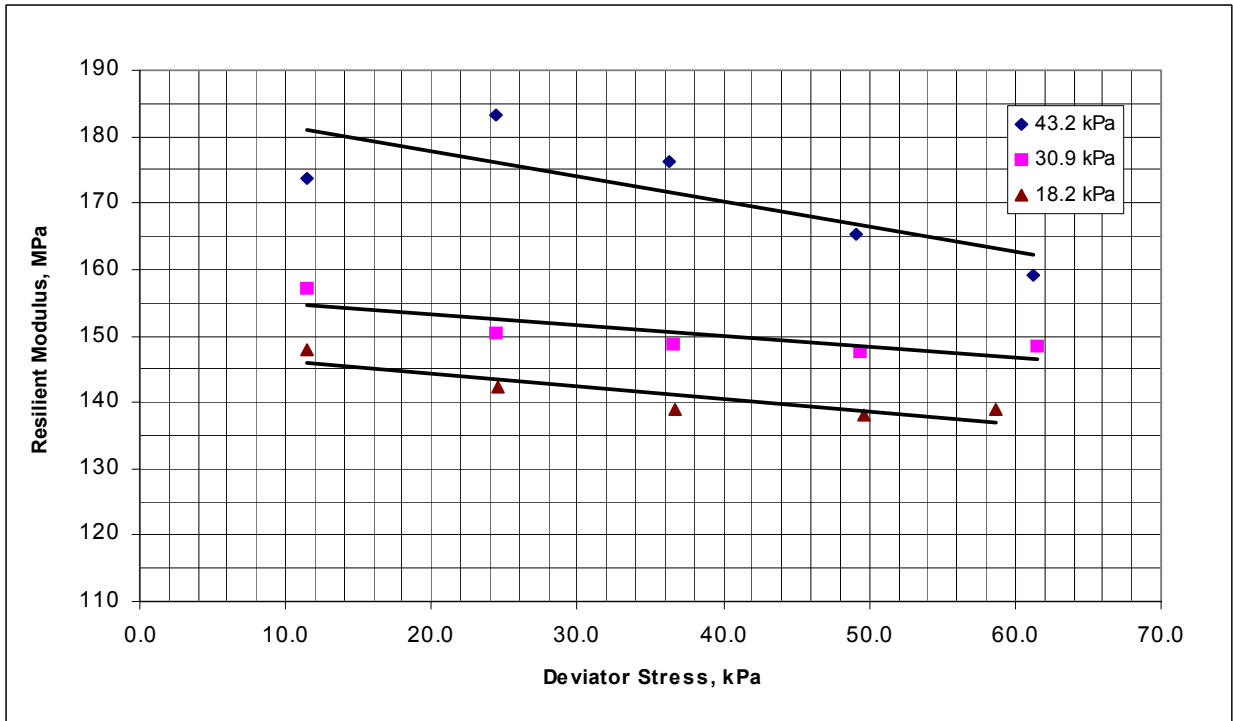


Figure C18 Resilient Modulus Test Results, Station 907+50, Section 4, Sample # 1, 1 MPa = 145 psi

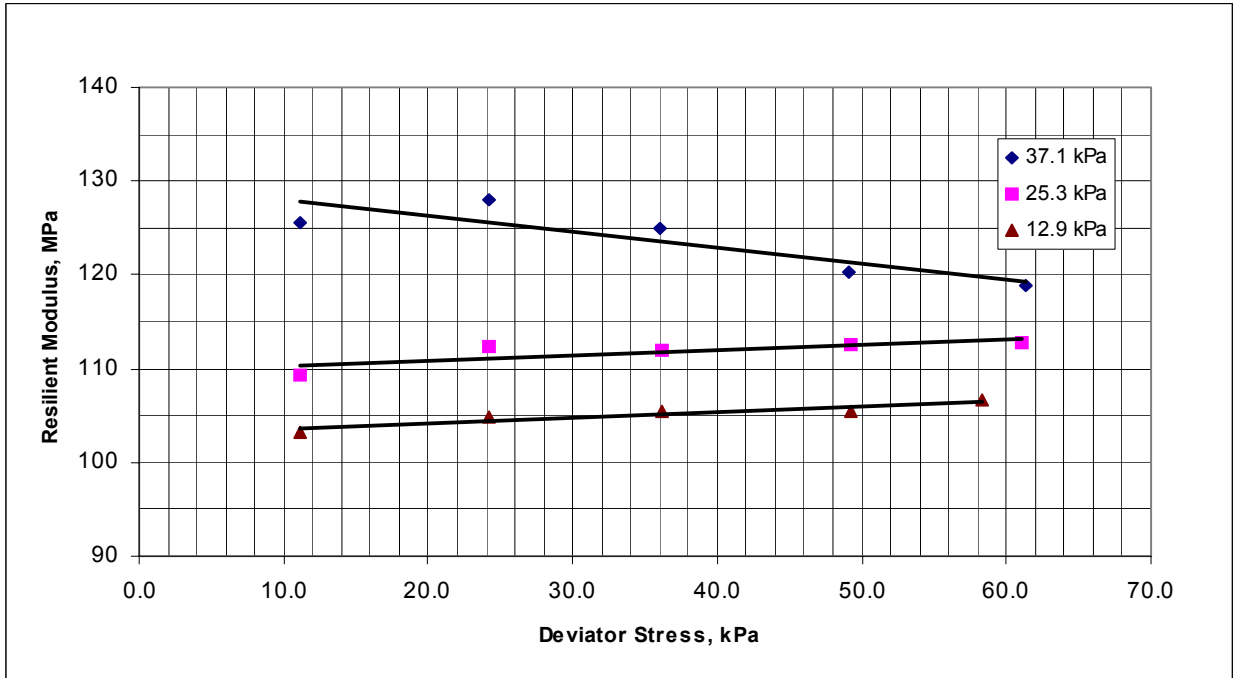


Figure C19 Resilient Modulus Test Results, Station 833+20, Section 5, Sample # 1, 1 MPa = 145 psi

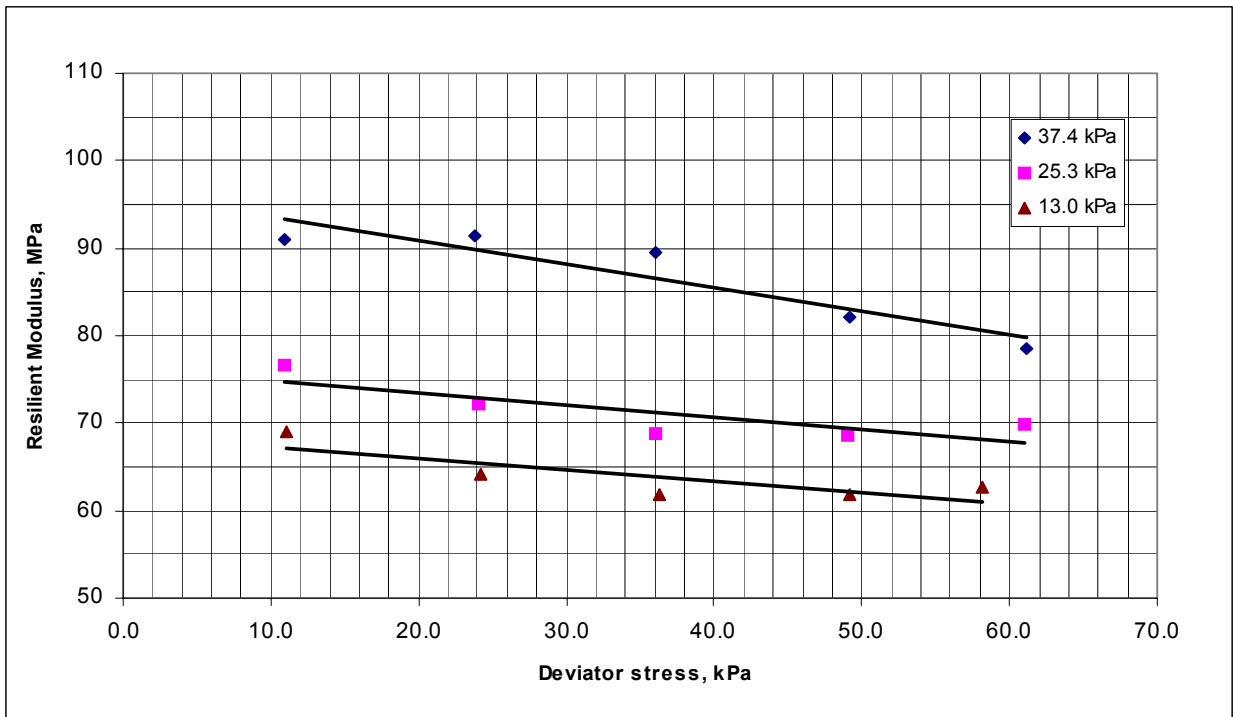


Figure C20 Resilient Modulus Test Results, Station 834+00, Section 5, Sample # 1, 1 MPa = 145 psi

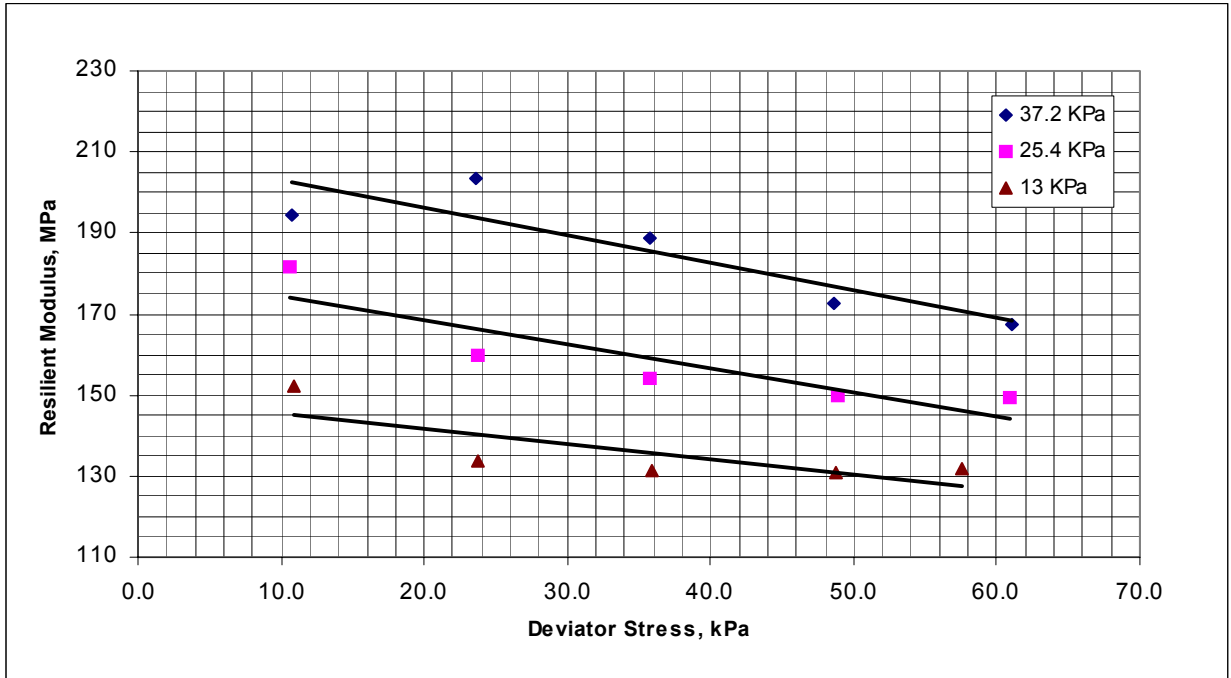


Figure C21 Resilient Modulus Test Results, Station 834+40, Section 5, Sample # 1, 1 MPa = 145 psi

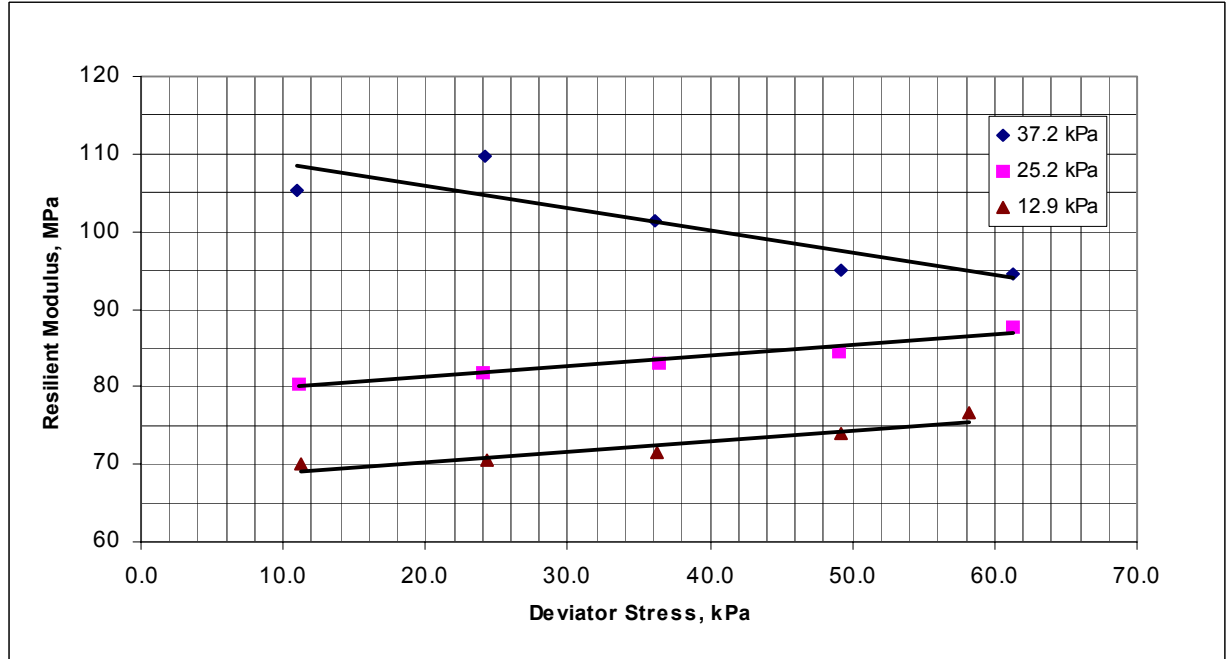


Figure C22 Resilient Modulus Test Results, Station 25+00, Section 6, Sample # 1, 1 MPa = 145 psi

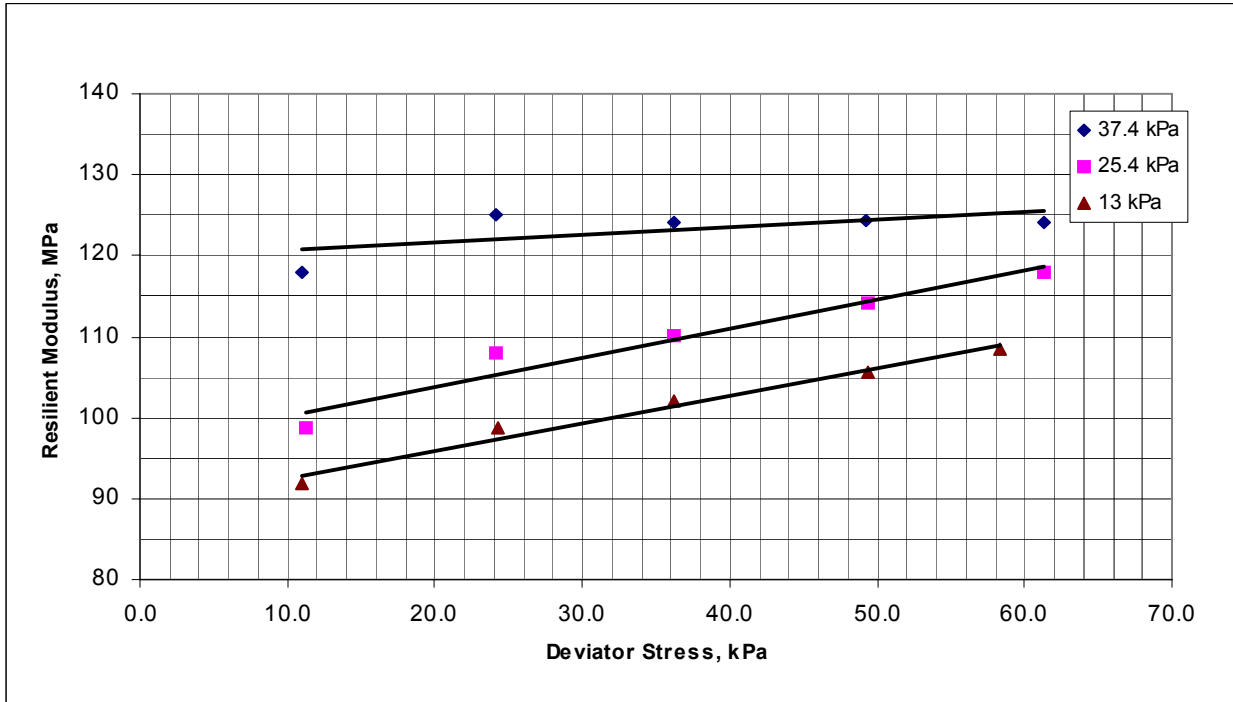


Figure C23 Resilient Modulus Test Results, Station 25+50, Section 6, Sample # 1, 1 MPa = 145 psi

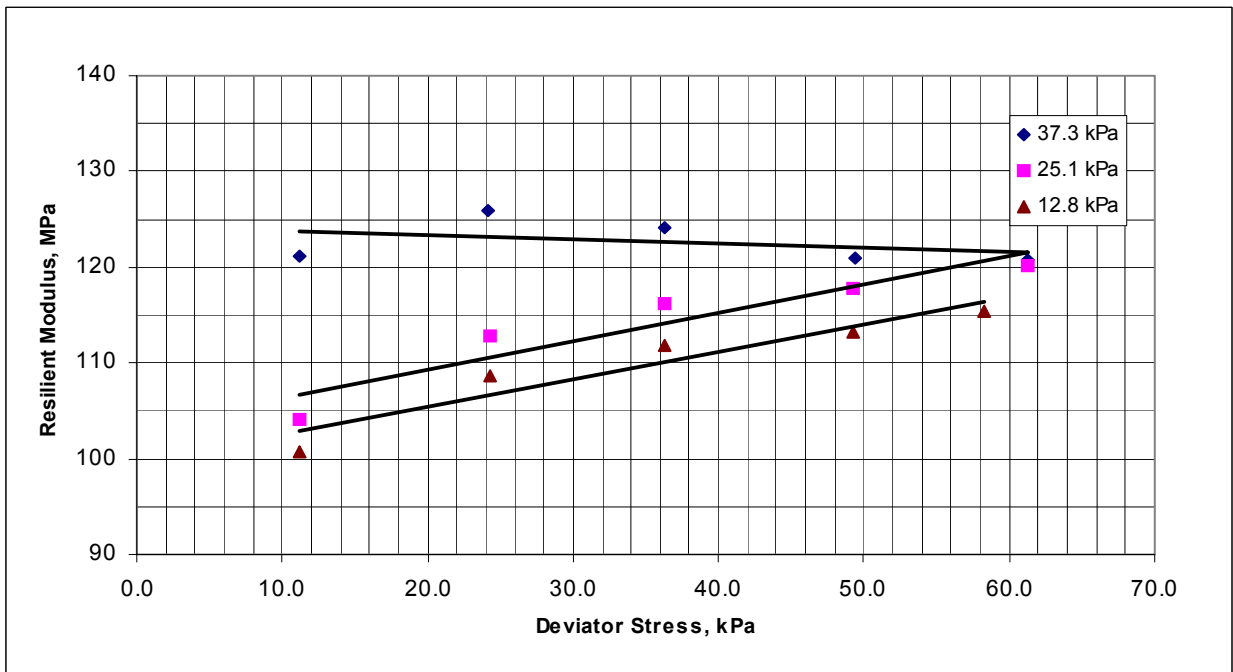


Figure C24 Resilient Modulus Test Results, Station 26+00, Section 6, Sample # 1, 1 MPa = 145 psi

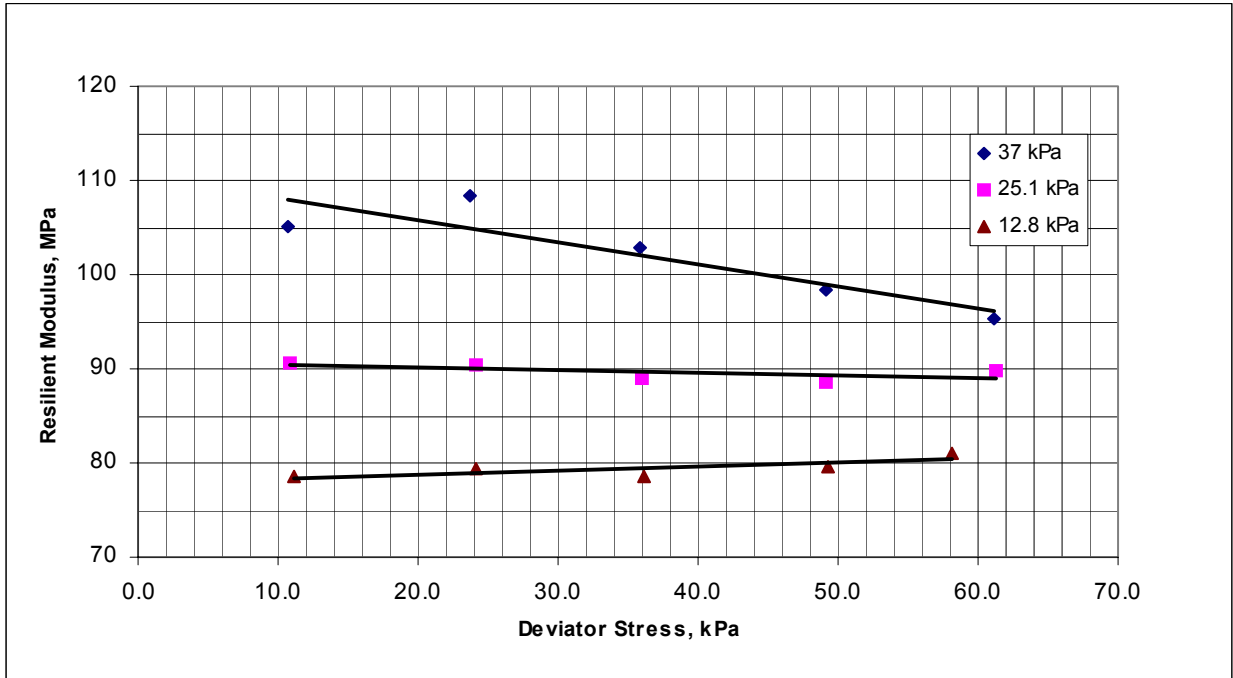


Figure C25 Resilient Modulus Test Results, Station 26+50, Section 6, Sample # 1, 1 MPa = 145 psi

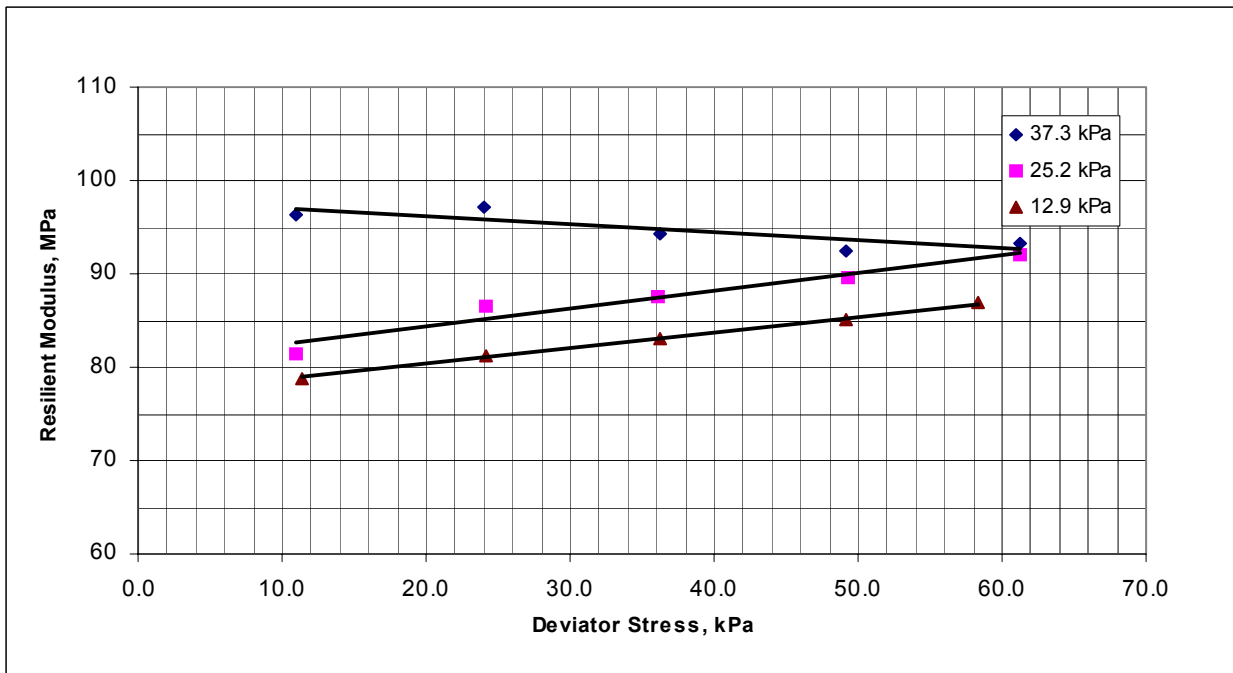


Figure C26 Resilient Modulus Test Results, Station 27+00, Section 6, Sample # 1, 1 MPa = 145 psi

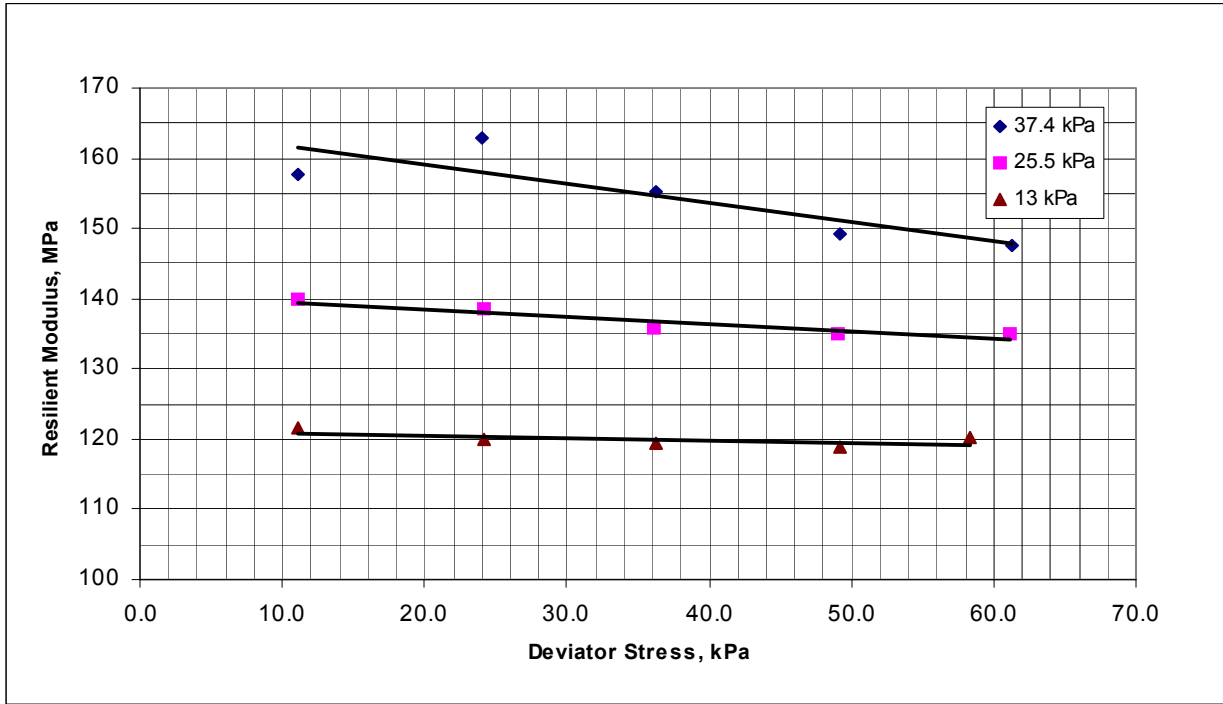


Figure C27 Resilient Modulus Test Results, Station 6+500, Section 7, Sample # 1, 1 MPa = 145 psi

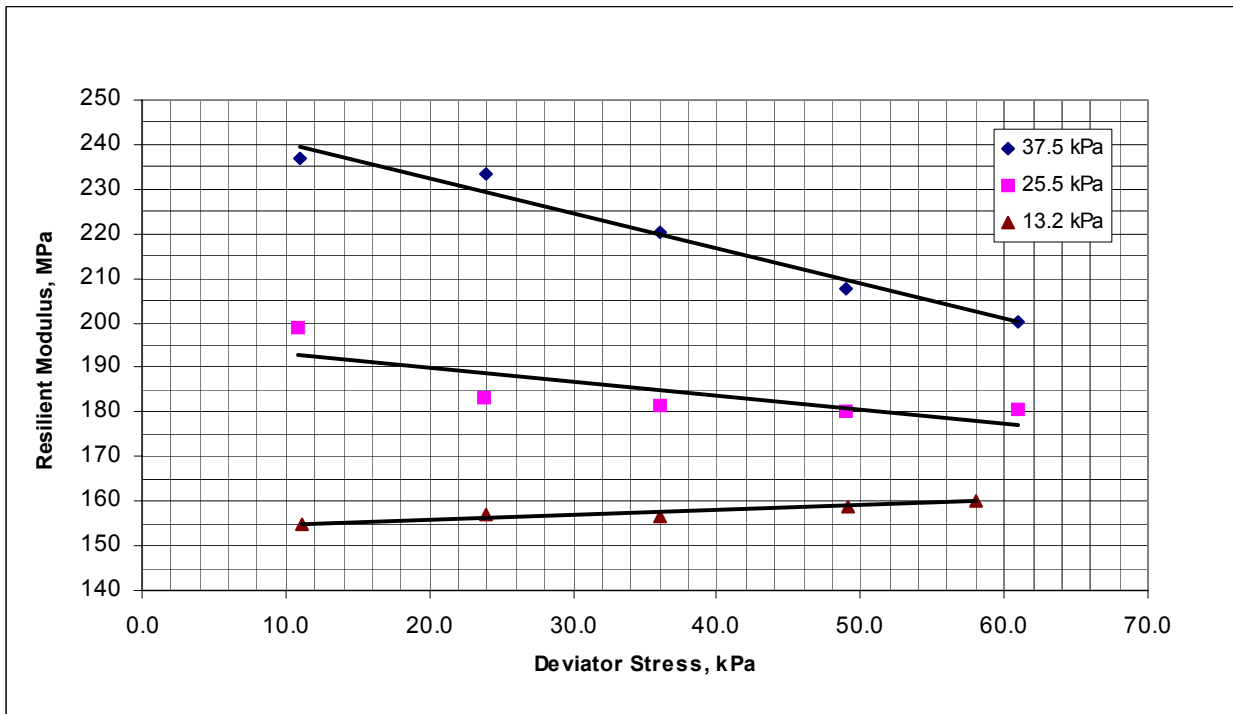


Figure C28 Resilient Modulus Test Results, Station 6+515, Section 7, Sample # 1, 1 MPa = 145 psi

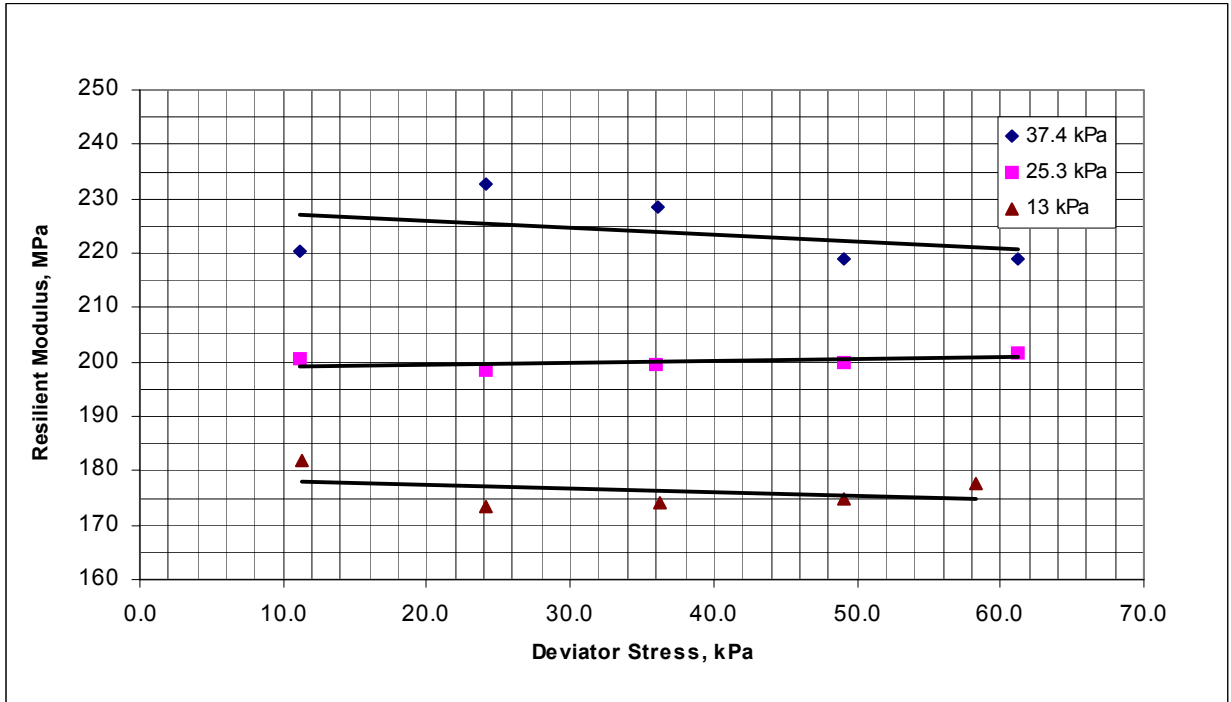


Figure C29 Resilient Modulus Test Results, Station 6+530, Section 7, Sample # 1, 1 MPa = 145 psi

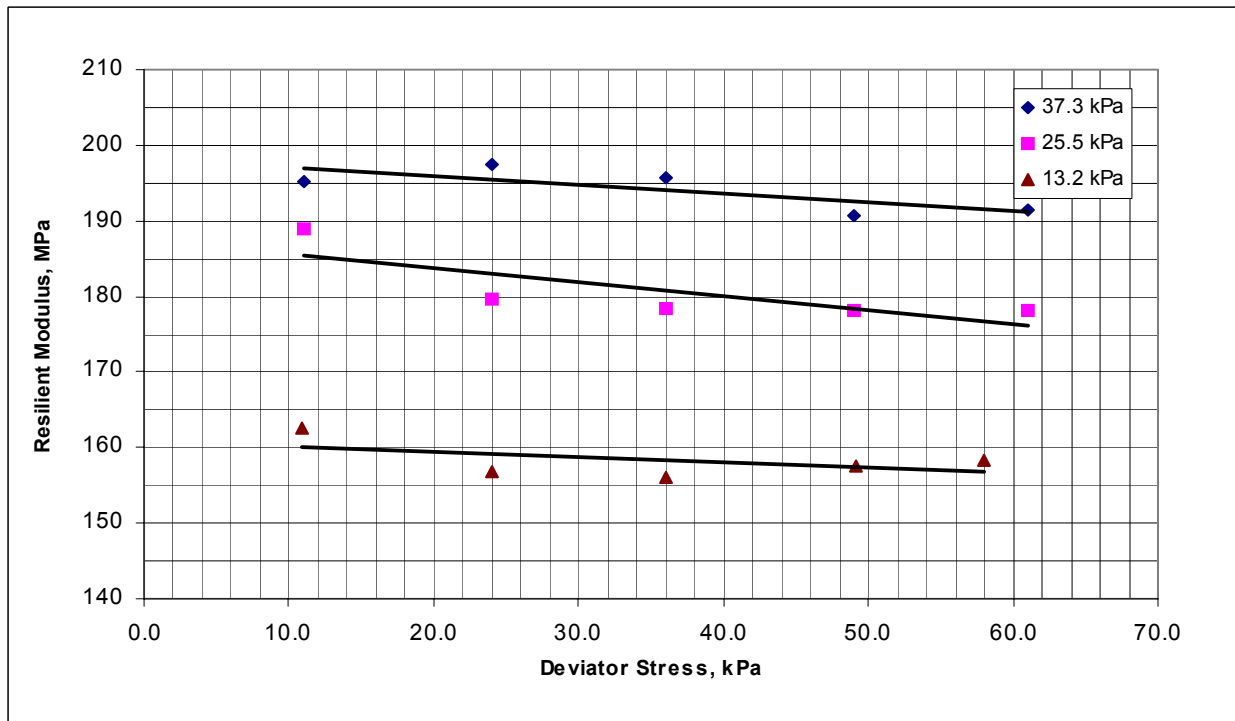


Figure C30 Resilient Modulus Test Results, Station 6+545, Section 7, Sample # 1, 1 MPa = 145 psi

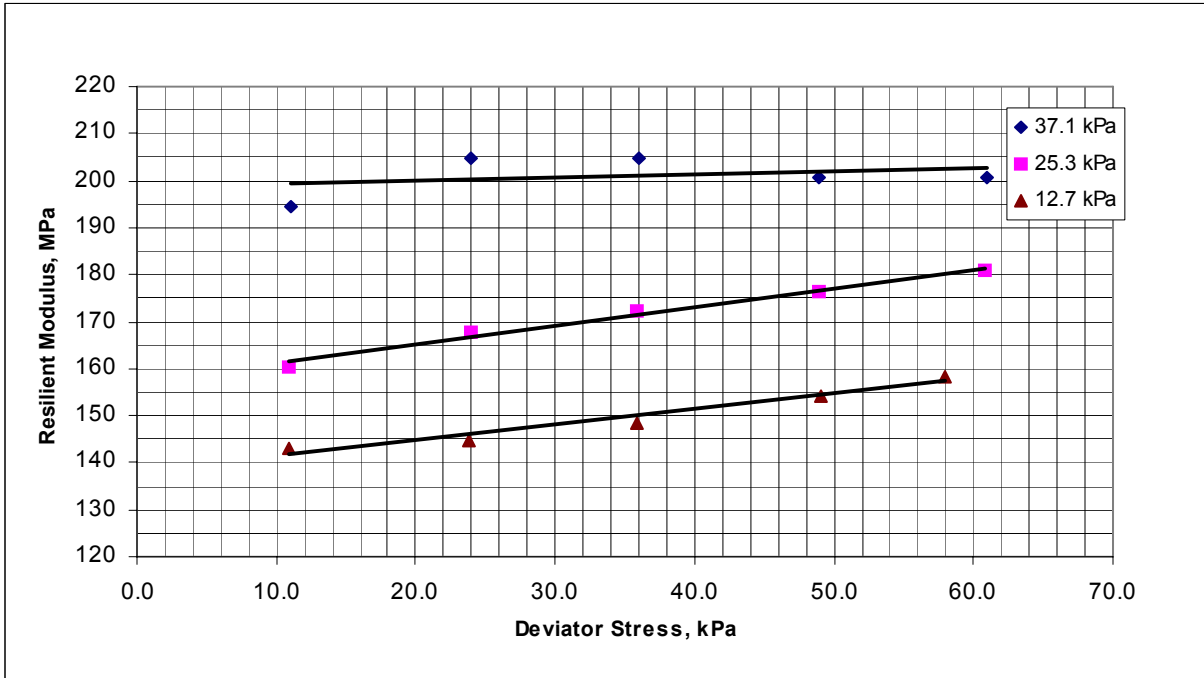


Figure C31 Resilient Modulus Test Results, Station 6+560, Section 7, Sample # 1, 1 MPa = 145 psi

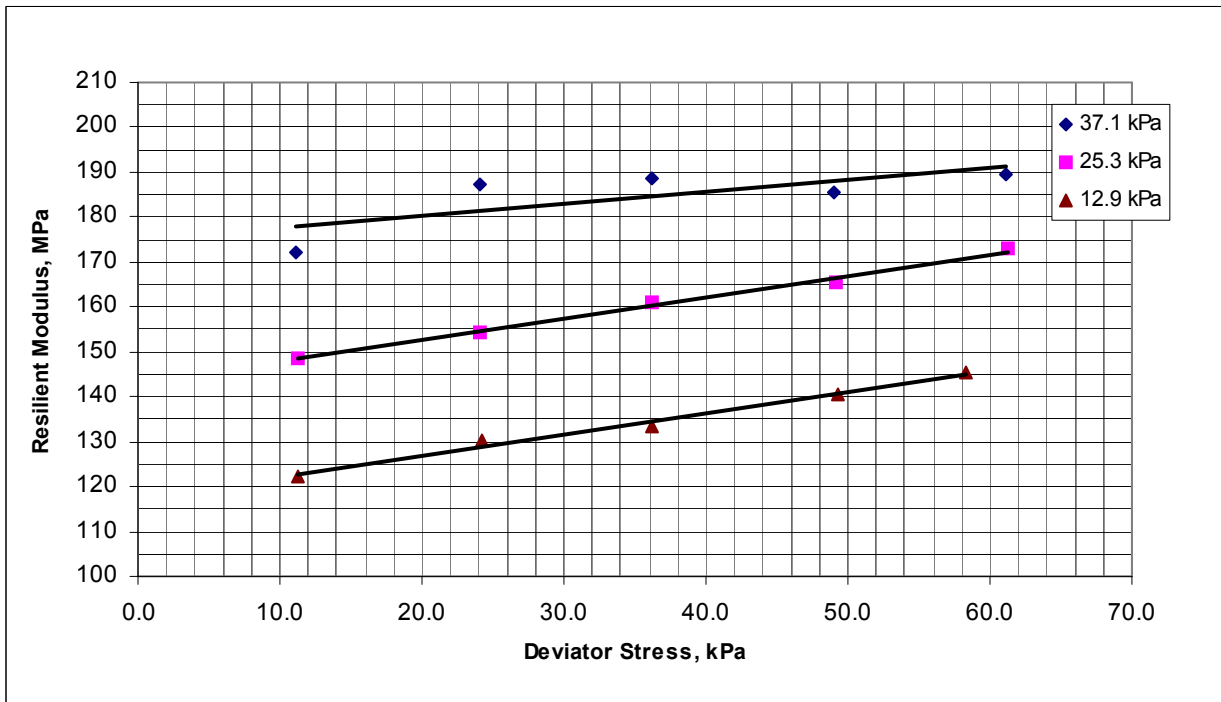


Figure C32 Resilient Modulus Test Results, Station 7+375, Section 8, Sample # 1, 1 MPa = 145 psi

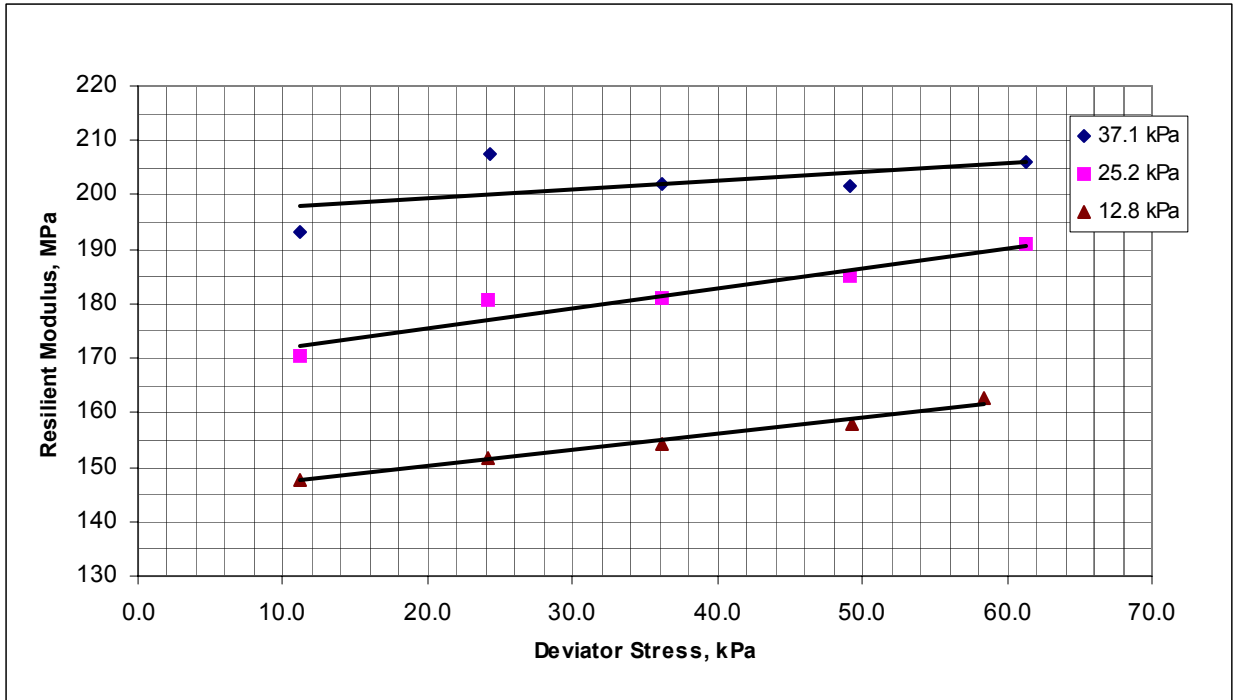


Figure C33 Resilient Modulus Test Results, Station 7+390, Section 8, Sample # 1, 1 MPa = 145 psi

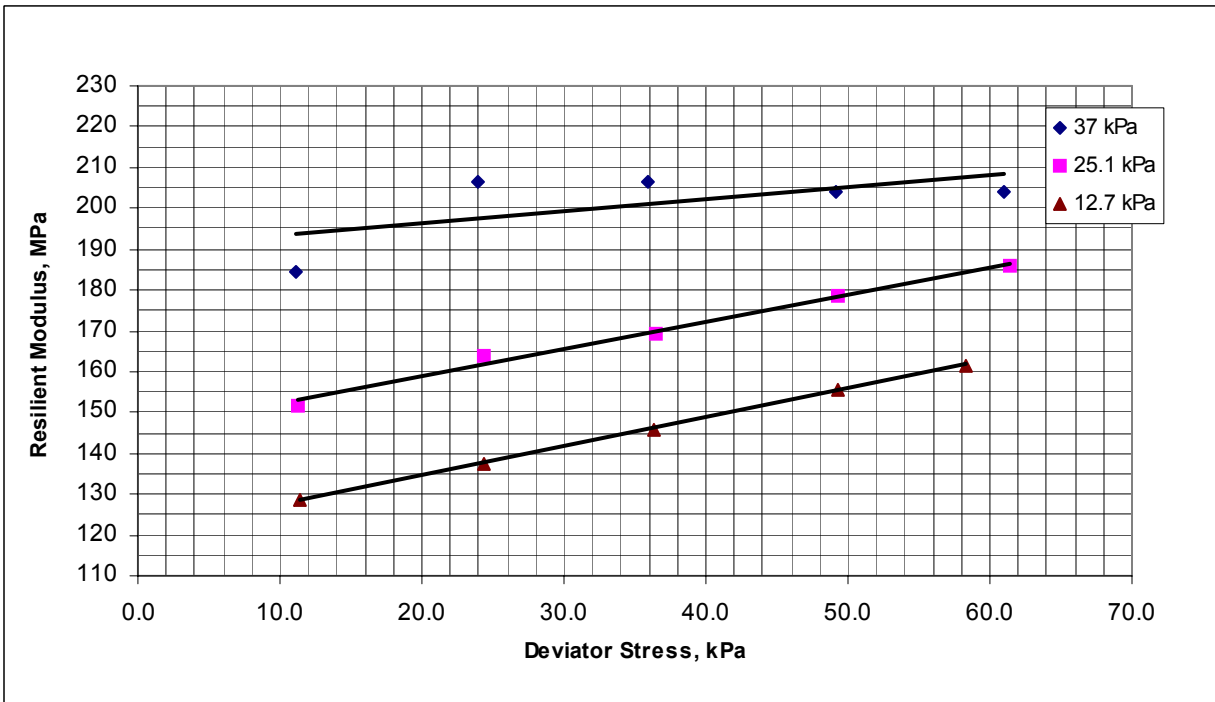


Figure C34 Resilient Modulus Test Results, Station 7+405, Section 8, Sample # 1, 1 MPa = 145 psi

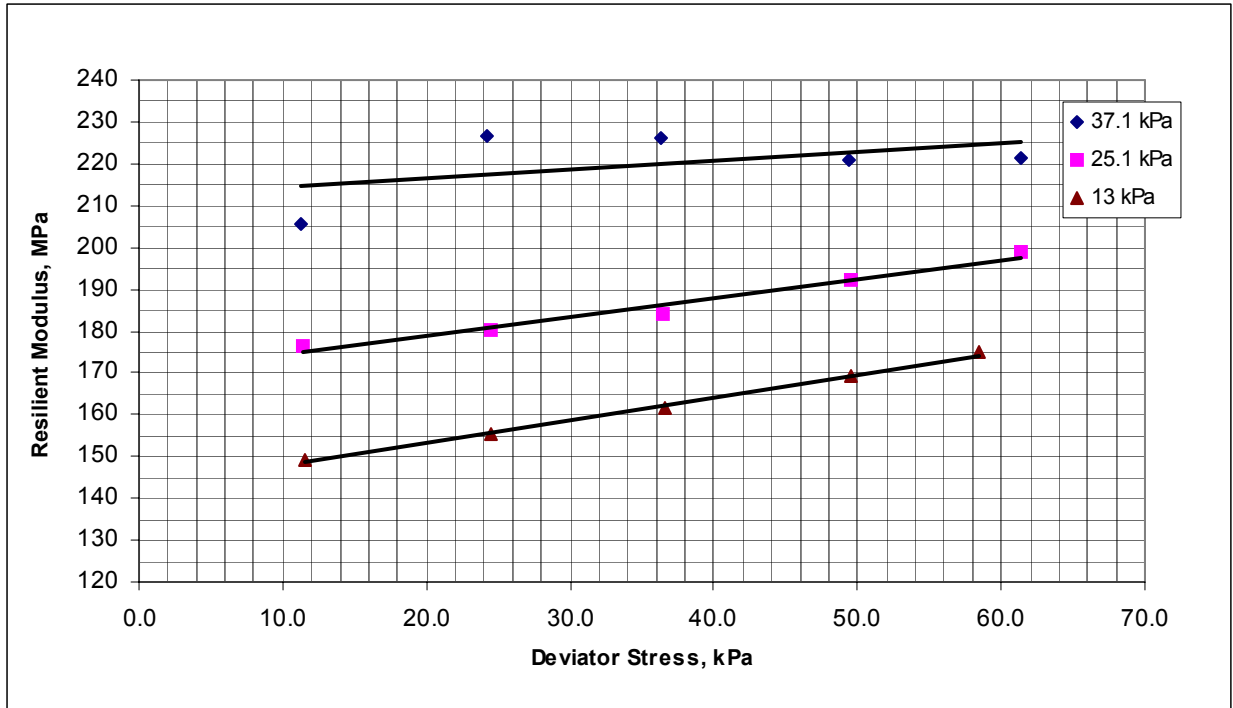


Figure C35 Resilient Modulus Test Results, Station 7+420, Section 8, Sample # 1, 1 MPa = 145 psi

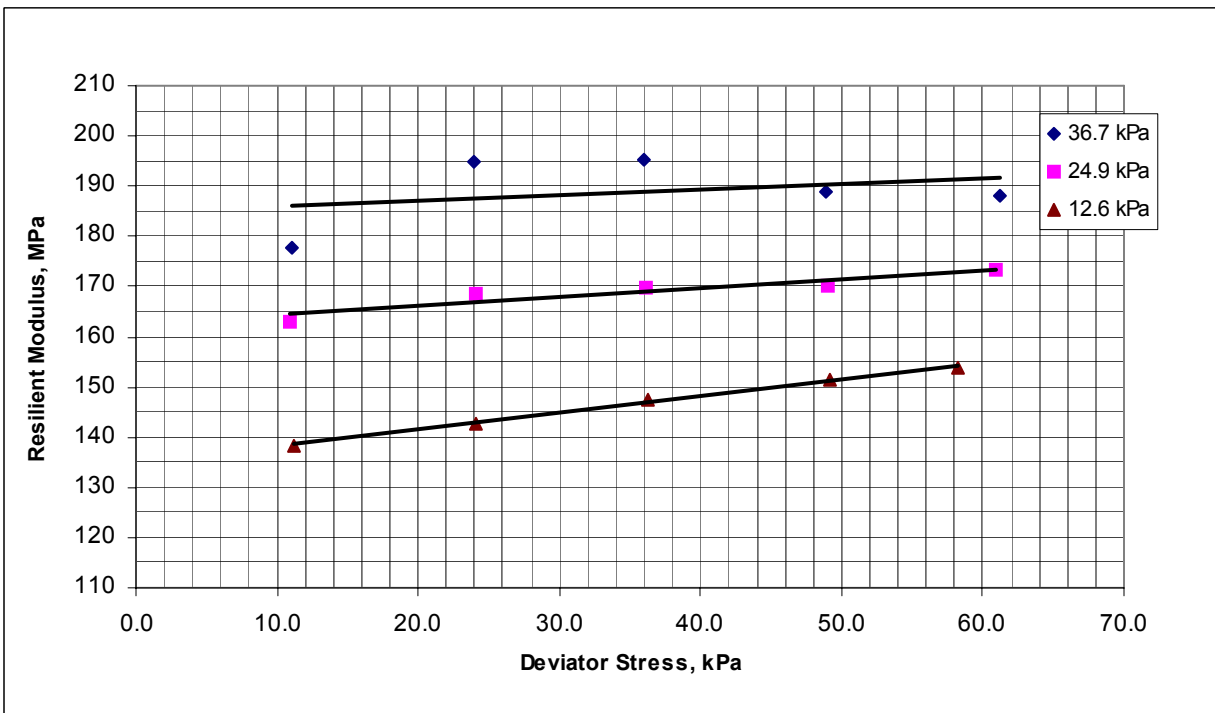


Figure C36 Resilient Modulus Test Results, Station 7+375, Section 9, Sample # 1, 1 MPa = 145 psi

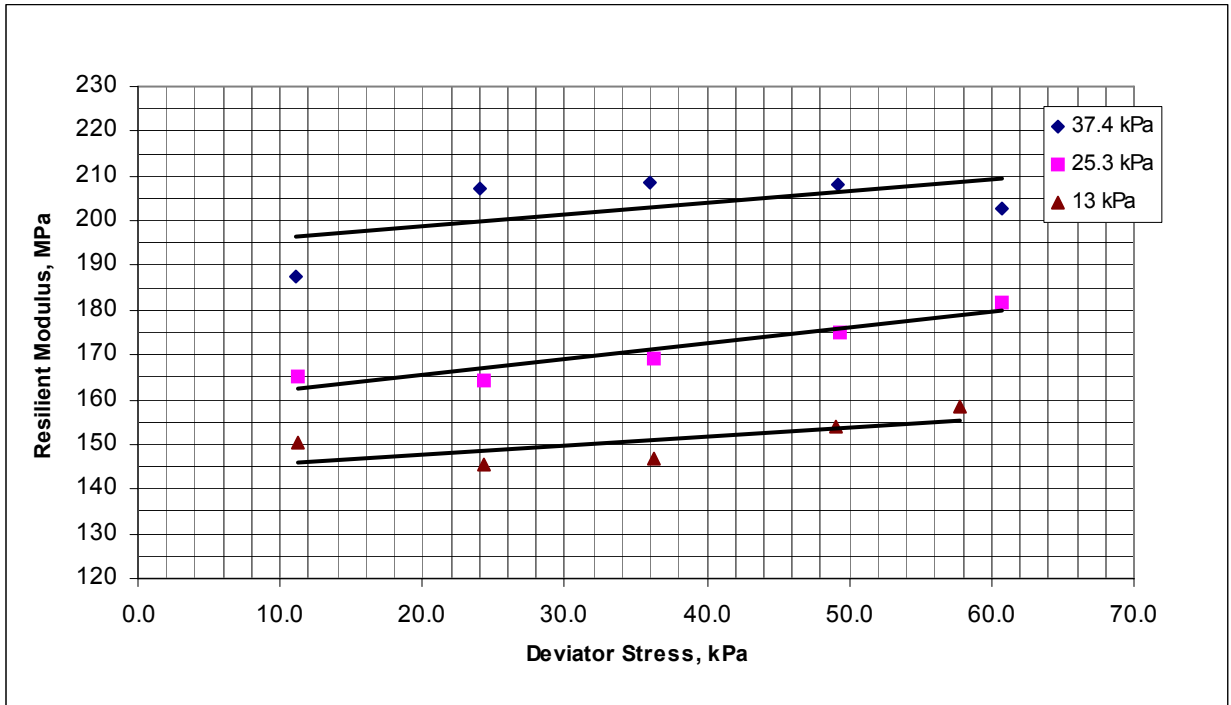


Figure C37 Resilient Modulus Test Results, Station 7+390, Section 9, Sample # 1, 1 MPa = 145 psi

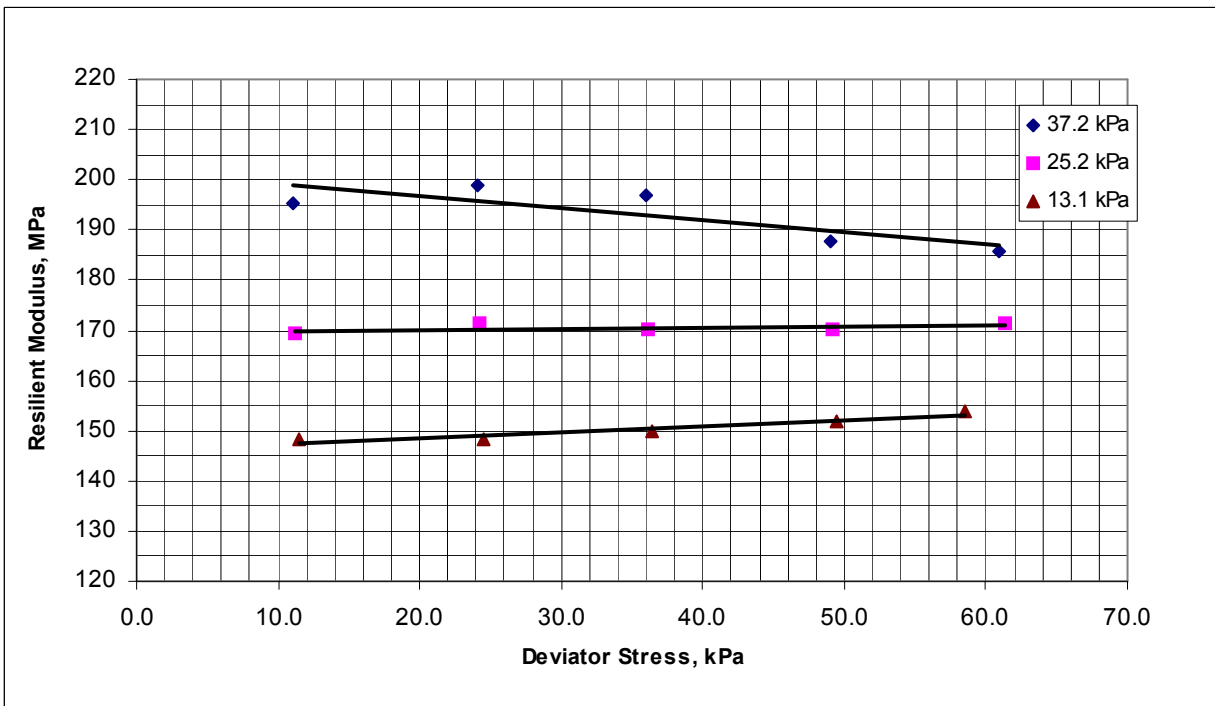


Figure C38 Resilient Modulus Test Results, Station 7+420, Section 9, Sample # 1, 1 MPa = 145 psi

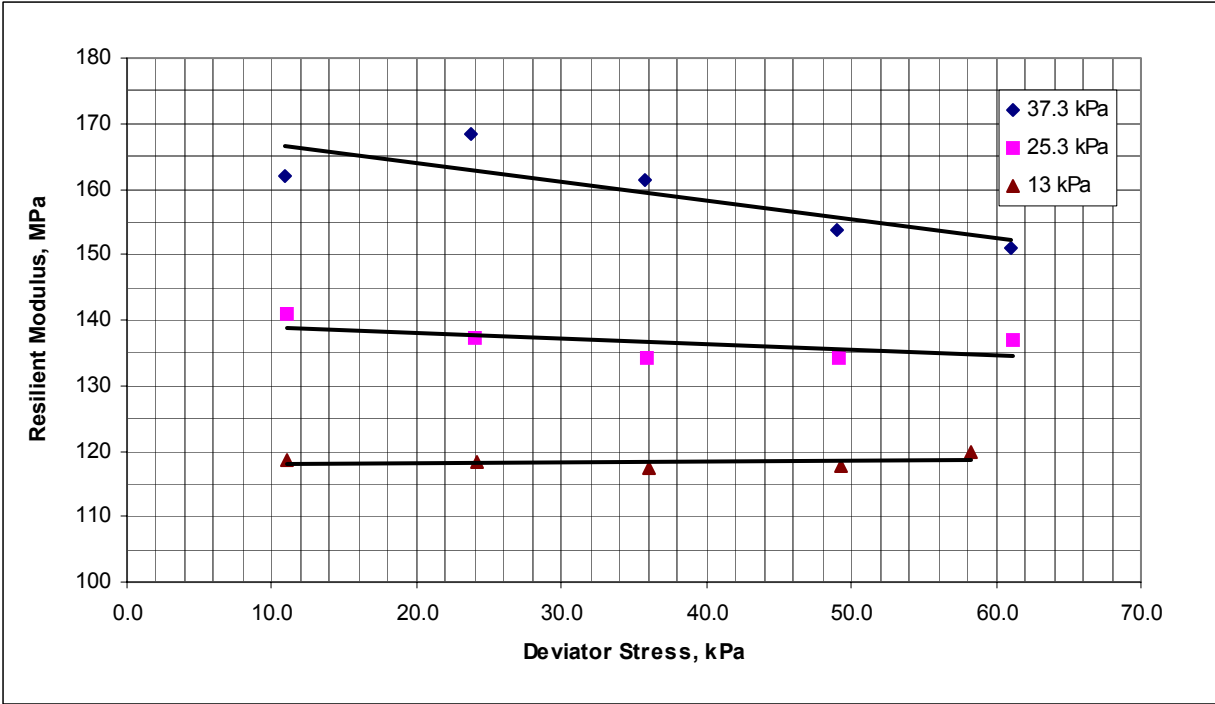


Figure C39 Resilient Modulus Test Results, Station 7+435, Section 9, Sample # 1, 1 MPa = 145 psi

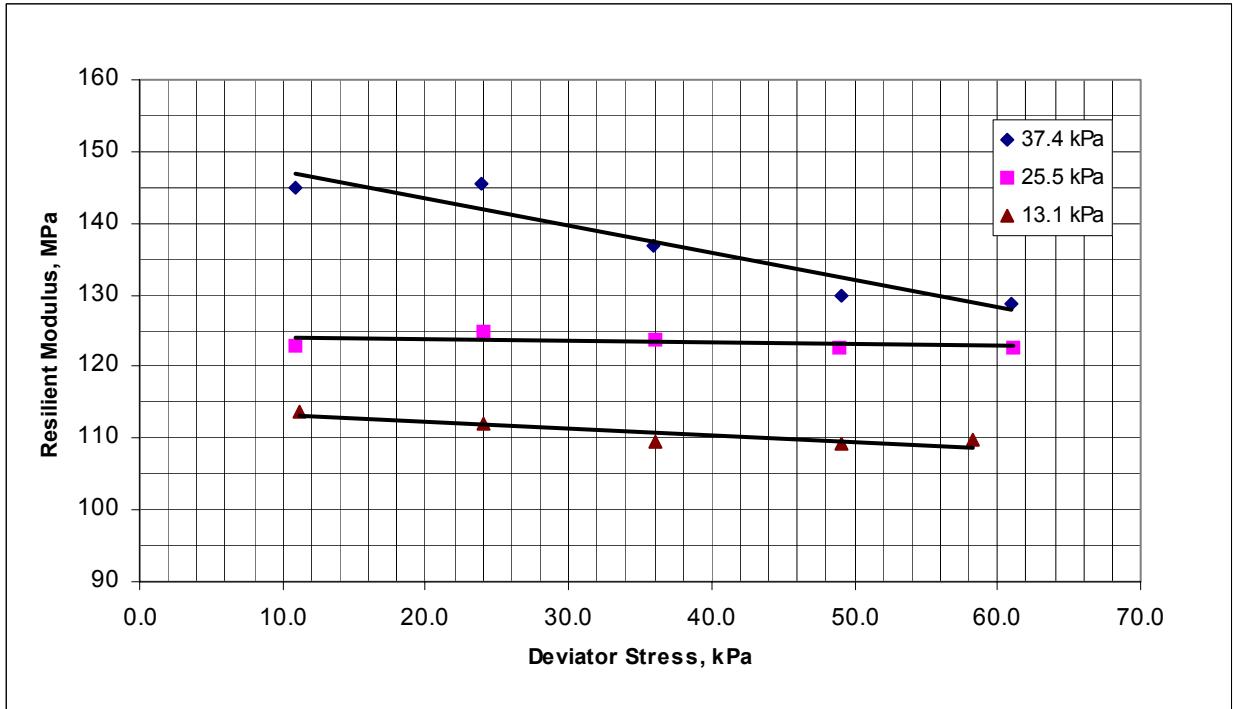


Figure C40 Resilient Modulus Test Results, Station 47+00, Section 10, Sample # 1, 1 MPa = 145 psi

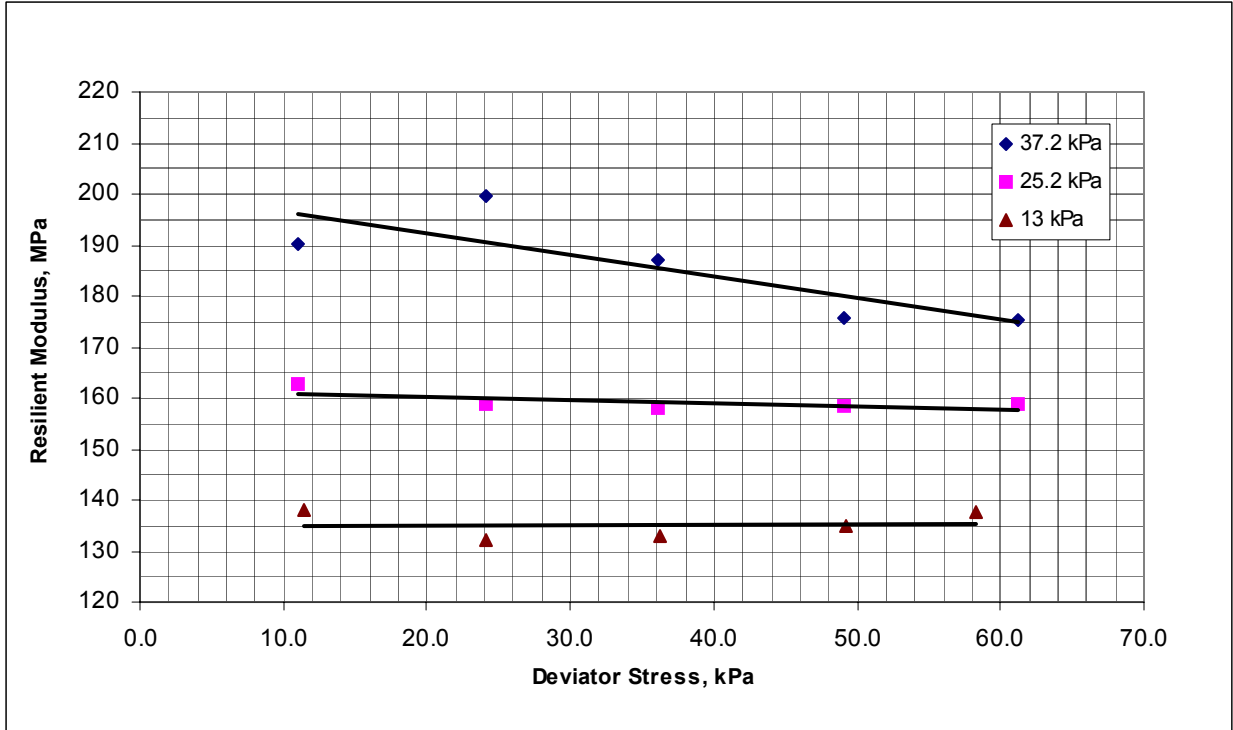


Figure C41 Resilient Modulus Test Results, Station 47+50, Section 10, Sample # 1, 1 MPa = 145 psi

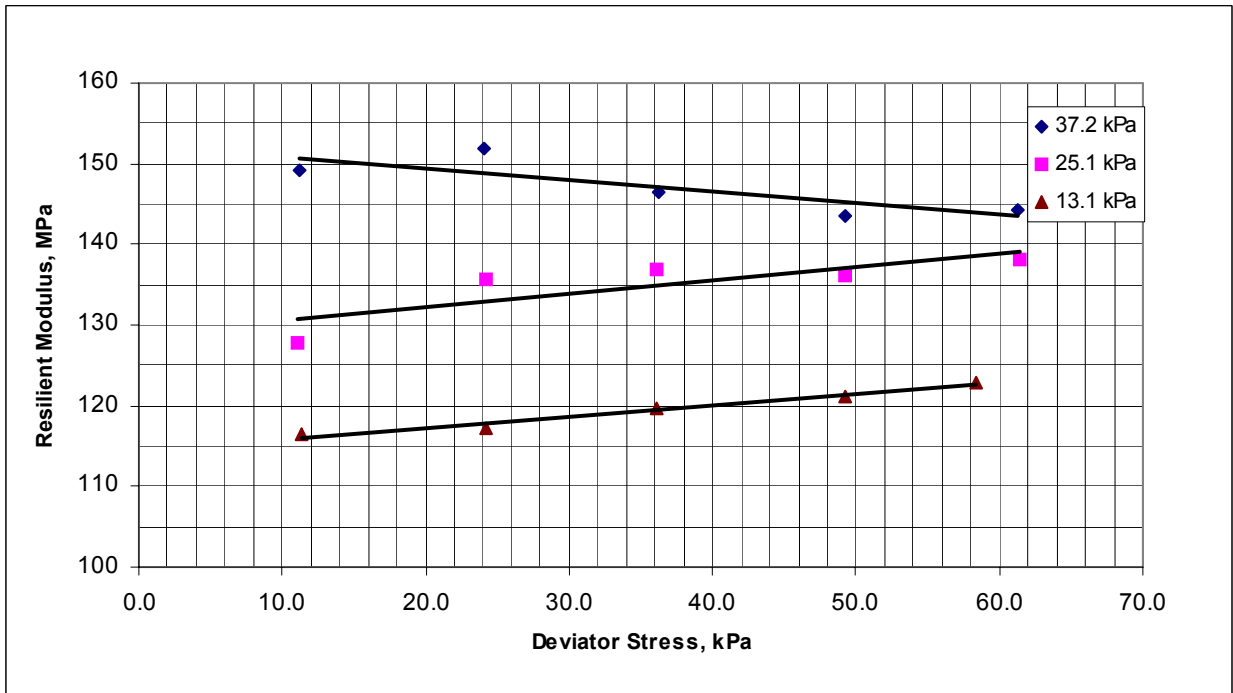


Figure C42 Resilient Modulus Test Results, Station 48+00, Section 10, Sample # 1, 1 MPa = 145 psi

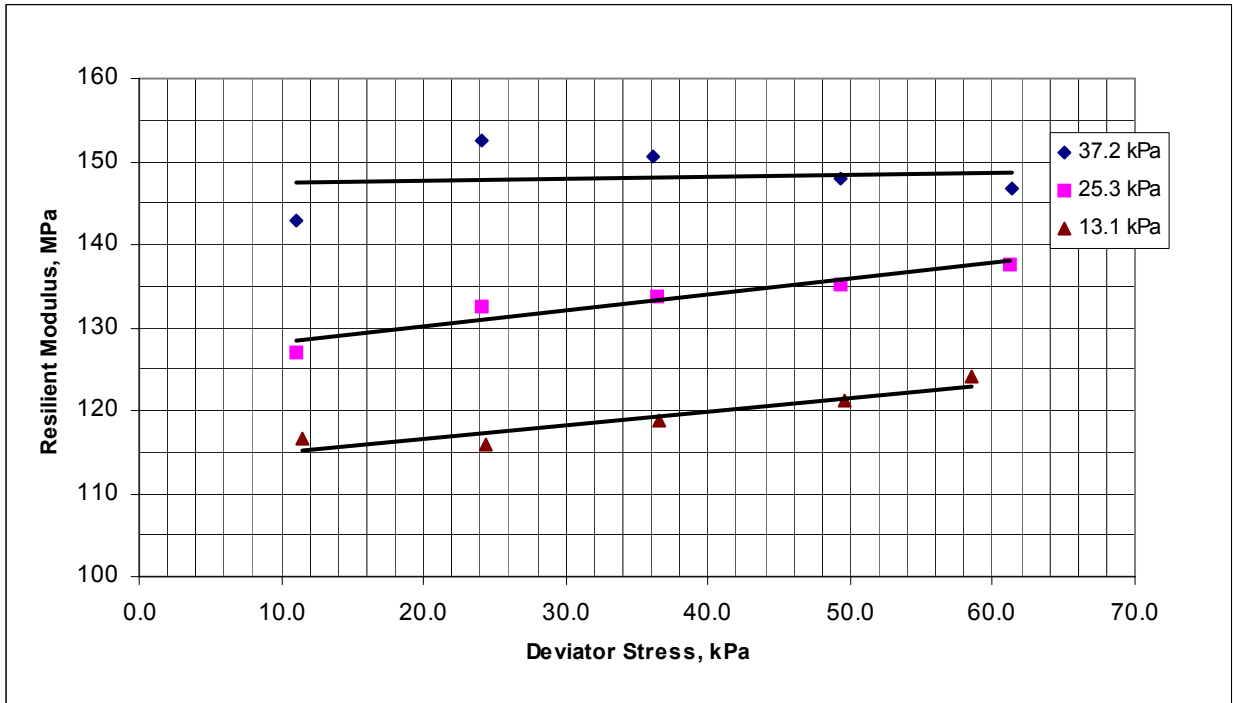


Figure C43 Resilient Modulus Test Results, Station 48+50, Section 10, Sample # 1, 1 MPa = 145 psi

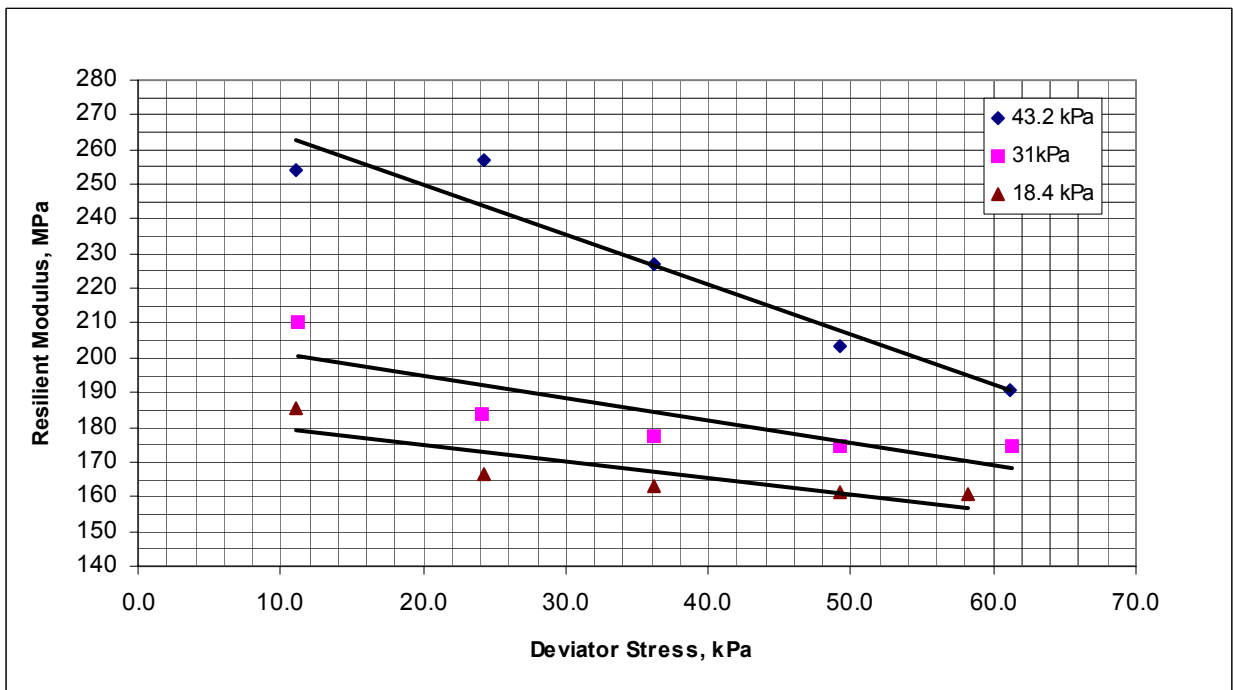


Figure C44 Resilient Modulus Test Results, Station 49+00, Section 10, Sample # 1, 1 MPa = 145 psi

APPENDIX D

**DETAILED FLOW CHARTS OF SOFTWARE PROGRAM
FWDSUBGRADE**

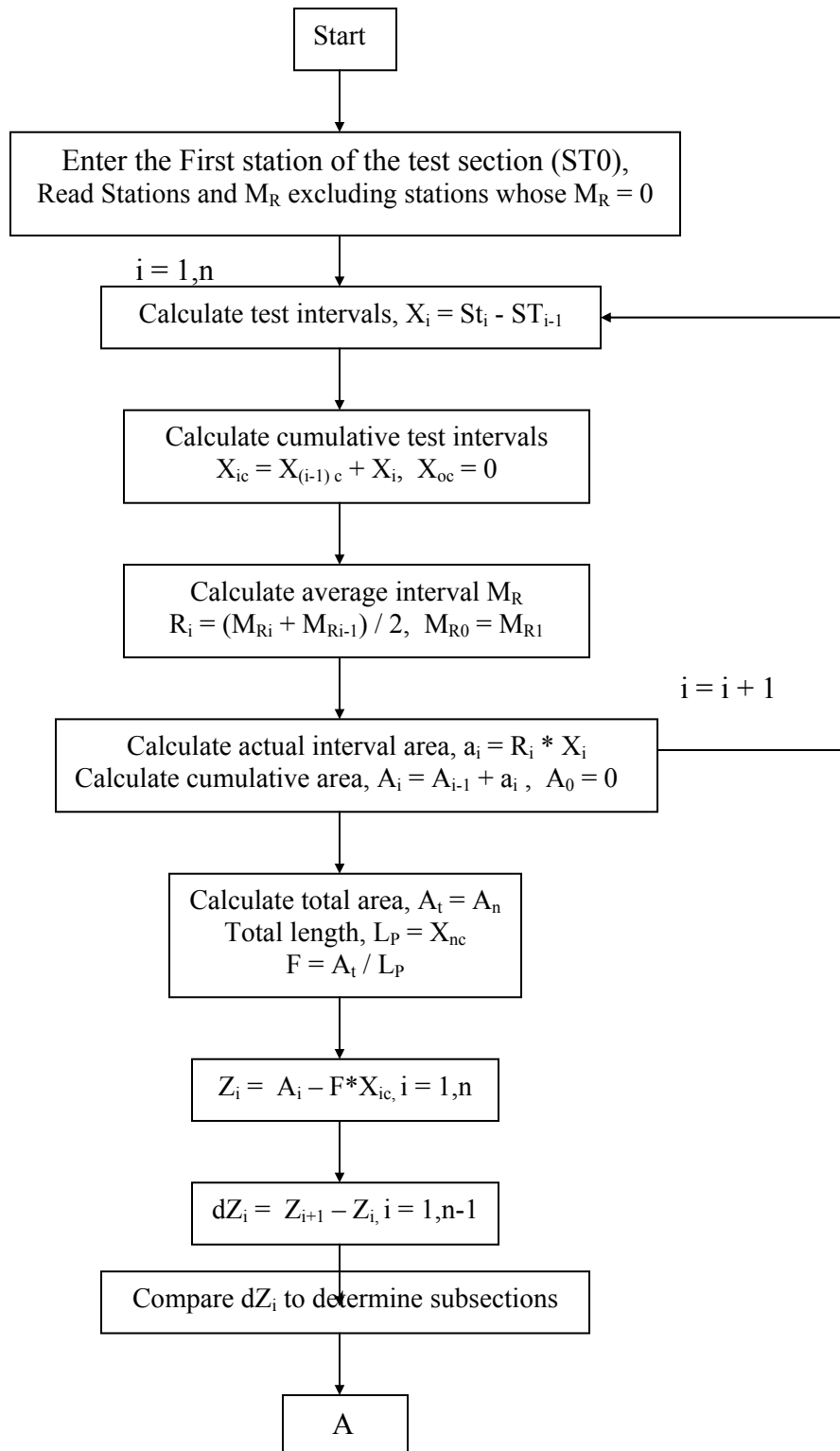


Figure D2 Flow Chart of Second Phase of Program Delineating Homogeneous Sections

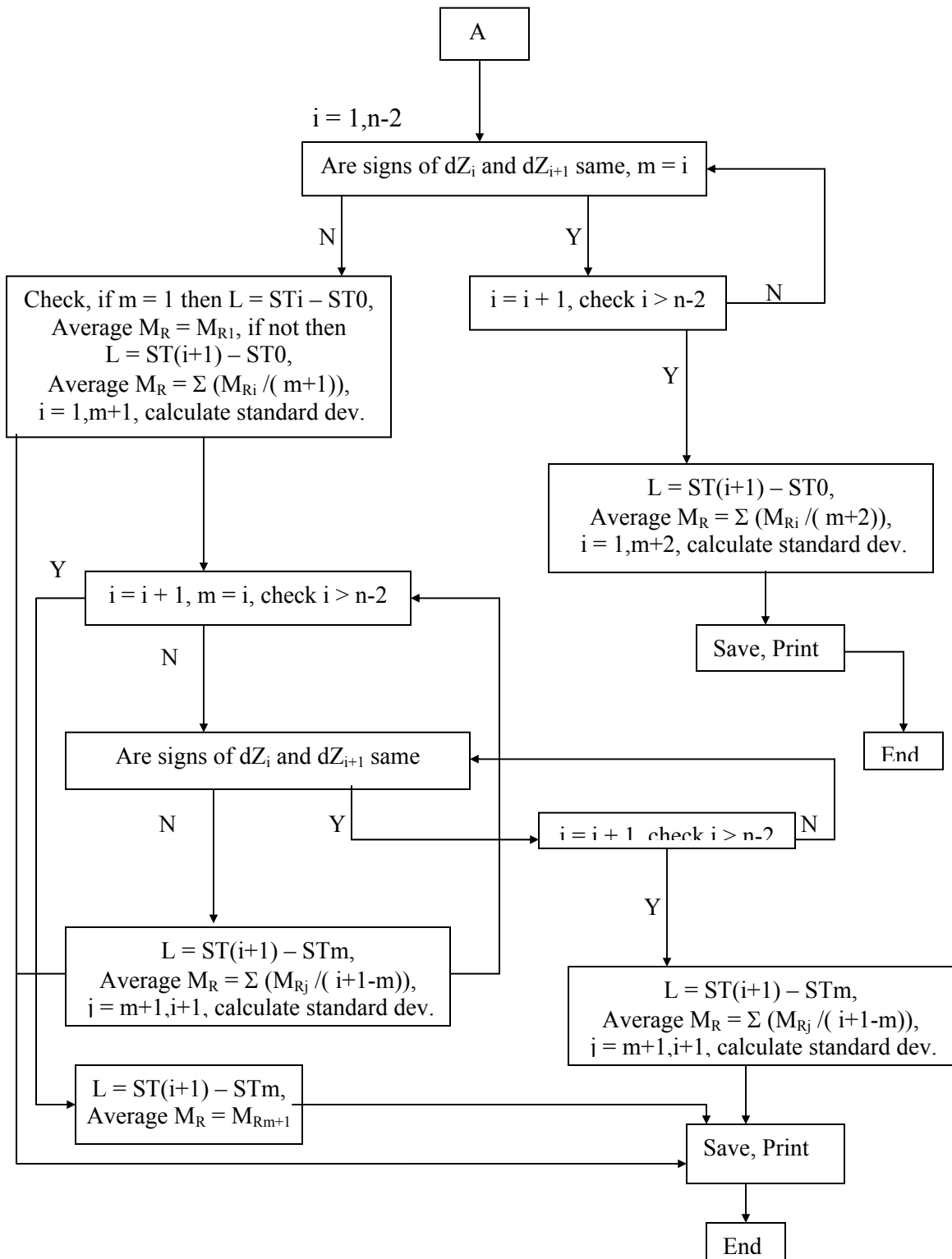


Figure D2 (Ctd) Flow Chart of Second Phase of Program Delineating Homogeneous Sections